



HAL
open science

Quantum theory of light in linear media : applications to quantum optics and quantum plasmonics

Vincent Dorier

► **To cite this version:**

Vincent Dorier. Quantum theory of light in linear media : applications to quantum optics and quantum plasmonics. Physics [physics]. Université Bourgogne Franche-Comté, 2020. English. NNT : 2020UBFCK006 . tel-02954369

HAL Id: tel-02954369

<https://theses.hal.science/tel-02954369>

Submitted on 1 Oct 2020

HAL is a multi-disciplinary open access archive for the deposit and dissemination of scientific research documents, whether they are published or not. The documents may come from teaching and research institutions in France or abroad, or from public or private research centers.

L'archive ouverte pluridisciplinaire **HAL**, est destinée au dépôt et à la diffusion de documents scientifiques de niveau recherche, publiés ou non, émanant des établissements d'enseignement et de recherche français ou étrangers, des laboratoires publics ou privés.

**THESE DE DOCTORAT DE L'ETABLISSEMENT UNIVERSITE BOURGOGNE FRANCHE-COMTE
PREPAREE AU LABORATOIRE INTERDISCIPLINAIRE CARNOT DE BOURGOGNE**

Ecole doctorale n°553

Carnot Pasteur

Doctorat de Physique

Par

M. Vincent Dorier

Quantum theory of light in linear media: Applications to quantum optics and quantum plasmonics

Thèse présentée et soutenue à Dijon, le 21/02/2020

Composition du Jury :

M. Gérard COLAS DES FRANCS	Professeur, Laboratoire ICB, UMR 6303 CNRS	Président
M. Michael FLEISCHHAUER	Professeur, Universitat Keiserslautern	Rapporteur
M. Stephan DE BIEVRE	Professeur, Laboratoire Paul Painlevé, UMR 8524 CNRS	Rapporteur
Mme Almut BEIGE	Professeur associé, School of Physics and Astronomy, University of Leeds	Examinatrice
M. Stéphane GUERIN	Professeur, Laboratoire ICB, UMR 6303 CNRS	Examineur
M. Hans-Rudolf JAUSLIN	Professeur, Laboratoire ICB, UMR 6303 CNRS	Directeur de thèse

Titre : Théorie quantique de la lumière dans les milieux linéaires : applications à l'optique quantique et la plasmonique quantique

Mots clés : Quantification, Plasmon, Optique

Résumé : Ce travail de thèse présente une stratégie de quantification de la lumière dans les milieux linéaire. Basée sur la construction de modèles hamiltoniens compatibles avec les équations de Maxwell, elle utilise la diagonalisation de l'hamiltonien par une transformation canonique pour préserver la structure du modèle, et un principe de correspondance pour transformer les variables canoniques en opérateurs agissant sur un espace de Fock quantique. Nous montrons que cette stratégie générale peut être appliquée au cas de photons dans des milieux passifs (i.e., sans dissipation), ainsi que pour les plasmons dans des milieux de type Kramers-Kronig. Nous utilisons ce formalisme pour décrire l'effet Hong-Ou-Mandel résolu en temps, ainsi que l'émission spontanée de plasmons.

Title : Quantum theory of light in linear media : applications to quantum optics and quantum plasmonics

Keywords : Quantization, Plasmon, Optics

Abstract : This PhD contains a strategy of quantization of light in linear media. Based on the construction of hamiltonian models compatible with Maxwell's equations, it uses the diagonalization of the Hamiltonian via a canonical transformation to preserved the structure of the model, and a principle of correspondence to transform the canonical variables into operators acting on a quantum Fock space. We show that this general strategy can be applied to the case of photons in passive media (i.e., without dissipation), as well as plasmons in Kramers-Kronig media. We use this formalism to describe the time-resolved Hong-Ou-Mandel effect, and the spontaneous emission of plasmons.

Contents

Contents	1
Acknowledgement	4
Introduction	5
1 Classical electromagnetism	13
1.1 Circuits of light	14
1.2 Maxwell's equations	15
1.2.1 Microscopic and macroscopic formulations	15
1.2.2 Vector and scalar potentials	17
1.2.3 Polarization density and electric susceptibility	17
1.2.4 Fourier domain and dielectric coefficient	19
1.3 Models for matter	20
1.3.1 Passive media	21
Definition of a passive medium	21
Maxwell's equations in a passive medium	22
Generalized Coulomb gauge	22
1.3.2 Drude model	23
1.3.3 Lorentz model	26
1.3.4 Drude-Lorentz model	26
1.4 Summary on classical electromagnetism	27
I Photons	29
2 Canonical optics	31
2.1 Hamiltonian structure	32
2.1.1 Starting equations	32
2.1.2 Hamiltonian function	32
2.2 Electromagnetic configurations	34
2.2.1 Phase space and complex representation	34
2.2.2 Modes and eigenconfigurations	36
2.2.3 Normal mode decomposition	38
2.2.4 Spectral structure (in vacuum)	39
2.3 Summary on the classical Hamiltonian system	41

3	Quantum optics	43
3.1	Quantization procedure in a reduced model	44
3.1.1	Principle of correspondence	44
3.1.2	General configurations	45
3.1.3	Ground states	46
3.1.4	Ladder space	46
3.2	Photons	47
3.2.1	Bosonic Fock space	47
3.2.2	Creation-annihilation operators	48
3.2.3	Number operator	49
3.2.4	Hilbert spaces of classical electromagnetic configurations	49
3.2.5	Electromagnetic field operators and Hamiltonian	51
3.2.6	The quantum field operator	52
3.3	Summary on the spaces	53
3.4	The key to the full model	54
3.4.1	The infinite Fock space	54
3.4.2	The different roles of operators in quantum optics	55
3.4.3	Remarks on the physical status of the reduced model	56
3.5	Summary on the quantum model	56
4	Photon dynamics	59
4.1	Time evolution of photon states	60
4.2	One photon through a beam splitter	61
4.2.1	Classical description	61
4.2.2	Quantum dynamics of the photon	63
4.3	Hong-Ou-Mandel effect	63
4.3.1	General setup	64
4.3.2	Usual HOM effect	65
4.3.3	Discussion on classical dynamics	67
4.4	Hong-Ou-Mandel with a fast detector	67
4.4.1	Time-resolved HOM effect	68
4.4.2	Time-resolved HOM with phase flip	69
4.4.3	Multi-pulses HOM with phase flips	71
4.5	Summary on the dynamics of photons	72
II	Plasmons	75
5	Canonical plasmonics	77
5.1	Microscopic model	78
5.1.1	Light	79
5.1.2	Matter	79
5.1.3	Interaction	80
5.1.4	Equivalence with Maxwell's macroscopic equations	81
5.1.5	Hamiltonian structure	83
5.1.6	Coupling function in standard models	84
	Drude model	85
	Lorentz model	85
5.2	Canonical diagonalization of the model	86
5.2.1	Pre-diagonalization of the electromagnetic part	86
5.2.2	Integral operators, matrix form and canonical transformations	87
5.2.3	Finding the harmonic-like Hamiltonian	89

5.2.4	Møller wave operator	90
5.2.5	Lippmann-Schwinger equation	92
5.2.6	Degeneracy and block structure	94
5.2.7	Phase space of plasmonic configurations	96
5.2.8	Orthonormalization and completeness of the eigenconfigurations	97
5.2.9	Diagonal Hamiltonian	98
5.3	Summary on the classical Hamiltonian system	99
6	Quantum plasmonics	101
6.1	Quantization	102
6.1.1	Bosonic operators and Hamiltonian	102
6.1.2	Fock space and quantum plasmons	103
6.1.3	Electric field operator	104
6.1.4	Other fields and commutation relations	105
6.1.5	No-coupling limit	106
6.2	Solving the Lippmann-Schwinger equation	107
6.2.1	Perturbative series	107
6.2.2	Small coupling regime	108
	Zeroth order	108
	First order	109
6.2.3	Small volume regime	111
	Partial exact diagonalization	111
	Zeroth order	114
	First order	114
	Second order	115
6.3	Comments on the literature	115
6.3.1	Summary of the previous approaches in literature	116
6.3.2	The problem of the no-coupling limit	118
	For the bosonic operators	118
	For the Hamiltonian	119
	For the electric field operator	119
	Remarks on an infinite bulk medium	120
6.3.3	Justifications and proposed corrections in the literature	120
	Addition of a fictitious homogeneous dissipative medium	120
6.3.4	Addition of a modified free field	121
6.4	Summary on the quantum model	121
7	Plasmon dynamics	123
7.1	The model	124
7.2	Fermi Golden rule	125
7.2.1	Emitter in a plasmonic environment	126
7.2.2	Emitter in vacuum	127
7.2.3	The Purcell factor	128
7.3	Wigner-Weisskopf theory	129
7.3.1	Emitted quantum state	129
7.3.2	Tracking the dissipation	130
7.4	Comments on the literature	132
7.4.1	Summary of the result in the literature	132
7.4.2	Fermi golden rule assuming Eq. (6.110)	133
7.4.3	Spontaneous emission in a 1D model assuming Eq. (6.110)	135
7.5	Summary on the dynamics of plasmons	138

Conclusion	138
A Classical energy of radiation	143
A.1 From the power transfer to a set of external charges	143
A.2 From the Hamiltonian structure	145
A.3 Equivalence of the two approaches	145
B Symplectic structure for the electromagnetic field	147
C Symmetry of the plasmonic frequency operator	149
C.1 Definition of symmetric integral operators	149
C.2 Symmetry of the diagonal blocks	150
C.3 Symmetry of the off diagonal blocks	150
D Derivation of the Green identity	151
E Green function for a 1D slab	153
E.1 Continuity conditions	153
E.2 Source on the right of the slab	154
E.3 Other positions of the source	156
E.3.1 On the left of the slab	156
E.3.2 Inside the slab	157
Bibliography	159

Acknowledgement

I want to first acknowledge my wife Narine, whom I met when starting this PhD, and whom I married right in the middle of it. She has been the most supportive, motivating and understanding person by my side during this long journey.

I would thank my family for being always faithful, and my colleagues for being very helpful both at work and outside of the lab. My closest friends, then, who have accompanied me throughout my years at university.

Finally, I want to express special thanks to my supervisor Hans, who has never lost faith in my abilities even when I had, and who gave me so much inspiration both as a researcher and as a human being.

Introduction

Articles linked to this work:

- [1] V. Dorier, J. Lampart, S. Guérin and H. R. Jauslin, **Canonical quantization for quantum plasmonics with finite nanostructures**, *Physical Review A* 100, 042111 (2019).
 - [2] V. Dorier, S. Guérin and H.R. Jauslin, **Critical review of quantum plasmonic models for finite-size media**, arXiv:1911.03134 (2019).
 - [3] V. Dorier, J. Lampart, S. Guérin and H. R. Jauslin, **Canonical quantization, spontaneous emission and dissipation of plasmon polaritons**, to be published.
-

The field of Quantum Optics has been growing in a unprecedented manner since the first experimental proofs, by Clauser [4, 5] and then Grangier *et al.* [6], that light can behave in a strictly non-classical manner. In 1987, Ghosh and Mandel [7] have studied experimentally the process of Spontaneous Parametric Down Conversion (SPDC, first observed in 1970 [8, 9]), which serves as the single-photon source of many experiments nowadays – one big advantage of this method being that it can create pairs of entangled photons. Other common devices include color centers in diamonds, single atoms in cavities, or quantum dots [10]. In order to understand how differently single photons should behave in experiments compared to classical fields, one needs a detailed theoretical description of how quantum light is created and how it evolves in time.

In many works, n -photons are theoretically described as a n -quantum state of a bosonic Fock space, and is noted $|n\rangle$ [11]. Although such a notation is sufficient in studies where the important question is the number of photons n and their distribution (e.g., when building computing protocols with multi inputs/outputs circuits), it hides all classical properties of light which may survive in the quantization, such as the frequency distribution (and reciprocally the temporal distribution), the spatial profile, and the polarization.

Historically, each photon state was associated with a plane wave. Such states are eigenfunctions of the Hamiltonian. In this regard, one could consider a photon to have a well-defined energy, $E = \hbar\omega$, where ω is the frequency of the plane wave.¹ However, such modes are hardly appropriate to define a quantum state, since they are delocalized over all space. In

¹Throughout this thesis, the word frequency is used for the angular frequency.

order to make sense to the quantum states in a Fock space, one needs to construct appropriate modes (generally described as *pulses*). In vacuum, this process is immediate since plane waves can be integrated to build a pulse. Such "pulse-states" are eigenfunctions of the number operator, and this is the necessary condition for one to speak of a "1-photon state" in an experiment. But as a consequence, one cannot associate to the photon-state a single frequency (or equivalently a single energy, since a pulse-state is not an eigenfunction of the Hamiltonian), and it is always associated with a specific *classical* mode with its own polarization, spectrum and temporal distribution, and spatial profile.

A detailed description of photon states in vacuum can be found, e.g., in [12]. In our perspective, the quantum theory of light is constructed from a classical one. We make the following statement: *Maxwell's equations (microscopic or macroscopic) can describe all classical light, and consequently a quantized version of them can describe all quantum light.* We thus start with Chapter 1 as an introduction of the classical theory of light. We describe the Maxwell equations and show how they relate to macroscopic quantities such as the dielectric function to describe linear interactions with matter. We emphasize that we consider only *linear* media, defined as such:

A material medium is linear if its polarization induced by the presence of an electromagnetic field is a linear function of the electric field.

We introduce two models for matter: a *passive* one, where the polarization response of matter is instantaneous, and a *Kramers-Kronig* one, where the response is retarded, which gives rise to dissipation and dispersion. Finally, we present some of the most common models to describe the response function: Drude, Lorentz, and a combination of both.

The quantization of the Maxwell equations we write in Chapter 1 leads to the emergence of two types of quantum excitation: *photons* and *plasmons*. The former come from the Maxwell equations in passive media, and the latter when the field interacts with the electrons of the medium, producing a polarization. Although both models rely on the classical theory of electromagnetism, they feature some fundamental differences, such as the presence of dissipation and dispersion in the latter while it is absent in the former. Nonetheless, we developed a strategy of quantization which can be applied to both systems, adapted from the quantization procedure described in Ref. [13–15]. It splits into two distinct steps:

1. Construction and diagonalization of a classical Hamiltonian model;
2. Quantization through a principle of correspondence and construction of a Fock space.

The first step establishes the concept of *canonical models*, where light is described in a Hamiltonian structure equivalent to the Maxwell equations. Appropriate canonical variables are introduced, and the model is diagonalized with canonical transformations to construct normal (optical or plasmonic) modes.

The second step relies on a principle of correspondence which is defined to construct creation-annihilation operators acting on a Fock space of quantum states. This step allows us to analyze some properties of the states such as their connection to classical solutions of Maxwell's equations.

This two-step scheme is very general and applies to most strategies of quantization of classical models. The fundamental ideas of our construction are the following:

- **Step 1** – We construct and transform the classical models such that they acquire the same structure as a continuous set of coupled harmonic oscillators. Although this is rather

common in vacuum (since the connection with harmonic oscillators is rather straightforward, especially when expanding the fields in the Fourier domain), it is not so common in the presence of matter, in particular when dispersion and dissipation is added. We call such a structure a *harmonic-like form*, whose Hamiltonian reads

$$H = \frac{1}{2}P \cdot P + \frac{1}{2}Q \cdot \Omega^2 Q. \quad (1)$$

The variables P and Q are the canonically conjugate variables, and Ω is called the *frequency operator*. This notation is very general: P and Q can contain many components (each corresponding to a different harmonic oscillator), or even an infinite number of them. The product \cdot is a sum (or integral in the continuous case) over all components.

In the case of a discrete set of N harmonic oscillators, the Hamiltonian (1) reads

$$H = \frac{1}{2} \sum_{\kappa=1}^N \left[p_{\kappa}^2 + q_{\kappa} \sum_{\kappa'} \Omega_{\kappa, \kappa'}^2 q_{\kappa'} \right]. \quad (2)$$

If the oscillators are independent, the matrix Ω is diagonal ($\Omega_{\kappa, \kappa'} \propto \delta_{\kappa \kappa'}$). Its diagonal terms are the frequency of each individual oscillator. Any additional off-diagonal term represents a coupling between oscillators. We show in Fig. 1 a scheme of the transformation from a general discrete quadratic Hamiltonian with non-trivial couplings to a harmonic-like form.

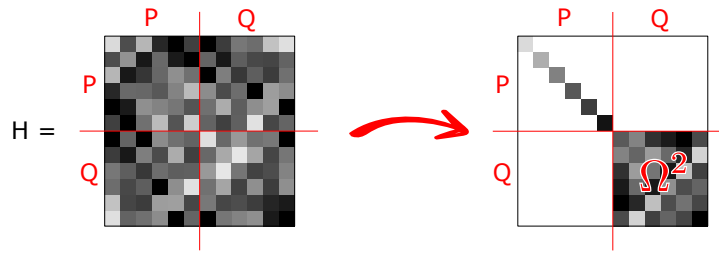


Figure 1 – Transformation from a discrete Hamiltonian of harmonic oscillators with non-trivial couplings, to a harmonic-like form with a frequency operator Ω .

If the oscillators form a continuous spectrum (i.e., their label κ is a continuous variable), the sum \sum_{κ} becomes an integral $\int d\kappa$:

$$H = \frac{1}{2} \int d\kappa [p^2(\kappa) + q(\kappa)(\Omega^2 q)(\kappa)]. \quad (3)$$

In this case, Ω is an *integral operator*, which is the continuous equivalent of a matrix. It acts as

$$(\Omega q)(\kappa) = \int d\kappa' W(\kappa, \kappa') q(\kappa'), \quad (4)$$

with $W(\kappa, \kappa')$ a rank-2 tensor called the *kernel* of Ω . Note that this kernel is not necessarily a continuous function; it can even be defined as a distribution. As an example, if Ω is diagonal, then $W(\kappa, \kappa') \propto \delta(\kappa - \kappa')$, with the δ function being the continuous equivalent of the Kronecker δ .

Once the model for light is described by a Hamiltonian in harmonic-like form, its diagonalization reduces to the diagonalization of the frequency operator.

- **Step 2** – Once the classical models are expressed in a harmonic-like form, the quantization is formulated similarly in both types of media. It relies on the definition of a complex representation of the classical phase space,

$$\Psi = \frac{1}{\sqrt{2}} (\Omega^{1/2} Q + i\Omega^{-1/2} P). \quad (5)$$

The following principle of correspondence is then applied:

$$\Psi \mapsto \sqrt{\hbar} \hat{B}_\Psi, \quad \Psi^* \mapsto \sqrt{\hbar} \hat{B}_\Psi^\dagger, \quad (6)$$

where the operators \hat{B}_Ψ^\dagger and \hat{B}_Ψ are creation and annihilation operators acting on a bosonic Fock space. The definition of the Fock space depends on the structure of the model (which will prove very different in the two types of media considered in the thesis). The interpretation is that \hat{B}_Ψ^\dagger creates one quantum of excitation associated with the classical configuration Ψ . The evolution of the quantum state is then entirely known from the evolution of Ψ and the symmetry property of bosons.

Inverting the canonical transformations performed in Step 1 provides a definition of the electric and magnetic fields as operators acting on the Fock space. They can then be used to evaluate measurable quantities such as the probability of measurement of specific states in optical circuits (Chap. 4) or the spontaneous decay rate of an emitter interacting with light in a material environment (Chap. 7).

In Chapters 2,3 we construct the quantum theory of light in passive media described by an inhomogeneous dielectric permittivity. Our construction is adapted from the approach of Refs. [16, 17].

In Chapter 4 we describe more precisely the properties of photon states, such as their spectrum or temporal shape. We describe one of the most fundamental experiment used to distinguish between classical and quantum light, or to characterize a photon source: the Hong-Ou-Mandel experiment [18]. This experiment was recently adapted [19–22] to systems where the photon state can be shaped and temporally resolved by the detector, which brings new counter-intuitive results. We use this Chapter to analyze this type of setups from the quantization procedure of Chapter 3.

The other three Chapters focus on plasmons. The basic classical theory is the macroscopic Maxwell equations, with a polarization density both induced by the interaction with the electric field and spontaneously emerging from the sources of the material medium. The macroscopic Maxwell equations do not have a Hamiltonian (canonical) structure because of the presence of dispersion and dissipation. This comes from the lack of material degrees of freedom in the equations: Maxwell's equations describe how the energy of the electromagnetic field is affected by the sources and currents in matter, but they do not describe the energy of the medium. In Chapter 5 we add to Maxwell's equations a microscopic model for matter such that all degrees of freedom are included and the dissipation and dispersion of light can be tracked. The model is justified by its compatibility with the initial macroscopic Maxwell equations when the degrees of freedom of the medium are eliminated. This construction is inspired by the one of Refs. [23–26]. The second part of Chapter 5 is new, since it provides an exact method of diagonalization of the Hamiltonian which differs from earlier treatments in the literature and is specifically adapted to situations where light interacts with finite media like nanostructures.

Chapter 6 is dedicated to the quantization of the model of Chapter 5 and the description of the quantum plasmon states. The former is based on similar principles as for photons (Chapter 3). The latter requires the explicit diagonalization of the Hamiltonian, which is performed using a Lippmann-Schwinger equation. We show how it can partially be solved exactly, and we give results of perturbation theory for the complete diagonalization. We also use this Chapter to raise some remarks on the validity of earlier treatments for finite and infinite media.

In the last Chapter, we study the spontaneous emission of plasmon states by a single emitter interacting with the plasmonic field. This study directly follows the diagonalization performed in Chapter 6 since the spontaneous decay rate is connected to the eigenfunctions calculated with the Lippmann-Schwinger equation. We construct it using the Fermi golden rule, and we use the Wigner-Weisskopf theory to extract the emitted plasmon state and to track the energy dissipated inside the medium. We also describe how the decay rate was constructed in the past, a method containing discrepancies which, to our knowledge, have not been addressed in the literature.

The main results of Chapters 5,6 were published in Ref. [1], and the derivation of spontaneous emission will be published later [3]. The comments on the past methods of quantization (Chapter 6) and calculation of spontaneous emission (Chapter 7) were published in Ref. [2].

Classical electromagnetism

This first chapter is dedicated to the basics of classical electromagnetism [27, 28]. It is generally assumed that since Maxwell's equations provide a well-grounded description of all classical light interacting with matter, one can build an a well-grounded theory of quantum light by applying to Maxwell's equations a rigorous quantization procedure. This assumption (and the existence of such a procedure) is particularly relevant to justify a continuity between the quantum and the classical description of the electromagnetic radiation.

We use this first Chapter to introduce the notations for the fields and variables. After brief general statements on the idea of photonic and plasmonic circuits in Section 1.1, we describe the microscopic and macroscopic formulations of Maxwell's equations in Section 1.2. We introduce important quantities such as the dielectric coefficient as well as the vector and scalar potentials, which are fundamental variables we will use in the quantization. In Section 1.3 we introduce two models that can describe the interaction between light and matter, one for passive media and the other for dispersive and dissipative media. The keystone of the models is the dielectric coefficient, which describes macroscopically the electric response of the medium and can be either measured experimentally or computed with (ab initio or not) models. We end the Chapter with the description of two such models: the Drude model and the Lorentz model, as well as combination of them.

Contents

1.1 Circuits of light	14
1.2 Maxwell's equations	15
1.2.1 Microscopic and macroscopic formulations	15
1.2.2 Vector and scalar potentials	17
1.2.3 Polarization density and electric susceptibility	17
1.2.4 Fourier domain and dielectric coefficient	19
1.3 Models for matter	20
1.3.1 Passive media	21
1.3.2 Drude model	23
1.3.3 Lorentz model	26
1.3.4 Drude-Lorentz model	26
1.4 Summary on classical electromagnetism	27

1.1 Circuits of light

Before getting into the equations and mathematical formalisms of classical electromagnetism, we start with an overview of the physical scenarios we may always keep in mind when we wish to construct the quantum theories for photons and plasmons. In a general point of view, many (if not most) of the experiments with light follow the scheme of a circuit, with three main parts:

- the *emission part*, where one or several devices can be triggered to emit classical or quantum light in a controlled way;
- the *propagation part*, which can consist of different material media whose roles are to guide and/or modify the emitted light;
- the *detection part*, where one or several devices can collect light and measure its property with the highest accuracy possible.



The description of how classical light propagates through lenses, bounces on mirrors or gets attenuated through filters is based on a well-established theory of electromagnetism. The emission part is generally absent from classical descriptions, we simply assume a specific structure of the emitted wave from what we know of the source. The detection part is usually based on approximations of what properties of light the detector is mostly sensitive to, with an efficiency of measurement which can be optimized with an adequate statistical sample of measures.

In the scope of linear quantum optics or quantum plasmonics, it is necessary to have a good understanding of the propagation part since, as we show in Chapter 3 and use in Chapter 4, the structure and time-evolution of the quantum state of light is directly associated with a classical wave. It is this direct connection which justifies that most experimental schemes used for quantum light (either photonics or plasmonics) can be used for classical light: the propagation of photons in fibers or the attenuation of their probability of measurement when passing through filters, for instance, are based on the knowledge of how fibers and filters act on classical light. As an example, the Hong-Ou-Mandel experiment we describe in Chapter 4, even though having different outcomes when using classical or quantum light, fundamentally relies on a description of the propagation and of the effect of the beam splitter inherited from the classical theory.

When describing purely quantum phenomena, it is common to use a mathematical formalism which hides the implicit classical behaviors associated with the quantum state (such as writing only the number of quanta in the state). But in some experiments, one must analyze precisely the propagation of the state. This is why we construct the theories of quantum photonics and quantum plasmonics based on manipulations and transformations of the classical theory of electromagnetism of which we give a brief overview in the present Chapter.

1.2 Maxwell's equations

1.2.1 Microscopic and macroscopic formulations

Any classical electromagnetic radiation obeys the microscopic Maxwell's equations:

$$\partial_t \vec{E} = c^2 \nabla \times \vec{B} - \vec{j} / \epsilon_0, \quad (1.1a)$$

$$\partial_t \vec{B} = -\nabla \times \vec{E}, \quad (1.1b)$$

$$\nabla \cdot \vec{E} = \rho / \epsilon_0, \quad (1.1c)$$

$$\nabla \cdot \vec{B} = 0, \quad (1.1d)$$

with \vec{E} the electric field, \vec{B} the magnetic field (also called “magnetic induction”), ρ the total density of charges, \vec{j} the total current density, c the speed of light in vacuum and ϵ_0 the vacuum permittivity. We use the notation $\partial_t \equiv \partial / \partial t$, $\nabla = (\partial_{x_1}, \partial_{x_2}, \partial_{x_3})$ is the *nabla* operator, \times is the vector product and \cdot is the scalar product.

The equations (1.1) are called the “microscopic” Maxwell equations because they relate the electric and magnetic fields to the behavior and distribution of microscopic charges. In particular:

- Eq. (1.1a) describes how a change in the electric field and the presence of currents produce a magnetic field,
- Eq. (1.1b) describes how a change in the magnetic field produces an electric field,
- Eq. (1.1c) shows the emergence of an electric field from the presence of electric charges,
- Eq. (1.1d) is a formulation of the non-existence of magnetic charges, also called “magnetic monopoles”.

We also have the continuity relation:

$$\partial_t \rho + \nabla \cdot \vec{j} = 0, \quad (1.2)$$

which is obtained by combining the time derivative of (1.1c) and the divergence of (1.1a). This relation shows that a variation of the density of charges is necessarily related to a variation of current (one can further use the Gauss divergence theorem to show that it implies a conservation of the number of charges if the system is isolated).

The microscopic Maxwell equations (1.1) are particularly useful when the number of charges is small and when their motion (or equivalently, the currents they produce) is easily tracked – and even more so in vacuum, where there is no charge nor current ($\rho = 0$, $\vec{j} = 0$). However, when the electromagnetic field interacts with a medium consisting of many charges moving in a disordered fashion, we have to use macroscopic quantities containing the large-scale response of the medium to the electromagnetic field. We will now describe how to build such a macroscopic model.

In a very general way, one can phenomenologically define a material medium by formally splitting the total charge and current densities into two groups: one bounded to the medium (ρ_m, \vec{j}_m), and one external/independent from the medium ($\rho_{ext}, \vec{j}_{ext}$). It is important to note that this distinction is *phenomenological*: the charges and currents in the first group are chosen for their contribution to specific phenomena (typically, a somewhat large-scale

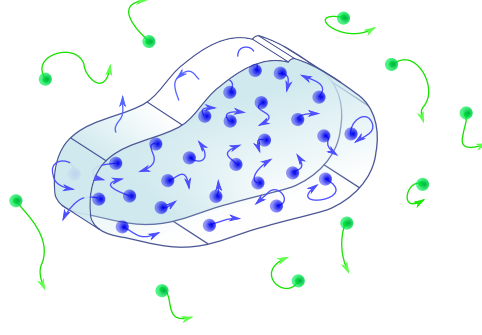


Figure 1.1 – Differentiation between charges and currents bounded to a macroscopic medium (in blue), and external charges and currents (in green).

response to the electromagnetic field). In the microscopic Maxwell's equations (1.1), one can therefore replace the total charge and current densities by

$$\rho = \rho_m + \rho_{ext}, \quad (1.3a)$$

$$\vec{j} = \vec{j}_m + \vec{j}_{ext}. \quad (1.3b)$$

One can show (using Poincaré's lemma) that the conservation equation (1.2) implies the existence of two vector fields $\vec{\mathfrak{P}}$ and $\vec{\mathfrak{M}}$, related to ρ and \vec{j} by:

$$\rho = -\nabla \cdot \vec{\mathfrak{P}}, \quad (1.4a)$$

$$\vec{j} = \nabla \times \vec{\mathfrak{M}} + \partial_t \vec{\mathfrak{P}}. \quad (1.4b)$$

The fields $\vec{\mathfrak{P}}$ and $\vec{\mathfrak{M}}$ are called *polarization density* and *magnetization* respectively.¹ These vector fields represent how the collective behavior of charges and currents produces a macroscopic response. In other words, they contain the averaged information of many electric and magnetic dipoles interacting, without requiring the knowledge of the number of dipoles nor of their individual action. For this reason, the polarization density and the magnetization are called *macroscopic fields*.

By replacing ρ and \vec{j} by their new expressions in the microscopic Maxwell equations, we obtain the *macroscopic Maxwell equations*:

$$\partial_t \vec{E} = c^2 \nabla \times \vec{B} - \frac{1}{\epsilon_0} \left[\nabla \times \vec{\mathfrak{M}} + \partial_t \vec{\mathfrak{P}} \right], \quad (1.5a)$$

$$\partial_t \vec{B} = -\nabla \times \vec{E}, \quad (1.5b)$$

$$\nabla \cdot \vec{E} = -\frac{1}{\epsilon_0} \nabla \cdot \vec{\mathfrak{P}}, \quad (1.5c)$$

$$\nabla \cdot \vec{B} = 0. \quad (1.5d)$$

In this thesis, we will consider non-magnetic media: $\vec{\mathfrak{M}} = 0$. The macroscopic Maxwell equations therefore read

¹ $\vec{\mathfrak{P}}$ is sometimes referred to simply as “polarization”, but it may lead to some confusion with the polarization of a light wave (both can be related when the polarization density is induced by a polarized light radiation, but they still are distinct concepts). Therefore we will always use the term “polarization density” to avoid confusion.

$$\partial_t \vec{E} = c^2 \nabla \times \vec{B} - \frac{1}{\epsilon_0} \partial_t \vec{\mathfrak{P}}, \quad (1.6a)$$

$$\partial_t \vec{B} = -\nabla \times \vec{E}, \quad (1.6b)$$

$$\nabla \cdot \vec{E} = -\frac{1}{\epsilon_0} \nabla \cdot \vec{\mathfrak{P}}, \quad (1.6c)$$

$$\nabla \cdot \vec{B} = 0. \quad (1.6d)$$

1.2.2 Vector and scalar potentials

For many purposes, and more specifically to study electromagnetism in a Lagrangian or Hamiltonian formalism, and to construct a quantum theory of electromagnetism (see Chapters 2,3 and 5,6), it is convenient to introduce the scalar and vector potentials associated with the electric and magnetic fields.

By Poincaré's lemma, the zero divergence of \vec{B} [Eq. (1.6d)] implies that there is a vector field $\vec{A}(\vec{x}, t)$ such that

$$\vec{B} = \nabla \times \vec{A}. \quad (1.7)$$

Inserting it into Eq. (1.6b), we get

$$\nabla \times (\partial_t \vec{A} + \vec{E}) = 0, \quad (1.8)$$

and using Poincaré's lemma again, this implies that there is a function $U(\vec{x}, t)$ such that

$$\partial_t \vec{A} + \vec{E} = -\nabla U. \quad (1.9)$$

\vec{A} and U are called *vector potential* and *scalar potential*, respectively. Maxwell's equations can be written as

$$\partial_t \vec{E} = c^2 \nabla \times \nabla \times \vec{A} - \frac{1}{\epsilon_0} \partial_t \vec{\mathfrak{P}}, \quad (1.10a)$$

$$\partial_t \vec{A} = -\vec{E} - \nabla U, \quad (1.10b)$$

$$\nabla \cdot \vec{E} = -\frac{1}{\epsilon_0} \nabla \cdot \vec{\mathfrak{P}}, \quad (1.10c)$$

$$\vec{B} = \nabla \times \vec{A}. \quad (1.10d)$$

The two first Maxwell equations can be merged into one second order equation:

$$\nabla \times \nabla \times \vec{A} + \frac{1}{c^2} \partial_t^2 \vec{A} + \frac{1}{c^2} \partial_t \nabla U = \mu_0 \partial_t \vec{\mathfrak{P}}, \quad (1.11)$$

with $\mu_0 = 1/(\epsilon_0 c^2)$. This equation is a general form of what is called the *wave equation* for \vec{A} . One can build similar wave equations for \vec{E} and \vec{B} .

1.2.3 Polarization density and electric susceptibility

We can split the polarization density into three contributions:

$$\vec{\mathfrak{P}} = \vec{\mathfrak{P}}_{ind} + \vec{\mathfrak{P}}_{sp} + \vec{\mathfrak{P}}_{ext}. \quad (1.12)$$

The first contribution describes the part of the field which is *induced* by the interaction of the medium with light; the second term describes the part *spontaneously* generated by the charges and currents of the medium – both of these contributions originate from the charges and currents inside the medium (ρ_m, \vec{j}_m) . The last term is the contribution from *external* charges and currents $(\rho_{ext}, \vec{j}_{ext})$.

The spontaneous polarization density $\vec{\mathfrak{P}}_{sp}$ is determined by initial conditions of the medium, which in experiments are difficult to choose in a controlled way. Hence, in classical theoretical descriptions it is often treated as a random noise term, or simply set to zero when its effect can be considered negligible (such as in optical fibers).

In the case of a non-magnetic, neutral medium (i.e., it is globally neutral before an electric field is applied), the effect of the electric field is to displace the negative charges with respect to the positive ones. Hence the induced polarization is proportional to the electric field and powers of it. In a *linear* medium as considered throughout this thesis, higher powers are neglected, and the induced polarization density can be written with a (dimensionless) response function χ :

$$\vec{\mathfrak{P}}_{ind}(\vec{x}, t) = \epsilon_0 \int_{-\infty}^{\infty} dt' \chi(\vec{x}, t - t') \vec{E}(\vec{x}, t'). \quad (1.13)$$

This function χ is called the *electric susceptibility*. It is a tensor in general, but reduces to a scalar function in case of an isotropic medium.

The expression (1.13) is too general in the sense that it seems to allow for a polarization density at time t dependent on the electric field evaluated at future times $t' > t$. Since this would violate causality, we have to constrain the response function in a way that excludes non-causal responses. We can identify two possible choices:

- A **retarded** susceptibility $\chi(\vec{x}, t - t') = \Lambda(\vec{x}, t - t')\theta(t - t')$, with Λ a continuous function and $\theta(t - t')$ the Heaviside function:

$$\theta(t - t') = \begin{cases} 1 & \text{if } t' < t \\ 0 & \text{if } t' > t \end{cases}, \quad (1.14)$$

which ensures the causality. We can write in this case:

$$\vec{\mathfrak{P}}_{ind}(\vec{x}, t) = \epsilon_0 \int_{-\infty}^t dt' \Lambda(\vec{x}, t - t') \vec{E}(\vec{x}, t'). \quad (1.15)$$

- An **instantaneous** response function $\chi(\vec{x}, t - t') = \Lambda(\vec{x})\delta(t - t')$, with $\delta(t - t')$ the Dirac delta function. We have therefore

$$\vec{\mathfrak{P}}_{ind}(\vec{x}, t) = \epsilon_0 \Lambda(\vec{x}) \vec{E}(\vec{x}, t). \quad (1.16)$$

In both cases, the function χ is called the *electric susceptibility*.

Remark: It is worth noting that the instantaneous response function is *not* a special case of the retarded one. Indeed, if one were to extract a delta function from the susceptibility in Eq. (1.15), the integral would not be well defined because of the singular point $t' = t$. In this regard, the literature can be misleading, since it is not unusual to find the instantaneous response derived after defining Eq. (1.15) as the general equation. The way it is justified is by first taking $t \rightarrow \infty$ in (1.15) and only then extracting the delta function. This would be a valid approach if the susceptibility were a continuous function falling to zero at $t = t'$ (in which case applying the delta function would lead to $\vec{\mathfrak{P}}_{ind} = 0$), but otherwise if it contains a discontinuity at $t = t'$, one can-

not apply $\delta(t - t')$.

Note that vacuum is the only case where both approaches are equivalent, since $\chi = 0$.

In this section, we consider the first case of a causal non-instantaneous response. The instantaneous response will be described in more details in Section 1.3.1.

Let us impose that $\chi(\vec{x}, t - t') = \Lambda(\vec{x}, t - t')\theta(t - t')$ is square-integrable in t' . Then, Titchmarsh's theorem shows that the two following statements are equivalent:

1. The function $\chi(\vec{x}, t - t')$ vanishes for $t - t' < 0$;
2. The real and imaginary parts of its Fourier transform $\tilde{\chi}(\vec{x}, \omega)$ are Hilbert transforms of each other.

Because of causality, the first condition is automatically fulfilled. Hence we can write the Hilbert transforms:

$$\tilde{\chi}_R(\omega) = \frac{2}{\pi} \mathcal{P} \int_0^{\infty} d\omega' \frac{\omega' \tilde{\chi}_I(\omega')}{\omega'^2 - \omega^2}, \quad (1.17a)$$

$$\tilde{\chi}_I(\omega) = -\frac{2}{\pi} \mathcal{P} \int_0^{\infty} d\omega' \frac{\omega' \tilde{\chi}_R(\omega')}{\omega'^2 - \omega^2}, \quad (1.17b)$$

where \mathcal{P} stands for the Cauchy principal value, defined as:

$$\mathcal{P} \int_a^b dx f(x) = \lim_{\delta \rightarrow 0} \left[\int_a^{x_0 - \delta} dx f(x) + \int_{x_0 + \delta}^b dx f(x) \right], \quad (1.18)$$

with $f(x)$ a function with a pole at $x_0 \in [a, b]$. The equations (1.17) are usually referred to as the *Kramers-Kronig relation*. A medium modeled with a susceptibility which satisfies such relations is sometimes called a *Kramers-Kronig medium*.

1.2.4 Fourier domain and dielectric coefficient

It is often more convenient to solve the wave equation (1.11) in the Fourier domain ($t \rightarrow \omega$) in order to remove the temporal derivatives. We use the following conventions for the Fourier transform and its inverse:

$$\tilde{f}(\omega) = \int_{-\infty}^{\infty} dt f(t) e^{i\omega t}, \quad f(t) = \frac{1}{2\pi} \int_{-\infty}^{\infty} d\omega \tilde{f}(\omega) e^{-i\omega t}. \quad (1.19)$$

By splitting up the polarization density as in (1.12), the wave equation reads in the Fourier domain:

$$\nabla \times \nabla \times \vec{\tilde{A}} - \frac{\omega^2}{c^2} \vec{\tilde{A}} - \frac{i\omega}{c^2} \nabla \tilde{U} = -i\mu_0 \omega \left[\vec{\tilde{\mathfrak{P}}}_{ind} + \vec{\tilde{\mathfrak{P}}}_{sp} + \vec{\tilde{\mathfrak{P}}}_{ext} \right]. \quad (1.20)$$

The induced polarization density (1.13) takes the form of a convolution, therefore its Fourier transform simply reads

$$\vec{\tilde{\mathfrak{P}}}_{ind}(\vec{x}, \omega) = \epsilon_0 \tilde{\chi}(\vec{x}, \omega) \vec{\tilde{E}}(\vec{x}, \omega), \quad (1.21)$$

and because of (1.9), we can write

$$\vec{\tilde{\mathfrak{P}}}_{ind} = \epsilon_0 \tilde{\chi} \left[i\omega \vec{\tilde{A}} - \nabla \tilde{U} \right]. \quad (1.22)$$

We insert it into the wave equation (1.20):

$$\nabla \times \nabla \times \vec{A} - \frac{\omega^2}{c^2} \epsilon \vec{A} = \frac{i\omega}{c^2} \epsilon \nabla \tilde{U} - i\omega\mu_0 \left[\vec{\mathfrak{P}}_{sp} + \vec{\mathfrak{P}}_{ext} \right]. \quad (1.23)$$

We have introduced in Eq. (1.23) the *relative dielectric coefficient* ϵ :

$$\epsilon(\vec{x}, \omega) = 1 + \tilde{\chi}(\vec{x}, \omega). \quad (1.24)$$

The dielectric coefficient $\epsilon(\vec{x}, \omega)$ (also called *dielectric constant* or *dielectric function*) is a fundamental tool to describe the macroscopic (linear) response of a medium. It can be directly related to the refraction index and the extinction coefficient, i.e., quantities measured in experiments,² and its imaginary part ϵ_I is associated with dissipation of energy inside the medium.

The real and imaginary parts of the dielectric coefficient are also related by Kramers-Kronig relations. Inserting (1.24) into (1.17) gives:

$$\epsilon_R(\vec{x}, \omega) = 1 + \frac{2}{\pi} \mathcal{P} \int_0^\infty d\omega' \frac{\omega' \epsilon_I(\vec{x}, \omega')}{\omega'^2 - \omega^2}, \quad (1.25a)$$

$$\epsilon_I(\vec{x}, \omega) = -\frac{2\omega}{\pi} \mathcal{P} \int_0^\infty d\omega' \frac{\epsilon_R(\vec{x}, \omega') - 1}{\omega'^2 - \omega^2}. \quad (1.25b)$$

Various models are used to compute the dielectric coefficient (some will be described later on in this Chapter), each model being appropriate for a certain class of materials and in a certain frequency range. We note however that in order to describe losses (instead of gain), the imaginary part ϵ_I must be positive.

1.3 Models for matter

With the macroscopic Maxwell equations written in the Fourier domain, matter is modeled through the relative dielectric coefficient $\epsilon = \epsilon_R + i\epsilon_I$. In other terms, the properties of the dielectric coefficient can serve to describe the physical (optical) response of the medium. In particular, a medium is:

- *inhomogeneous* if ϵ varies in space;
- *dispersive* if ϵ varies with the frequency of light;
- *refractive* if $\epsilon_R \neq 1$;
- *dissipative* (or *lossy*) if $\epsilon_I \neq 0$.

Note that if $\epsilon \neq 1$ and if it satisfies the Kramers-Kronig relation, then the medium is necessarily dispersive, refractive **and** dissipative. Many materials can however obey one condition more than the other, depending on the range of frequency of light that one would consider in a given situation. For instance, materials that exhibit a very low absorption of light in visible frequencies (eg., glass or water) are considered refractive ($\epsilon_R > 1$) but negligibly dispersive and dissipative. For this reason, they are also called *passive media* for visible light. We will describe in more detail the approximation made to treat easily such media in Section 1.3.1.

²A wide database of these coefficients is available on <https://refractiveindex.info/>.

On the other side, materials like metals exhibit a very high coefficient of losses: they absorb fast and on small distances the energy of electromagnetic radiations in the visible range. Such materials are characterized by a rather large ϵ_I and a negative ϵ_R , and the two main models to compute them (described in Sections 1.3.3 and 1.3.2 respectively) are the Lorentz model and the Drude model.

Some works [29, 30] have shown that the standard models for the dielectric coefficient of metals should be modified when the size of the medium is very small. We will not consider this problem in this thesis, but we expect that one could always adapt the model by replacing the usual dielectric coefficient by a modified one, taking this effect into account.

We also emphasize that the dielectric coefficient is a *macroscopic* quantity. One cannot infer the microscopic motion and distribution of charges inside the medium simply from the values of ϵ_R and ϵ_I . These microscopic properties, however, are useful to build a theoretical model to compute ϵ .

1.3.1 Passive media

One of the simplest models of dielectric response one can build is the one of passive media (typically, silicon glass in visible light). In this model, we neglect absorption and dispersion to focus on the refractive property of the medium. In other terms, we neglect ϵ_I , exclude the Kramers-Kronig relations (and all frequency dependence), and allow an arbitrary choice of ϵ_R .

Although these conditions are easy to implement in the macroscopic Maxwell's equations in the Fourier domain (and then one can easily return to the temporal domain since ϵ does not depend on ω), it is interesting to see how (and under which approximations) this model is justified from the initial equations in the temporal domain.

Definition of a passive medium

The key ingredient to define a passive medium is the assumption of *instantaneous response*: after giving to the induced polarization density its general linear expression [Eq. (1.13)], we assume that the response function χ has an instantaneous effect:

$$\chi(\vec{x}, t - t') = \Lambda(\vec{x})\delta(t - t'), \quad (1.26)$$

where $\Lambda(\vec{x})$ is a (potentially inhomogeneous) function which is zero in the exterior of the medium, and $\delta(t - t')$ is the Dirac delta distribution, defined as

$$\int_{-\infty}^{\infty} dt' f(t')\delta(t - t') = f(t), \quad (1.27)$$

for any test function f . The polarization density reads

$$\vec{\mathfrak{P}}_{ind}(\vec{x}, t) = \epsilon_0 \Lambda(\vec{x}) \vec{E}(\vec{x}, t). \quad (1.28)$$

Since the fields are real, the function Λ is real as well. We introduce the dielectric coefficient as

$$\epsilon_R(\vec{x}) = 1 + \Lambda(\vec{x}), \quad (1.29)$$

where we add the index R to emphasize that ϵ is real. Because of this, the dielectric coefficient in a passive medium does not fulfill the Kramers-Kronig relations (1.25) unless $\epsilon_R = 1$.

Additionally to the instantaneous response assumption, the spontaneous polarization of the medium can be neglected in a passive medium:

$$\vec{\mathfrak{P}}_{sp} = 0. \quad (1.30)$$

A justification for this is that the spontaneous polarization emerges from the natural movement of charges inside the medium. This movement is linked to very high frequency dynamics which is well beyond the range of frequencies for which we would describe a medium as *passive* (typically, optical frequencies for glass). A more detailed discussion on this can be found in Ref. [31], Section 7.3.

Maxwell's equations in a passive medium

In order to simplify the study, we consider that there is no charge at the exterior of the medium, leading to

$$\vec{\mathfrak{P}}_{ext} = 0. \quad (1.31)$$

Because of this, and together with (1.28) and (1.29), Maxwell's equations (1.10) become in a passive medium:

$$\epsilon_R \partial_t \vec{E} = c^2 \nabla \times \nabla \times \vec{A}, \quad (1.32a)$$

$$\partial_t \vec{A} = -\vec{E} - \nabla U, \quad (1.32b)$$

$$\nabla \cdot \epsilon_R \vec{E} = 0, \quad (1.32c)$$

$$\vec{B} = \nabla \times \vec{A}. \quad (1.32d)$$

The wave equation of \vec{A} (1.23) can also be rewritten in the temporal domain:

$$\nabla \times \nabla \times \vec{A} + \frac{1}{c^2} \epsilon_R \partial_t^2 \vec{A} = -\frac{1}{c^2} \epsilon_R \partial_t \nabla U. \quad (1.33)$$

Generalized Coulomb gauge

In order to solve the wave equation (1.33) (or the equivalent for the electric or magnetic field), and hence obtain an expression for the electromagnetic waves that can propagate in the medium described by ϵ_R , one needs to know the scalar potential U . However the potentials are not unique. Indeed, for any function $f(\vec{x}, t)$, the potentials

$$\vec{A}' = \vec{A} + \nabla f, \quad (1.34a)$$

$$U' = U - \partial_t f, \quad (1.34b)$$

lead to the same fields \vec{E} and \vec{B} . The transformation from (\vec{A}, U) to (\vec{A}', U') is called a *gauge transformation*. For an arbitrary pair (\vec{A}, U) , one can choose a function f which simplifies the wave equation.

A very standard choice of gauge in vacuum is the *Coulomb gauge* (also called *transverse gauge*), where f is chosen in Eq. (1.34) in such a way that the new vector potential \vec{A}_C is transverse and the scalar potential is zero, i.e.,

$$\nabla \cdot \vec{A}_C = 0, \quad U_C = 0. \quad (1.35)$$

Remark: This gauge is particularly convenient in vacuum, where $\epsilon_R = 1$. In this situation, the polarization density is zero, which implies that the electric field is also transverse [see Maxwell's equation (1.10c)]. The right-hand side of the wave equation (1.33) vanishes and we obtain a much simpler wave equation:

$$\nabla \times \nabla \times \vec{A} + \frac{1}{c^2} \partial_t^2 \vec{A} = 0. \quad (1.36)$$

Since $\nabla \cdot \vec{A} = 0$ and $\Delta = (\nabla \nabla \cdot) - (\nabla \times \nabla \times)$ is the Laplacian operator, the wave equation in vacuum can be written equivalently

$$c^2 \Delta \vec{A} = \partial_t^2 \vec{A}. \quad (1.37)$$

Plane waves are solutions of this equation, and any other solution can be written as a linear combination of these plane waves.³

Despite its usefulness in vacuum, the Coulomb gauge is not compatible with Maxwell's equations in a inhomogeneous passive dielectric. Indeed, Eqs. (1.32b) and (1.32c) imply $\rho/\epsilon_0 = \nabla \cdot \epsilon_R \vec{E} = \nabla \epsilon_R \cdot \vec{E} + \epsilon_R \nabla \cdot \vec{E}$, and thus

$$\partial_t \nabla \cdot \vec{A} = -\nabla \cdot \vec{E} = \frac{\nabla \epsilon_R}{\epsilon_R} \cdot \vec{E} - \frac{\rho}{\epsilon_0 \epsilon_R} \neq 0, \quad (1.38)$$

which would contradict $\nabla \cdot \vec{A} = 0$. In the case of the macroscopic Maxwell equations with a non unit dielectric permittivity ϵ_R , it is more convenient to use a *generalized Coulomb gauge*, which consists in finding a gauge transformation f such that

$$\nabla \cdot [\epsilon_R \vec{A}_{GC}] = 0, \quad U_{GC} = 0, \quad (1.39)$$

which greatly simplifies the wave equations (1.33) into:

$$\nabla \times \nabla \times \vec{A}_{GC} + \frac{1}{c^2} \epsilon_R \partial_t^2 \vec{A}_{GC} = 0. \quad (1.40)$$

Note that since ϵ_R may depend on the position \vec{x} , we have in general $\nabla \cdot [\epsilon_R \vec{A}_{GC}] = \epsilon_R \nabla \cdot \vec{A} + \nabla \epsilon_R \cdot \vec{A}$. In an infinite and homogeneous medium, $\nabla \epsilon_R(\vec{x}) = 0$ for all \vec{x} and the generalized Coulomb gauge is equivalent to the usual Coulomb gauge for \vec{A} . In a homogeneous but finite medium however, $\nabla \epsilon_R(\vec{x})$ is not zero at the boundary, thus the two gauges are not equivalent.

Note also, that since we need $\nabla U = 0$, we could define other equivalent gauges with U constant but different from zero.

1.3.2 Drude model

The Drude model is a simple classical model which is particularly adapted to describe the electric response of metals. It is based on the equation of motion for an electron at position \vec{x} under the action of an electric field $\vec{E}(t)$ subjected to a dissipative force proportional to the velocity:

$$\partial_t^2 \vec{x} = -\gamma \partial_t \vec{x} + \frac{e}{m} \vec{E}(t), \quad (1.41)$$

³In fact, since plane waves expand infinitely far in space, they have infinite energy. They cannot be considered physical, they are used as mathematical tools to describe more realistic radiation, such as pulses.

where e is the elementary charge, m is the mass of the electron, and γ is the damping coefficient. After relaxation of the initial condition, this equation has the following solution,

$$\vec{x}(t) = \int_0^\infty dt'' \frac{1}{\gamma} (1 - e^{-\gamma t''}) \frac{e}{m} \vec{E}(t - t''). \quad (1.42)$$

Proof: The equation of motion (1.41) can be written as a system for the pair of variables (\vec{v}, \vec{x}) , with $\vec{v} = \partial_t \vec{x}$:

$$\partial_t \begin{bmatrix} \vec{v} \\ \vec{x} \end{bmatrix} = M \begin{bmatrix} \vec{v} \\ \vec{x} \end{bmatrix} + \begin{bmatrix} \frac{e}{m} \vec{E}(t) \\ 0 \end{bmatrix}, \quad (1.43)$$

with

$$M := \begin{bmatrix} -\gamma & 0 \\ 1 & 0 \end{bmatrix}. \quad (1.44)$$

We define the propagator

$$\begin{aligned} U(t) &:= e^{Mt} & (1.45) \\ &= \sum_{n=0}^{\infty} \frac{t^n M^n}{n!} \\ &= \mathbb{1} + \frac{1}{\gamma} (1 - e^{-\gamma t}) M \\ &= \begin{bmatrix} e^{-\gamma t} & 0 \\ \frac{1}{\gamma} (1 - e^{-\gamma t}) & 1 \end{bmatrix}, & (1.46) \end{aligned}$$

where we have used the fact that for $n \geq 1$, $M^n = (-\gamma)^{n-1} M$. The general solution can be written as

$$\begin{bmatrix} \vec{v}(t) \\ \vec{x}(t) \end{bmatrix} = U(t - t_i) \begin{bmatrix} \vec{v}_i \\ \vec{x}_i \end{bmatrix} + \int_{t_i}^t dt' U(t - t') \begin{bmatrix} \frac{e}{m} \vec{E}(t') \\ 0 \end{bmatrix}, \quad (1.47)$$

with \vec{x}_i and \vec{v}_i the position and velocity at the initial time t_i . The expression (1.46) gives

$$\vec{v}(t) = e^{-\gamma(t-t_i)} \vec{v}_i + \int_{t_i}^t dt' e^{-\gamma(t-t')} \frac{e}{m} \vec{E}(t'), \quad (1.48)$$

$$\vec{x}(t) = \frac{1}{\gamma} (1 - e^{-\gamma(t-t_i)}) \vec{v}_i + \vec{x}_i + \int_{t_i}^t dt' \frac{1}{\gamma} (1 - e^{-\gamma(t-t')}) \frac{e}{m} \vec{E}(t'). \quad (1.49)$$

If we choose the initial time $t_i = -\infty$ this expression becomes

$$\vec{v}(t) = \int_{-\infty}^t dt' e^{-\gamma(t-t')} \frac{e}{m} \vec{E}(t'), \quad (1.50)$$

$$\vec{x}(t) = \vec{x}_i + \int_{-\infty}^t dt' \frac{1}{\gamma} (1 - e^{-\gamma(t-t')}) \frac{e}{m} \vec{E}(t'). \quad (1.51)$$

Relaxing the initial condition and making the change of variable $t'' = t - t'$, we obtain Eq. (1.42).

From this we can deduce the dipole moment of the electron, defined as $\vec{d} = -q\vec{x}$ with $q = -e$

the charge:

$$\vec{d} = \int_0^\infty dt'' \frac{1}{\gamma} (1 - e^{-\gamma t''}) \frac{e^2}{m} \vec{E}(t - t''). \quad (1.52)$$

The induced polarization density of an ensemble of such electrons can be written

$$\vec{\mathfrak{P}}_{\text{ind}} = \mathcal{N} \vec{d}, \quad (1.53)$$

with \mathcal{N} the averaged number of electrons per volume unit. But since

$$\vec{\mathfrak{P}}_{\text{ind}}(t) = \epsilon_0 \int_{-\infty}^\infty dt' \chi(t - t') \vec{E}(t'), \quad (1.54)$$

we can identify

$$\chi(t) = \frac{\omega_p^2}{\gamma} (1 - e^{-\gamma t}) \Theta(t), \quad \text{with } \omega_p^2 = \frac{\mathcal{N} e^2}{m \epsilon_0}, \quad (1.55)$$

where $\Theta(t)$ is the Heaviside function, and ω_p is called the *plasma frequency*. Taking the Fourier transform gives

$$\tilde{\chi}(\omega) = \frac{\omega_p^2}{\gamma} \left(\tilde{\Theta}(\omega) - \frac{i}{\omega + i\gamma} \right). \quad (1.56)$$

$\tilde{\Theta}(\omega)$ is the Fourier transform of the Heaviside function, which can be written

$$\tilde{\Theta}(\omega) = \frac{i}{\omega + i0^+} = i\mathcal{P} \frac{1}{\omega} + \pi\delta(\omega), \quad (1.57)$$

where $\frac{1}{\omega + i0^+}$ denotes the distribution defined by the limit

$$\lim_{\varepsilon \rightarrow 0^+} \frac{1}{\omega + i\varepsilon}.$$

It can be shown that (1.56) can be written in an equivalent way as

$$\tilde{\chi}(\omega) = -\frac{\omega_p^2}{(\omega + i0^+)(\omega + i\gamma)}. \quad (1.58)$$

Remark: Since the Fourier transform $\tilde{\chi}(\omega)$ of the susceptibility of the Drude model is a distribution and does not go to zero for $t \rightarrow \infty$, it satisfies the Kramers-Kronig relation (1.17) in the sense of distribution only.

We can finally write the dielectric permittivity as

$$\epsilon(\omega) = 1 + \tilde{\chi}(\omega) = 1 - \frac{\omega_p^2}{(\omega + i0^+)(\omega + i\gamma)}. \quad (1.59)$$

1.3.3 Lorentz model

The Lorentz model consists in assuming that the electrons are somewhat attached to the (relatively) fixed nuclei. Hence their equation of motion is the same as Eq. (1.41), but with an additional restoring force $\vec{F} = -\omega_0^2 \vec{x}$:

$$\partial_t^2 \vec{x} = -\omega_0^2 \vec{x} - \gamma \partial_t \vec{x} + \frac{e}{m} \vec{E}(t). \quad (1.60)$$

In the same way as above, one can show that the corresponding (Fourier transformed) susceptibility is

$$\tilde{\chi}(\omega) = -\frac{\omega_p^2}{-\omega_0^2 + \omega(\omega + i\gamma)}, \quad (1.61)$$

which satisfies the standard Kramers-Kronig relations. We can also express the dielectric permittivity:

$$\epsilon(\omega) = 1 + \tilde{\chi}(\omega) = 1 - \frac{\omega_p^2}{-\omega_0^2 + \omega(\omega + i\gamma)}. \quad (1.62)$$

The Lorentz model is considered to be well-adapted to dielectrics, but less to metals.

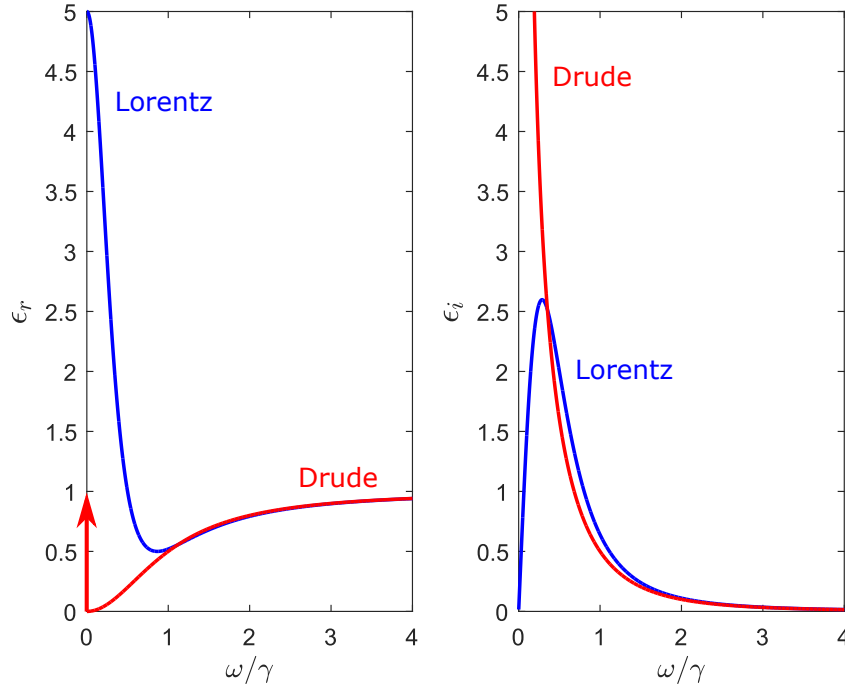


Figure 1.2 – Real and imaginary parts of the dielectric permittivity calculated with the Drude model (blue) and the Lorentz model (red). The arrow represents the delta distribution in the Drude model. The permittivity is in units of ω_p^2/γ^2 and we chose $\omega_0/\gamma = 0.5$ in the Lorentz model.

1.3.4 Drude-Lorentz model

The Drude-Lorentz model is a combination of the Drude and the Lorentz models. It is based on the hypothesis that there are some charges that are free and some that stay bounded

close to the nuclei or to impurities or to defects. Both contribute to the susceptibility. This model can allow for several binding constants $\omega_{0,j}^2$ for different charges, leading to a susceptibility of the form

$$\tilde{\chi}(\omega) = -\frac{(\omega_p^D)^2}{(\omega + i0^+)(\omega + i\gamma)} - \sum_j \frac{(\omega_{p,j}^L)^2}{-\omega_{0,j}^2 + \omega(\omega + i\gamma)}, \quad (1.63)$$

where

$$(\omega_p^D)^2 = \mathcal{N}_{\text{free}} \frac{e^2}{m}, \quad (1.64)$$

$$(\omega_p^L)^2 = \mathcal{N}_{\text{bound},j} \frac{e^2}{m}, \quad (1.65)$$

and $\mathcal{N}_{\text{free}}$ is the density of free charges, and $\mathcal{N}_{\text{bound},j}$ is the density of bound charges for each of the binding constant $\omega_{0,j}^2$. In this model, we assume that all charges have the same damping coefficient γ . The Drude-Lorentz model can be applied to describe both metals and dielectrics by different choices of the parameters.

1.4 Summary on classical electromagnetism

In this chapter we have introduced the main equations and constructions used to describe classical light propagating in linear media. In particular, from the macroscopic Maxwell equations, we have shown how to define explicitly the (causal) response of both passive media and Kramers-Kronig media. This is mostly based on assuming a certain expression of the induced polarization density $\vec{\mathfrak{P}}_{\text{ind}}$. The quantum theories of light we construct in this thesis fundamentally rely on these classical descriptions.

Finally we have described some of the main models used to calculate the susceptibility of dissipative and dispersive media. This will give an empirical basis for the quantum model of plasmons built in Chapters 5, 6 and 7.

Part I
Photons

Canonical optics

Although electromagnetic fields can interact with either passive or dispersive and dissipative media, the quantum states in passive media are usually the ones we refer to as photons, and the name plasmons is reserved for quantum electromagnetic radiations in dissipative environments such as metals. In this Chapter, we are interested in optics and thus we will consider passive media, either the vacuum or a passive dielectric.

In order to introduce the concept of photons, we could simply assess that photons are theoretically described by creation-annihilation operators acting on a Fock space, whose accessible quantum states have symmetric properties. Such a brief introduction would suffice for many studies in quantum optics and quantum information in which one only needs to manipulate the bosonic n -photon states. However, we wish to enter in more details in the construction of the theory. For this purpose, in this Chapter we follow the first step of the strategy described in the introduction: we construct in Section 2.1 a Hamiltonian structure we may call canonical optics. Then in Section 2.2 we analyze more deeply this structure, in particular we define the concept of modes and electromagnetic configurations, which are key elements in the quantization procedure.

This Chapter (and the next) is partially an adaptation of the approach of Refs. [16, 17].

Contents

2.1 Hamiltonian structure	32
2.1.1 Starting equations	32
2.1.2 Hamiltonian function	32
2.2 Electromagnetic configurations	34
2.2.1 Phase space and complex representation	34
2.2.2 Modes and eigenconfigurations	36
2.2.3 Normal mode decomposition	38
2.2.4 Spectral structure (in vacuum)	39
2.3 Summary on the classical Hamiltonian system	41

2.1 Hamiltonian structure

2.1.1 Starting equations

We first recall some of the main equations of classical electromagnetism in passive media introduced in Chapter 1 (this subsection is a very abridged version of Sec. 1.3.1). The macroscopic Maxwell equations written with the potentials are

$$\partial_t \vec{E} = c^2 \nabla \times \nabla \times \vec{A} - \frac{1}{\epsilon_0} \partial_t \vec{\mathfrak{P}}, \quad (2.1a)$$

$$\partial_t \vec{A} = -\vec{E} - \nabla U, \quad (2.1b)$$

$$\nabla \cdot \vec{E} = -\frac{1}{\epsilon_0} \nabla \cdot \vec{\mathfrak{P}}, \quad (2.1c)$$

$$\vec{B} = \nabla \times \vec{A}. \quad (2.1d)$$

We make the approximation of passive media introduced in Section 1.3.1: We write the instantaneous response approximation $\chi(\vec{x}, t - t') = \Lambda(\vec{x})\delta(t - t')$ and we have the (real) dielectric coefficient $\epsilon_R(\vec{x}) = 1 + \Lambda(\vec{x})$. Furthermore, we neglect the spontaneous polarization of the medium. Hence, the polarization density reads

$$\vec{\mathfrak{P}} = \vec{\mathfrak{P}}_{ind} = \epsilon_0(\epsilon_R - 1)\vec{E}, \quad (2.2)$$

and Eq. (2.1a) becomes

$$\partial_t \vec{E} = \frac{c^2}{\epsilon_R} \nabla \times \nabla \times \vec{A}. \quad (2.3)$$

We insert Eq. (2.1b) into (2.3):

$$\partial_t^2 \vec{A} = -\frac{c^2}{\epsilon_R} \nabla \times \nabla \times \vec{A} - \partial_t \nabla U. \quad (2.4)$$

We now impose the generalized Coulomb gauge (1.39), and we obtain

$$\partial_t^2 \vec{A} = -\frac{c^2}{\epsilon_R} \nabla \times \nabla \times \vec{A}, \quad (2.5a)$$

$$\text{with } \nabla \cdot [\epsilon_R \vec{A}] = 0, \quad U = 0. \quad (2.5b)$$

This is the wave equation in the time domain for \vec{A} in a passive medium and the conditions on \vec{A} and U in the generalized Coulomb gauge. We also have $\nabla \cdot [\epsilon_R \vec{E}] = 0$.

2.1.2 Hamiltonian function

Once we have described classical electromagnetism in a passive medium (see Section 1.3.1 for more details), our first step to prepare for the quantization is to find a Hamiltonian system equivalent to the Maxwell equations. In the classical domain, the Hamilton function should correspond to the classical energy of electromagnetic radiations one can measure in experiments. The current subsection is dedicated to finding a Hamiltonian from the Maxwell equations (more specifically from the wave equation of the vector potential) and

to verify that it gives the classical energy of light. Our approach is essentially equivalent to the one first proposed by Glauber and Lewenstein in Ref. [16], and developed further in Ref. [17].

For a reason that will become clear below, it is convenient to make the following change of variable:

$$\vec{A}' = \sqrt{\epsilon_0 \epsilon_R} \vec{A}, \quad (2.6)$$

so that the wave equation (2.5a) reads

$$\partial_t^2 \vec{A}' = -\frac{c}{\sqrt{\epsilon_R}} \nabla \times \nabla \times \left[\frac{c}{\sqrt{\epsilon_R}} \vec{A}' \right]. \quad (2.7)$$

We can therefore write

$$\partial_t^2 \vec{A}' = -\Omega^2 \vec{A}', \quad (2.8)$$

with Ω the *frequency operator* defined as

$$\Omega^2 := \frac{c}{\sqrt{\epsilon_R}} \nabla \times \nabla \times \frac{c}{\sqrt{\epsilon_R}}. \quad (2.9)$$

Since the (real) frequency operator can be written as $\Omega^2 = \Xi^\dagger \Xi$, with $\Xi^\dagger = \frac{c}{\sqrt{\epsilon_R}} \nabla \times$, it is symmetric: $(\Omega^2)^T = \Omega^2$. This is the reason for the change of variable (2.6).

The wave equation (2.8) is a second order differential equation in time. It can be split into two coupled first order equations as

$$\partial_t \vec{A}' = \vec{\Pi}', \quad (2.10a)$$

$$\partial_t \vec{\Pi}' = -\Omega^2 \vec{A}', \quad (2.10b)$$

where we have introduced a new vector $\vec{\Pi}'$ (we add a prime for the sake of symmetry with \vec{A}'), which can be directly related to the electric field using Eq. (2.1b) with the change of variable (2.6):

$$\partial_t \vec{A}' = -\sqrt{\epsilon_0 \epsilon_R} \vec{E}, \quad (2.11)$$

implying

$$\vec{\Pi}' = -\sqrt{\epsilon_0 \epsilon_R} \vec{E}. \quad (2.12)$$

We can now introduce the Hamiltonian of the system, at first without including the transversality constraints:

$$H = \frac{1}{2} \int d^3x [\vec{\Pi}' \cdot \vec{\Pi}' + \vec{A}' \cdot \Omega^2 \vec{A}']. \quad (2.13)$$

\vec{A}' and $\vec{\Pi}'$ are the *canonically conjugate variables* (or simply *canonical variables*) of this Hamiltonian system. They satisfy the Hamilton equations:

$$\partial_t \vec{\Pi}' = -\frac{\delta H}{\delta \vec{A}'}, \quad \partial_t \vec{A}' = \frac{\delta H}{\delta \vec{\Pi}'} \quad (2.14a)$$

which one can verify to be equivalent to the wave equation (2.10). Replacing the canonical variables in Eq. (2.13) by their expression in terms of the fields and using $\epsilon_0\mu_0c^2 = 1$, we obtain

$$H = \frac{1}{2} \int d^3x \left[\epsilon_0 \epsilon_R \vec{E} \cdot \vec{E} + \frac{1}{\mu_0} \vec{B} \cdot \vec{B} \right], \quad (2.15)$$

which is the usual expression of the energy of the classical radiation generated by (\vec{E}, \vec{B}) in a passive medium. This is consistent with the interpretation of the Hamiltonian as the energy of the system in the classical domain. We show in Appendix A that this interpretation can be justified from Maxwell's equations by expressing the transfer of energy from external charges to the electromagnetic field.

In order to take into account the transversality constraints, we first show that Eqs. (2.10) imply that if the initial conditions satisfy the constraints, then they are preserved by the time evolution. This follows from

$$\vec{\Pi}'(t + \delta t) = \vec{\Pi}'(t) - \delta t \Omega^2 \vec{A}'(t), \quad (2.16)$$

$$\vec{A}'(t + \delta t) = \vec{A}'(t) + \delta t \vec{\Pi}'(t), \quad (2.17)$$

and the fact that

$$\begin{aligned} \nabla \cdot [\sqrt{\epsilon_R} \Omega^2 \vec{A}'(t)] &= \nabla \cdot \left[\sqrt{\epsilon_R} \left(\frac{1}{\sqrt{\epsilon_R}} \nabla \times \nabla \times \right) \frac{1}{\sqrt{\epsilon_R}} \vec{A}'(t) \right] \\ &= \nabla \cdot \left[(\nabla \times \nabla \times) \frac{1}{\sqrt{\epsilon_R}} \vec{A}'(t) \right] = 0. \end{aligned}$$

Thus, one can take the Hamiltonian (2.13) restricted to the subspace defined by the constraints.

Note that we must ensure a finite energy of the system, i.e., we impose:

$$\int d^3x \vec{\Pi}' \cdot \vec{\Pi}' < \infty, \quad \int d^3x \vec{A}' \cdot \Omega^2 \vec{A}' < \infty. \quad (2.18)$$

We introduce the (identical) spaces where the canonical variables live:

$$\mathcal{E}[\vec{A}'] = \left\{ \vec{A}'(\vec{x}) \in L_2(\mathbb{R}^3 \rightarrow \mathbb{R}^3, d^3x) \mid \nabla \cdot [\sqrt{\epsilon_R} \vec{A}'] = 0 \right\}, \quad (2.19)$$

$$\mathcal{E}[\vec{\Pi}'] = \left\{ \vec{\Pi}'(\vec{x}) \in L_2(\mathbb{R}^3 \rightarrow \mathbb{R}^3, d^3x) \mid \nabla \cdot [\sqrt{\epsilon_R} \vec{\Pi}'] = 0 \right\}, \quad (2.20)$$

with a generalized Coulomb gauge due to the presence of the passive medium.

2.2 Electromagnetic configurations

2.2.1 Phase space and complex representation

An important tool in Hamiltonian systems is to describe a configuration of the system as a point in a phase space generated by the canonical variables. We build a real phase space

which contains all electromagnetic fields with finite energy:

$$\mathcal{P}_{\mathbb{R}}[\vec{A}', \vec{\Pi}'] = \left\{ (\vec{A}'(\vec{x}), \vec{\Pi}'(\vec{x})) \mid \int d^3x (\vec{\Pi}' \cdot \vec{\Pi}' + \vec{A}' \cdot \Omega^2 \vec{A}') < \infty, \right. \\ \left. \nabla \cdot [\sqrt{\epsilon_R} \vec{A}'] = 0, \nabla \cdot [\sqrt{\epsilon_R} \vec{\Pi}'] = 0 \right\}. \quad (2.21)$$

An electromagnetic field described by a pair $(\vec{A}', \vec{\Pi}')$ in the phase space $\mathcal{P}_{\mathbb{R}}[\vec{A}', \vec{\Pi}']$ will be called a $(\vec{A}', \vec{\Pi}')$ -*configuration*.

For reasons that will become clear later, we introduce a complex representation of this phase space, where the information of the fields \vec{A} and $\vec{\Pi}$ is combined into the complex vector field $\vec{\Psi}(\vec{x})$, defined as

$$\vec{\Psi} = \frac{1}{\sqrt{2}} (\Omega^{1/2} \vec{A}' + i\Omega^{-1/2} \vec{\Pi}'). \quad (2.22)$$

The new phase space of $\vec{\Psi}$ -configurations, $\mathcal{P}_{\mathbb{C}, \Omega}[\vec{\Psi}]$, now depends on the operator Ω (and hence, on the geometry of the medium through ϵ_R). Note that the complex phase space has the structure of a Hilbert space, since we define a scalar product:

$$\vec{\Psi} \cdot \vec{\Psi}' := \int d^3x \sum_j \Psi_j^*(\vec{x}) \Psi'_j(\vec{x}). \quad (2.23)$$

From Eq. (2.22) it is not immediate to see how the divergence constraint is expressed in terms of $\vec{\Psi}$ in a given gauge, since we do not know the effect of the operators $\Omega^{\pm 1/2}$ on the transversality of the fields. We will show in Section 2.2.3 how it can be constructed.

Remark: One can show that the operator Ω^2 given in Eq. (2.9) has no kernel on the subspace of functions \vec{v} verifying the generalized Coulomb constraint $\nabla \cdot [\epsilon_R \vec{v}] = 0$. Furthermore it is hermitian with real positive spectrum:

$$\Omega^2 \vec{\varphi}_{\lambda, d^\lambda} = \lambda^2 \vec{\varphi}_{\lambda, d^\lambda}, \quad (2.24)$$

with d^λ a possible index of degeneracy. Therefore, in the constrained subspace, any power of Ω is well-defined and we can write

$$\Omega^a \vec{\varphi}_{\lambda, d^\lambda} = \lambda^a \vec{\varphi}_{\lambda, d^\lambda}, \quad (2.25)$$

with $\lambda > 0$, for any real number a . Hence, the vector (2.22) is well defined.

In terms of the complex vector, the Maxwell equations take the form

$$i\partial_t \vec{\Psi} = \Omega \vec{\Psi}. \quad (2.26)$$

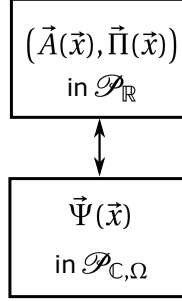
This can be shown easily by expressing \vec{A}' and $\vec{\Pi}'$ in terms of $\vec{\Psi}$ by inverting Eq. (2.22), inserting them into Eqs. (2.10a) and (2.10b) and summing up the two resulting equations.

We remark that Eq. (2.26) has the form of a Schrödinger equation. The Hamiltonian (2.13) can be written with the complex vectors as

$$H = \frac{1}{2} \int d^3x [\vec{\Psi}^* \cdot \Omega \vec{\Psi} + \vec{\Psi} \cdot \Omega \vec{\Psi}^*]. \quad (2.27)$$

Because of the structure of these equations which is reminiscent of harmonic oscillators, one can already presuppose a link between the complex vector $\vec{\Psi}$ and creation-annihilation operators. This link will be made clear in the quantization process.

In summary, the real electromagnetic $(\vec{A}', \vec{\Pi}')$ -configurations can be represented equivalently as complex $\vec{\Psi}$ -configurations.



2.2.2 Modes and eigenconfigurations

An important concept to understand classical light is the concept of *modes*. We define it in this subsection.

Starting in the real phase space defined by Eq. (2.21), an initial condition $(\vec{\Pi}'(\vec{x}, t_0), \vec{A}'(\vec{x}, t_0))$ at an (arbitrarily chosen) initial time t_0 determines uniquely the time evolution given by $(\vec{\Pi}'(\vec{x}, t), \vec{A}'(\vec{x}, t))$. In the complex representation, the initial condition $\vec{\Psi}(\vec{x}, t_0)$ determines uniquely the trajectory $\vec{\Psi}(\vec{x}, t)$.

Since the Maxwell equations are linear, if we multiply an initial $\vec{\Psi}$ -configuration, $\vec{\Psi}(t_0)$, by an arbitrary constant $\alpha \in \mathbb{C}$, its time evolution will also be simply multiplied by α .

Definition: In the complex representation, a *classical mode* (on the electromagnetic configuration $\vec{\Psi}$) is a one dimensional subspace of configurations

$$\mathcal{M}_{\vec{\Psi}} = \{ \alpha \vec{\Psi}(\vec{x}), \alpha \in \mathbb{C} \}. \quad (2.28)$$

In other terms, a solution $\vec{\Psi}$ of the Maxwell equation (2.26) at a time t , and the same solution multiplied by a complex constant α , correspond to the same mode.

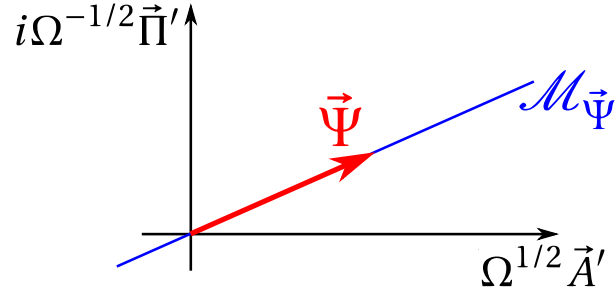
In the real representation, the mode corresponds to a 2-dimensional subspace

$$\mathcal{M}_{(\vec{\Pi}', \vec{A}')} = \left\{ c \begin{bmatrix} \vec{\Pi}' \\ \vec{A}' \end{bmatrix} + s \begin{bmatrix} \Omega \vec{A}' \\ -\Omega^{-1} \vec{\Pi}' \end{bmatrix}, (c, s) \in \mathbb{R}^2 \right\}, \quad (2.29)$$

where $\alpha = c + is$.

We can draw two remarks from this definition:

- To a $(\vec{A}', \vec{\Pi}')$ -configuration, one can associate a unique mode $\mathcal{M}_{(\vec{\Pi}', \vec{A}')}$;
- However, the mode also contains infinitely many other possible configurations.



In the phase space of $\vec{\Psi}$ -configurations, an electromagnetic configuration is a vector, and the associated mode is the line generated by this vector.

An interesting consequence of this construction is the following. One can theoretically construct a *purely electric* configuration ($\vec{\Pi}', \vec{A}' = \vec{0}$). The corresponding mode is

$$\mathcal{M}_{(\vec{\Pi}', \vec{0})} = \left\{ c \begin{bmatrix} \vec{\Pi}' \\ \vec{0} \end{bmatrix} + s \begin{bmatrix} \vec{0} \\ -\Omega^{-1}\vec{\Pi}' \end{bmatrix} = \begin{bmatrix} c\vec{\Pi}' \\ -s\Omega^{-1}\vec{\Pi}' \end{bmatrix}, (c, s) \in \mathbb{R}^2 \right\}. \quad (2.30)$$

This shows that a mode always contains configurations that have both an electric and a magnetic field. There are no purely electric nor purely magnetic modes, even though one can construct a configuration as such at a certain time t . This plays an important role for the quantized electromagnetic field and the nature of photons. We will see that there is a one-to-one correspondence between one photon states and classical modes. As a consequence we will be able to state that there are no “electric photons” nor “magnetic photons”.

In the quantization of the electromagnetic field we will use normalized vectors defined as follows:

Definition: A *normalized $\vec{\Psi}$ -configuration* is defined by an initial condition $\vec{\Psi}$ such that

$$\int d^3x |\vec{\Psi}|^2 = 1, \quad (2.31)$$

or equivalently in the real representation.

Furthermore, we introduce the concept of normal modes, which will be of prime importance in the next subsection.

Definition: A *normal mode* is a mode whose electromagnetic configurations are eigenvectors of the frequency operator Ω , with a certain eigenvalue ω :

$$\Omega\vec{\Psi} = \omega\vec{\Psi}, \quad (2.32)$$

or equivalently,

$$\begin{cases} \Omega\vec{\Pi}' = \omega\vec{\Pi}', \\ \Omega\vec{A}' = \omega\vec{A}'. \end{cases} \quad (2.33)$$

We remark that if $\vec{\Psi}$ belongs to a normal mode $\mathcal{M}_{\vec{\Psi}}$, then all vectors $\alpha\vec{\Psi}$ of the same mode are also eigenvectors of Ω with the same eigenvalue. It is very common to use the term *normal mode* to refer to an arbitrary (or eventually normalized) vector $\vec{\Psi}$ of the mode $\mathcal{M}_{\vec{\Psi}}$. In order not to confuse the two,

a vector $\vec{\Psi}$ of a normal mode will be referred to as an *eigenconfiguration*.

We remark that since Ω is positive, Eqs. (2.32) and (2.33) are equivalent to

$$\Omega^2 \vec{\Psi} = \omega^2 \vec{\Psi} \quad (2.34)$$

and

$$\begin{cases} \Omega^2 \vec{\Pi}' = \omega^2 \vec{\Pi}', \\ \Omega^2 \vec{A}' = \omega^2 \vec{A}'. \end{cases} \quad (2.35)$$

2.2.3 Normal mode decomposition

The Hamiltonian (2.13) [or equivalently (2.27)] cannot be quantized straightforwardly since its canonical variables must satisfy the divergence constraints:

$$\nabla \cdot [\sqrt{\epsilon_R} \vec{A}'] = 0, \quad \nabla \cdot [\sqrt{\epsilon_R} \vec{\Pi}'] = 0. \quad (2.36)$$

Such constraints imply a redundancy of variables, in other terms one of the components of the fields is dependent on the two others. This is not desirable for applying a principle of correspondence since it presupposes that the new quantum variables are all independent. The key idea to remove this constraint from the canonical variables is to expand them on an orthonormal basis of real vectors $\{\vec{\varphi}_\kappa\}$ satisfying the constraint:

$$\begin{cases} \vec{A}'(\vec{x}) = \int d\kappa q_\kappa \vec{\varphi}_\kappa(\vec{x}) \\ \vec{\Pi}'(\vec{x}) = \int d\kappa p_\kappa \vec{\varphi}_\kappa(\vec{x}) \end{cases}, \quad \nabla \cdot [\sqrt{\epsilon_R} \vec{\varphi}_\kappa] = 0, \quad (2.37)$$

with some scalar coefficients q_κ and p_κ . The notation κ is implicit and contains both frequencies and degeneracy indices. The orthonormality condition reads

$$\int d^3x \vec{\varphi}_\kappa(\vec{x}) \cdot \vec{\varphi}_{\kappa'}(\vec{x}) = \delta(\kappa - \kappa'). \quad (2.38)$$

We show in Appendix B that this transformation $(\vec{A}', \vec{\Pi}') \mapsto (q, p)$ is canonical, i.e., it preserves the Hamiltonian structure of the model. The new variables live in a phase space $\mathcal{P}_\ell = \ell_2 \oplus \ell_2$, with $\ell_2(\mathcal{J}) = \{(q_1, q_2, \dots) \mid \sum_{\kappa \in \mathcal{J}} |q_\kappa|^2 < \infty\}$.

Note that we can invert Eq. (2.37) to obtain:

$$q_\kappa = \int d^3x \vec{\varphi}_\kappa(\vec{x}) \cdot \vec{A}'(\vec{x}), \quad (2.39a)$$

$$p_\kappa = \int d^3x \vec{\varphi}_\kappa(\vec{x}) \cdot \vec{\Pi}'(\vec{x}). \quad (2.39b)$$

What contains κ precisely (i.e., its degeneracy structure) will be investigated in detail in the next subsection. So far, we simply consider that it contains a continuous spectrum of frequencies ω_κ and possibly degeneracy indices, either continuous or discrete, leading either to extra integrals or sums in the equations.

The basis $\{\vec{\varphi}_\kappa\}$ is chosen so that its vectors $\vec{\varphi}_\kappa$ are real generalized eigenfunctions of the frequency operator Ω :

$$\Omega \vec{\varphi}_\kappa(\vec{x}) = \omega_\kappa \vec{\varphi}_\kappa(\vec{x}), \quad \omega_\kappa > 0, \quad (2.40)$$

in other terms, the expansion is made on a basis of eigenconfigurations as described in Section 2.2.2. We can now go to the complex representation by introducing the expansions (2.37) into the complex vector (2.22). We obtain, using (2.40),

$$\vec{\Psi}(\vec{x}) = \int d\kappa z_\kappa \vec{\varphi}_\kappa(\vec{x}), \quad (2.41)$$

where

$$z_\kappa = \frac{1}{\sqrt{2}} [\omega_\kappa^{1/2} q_\kappa + i\omega_\kappa^{-1/2} p_\kappa]. \quad (2.42)$$

Since the constraint of \vec{A}' and $\vec{\Pi}'$ is translated to the vectors of the basis ($\nabla \cdot [\sqrt{\epsilon_R} \vec{\varphi}_\kappa(\vec{x})] = 0$), the coefficients q , p and z in the expansions (2.37) and (2.41) are *free of constraint*. This also implies the divergence constraint on all $\vec{\Psi}$ -configurations:

$$\nabla \cdot [\sqrt{\epsilon_R} \vec{\Psi}] = 0. \quad (2.43)$$

The Hamiltonian can now be written as

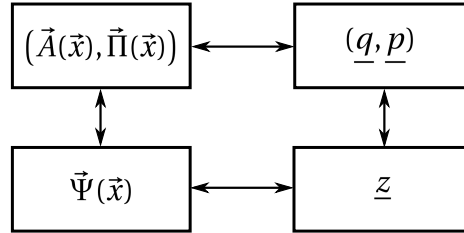
$$H = \frac{1}{2} \int d\kappa [p_\kappa^2 + \omega_\kappa^2 q_\kappa^2], \quad (2.44)$$

or

$$H = \frac{1}{2} \int d\kappa \omega_\kappa [z_\kappa^* z_\kappa + z_\kappa z_\kappa^*]. \quad (2.45)$$

We can therefore use the functions q_κ and p_κ as new canonical variables of the Hamiltonian system. The passage $(\vec{A}', \vec{\Pi}') \mapsto (q, p)$ [where we use the underline notation as $\underline{q} = (q_1, q_2, \dots)$] is a *canonical transformation*, a concept that will be developed in more detail in Chapter 3 and that is crucial for the quantization process.

We can now describe all electromagnetic configurations as $(\underline{q}, \underline{p})$ -configurations or equivalently as \underline{z} -configurations.



2.2.4 Spectral structure (in vacuum)

The spectral structure (i.e., the distribution of frequencies and the degeneracy) of the Hamiltonian system in study is given by the one of the eigenconfigurations of the operator Ω . What is contained in the implicit label κ depends on the necessity for these eigenconfigurations to verify the completeness condition:

$$\int d\kappa \vec{\varphi}_\kappa(\vec{x}) \cdot \vec{\varphi}_\kappa(\vec{x}') = \delta^{\perp, \sqrt{\epsilon_R}}(\vec{x} - \vec{x}'), \quad (2.46)$$

where $\delta^{\perp, \sqrt{\epsilon_R}}(\vec{x} - \vec{x}')$ is the transverse delta function modified by the dielectric coefficient:

Definition: for any test function f which can be decomposed into $g + h$, where $\nabla \cdot [\sqrt{\epsilon_R}g] = 0$ and $\nabla \times [\sqrt{\epsilon_R}h] = 0$, we have

$$\int d^3x' f(\vec{x}') \delta^{\perp, \sqrt{\epsilon_R}}(\vec{x} - \vec{x}') = g(\vec{x}). \quad (2.47)$$

Since the frequency operator depends on the dielectric coefficient ϵ_R , the eigenconfigurations vary for each particular medium in consideration, and therefore the spectral structure may change as well. In this section we describe the structure of Ω^2 in vacuum ($\epsilon_R = 1$).

In a very general way, we can describe the label κ as the combination of a frequency ω that may span over the whole spectrum, and an index of degeneracy. In free electromagnetism, the spectrum spans from 0 to $+\infty$. Moreover, the degeneracy consists of:

- A continuous index spanning the possible directions of the wave vector \vec{k} (with $|\vec{k}| = \omega/c$);
- An index σ corresponding to the polarization of the eigenfunction, dependent on the polarization basis that has been chosen (typically vertical/horizontal or circular left/right).

A widely used choice of eigenconfigurations of $\Omega^2 = -c^2\Delta$ is plane waves. It is often used as a complex basis:

$$\vec{\varphi}_{\vec{k}, \sigma}(\vec{x}) = \vec{\epsilon}_\sigma(\vec{k}) e^{i\vec{k} \cdot \vec{x}}, \quad (2.48)$$

with $\vec{\epsilon}_\sigma(\vec{k})$ two unit vectors (one for each polarization) orthogonal to \vec{k} and to each other. In the real basis, the equivalent waves are

$$\vec{\varphi}_{\vec{k}, \sigma, \zeta}(\vec{x}) = \begin{cases} \frac{1}{2\pi^{3/2}} \vec{\epsilon}_\sigma(\vec{k}) \cos(\vec{k} \cdot \vec{x}), & \zeta = c, \\ \frac{1}{2\pi^{3/2}} \vec{\epsilon}_\sigma(\vec{k}) \sin(\vec{k} \cdot \vec{x}), & \zeta = s, \end{cases} \quad (2.49)$$

where we needed to add a degeneracy index of parity ζ in order to recover the full structure of the plane waves (where the direction of \vec{k} generates either propagating or counter-propagating waves).

In vacuum the eigenconfigurations (2.49) satisfy the Coulomb gauge, $\nabla \cdot \vec{\varphi}_{\vec{k}, \sigma, \zeta}(\vec{x}) = 0$, and they form a complete basis of $\Omega^2 = c^2 \nabla \times \nabla \times$ restricted to the transverse subspace (where we can identify $\nabla \times \nabla \times = -\Delta$).

Remark: When using the complex basis in vacuum, the expansions of the fields (2.37) are very similar to Fourier transforms, where the frequency plays the role of the Fourier variable and the new canonical variables (q, p) are the Fourier coefficients. Although it seems easier to manipulate the Fourier transform than the real basis (2.49), one must keep in mind that it can be used so straightforwardly only because plane waves are eigenfunctions of the frequency operator in vacuum. In an inhomogeneous passive medium, however, plane waves are no longer eigenconfigurations and one cannot use the standard Fourier transform to expand the fields.

The structure of the spectrum and its degeneracy can be written $\kappa = (\omega, d^\omega)$ as it is usual with degenerate harmonic oscillators. However, this notation is rarely appropriate for the

electromagnetic field, since the integral over all degrees of freedom has a complicated expression:

$$\int d\kappa \equiv \frac{1}{c^3} \int_0^\infty d\omega \omega^2 \int_0^{\pi/2} d\vartheta \sin \vartheta \int_0^{2\pi} d\varphi \sum_{\sigma, \zeta}, \quad (2.50)$$

with (ϑ, φ) the angles in spherical coordinates. This is obtained from the projection onto spherical coordinates of the wave vector \vec{k} , using $|\vec{k}| = \omega/c$. It is in general more practical to use the notation $\kappa = \vec{k}, \sigma, \zeta$, since (2.50) reduces to

$$\int d\kappa \equiv \int d\vec{k} \sum_{\sigma, \zeta}. \quad (2.51)$$

This exhibits the inherent complicated degeneracy structure of the electromagnetic field, a complexity necessary to take into account all geometrical properties of light waves.

As mentioned above, the degeneracy structure of the frequency operator in a passive dielectric depends on the geometry of the medium. In the special cases studied in Chapter 4, this structure is the same as in vacuum and the passive medium modifies the configurations by simply adding extra coefficients of reflection on and transmission through the medium.

In Chapter 5 where we consider dissipative and dispersive media, however, the question of the degeneracy structure of the model will be crucial.

2.3 Summary on the classical Hamiltonian system

In this Chapter we have seen that the Maxwell equations in a passive medium (i.e., with no dispersion nor dissipation, or equivalently, with an instantaneous electric response) can be reformulated as Hamilton equations with a Hamiltonian function corresponding to the classical energy of radiation:

$$H = \frac{1}{2} \int d^3x [\vec{\Pi}' \cdot \vec{\Pi}' + \vec{A}' \cdot \Omega^2 \vec{A}']. \quad (2.52)$$

This has been shown with a particular choice of canonical variables which can be directly related to the magnetic vector potential and the electric field – a choice of variables that is not unique.

The spectral and degeneracy structure of the system has been discussed with an explicit description for the case of vacuum. The precise analysis of the spectral structure in the case of an inhomogeneous passive medium can be performed provided that one can determine the eigenfunctions of the operator Ω^2 (referred to as eigenconfigurations).

We have used these eigenconfigurations (equivalent to the plane waves in vacuum) to perform a change of basis where we can use new canonical variables $(\underline{q}, \underline{p})$ which are not constrained by any transversality condition. We have also introduced a complex representation:

$$(\vec{A}', \vec{\Pi}') \mapsto (\vec{\Psi}, \vec{\Psi}^*), \quad (2.53)$$

$$(\underline{q}, \underline{p}) \mapsto (\underline{z}, \underline{z}^*), \quad (2.54)$$

that will be useful in the quantization procedure. The Hamiltonian can finally be written both in the real or in the complex representation as

$$H = \frac{1}{2} \int d\kappa [p_\kappa^2 + \omega^2 q_\kappa^2], \quad (2.55a)$$

$$= \frac{1}{2} \int d\kappa \omega [z_\kappa^* z_\kappa + z_\kappa z_\kappa^*]. \quad (2.55b)$$

We now have all the ingredients to quantize the model.

Quantum optics

The goal of this Chapter is to quantize the Hamiltonian model developed in Chapter 2. The quantization cannot be performed too naively because of dimension issues that we describe in Section 3.4. We start by quantizing a reduced model equivalent to an ensemble of uncoupled harmonic oscillators, and we use this construction to justify the passage from the reduced model to the full model (which corresponds to a limit from finite degrees of freedom to infinite degrees of freedom).

In Section 3.1 we write explicitly the quantization procedure based on a principle of correspondence. In Section 3.2 we construct a Fock space of photon states and express the fields and Hamiltonian as operators acting on this space. We use Section 3.3 as a brief summary of the different spaces of photon states in the reduced model. In Section 3.4 we show how to extend the theory from the reduced model to the full model of infinite dimensions.

Before and after the quantization process, there are several changes of variables and many changes of space performed. All these changes have their own pertinence which we describe along the way. In order to have a clearer vision of where each mathematical object fits in the general procedure, we summarize these relations in Figure 3.2 at the end of this section.

This Chapter is an adaptation of the approach of Refs. [16, 17] with the general procedure of quantization of linear fields described in [13–15].

Contents

3.1	Quantization procedure in a reduced model	44
3.1.1	Principle of correspondence	44
3.1.2	General configurations	45
3.1.3	Ground states	46
3.1.4	Ladder space	46
3.2	Photons	47
3.2.1	Bosonic Fock space	47
3.2.2	Creation-annihilation operators	48
3.2.3	Number operator	49
3.2.4	Hilbert spaces of classical electromagnetic configurations	49
3.2.5	Electromagnetic field operators and Hamiltonian	51
3.2.6	The quantum field operator	52

3.3 Summary on the spaces	53
3.4 The key to the full model	54
3.4.1 The infinite Fock space	54
3.4.2 The different roles of operators in quantum optics	55
3.4.3 Remarks on the physical status of the reduced model	56
3.5 Summary on the quantum model	56

3.1 Quantization procedure in a reduced model

A rough procedure of quantization is to reinterpret the variables of the model as operators (usually exhibited in the notation by the passage from x to \hat{x}). However, to do so in a rigorous way, one needs to specify the Hilbert space on which the operators are going to act (note that there are various possible choices for the Hilbert space). To prepare the quantization of the full model of Chapter 2, we first describe the quantization of a *reduced* model.

The reduced model is a model where the fields are expanded on a reduced N -dimensional basis of eigenconfigurations, with $N < \infty$. Thus all integrals over κ in Sections 2.2.3, 2.2.4 and 2.3 become sums of N elements. This reduced model can be justified if the electromagnetic field is confined in a perfect cavity (which discretizes the frequencies of the modes) and by imposing an ultraviolet cutoff (otherwise the basis would still be infinite). The formulation of the quantization we use is based on Refs. [13–15] and on [32].

3.1.1 Principle of correspondence

In such a reduced model with a Hamiltonian function

$$H = \frac{1}{2} \sum_{\kappa=1}^N [p_{\kappa}^2 + \omega^2 q_{\kappa}^2], \quad (3.1)$$

the standard choice of Hilbert space is the space of real square-integrable functions of the variable q : $L_2(\mathbb{R}^N, d^N q)$, where $q = (q_1, q_2, \dots)$. We can apply a general correspondence principle for the canonical variables q_{κ}, p_{κ} :

$$q_{\kappa} \mapsto \hat{q}_{\kappa} := \text{multiplication by } q_{\kappa}, \quad p_{\kappa} \mapsto \hat{p}_{\kappa} := -i\hbar \frac{\partial}{\partial q_{\kappa}}, \quad (3.2)$$

with \hbar the reduced Planck constant, and \hat{q}_{κ} and \hat{p}_{κ} are two operators acting on the Hilbert space. We have automatically the commutation relations:

$$[\hat{q}_{\kappa}, \hat{p}_{\kappa'}] = i\hbar \delta_{\kappa\kappa'}, \quad [\hat{q}_{\kappa}, \hat{q}_{\kappa'}] = [\hat{p}_{\kappa}, \hat{p}_{\kappa'}] = 0. \quad (3.3)$$

To the Hamiltonian function (3.1) corresponds the operator

$$\hat{H} = \frac{1}{2} \sum_{\kappa=1}^N [\hat{p}_{\kappa}^2 + \omega^2 \hat{q}_{\kappa}^2], \quad (3.4)$$

which is the usual Hamiltonian of a set of N uncoupled *quantum* harmonic oscillators, where \hat{q}_{κ} is the position operator of the κ -th oscillator and \hat{p}_{κ} is its momentum operator. One can also use the equivalent correspondence principle with the complex coordinates:

$$z_{\kappa} \mapsto \sqrt{\hbar} \hat{a}_{\kappa}, \quad z_{\kappa}^* \mapsto \sqrt{\hbar} \hat{a}_{\kappa}^{\dagger}, \quad (3.5)$$

with

$$\hat{a}_\kappa = \frac{1}{\sqrt{2\hbar}} (\omega_\kappa^{1/2} \hat{q}_\kappa + i\omega_\kappa^{-1/2} \hat{p}_\kappa), \quad (3.6)$$

and

$$[\hat{a}_\kappa, \hat{a}_{\kappa'}^\dagger] = \delta_{\kappa\kappa'}, \quad [\hat{a}_\kappa, \hat{a}_{\kappa'}] = 0. \quad (3.7)$$

The Hamiltonian becomes

$$\hat{H} = \sum_{\kappa=1}^N \frac{\hbar\omega_\kappa}{2} [\hat{a}_\kappa^\dagger \hat{a}_\kappa + \hat{a}_\kappa \hat{a}_\kappa^\dagger]. \quad (3.8)$$

The operators \hat{a}_κ and \hat{a}_κ^\dagger are called annihilation and creation operators, respectively.

3.1.2 General configurations

The passage from the classical complex configurations of the fields z_κ and the creation-annihilation operators $(\hat{a}_\kappa, \hat{a}_\kappa^\dagger)$ is a quantization of an individual oscillator (typically, the one labeled by κ). However, there exist more general configurations where several oscillators are in motion simultaneously. We note such configurations $\underline{z} = (z_1, \dots, z_N) \in \mathbb{C}^N$, where each component z_κ given by Eq. (2.42) corresponds to a certain configuration of the κ -th oscillator.

We can then define creation-annihilation operators $(\hat{b}_{\underline{z}}, \hat{b}_{\underline{z}}^\dagger)$ associated with the superposition \underline{z} . They are connected with the single-oscillator operators by

$$\hat{b}_{\underline{z}} = \underline{z}^* \cdot \hat{\underline{a}}, \quad (3.9a)$$

$$\hat{b}_{\underline{z}}^\dagger = \underline{z} \cdot \hat{\underline{a}}^\dagger, \quad (3.9b)$$

with $\hat{\underline{a}} = (\hat{a}_1, \dots, \hat{a}_N)$. The scalar product here corresponds to a summation over the components κ . We can identify the special case:

$$\hat{b}_{\underline{e}_\kappa} \equiv \hat{a}_\kappa, \quad (3.10)$$

where $\underline{e}_\kappa = (0, \dots, 1, \dots, 0)$ is a configuration where only one oscillator is excited. We represent in Figure 3.1 the two types of configurations: one moving oscillator, and a collection of oscillations.

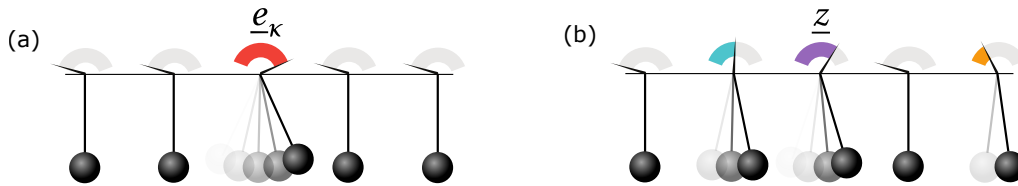


Figure 3.1 – Representation of the two types of excitations that can be generated by the creation-annihilation operators in the reduced model: (a) only one oscillator of normal frequency ω_κ is excited by $\hat{b}_{\underline{e}_\kappa}^\dagger$, (b) a collection of oscillators (of different normal frequency or different degenerate index) are excited by $\hat{b}_{\underline{z}}^\dagger$, giving rise to a superposition characterized by the components z_κ .

The superposition implies that the commutator of the creation-annihilation operators depends on the associated configuration:

$$[\hat{b}_{\underline{z}}, \hat{b}_{\underline{z}'}^\dagger] = \underline{z}^* \cdot \underline{z}'. \quad (3.11)$$

3.1.3 Ground states

A first important use of the creation-annihilation operators is in the determination of the ground states of the oscillators. We denote them $\phi_{g,\kappa}(\underline{q})$. Each ground state is defined by

$$\hat{a}_\kappa \phi_{g,\kappa}(q_\kappa) = 0. \quad (3.12)$$

We can calculate it for each κ using the expression of \hat{a}_κ (3.6):

$$\frac{1}{\sqrt{2\hbar}} (\omega_\kappa^{1/2} \hat{q}_\kappa + i\omega_\kappa^{-1/2} \hat{p}_\kappa) \phi_{g,\kappa}(q_\kappa) = 0, \quad (3.13)$$

and inserting the definition of the operators \hat{q}_κ and \hat{p}_κ [Eq. (3.2)]:

$$\frac{\partial}{\partial q_\kappa} \phi_{g,\kappa}(q_\kappa) = -\frac{\omega_\kappa q_\kappa}{\hbar} \phi_{g,\kappa}(q_\kappa). \quad (3.14)$$

The normalized solution of this equation reads

$$\phi_{g,\kappa}(q_\kappa) = \left(\frac{\omega_\kappa}{\pi\hbar}\right)^{\frac{1}{4}} e^{-\frac{\omega_\kappa q_\kappa^2}{2\hbar}}, \quad (3.15)$$

which is a Gaussian function of the position variable q_κ .

3.1.4 Ladder space

The ground state of each individual oscillator is given by Eq. (3.15). In order to have a clearer view on the number of quantum excitations attached to a given state, we use a different representation of the Hilbert space $L_2(\mathbb{R}^N, d^N \underline{q})$, which we call a ‘‘ladder space’’, denoted by \mathcal{L} .

In order to define \mathcal{L} , we call ϕ_g the ground state of the whole system of N oscillators, which contains the knowledge of the ground states of all individual oscillators:

$$\phi_g = \otimes_{\kappa=1}^N \phi_{g,\kappa}, \quad (3.16)$$

with $\phi_{g,\kappa}$ given by Eq. (3.15), and \otimes denoting the tensor product. From this, the ladder space \mathcal{L} is defined by

$$\mathcal{L} := \oplus_{n=0}^{\infty} \mathcal{L}_n, \quad (3.17)$$

where \oplus denotes the direct sum, and the subspaces \mathcal{L}_n are

$$\begin{aligned} \mathcal{L}_0 &:= \left\{ \phi_0 \in \mathcal{L} \mid \phi_0 = c\phi_g, \quad c \in \mathbb{C} \right\}, \\ \mathcal{L}_1 &:= \left\{ \phi_1 \in \mathcal{L} \mid \phi_1 = \hat{b}_{\underline{z}}^\dagger \phi_g, \quad \underline{z} \in \mathbb{C}^N \right\}, \\ \mathcal{L}_2 &:= \left\{ \phi_2 \in \mathcal{L} \mid \phi_2 = \hat{b}_{\underline{z}_1}^\dagger \hat{b}_{\underline{z}_2}^\dagger \phi_g, \quad \underline{z}_1, \underline{z}_2 \in \mathbb{C}^N \right\}, \\ &\vdots \end{aligned} \quad (3.18)$$

\mathcal{L}_0 is the space of functions that are simply the ground state multiplied by an arbitrary complex constant, and \mathcal{L}_n is the space of functions defined by the application of n creation operators on the ground state (on possibly n different \underline{z} -configurations). Therefore, we use the creation-annihilation operators to climb up or down from one subspace of the ladder space to another.

3.2 Photons

3.2.1 Bosonic Fock space

For reasons that will be made clear in the next section, we now define an abstract bosonic Fock space \mathcal{F} by [13–15, 32–34]

$$\mathcal{F} = \oplus_{n=0}^{\infty} \mathcal{F}_n \quad (3.19)$$

(with \oplus the direct sum), built with a (suitably chosen) Hilbert space of configurations $\mathcal{H}_{\text{config}}$ as

$$\begin{aligned} \mathcal{F}_0 &:= \mathbb{C}, \\ \mathcal{F}_1 &:= \mathcal{H}_{\text{config}}, \\ \mathcal{F}_2 &:= \hat{S}_2(\mathcal{H}_{\text{config}} \otimes \mathcal{H}_{\text{config}}), \\ &\vdots \\ \mathcal{F}_n &:= \hat{S}_n(\mathcal{H}_{\text{config}} \otimes \dots \otimes \mathcal{H}_{\text{config}}), \\ &\vdots \end{aligned} \quad (3.20)$$

where we call \mathcal{F}_0 the 0-quantum space, \mathcal{F}_1 the 1-quantum space, and so on. A vector in \mathcal{F}_n is called a n -quanta *state*, and it can be written in general as a linear combination of vectors of the form

$$\hat{S}_n |\xi_1 \otimes \dots \otimes \xi_n\rangle, \quad (3.21)$$

with all ξ_j being configurations in $\mathcal{H}_{\text{config}}$. From now on, we will use the “bra-ket” notation exclusively for states in a Fock space.

The operator \hat{S}_n is a projector onto symmetric states, constructed with the permutations of the 1-quantum states. It can be formally defined by

$$\hat{S}_n := \frac{1}{n!} \sum_{\text{perm.}} \quad \text{and} \quad \hat{S}_0 := \mathbb{1}. \quad (3.22)$$

For instance

$$\hat{S}_2 |\xi \otimes \xi'\rangle = \frac{1}{2} [|\xi \otimes \xi'\rangle + |\xi' \otimes \xi\rangle]. \quad (3.23)$$

The resulting state is said to be *symmetric* or *bosonic*.

Remark: For states in \mathcal{F}_2 , we adopt the standard notation $|\xi \otimes_s \xi'\rangle \equiv \hat{S}_2 |\xi \otimes \xi'\rangle$, with \otimes_s called the *symmetrized tensor product* defined by

$$\xi \otimes_s \xi' := \frac{1}{2} (\xi \otimes \xi' + \xi' \otimes \xi) \equiv \hat{S}_2 (\xi \otimes \xi'). \quad (3.24)$$

This notation is widely used in the literature even for high subspaces ($n > 2$), but it is more difficult to define unambiguously the associative property of many symmetrized tensor products, whereas the definition (3.22) of the operators \hat{S}_j is very clear.

The Fock space \mathcal{F} is called *bosonic* because its n -quanta states (i.e., the vectors of \mathcal{F}_n) with $n > 1$ are linear combinations of symmetric tensor products of n states of \mathcal{F}_1 . This symmetry is a signature of bosonic states.

This construction of the bosonic Fock space is abstract. In order to relate it to a physical model, one needs to specify which space of configurations $\mathcal{H}_{\text{config}}$ the Fock space is built with. This will be investigated more closely later on.

3.2.2 Creation-annihilation operators

In the Fock space \mathcal{F} defined in the preceding section, we can define creation-annihilation operators for any configuration $\xi \in \mathcal{H}_{\text{config}}$, as operators that allow one to go up or down on the series of Fock subspaces (one can already foretell a link with the ladder space \mathcal{L}):

$$\hat{B}_\xi : \mathcal{F}_n \mapsto \mathcal{F}_{n-1}, \quad (3.25)$$

$$\hat{B}_\xi^\dagger : \mathcal{F}_n \mapsto \mathcal{F}_{n+1}, \quad (3.26)$$

and verifying the bosonic commutation relations

$$[\hat{B}_\xi, \hat{B}_{\xi'}^\dagger] = (\xi \cdot \xi') \mathbb{1}, \quad [\hat{B}_\xi, \hat{B}_{\xi'}] = 0. \quad (3.27)$$

Note that the definition of the scalar product $\xi \cdot \xi'$ depends on the representation of the electromagnetic configurations, i.e., on the Hilbert space $\mathcal{H}_{\text{config}}$ that has been chosen.

The 0-quantum state (i.e., ground state) is written $|\emptyset\rangle \in \mathcal{F}_0$ and verifies

$$\hat{B}_\xi |\emptyset\rangle = 0, \quad \forall \xi \in \mathcal{H}_{\text{config}}. \quad (3.28)$$

We denote $|\xi\rangle$ any 1-quantum state associated with the classical configuration ξ . It is generated by applying the corresponding creation operator on the ground state:

$$|\xi\rangle = \hat{B}_\xi^\dagger |\emptyset\rangle. \quad (3.29)$$

Multi-quanta states can be generally defined by the application of several creation operators and the introduction of the number of excitations in each configuration. The general application rules of the operators on n -quanta states ($n > 0$) read

$$\hat{B}_\xi^\dagger |\xi_1 \otimes \dots \otimes \xi_n\rangle = \sqrt{n+1} \hat{S}_{n+1} |\xi \otimes \xi_1 \otimes \dots \otimes \xi_n\rangle, \quad (3.30)$$

$$\hat{B}_\xi |\xi_1 \otimes \dots \otimes \xi_n\rangle = \frac{1}{\sqrt{n}} \sum_{j=1}^n (\xi \cdot \xi_j) \hat{S}_{n-1} |\xi_1 \otimes \dots \otimes \check{\xi}_j \otimes \dots \otimes \xi_n\rangle, \quad (3.31)$$

where the notation $\check{\xi}_j$ indicates that this term is missing.

Remark: The creation-annihilation operators act first by symmetrizing the state (with the application of \hat{S}). Thus if the state on which we apply \hat{B} or \hat{B}^\dagger is already symmetric, \hat{S} has no effect. Another way of looking at it is: $\hat{B}_\xi \hat{S} = \hat{B}_\xi$, which comes naturally from the fact that $\hat{S}^2 = \hat{S}$ (i.e., \hat{S} is a projector).

Examples: the creation and annihilation of quanta on configuration ξ , applied on the 0-quantum state or on arbitrary 1-quantum and 2-quanta states give:

$$\hat{B}_\xi^\dagger |\emptyset\rangle = |\xi\rangle$$

$$\hat{B}_\xi |\emptyset\rangle = 0$$

$$\hat{B}_\xi^\dagger |\xi_1\rangle = \frac{\sqrt{2}}{2} [|\xi \otimes \xi_1\rangle + |\xi_1 \otimes \xi\rangle]$$

$$\hat{B}_\xi |\xi_1\rangle = (\xi \cdot \xi_1) |\emptyset\rangle$$

$$\begin{aligned} \hat{B}_\xi^\dagger |\xi_1 \otimes \xi_2\rangle &= \frac{\sqrt{3}}{3!} [|\xi \otimes \xi_1 \otimes \xi_2\rangle + |\xi \otimes \xi_2 \otimes \xi_1\rangle \\ &\quad + |\xi_1 \otimes \xi \otimes \xi_2\rangle + |\xi_2 \otimes \xi \otimes \xi_1\rangle \\ &\quad + |\xi_1 \otimes \xi_2 \otimes \xi\rangle + |\xi_2 \otimes \xi_1 \otimes \xi\rangle] \end{aligned}$$

$$\hat{B}_\xi |\xi_1 \otimes \xi_2\rangle = \frac{1}{\sqrt{2}} [(\xi \cdot \xi_1) |\xi_2\rangle + (\xi \cdot \xi_2) |\xi_1\rangle]$$

In particular, we have the usual expression for the annihilation in a single harmonic oscillator with normalized configurations ($\xi \cdot \xi = 1$):

$$\hat{B}_\xi |\xi \otimes_s \xi\rangle = \sqrt{2} |\xi\rangle. \quad (3.32)$$

The creation-annihilation operators furthermore satisfy the following properties:

$$\hat{B}_{\xi_1 + \xi_2}^\dagger = \hat{B}_{\xi_1}^\dagger + \hat{B}_{\xi_2}^\dagger, \quad \hat{B}_{c\xi}^\dagger = c \hat{B}_\xi^\dagger \quad \text{for } c \in \mathbb{C}, \quad (3.33a)$$

$$\hat{B}_{\xi_1 + \xi_2} = \hat{B}_{\xi_1} + \hat{B}_{\xi_2}, \quad \hat{B}_{c\xi} = c^* \hat{B}_\xi \quad \text{for } c \in \mathbb{C}. \quad (3.33b)$$

3.2.3 Number operator

A central idea when speaking of quantum light is the possibility to *count* individual photons. This is already encompassed in the splitting of the ladder space and the Fock space into countable subspaces, one for each number of quanta, but there is a practical mathematical object which is appreciated to address this matter: the *number operator* \hat{N} . The definition is very straightforward:

Consider an arbitrary state $|\Phi\rangle$ in the Fock space \mathcal{F} . Since \mathcal{F} is an infinite direct sum of the subspaces \mathcal{F}_j , $|\Phi\rangle$ can be written as an array of states:

$$|\Phi\rangle = (|\phi_0\rangle, |\phi_1\rangle, |\phi_2\rangle, |\phi_3\rangle, \dots), \quad (3.34)$$

with $|\phi_n\rangle \in \mathcal{F}_n$. The number operator is the operator that attaches the corresponding number of quanta to each state in $|\Phi\rangle$:

$$\hat{N}|\Phi\rangle := (0, 1|\phi_1\rangle, 2|\phi_2\rangle, 3|\phi_3\rangle, \dots). \quad (3.35)$$

It is usually directly applied to an n -quanta state of \mathcal{F}_n :

$$\text{if } |\phi_n\rangle \in \mathcal{F}_n, \quad \text{then } \hat{N}|\phi_n\rangle = n|\phi_n\rangle. \quad (3.36)$$

This implies that **all n -quanta states are eigenvectors of the number operator.**

Remark: It can be shown that the definition of the bosonic creation-annihilation operators implies that for any orthonormal basis of eigenconfigurations $\{\vec{\varphi}_\kappa\}$,

$$\hat{N} = \sum_\kappa \hat{B}_{\vec{\varphi}_\kappa}^\dagger B_{\vec{\varphi}_\kappa}. \quad (3.37)$$

This is also a usual way of defining the number operator, but the definition (3.35) emphasizes that the number operator can be used and interpreted independently of the creation-annihilation operators.

3.2.4 Hilbert spaces of classical electromagnetic configurations

As mentioned earlier, the Hilbert space of configurations $\xi \in \mathcal{H}_{\text{config}}$ tells us to which physical model the Fock space can be related (mechanical oscillators, light...). We now describe what possible Hilbert spaces can be chosen to give to the states in \mathcal{F} the interpretation of *photon states*.

One can recall from our construction (see e.g. the scheme at the end of Section 2.2.3) that we have several equivalent choices for the Hilbert space of electromagnetic configurations: we can choose the real space of $(\vec{A}', \vec{\Pi}')$ -configurations, the complex space of $\vec{\Psi}$ -configurations, the real space of $(\underline{q}, \underline{p})$ -configurations, or the complex space of \underline{z} -configurations. One can see this flexibility as equivalent to the choice of dealing with Fourier representations instead of the initial fields in classical optics.

Let us start with the latter because it has a straightforward relation to the functions of the ladder space: we choose $\mathcal{H}_{\text{config}} \equiv \{\underline{z} \in \mathbb{C}^N\}$ and the configurations are $\xi \equiv \underline{z}$. This Fock space can be shown [13–15] to be isomorphic to the ladder space \mathcal{L} . We have the one-to-one correspondence:

$$\begin{aligned}\mathcal{L} &\leftrightarrow \mathcal{F}(\mathbb{C}^N), \\ \hat{b}_{\underline{z}} &\leftrightarrow \hat{B}_{\underline{z}}, \\ \phi_0 &\leftrightarrow |\emptyset\rangle, \\ \phi_n &\leftrightarrow \hat{S}_n |\underline{z}_1 \otimes \dots \otimes \underline{z}_n\rangle.\end{aligned}\tag{3.38}$$

Remark: This isomorphism is valid only if the Fock space is bosonic, i.e., if we have imposed the symmetry of the many-quanta states ($n > 1$). This is as a key argument to justify the bosonic nature of the quanta of the system.

The quantum states of the Fock space $\mathcal{F}(\mathbb{C}^N)$ are always associated to classical electromagnetic configurations (here of the \underline{z} -type). For instance, the 1-quantum state $|\underline{z} = \underline{e}_\kappa\rangle$ is the quantum state corresponding to an excitation on the κ -th oscillator, and all others in their ground state. Any state $|\underline{z}\rangle$ is in general a superposition of such states:

$$|\underline{z}\rangle = \sum_{\kappa=1}^N c_\kappa |\underline{e}_\kappa\rangle.\tag{3.39}$$

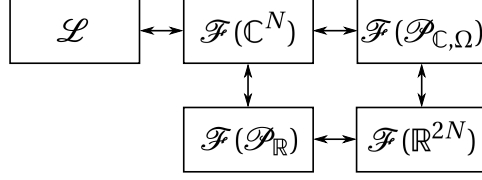
One can also choose to associate the quantum states with $\vec{\Psi}$ -configurations instead of \underline{z} -configurations. Since in the next section we focus on a description of photons and properties of *locality*, we will base our study on the space of $\vec{\Psi}$ -configurations. The isomorphism between the two spaces of configurations implies the isomorphism between the Fock spaces:

$$\begin{aligned}\mathcal{F}(\mathbb{C}^N) &\leftrightarrow \mathcal{F}(\mathcal{P}_{\mathbb{C},\Omega}), \\ \hat{B}_{\underline{z}} &\leftrightarrow \hat{B}_{\vec{\Psi}}, \\ |\underline{z}\rangle &\leftrightarrow |\vec{\Psi}\rangle.\end{aligned}\tag{3.40}$$

In the same way as for $\hat{B}_{\underline{e}_\kappa}$, we have in $\mathcal{F}(\mathcal{P}_{\mathbb{C},\Omega})$ the special case of single-oscillator excitations $\hat{B}_{\vec{\varphi}_\kappa}$ where $\vec{\varphi}_\kappa(\vec{x})$ are eigenconfigurations (i.e., eigenfunctions of Ω , plane waves in the vacuum case). In general, we identify the expansion (2.41) in the Fock space:

$$|\vec{\Psi}\rangle = \sum_{\kappa=1}^N z_\kappa |\vec{\varphi}_\kappa\rangle.\tag{3.41}$$

We do not explicitly describe the quantum states in the two other possible Fock spaces, but one can refer to the following scheme to follow the isomorphism chain of the classical phase spaces of configurations in the quantum domain.



3.2.5 Electromagnetic field operators and Hamiltonian

Now that the quantization of the reduced model is constructed in the framework of a bosonic Fock space, we can invert the transformations and express the electric field as an operator acting on the Fock space.

The quantum versions of the canonical variables obey the same relations as in the classical domain, i.e., from Eq. (2.37):

$$\vec{A}'(\vec{x}) = \sum_{\kappa=1}^N \vec{\varphi}_{\kappa}(\vec{x}) \hat{q}_{\kappa}, \quad (3.42a)$$

$$\vec{\Pi}'(\vec{x}) = \sum_{\kappa=1}^N \vec{\varphi}_{\kappa}(\vec{x}) \hat{p}_{\kappa}. \quad (3.42b)$$

Because of Eq. (3.6), it gives

$$\vec{A}'(\vec{x}) = \sum_{\kappa=1}^N \sqrt{\frac{\hbar}{2\omega_{\kappa}}} \vec{\varphi}_{\kappa}(\vec{x}) [\hat{a}_{\kappa} + \hat{a}_{\kappa}^{\dagger}], \quad (3.43a)$$

$$\vec{\Pi}'(\vec{x}) = -i \sum_{\kappa=1}^N \sqrt{\frac{\hbar\omega_{\kappa}}{2}} \vec{\varphi}_{\kappa}(\vec{x}) [\hat{a}_{\kappa} - \hat{a}_{\kappa}^{\dagger}]. \quad (3.43b)$$

Using the isomorphism with the Fock space $\mathcal{F}(\mathcal{P}_{\mathbb{C}, \Omega})$, we have the one-to-one correspondence $\hat{a}_{\kappa} \leftrightarrow \hat{B}_{\vec{\varphi}_{\kappa}}$, implying

$$\vec{A}'(\vec{x}) = \sum_{\kappa=1}^N \sqrt{\frac{\hbar}{2\omega_{\kappa}}} \vec{\varphi}_{\kappa}(\vec{x}) [\hat{B}_{\vec{\varphi}_{\kappa}} + \hat{B}_{\vec{\varphi}_{\kappa}}^{\dagger}], \quad (3.44a)$$

$$\vec{\Pi}'(\vec{x}) = -i \sum_{\kappa=1}^N \sqrt{\frac{\hbar\omega_{\kappa}}{2}} \vec{\varphi}_{\kappa}(\vec{x}) [\hat{B}_{\vec{\varphi}_{\kappa}} - \hat{B}_{\vec{\varphi}_{\kappa}}^{\dagger}]. \quad (3.44b)$$

Finally, using Eq. (2.12) on one side, and Eqs. (2.1d) and (2.6) on the other side, we obtain the electric and magnetic fields as operators acting on the Fock space:

$$\vec{E}(\vec{x}) = i \sum_{\kappa=1}^N \sqrt{\frac{\hbar\omega_{\kappa}}{2\epsilon_0\epsilon_R}} \vec{\varphi}_{\kappa}(\vec{x}) [\hat{B}_{\vec{\varphi}_{\kappa}} - \hat{B}_{\vec{\varphi}_{\kappa}}^{\dagger}], \quad (3.45a)$$

$$\vec{B}(\vec{x}) = \sum_{\kappa=1}^N \sqrt{\frac{\hbar\epsilon_0}{2\omega_{\kappa}}} \nabla \times (\sqrt{\epsilon_R} \vec{\varphi}_{\kappa}(\vec{x})) [\hat{B}_{\vec{\varphi}_{\kappa}} + \hat{B}_{\vec{\varphi}_{\kappa}}^{\dagger}]. \quad (3.45b)$$

Similarly, we can express the quantum Hamiltonian (3.8) in terms of the operators of the Fock space:

$$\hat{H} = \sum_{\kappa=1}^N \frac{\hbar\omega_{\kappa}}{2} [\hat{B}_{\vec{\varphi}_{\kappa}}^{\dagger} \hat{B}_{\vec{\varphi}_{\kappa}} + \hat{B}_{\vec{\varphi}_{\kappa}} \hat{B}_{\vec{\varphi}_{\kappa}}^{\dagger}]. \quad (3.46)$$

Because of the commutation relation (3.27), we can write $\hat{B}_{\vec{\varphi}_\kappa} \hat{B}_{\vec{\varphi}_\kappa}^\dagger = \hat{B}_{\vec{\varphi}_\kappa}^\dagger \hat{B}_{\vec{\varphi}_\kappa} + 1$, which gives

$$\hat{H} = \sum_{\kappa=1}^N \hbar \omega_\kappa \left[\hat{B}_{\vec{\varphi}_\kappa}^\dagger \hat{B}_{\vec{\varphi}_\kappa} + \frac{1}{2} \mathbb{1} \right]. \quad (3.47)$$

The Hamiltonian therefore contains a *zero-point energy* term $\sum_{\kappa} \hbar \omega_\kappa / 2$ (which is finite in the reduced model). Since one can add an arbitrary finite constant to the Hamiltonian without changing the dynamics, we remove this constant. This procedure is sometimes referred to as *normal ordering*, or *Wick ordering*, where the products of creation and annihilation operators are ordered in such a way that the annihilation operators are applied before the creation operators.

Thus finally, the quantized (diagonal) Hamiltonian reads

$$\hat{H} = \sum_{\kappa=1}^N \hbar \omega_\kappa \hat{B}_{\vec{\varphi}_\kappa}^\dagger \hat{B}_{\vec{\varphi}_\kappa}. \quad (3.48)$$

3.2.6 The quantum field operator

One can find useful to define a position dependent quantum operator acting on the bosonic Fock space, instead of the creation-annihilation operators introduced in Sec. 3.2.2. We thus introduce the *quantum field operator* $\vec{\Psi}(\vec{x})$,

$$\vec{\Psi}(\vec{x}) := \frac{1}{\sqrt{2\hbar}} \left(\Omega^{1/2} \vec{A}'(\vec{x}) + i\Omega^{-1/2} \vec{\Pi}'(\vec{x}) \right), \quad (3.49)$$

with Ω the frequency operator (2.9), i.e., it is the quantum equivalent of the complex field Ψ introduced in Sec. 2.2.1. Because of the expansion (2.41) and the principle of correspondence (3.5), it can also be linked to the creation-annihilation operators by

$$\vec{\Psi}(\vec{x}) = \sum_{\kappa=1}^N \vec{\varphi}_\kappa(\vec{x}) \hat{B}_{\vec{\varphi}_\kappa}, \quad (3.50)$$

with $\{\vec{\varphi}_\kappa\}$ the real basis of eigenconfigurations of Ω . Note however that the definition (3.50) holds for any basis of eigenfunctions of Ω .

As a consequence, the electromagnetic field observables can be expressed in terms of the field operator $\vec{\Psi}$,

$$\vec{E}(\vec{x}) = i \sqrt{\frac{\hbar}{2\epsilon_0 \epsilon_R}} \Omega^{1/2} \left[\vec{\Psi}(\vec{x}) - \vec{\Psi}^\dagger(\vec{x}) \right], \quad (3.51a)$$

$$\vec{B}(\vec{x}) = \sqrt{\frac{\hbar \epsilon_0}{2}} \nabla \times \left\{ \epsilon_R \Omega^{-1/2} \left[\vec{\Psi}(\vec{x}) + \vec{\Psi}^\dagger(\vec{x}) \right] \right\}, \quad (3.51b)$$

and the Hamiltonian alike,

$$\hat{H} = \hbar \int d^3x \vec{\Psi}^\dagger(\vec{x}) \Omega \cdot \vec{\Psi}(\vec{x}). \quad (3.52)$$

Furthermore, because of Eq. (3.27) and the completeness (2.46) (with discrete spectrum) of the eigenconfigurations $\vec{\varphi}_\kappa$, it is easy to see that the field operators satisfy the commutation relations

$$[\hat{\Psi}_i(\vec{x}), \hat{\Psi}_j^\dagger(\vec{x}')] = \delta_{ij}^{\perp, \sqrt{\epsilon_R}}(\vec{x} - \vec{x}'), \quad (3.53a)$$

$$[\hat{\Psi}_i(\vec{x}), \hat{\Psi}_j(\vec{x}')] = 0. \quad (3.53b)$$

For each fixed position \vec{x}_0 and each component j , one can interpret $\hat{\Psi}_j^\dagger(\vec{x}_0)$ as a photon creation operator on a mode $\vec{\xi}_{\vec{x}_0, j}(\vec{x})$. This can be seen by applying it on the vacuum Fock state,

$$\begin{aligned} |\vec{\xi}_{\vec{x}_0, j}(\vec{x})\rangle &:= \hat{\Psi}_j^\dagger(\vec{x}_0)|\emptyset\rangle = \sum_{\kappa} \varphi_{\kappa}^{j*}(\vec{x}_0) \hat{B}_{\vec{\varphi}_{\kappa}}^\dagger |\emptyset\rangle \\ &= \sum_{\kappa} \varphi_{\kappa}^{j*}(\vec{x}_0) |\vec{\varphi}_{\kappa}\rangle. \end{aligned} \quad (3.54)$$

In the representation of the one-photon Fock space by the mode functions, we have

$$\vec{\xi}_{\vec{x}_0, j}(\vec{x}) = \sum_{\kappa} \varphi_{\kappa}^{j*}(\vec{x}_0) \vec{\varphi}_{\kappa}(\vec{x}). \quad (3.55)$$

Thus, using the completeness relation (2.46), the configuration $\vec{\xi}_{\vec{x}_0, j}(\vec{x})$ reads

$$\xi_{\vec{x}_0, j}^i(\vec{x}) = \sum_{\kappa} \varphi_{\kappa}^{j*}(\vec{x}_0) \varphi_{\kappa}^i(\vec{x}) = \delta_{ij}^{\perp, \sqrt{\epsilon_R}}(\vec{x} - \vec{x}_0). \quad (3.56)$$

The components of the configuration created by the field operator are equal to the transverse delta function (modified by the dielectric permittivity, as described in Sec. 2.2.4). Since this function is a distribution, the operators $\vec{\Psi}(\vec{x})$ are *operator valued distributions*, i.e., they only yield a regular operator when integrated over a test function (see, e.g., [32] and [35] p.778). This is also the case for the electromagnetic observables since they can be written as linear combinations of $\vec{\Psi}$ and $\vec{\Psi}^\dagger$.

3.3 Summary on the spaces

The reduced model is now thoroughly described. The Hamiltonian structure of the electromagnetic field is shown to be equivalent to an ensemble of quantum harmonic oscillators. We have a well-defined way of describing any multi-quanta excitation of such ensemble, and we have a choice of space of quantum states:

- **The Hilbert space** $L_2(\mathbb{R}^N, d^N \underline{q})$, where the states $f(\underline{q})$ are functions of the position variables of the oscillators, q_κ ;
- **The ladder space** \mathcal{L} , which is another representation of $L_2(\mathbb{R}^N, d^N \underline{q})$ as a series of subspaces, where the states $\phi_n(\underline{q})$ can be labeled with the corresponding number of quantum excitations;
- **The bosonic Fock space** \mathcal{F} , which is isomorphic to \mathcal{L} , where the many-quanta ($n > 1$) states are written as symmetric tensor products of 1-quantum states. The states are associated with functions of the space chosen for the construction of the Fock space: it can be the space of ‘‘Fourier’’ configurations $\underline{z} \in \mathbb{C}^N$, but we prefer to use the space of the complex representation of the electromagnetic fields $\vec{\Psi}(\vec{x}) \in \mathcal{P}_{\mathbb{C}, \Omega}$.

Once all of it is well-defined, we can express the electric field and magnetic field observables, which act in the Fock space and can be used to calculate measurable quantities in a given passive environment.

The full construction may look exaggeratedly complicated: why use and construct \mathcal{L} and \mathcal{F} when we could study all possible configurations and quantum excitations of the system of N oscillators in $L_2(\mathbb{R}^N, d^N q)$? The reason is the following: we define \mathcal{L} so that the isomorphism to the Fock space \mathcal{F} seems more natural and straightforward. But the reason for defining a Fock space is hardly justifiable in the reduced model of N oscillators (corresponding to the electromagnetic field in a perfect cavity). However, as we shall see now, the construction of the Fock space is necessary to quantize the full model of the electromagnetic field with infinitely many degrees of freedom.

3.4 The key to the full model

3.4.1 The infinite Fock space

We have shown in the preceding section how the classical Hamiltonian system describing the electromagnetic field interacting with passive media can be reduced to a collection of N discrete oscillators, provided that we consider only fields that can be expanded on a *discrete* and *finite* basis of eigenvectors $\vec{\varphi}_\kappa(\vec{x})$ of the frequency operator Ω (which corresponds to enclosing the electromagnetic field in a perfect cavity and imposing a cutoff in high frequencies). We have then shown how to quantize such a model, and we completed the construction to the definition of a (bosonic) Fock space to describe the quantum states.

We now wish to turn back to the full model, and here an issue emerges. In the classical model, we can always turn back to a continuous (infinite) basis $\sum_\kappa \rightarrow \int d\kappa$. However, at the time of the quantization procedure, we cannot take this limit since the Hilbert space $L_2(\mathbb{R}^N, d^N q)$ is not mathematically well-defined when $N \rightarrow \infty$ (no Lebesgue measure $d^N q$ exists in that case, and without it one cannot construct a Hilbert space, see, e.g., [36]). Without this Hilbert space, the operators \hat{q} , \hat{p} , \hat{a} or \hat{b} are ill-defined, we cannot construct \mathcal{L} , and we cannot go isomorphically to a Fock space [36].

The key to solve this problem lies in the fact that the Fock space \mathcal{F} is well-defined with $N \rightarrow \infty$. One can indeed construct an abstract bosonic Fock space similar to (3.20) in that limit. This does not change the fact that one cannot revert the process and go back isomorphically to an expression of the electric and magnetic fields in terms of the bosonic operators of the Fock space. But since the isomorphism is well-defined in the cavity case, we postulate that we can impose all the relations of the reduced model in the full model, and thus we define the electric and magnetic fields as in Eq. (3.45) but with the limit $\sum_\kappa \rightarrow \int d\kappa \equiv \int d\vec{k} \sum_{\sigma,\zeta}$ and $\omega_\kappa \rightarrow \omega$:

$$\vec{\tilde{E}}(\vec{x}) = i \int d\vec{k} \sum_{\sigma,\zeta} \sqrt{\frac{\hbar\omega}{2\epsilon_0\epsilon_R}} \vec{\varphi}_{\vec{k},\sigma,\zeta}(\vec{x}) \left[\hat{B}_{\vec{\varphi}_{\vec{k},\sigma,\zeta}} - \hat{B}_{\vec{\varphi}_{\vec{k},\sigma,\zeta}}^\dagger \right], \quad (3.57a)$$

$$\vec{\tilde{B}}(\vec{x}) = \int d\vec{k} \sum_{\sigma,\zeta} \sqrt{\frac{\hbar\epsilon_0}{2\omega}} \nabla \times \left(\sqrt{\epsilon_R} \vec{\varphi}_{\vec{k},\sigma,\zeta}(\vec{x}) \right) \left[\hat{B}_{\vec{\varphi}_{\vec{k},\sigma,\zeta}} + \hat{B}_{\vec{\varphi}_{\vec{k},\sigma,\zeta}}^\dagger \right]. \quad (3.57b)$$

Similarly, the diagonal Hamiltonian of the full model reads

$$\hat{H} = \int d\vec{k} \sum_{\sigma, \zeta} \hbar \omega \hat{B}_{\vec{k}, \sigma, \zeta}^\dagger \hat{B}_{\vec{k}, \sigma, \zeta}. \quad (3.58)$$

We note that the Hamiltonian is defined in the Fock space with the Wick ordering (since the constant in Eq. (3.47) would become infinite when the limit of infinite dimensions is taken).

We emphasize that there is no argument which would entirely solve the problem of the limit $N \rightarrow \infty$. The key we describe here, i.e., to define a Fock space with $N \rightarrow \infty$ and to postulate that the relations of the reduced model are preserved, is an *ad hoc* assumption justified by the existence of all isomorphisms in the reduced model.

We show in Figure 3.2 a scheme of all changes of variables and all isomorphisms used in the construction.

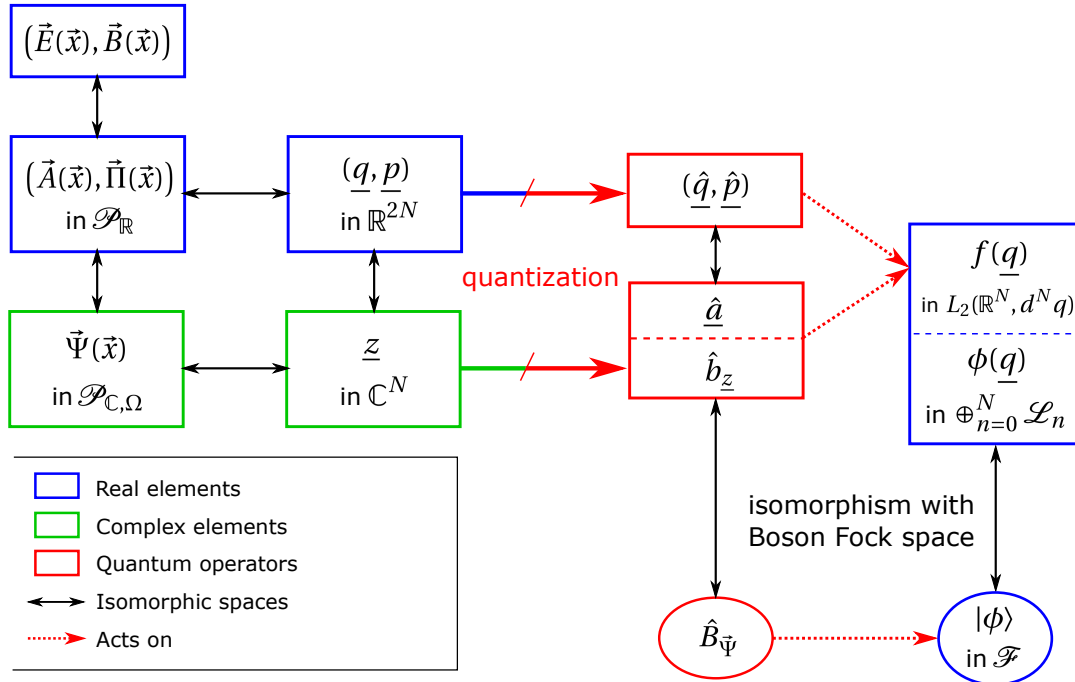


Figure 3.2 – Scheme of all changes of variables (and corresponding spaces) used in the quantization of electromagnetic radiations in a passive medium (i.e., with real, non-dispersive dielectric permittivity).

3.4.2 The different roles of operators in quantum optics

There are four different roles played by the various operators which have been introduced in this Chapter. In order to understand the conceptual implications of the quantum theory, it is important to keep in mind what these different roles are.

(i) The first type are operators representing observables, i.e., quantities that can be measured by a particular device. For each type of measuring instrument one has to construct appropriate operators that represent its function. Since instruments are in general quite complicated objects, one aims to construct simple model operators that codify at least the essential aspects of the function of the device. The electromagnetic field operators such as \vec{E} or \vec{B} are of this type.

(ii) The Hamiltonian operator \hat{H} plays a dual role: it corresponds to the total energy observable, and it is also the generator of the time evolution of the system through the Schrödinger equation. As the generator of the dynamics, it is not associated to a particular measuring instrument.

(iii) The creation and annihilation operators are defined in order to construct the different states in Fock space. They are also used as the basic building blocks to construct the representation of the observables in Fock space. In fact one can argue that the only way one can define operators in Fock space is by combining creation and annihilation operators and projectors of states $|\Phi\rangle\langle\Phi|$.

(iv) The field operator $\vec{\Psi}(\vec{x})$ introduced in Sec. 3.2.6 plays a similar role as the creation-annihilation operators in the construction of observables. It has the advantage that it does not involve explicitly any particular basis or set of modes. It is however a more singular object: it is an *operator valued distribution* [32, 35]. When applied formally on the vacuum it does not yield a state but a singular object that is not in the Hilbert space and which can be interpreted as a distribution. Its role could be considered only technical, i.e., as a convenient way to summarize information and as a convenient notation. On the other hand its independence on a particular choice of basis is an argument for considering it as the general intrinsic definition of the quantum field. This point of view is often prevalent in quantum field theory [33]. Moreover, it has been argued by Mandel [37] to help defining the localizability of quantum states of the free field.

3.4.3 Remarks on the physical status of the reduced model

The reduced model (with discrete and finite dimensions) has been constructed in order to have a well-defined Hilbert space in terms of L_2 functions of the electromagnetic configurations. It can be considered as an intermediate step that suggests the structure and interpretation that one should associate to the postulated Fock space model, that allows one a well-defined $N \rightarrow \infty$ model. One can however try to clarify the conceptual status and domain of validity of the reduced model for applications in (non-relativistic) quantum optics. For quantum optics in a cavity one can make the argument that the eigenmodes that have been projected out with a cutoff correspond to high energies, and therefore in usual quantum optics experiments these modes are never populated. Hence, the reduced model and the more general Fock space model should lead to essentially identical predictions for the considered experiments. In the same spirit, the propagation in free space can be reduced to a finite set of modes by considering large but finite cavities. However, for the description of propagating localized pulses one needs a continuum of modes, and thus the formulation in Fock space is necessary.

3.5 Summary on the quantum model

In this chapter we have quantized the canonical model of Chapter 2 in a perfect cavity where the fields are expanded on a discrete and finite set of modes. We have described the principle of correspondence which transforms the classical variables into quantum operators, and we have given several formulations of the theory depending on how we choose to construct the Hilbert space of quantum states. We have seen that a bosonic Fock space can be constructed and then extended to infinite dimensions (i.e., to more realistic scenarios with a continuous spectrum). This can serve as a theoretical justification of the bosonic property of the states. Observables like the electric field operator were derived and expressed in

a way that can be used to evaluate measurable quantities.

Moreover, the quantization scheme presented in this chapter highlights two sets of properties attached to the photon states: classical properties of the electromagnetic configurations, and quantum properties emerging from the principle of correspondence and from the construction of the Fock space. Some properties are more important than others depending on the context or what a given experimental setup stresses out. In the next chapter, we describe recent experiments where both classical and quantum properties of photons play crucial roles.

Photon dynamics

From the quantization of light in passive media, one must be able to extract a precise description of the photon states, and in particular what is usually referred to as the “mode profile” in classical electromagnetism, or the “wave packet” in quantum optics. This is what we investigate in this Chapter, and we use it to describe some fundamental quantum optics experiments.

In Section 4.1 we comment on the usual Planck-Einstein formula stating that the energy of a photon is given by a unique frequency. We argue that this formula, although useful in some specific conditions, is generally unadapted to describe propagating localized states. In Section 4.2 we give a precise description of “pulse” electromagnetic configurations associated with photons and we show how the quantum state is modified by its interaction with a beam splitter. Finally in Section 4.3 we investigate how the preceding description can be used to describe the Hong-Ou-Mandel experiment and some generalization of it.

Contents

4.1 Time evolution of photon states	60
4.2 One photon through a beam splitter	61
4.2.1 Classical description	61
4.2.2 Quantum dynamics of the photon	63
4.3 Hong-Ou-Mandel effect	63
4.3.1 General setup	64
4.3.2 Usual HOM effect	65
4.3.3 Discussion on classical dynamics	67
4.4 Hong-Ou-Mandel with a fast detector	67
4.4.1 Time-resolved HOM effect	68
4.4.2 Time-resolved HOM with phase flip	69
4.4.3 Multi-pulses HOM with phase flips	71
4.5 Summary on the dynamics of photons	72

4.1 Time evolution of photon states

The design of quantum optics experiments relies on the understanding of the dynamics of the photon states. The formulation developed in the preceding chapter allows us to make the following statement: starting from a given initial condition, the quantum evolution of an N -photon state is entirely determined by the classical evolution of its N classical configurations, combined with the bosonic condition of symmetry. We can show it easily with a 1-photon state:

We start with an initial classical configuration $\vec{\psi}(t=0)$. This configuration evolves according to the wave equation in the complex representation:

$$i\partial_t\vec{\psi}(t) = \Omega\vec{\psi}(t), \quad (4.1)$$

such that in terms of the eigenfunctions $\vec{\varphi}_\kappa$ of Ω , we have

$$\vec{\psi}(t) = \int d\kappa e^{-i\omega_\kappa t} \vec{\varphi}_\kappa \alpha_\kappa, \quad \alpha_\kappa = \vec{\varphi}_\kappa^* \cdot \vec{\psi}(t=0). \quad (4.2)$$

The quantum state associated with $\vec{\psi}(t)$ is

$$|\vec{\psi}(t)\rangle = \hat{B}_{\vec{\psi}(t)}^\dagger |\emptyset\rangle = \hat{B}_{\int d\kappa e^{-i\omega_\kappa t} \vec{\varphi}_\kappa \alpha_\kappa}^\dagger |\emptyset\rangle = \int d\kappa e^{-i\omega_\kappa t} \alpha_\kappa \hat{B}_{\vec{\varphi}_\kappa}^\dagger |\emptyset\rangle. \quad (4.3)$$

Using this representation, we can write

$$i\hbar\partial_t|\vec{\psi}(t)\rangle = \int d\kappa \hbar\omega_\kappa e^{-i\omega_\kappa t} \alpha_\kappa \hat{B}_{\vec{\varphi}_\kappa}^\dagger |\emptyset\rangle. \quad (4.4)$$

On the other hand, since the Hamiltonian reads $\hat{H} = \int d\kappa \hbar\omega_\kappa \hat{B}_{\vec{\varphi}_\kappa}^\dagger \hat{B}_{\vec{\varphi}_\kappa}$ (see Section 3.4.1), we have

$$\begin{aligned} \hat{H}|\vec{\psi}(t)\rangle &= \iint d\kappa d\kappa' \hbar\omega_{\kappa'} e^{-i\omega_{\kappa'} t} \alpha_{\kappa'} \hat{B}_{\vec{\varphi}_{\kappa'}}^\dagger \hat{B}_{\vec{\varphi}_{\kappa'}} \hat{B}_{\vec{\varphi}_\kappa}^\dagger |\emptyset\rangle, \\ &= \iint d\kappa d\kappa' \hbar\omega_{\kappa'} e^{-i\omega_{\kappa'} t} \alpha_{\kappa'} \hat{B}_{\vec{\varphi}_{\kappa'}}^\dagger \left(\hat{B}_{\vec{\varphi}_{\kappa'}} \hat{B}_{\vec{\varphi}_\kappa} + \delta(\kappa - \kappa') \right) |\emptyset\rangle, \\ &= \int d\kappa \hbar\omega_\kappa e^{-i\omega_\kappa t} \alpha_\kappa \hat{B}_{\vec{\varphi}_\kappa}^\dagger |\emptyset\rangle, \end{aligned} \quad (4.5)$$

where we have used the commutation relation $\hat{B}_{\vec{\varphi}_\kappa}^\dagger \hat{B}_{\vec{\varphi}_{\kappa'}} = \hat{B}_{\vec{\varphi}_{\kappa'}} \hat{B}_{\vec{\varphi}_\kappa}^\dagger + \delta(\kappa - \kappa')$ and the fact that $\hat{B}_{\vec{\varphi}_{\kappa'}} |\emptyset\rangle = 0$. Identification with (4.4) shows that the state $|\vec{\psi}(t)\rangle$ satisfies the Schrödinger equation

$$\hat{H}|\vec{\psi}(t)\rangle = i\hbar\partial_t|\vec{\psi}(t)\rangle, \quad (4.6)$$

which proves that the time evolution of $\vec{\psi}(t=0)$ coincides with the time evolution of the quantum state. In other words, starting with a quantum state $|\vec{\psi}(t=0)\rangle$, one can deduce the evolved state $|\vec{\psi}(t)\rangle$ at any time t by calculating the classical evolution $\vec{\psi}(t)$.

The above proof can easily be extended to states with a higher number of quanta. When calculating the time evolution of the state, one has to remember to add the bosonic condition of symmetry introduced in Section 3.2.1. This requirement is actually the only difference between the quantum and the classical evolution in the propagation (i.e., apart from the processes of emission and detection). As we will see in the next Sections, a simple experimental setup involving a beam splitter can be used to distinguish between classical and

quantum light only when at least two quanta are used.

When a classical configuration $\vec{\psi}$ propagates through a passive optical element X , we will note

$$|\vec{\psi}(t_1)\rangle \xrightarrow{X} |\vec{\psi}(t_2)\rangle, \quad (4.7)$$

with $t_2 > t_1$, the evolution of the associated quantum state. Thus the symbol \xrightarrow{X} implies the Schrödinger evolution of the state through the element X .

4.2 One photon through a beam splitter

A good, first way to confront the quantum description of photons to classical descriptions of light is to investigate the action of a beam splitter on a single photon. A beam splitter (BS) is a device widely used in classical optics which spatially separates a radiation of light into two distinct paths. It takes various forms (a superposition of layers of glass, a metallic film, a split cube of glass or a fiber coupler and equivalent integrated devices), and some of these forms allow the control of the ratio of transmitted light in each path. A beam splitter is called *balanced* when this ratio is 50/50, i.e., the radiation is equally guided onto each of the two paths.

Beam splitters can also have an effect on the polarization of the radiation, in which case we use the term *polarizing beam splitter*. In this thesis we do not study the effect of polarization.

It is worth noting that some designs of plasmonic beam splitters have recently been used in experiments [38–43]. Hence, everything we describe in the present Chapter can be extrapolated to quantum plasmonics experiments (of course one should also consider losses in the material [42–46], a feature that we neglect for photons).

4.2.1 Classical description

We first describe the effect of the beam splitter on a classical pulse. We will then use this description to build the corresponding quantum state.

We consider an initial classical configuration that is sent onto a beam splitter as represented in Figure 4.1 (a), and we place two detectors, one on each outgoing path (horizontal and vertical). We choose the origin of the coordinates at the center of the BS.

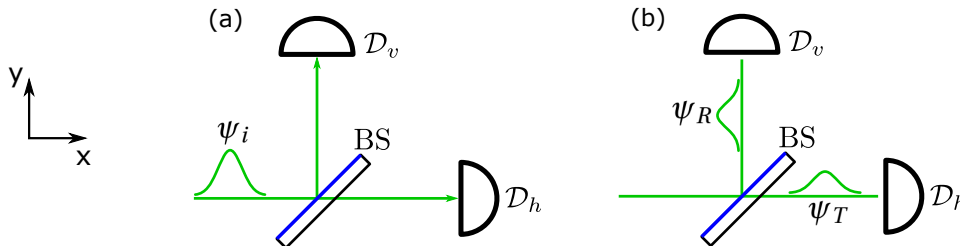


Figure 4.1 – (a) Initial classical configuration; (b) classical configuration after reflection and transmission.

We define the following *pulse shape function* $\vec{S}(r_1, r_2, r_3, \tau; k, L, L_0, \sigma)$, depending on three spatial arguments r_1, r_2, r_3 , a temporal variable τ , and several parameters k, L, L_0, σ ,

$$\vec{S}(r_1, r_2, r_3, \tau; k, L, L_0, \sigma) := \vec{e}_z \mathcal{E}(r_1 - c\tau) e^{i(kr_1 - \omega\tau)} g(r_2, r_3), \quad (4.8)$$

where $\vec{e}_z = (0, 0, 1)$ is the linear polarization vector, $\omega = ck > 0$ is the carrier frequency, and

$$\mathcal{E}(r) = \chi_{[-L_0-L, -L_0]}(r) \sin^2\left(r \frac{\pi}{L}\right), \quad (4.9)$$

$$g(r_2, r_3) = e^{-(r_2^2 + r_3^2)/\sigma^2} \chi_{[0, 9\sigma^2]}(r_2^2 + r_3^2), \quad (4.10)$$

with

$$\chi_{[a, b]}(r) := \begin{cases} 1 & \text{for } r \in [a, b], \\ 0 & \text{otherwise.} \end{cases} \quad (4.11)$$

$\mathcal{E}(r)$ is the pulse envelope in the direction of propagation. The function $g(r_2, r_3)$ is the transverse profile, for which we take a truncated Gaussian of width 3σ , to ensure that the pulses occupy a finite volume (which is what we can assume is a good description of what happens in experiments). L is the length of the pulse and L_0 determines the position of the pulse at time $\tau = 0$. For the pulse envelope \mathcal{E} we have taken a \sin^2 function with a finite support of size L , so that there is no ambiguity about when the process starts.

The initial configuration is chosen as

$$\psi_i(\vec{x}) = \vec{S}(x, y, z, \tau = 0; k, L, L_0, \sigma) =: \vec{S}(x, \tau = 0), \quad (4.12)$$

where we introduce an abridged notation for \vec{S} indicating only the first spatial argument and the time argument.

After interacting with the beam splitter, for $\tau \gg (L_0 + L)/c$, the classical mode evolves into a reflected pulse and a transmitted pulse

$$\psi_i \rightarrow \psi_R + \psi_T, \quad (4.13)$$

where

$$\psi_R(\vec{x}, \tau) = r \vec{S}(y - c\tau, \tau) =: r \nu(y), \quad (4.14)$$

$$\psi_T(\vec{x}, \tau) = t \vec{S}(x - c\tau, \tau) =: t h(x). \quad (4.15)$$

Assuming that we can neglect losses in the material, the reflection and transmission coefficients r, t satisfy the relation $|r|^2 + |t|^2 = 1$ and $r^* t + r t^* = 0$. For a balanced beam splitter they satisfy furthermore

$$t = ir, \quad \text{i.e., } r^2 + t^2 = 0. \quad (4.16)$$

We have also introduced the notations $\nu(y)$ and $h(x)$ (standing for *vertical* and *horizontal*) to improve the readability of the constructions of this Chapter. We emphasize that these notations do not refer to the polarization state of the pulse, but only to its propagation axis x (horizontal) or y (vertical).

It is worth noticing that the equations (4.14)–(4.15) are approximations since we do not consider any dispersion or spatial deformation effect during the propagation.

Remark: The classical description of a beam splitter we provide here does not modify the spectral structure of the Hamiltonian model built in Chapter 2, since it only adds transmission and reflection coefficients in the propagation. This is the case providing we do not look into local effects inside the beam splitter. As a consequence, configurations of the field in the exterior of the beam splitter can be mapped onto the basis of eigenconfigurations in vacuum (i.e., plane waves).

4.2.2 Quantum dynamics of the photon

Let us now assume that the radiation of light is not classical but made of a 1-photon state associated with the initial configuration ψ_i . In the Fock space, this state is

$$|\psi_i\rangle := \hat{B}_{\psi_i}^\dagger |\emptyset\rangle. \quad (4.17)$$

In order to use a probabilistic interpretation later on, we should assume this configuration to be normalized:

$$\int d^3r |\psi_i(\vec{r})|^2 = 1, \quad (4.18)$$

which entails [see Eq. (3.27)]

$$[\hat{B}_{\psi_i}, \hat{B}_{\psi_i}^\dagger] = \mathbb{1}. \quad (4.19)$$

This implies that the initial quantum state (4.17) is normalized:

$$\langle \psi_i | \psi_i \rangle = 1. \quad (4.20)$$

Using the classical evolution to calculate the quantum evolution as described in Section 4.1, the 1-photon state evolves to

$$\begin{aligned} |\psi_i\rangle &\xrightarrow{BS} |\psi_R + \psi_T\rangle = \hat{B}_{\psi_R + \psi_T}^\dagger |\emptyset\rangle, \\ &= |r\nu(y) + th(x)\rangle. \end{aligned} \quad (4.21)$$

The physical interpretation of the state at time t after the crossing of the beam splitter is as follows:

$|\psi_R + \psi_T\rangle$ is a 1-photon state on the *single* classical configuration $\psi_R + \psi_T$, which has two spatially disjoint components, one propagating in the x direction and the other one in the y direction.

We emphasize that the evolution of the state is studied far enough of the beam splitter such that we can neglect all local effects and in particular non-trivial deformations of the state inside the beam splitter. This approximation is therefore equivalent to a scattering perspective although the time-scale is finite and can be rather small depending on the classical configuration associated with the photon.

4.3 Hong-Ou-Mandel effect

When 2-photon states propagate onto a beam splitter from opposite ports, an interesting phenomenon can appear. This phenomenon is referred to as *Hong-Ou-Mandel effect* (HOM, [18]). It is fundamental in quantum optics since it is probably the simplest experimental setup which is able to clearly show a quantum behavior of light [19]. It can thus

serve as a way to check that the source used is indeed a single-photon source, and for this reason it is widely used in quantum optics experiments.

The HOM effect has been observed with photons in many different platforms. It was also used to study single plasmons [38–43], as well as electrons and holes in condensed matter [47], and even free atoms [48]. In this section, we consider only photons, which is the first and most common quantum object used in a HOM setup. It is thus well known, but we will see along this section some extensions of the phenomenon which challenges the usual intuition and that requires us to analyze more precisely how single-photon detectors actually work.

4.3.1 General setup

We consider the general setup as sketched on Figure 4.2, where two classical configurations are impinging a beam splitter from opposite ports.

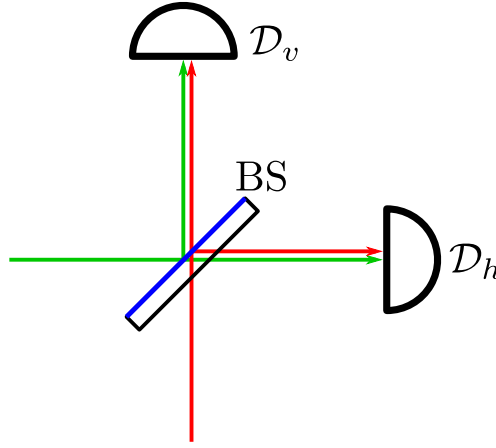


Figure 4.2 – General scheme for the HOM effect. Red and green arrows are the paths followed by the classical configurations which may carry 1-photon states.

The initial state (before the BS) is defined by

$$|\Psi_i\rangle = \hat{B}_{\psi_B}^\dagger \hat{B}_{\psi_A}^\dagger |\emptyset\rangle = |\psi_A\rangle \otimes_s |\psi_B\rangle, \quad (4.22)$$

where ψ_A and ψ_B are the classical configurations carrying the photons. They can have a Gaussian profile or any kind which is compatible with the complex Hilbert phase space of configurations as constructed in Chapter 2.

It is crucial for the interpretation of the phenomenon to emphasize that Ψ_i is a 2-photon state. It is **not** the sum of two 1-photon states – this would mean adding a photon on two distinct electromagnetic vacuums. A 2-photon state is not the sum of two 1-photon states, it is the vacuum state that has been excited twice [on potentially different classical configurations as in (4.22)], and therefore it is the symmetric tensor product of the 1-photon states.

We recall that, in order to have $\langle \Psi_i | \Psi_i \rangle = 1$ and knowing that the classical configurations are both normalized and orthogonal with one another, we have the definitions:

$$|\psi_j\rangle \otimes_s |\psi_k\rangle = \frac{1}{\sqrt{2}} (|\psi_j\rangle \otimes |\psi_k\rangle + |\psi_k\rangle \otimes |\psi_j\rangle), \quad j \neq k, \quad (4.23)$$

$$|\psi_j\rangle \otimes_s |\psi_j\rangle = |\psi_j\rangle \otimes |\psi_j\rangle. \quad (4.24)$$

As in the previous section, we denote by h and v the configurations propagating on the corresponding paths:

$$|\Psi_i\rangle = \hat{B}_v^\dagger \hat{B}_h^\dagger |\emptyset\rangle = |h\rangle \otimes_s |v\rangle. \quad (4.25)$$

We assume that the two pulses have the same profile and that they are not temporally or spectrally compressed nor stretched during the propagation (i.e., we neglect dispersion effects).

4.3.2 Usual HOM effect

We consider a simplified version of the original experiment of Hong, Ou and Mandel [18], where two Gaussian pulses h and v carrying the 1-photon states [as described in Eq. (4.2.1)] arrive simultaneously on the BS.

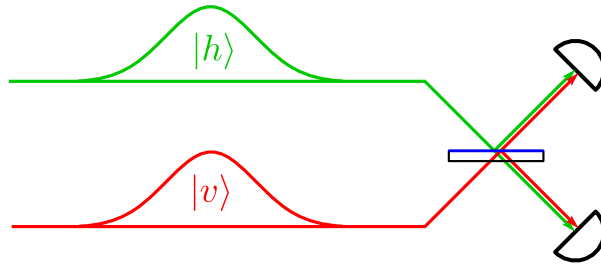


Figure 4.3 – Initial input of the usual HOM effect. The two 1-photon states are carried by classical configuration of the same shape, only spatially separated. They are prepared to arrive simultaneously on the beam splitter, making their respective configurations overlap exactly.

The state evolves as

$$|\Psi_i\rangle = |v\rangle \otimes_s |h\rangle \xrightarrow{BS} |\Psi_f\rangle = |tv + rh\rangle \otimes_s |th + rv\rangle. \quad (4.26)$$

We can calculate this final state more precisely using Eq. (4.23):

$$|\Psi_f\rangle = (r^2 + t^2) \left(|h\rangle \otimes |v\rangle + |v\rangle \otimes |h\rangle \right) + r t \left(|v\rangle \otimes |v\rangle + |h\rangle \otimes |h\rangle \right). \quad (4.27)$$

Assuming that the beam splitter is balanced, we have $|r| = |t| = 1/\sqrt{2}$, $r = it$, and $t^2 + r^2 = 0$. The final state reduces to

$$|\Psi_f\rangle = \frac{i}{2} \left(|v\rangle \otimes |v\rangle + |h\rangle \otimes |h\rangle \right). \quad (4.28)$$

We see that there is no cross terms of the form $|v\rangle \otimes |h\rangle$. This is the main result of the HOM experiment:

If the beam splitter is balanced, the photons bunch together and only pairs are detected, either on \mathcal{D}_h or on \mathcal{D}_v .

The vanishing of cross terms (called *coincidences*) is reduced if the configurations are not exactly equal, if they do not impinge the beam splitter perfectly synchronized, or if the beam splitter is not exactly balanced.

Remark: This result can be shown more precisely by defining the observables corresponding to the different possible detections:

- Detection of one photon in the considered configuration on detector \mathcal{D}_h :

$$\hat{O}_{1h} = |h\rangle\langle h| \otimes \mathbb{1} + \mathbb{1} \otimes |h\rangle\langle h|, \quad (4.29)$$

- correspondingly on detector \mathcal{D}_v :

$$\hat{O}_{1v} = |v\rangle\langle v| \otimes \mathbb{1} + \mathbb{1} \otimes |v\rangle\langle v|. \quad (4.30)$$

- Detection of two photons in \mathcal{D}_h :

$$\hat{O}_{2hh} = |h\rangle\langle h| \otimes |h\rangle\langle h|, \quad (4.31)$$

- correspondingly on detector \mathcal{D}_v :

$$\hat{O}_{2vv} = |v\rangle\langle v| \otimes |v\rangle\langle v|. \quad (4.32)$$

- Detection of one photon on \mathcal{D}_h and one photon on \mathcal{D}_v simultaneously (i.e., *coincidences*):

$$\hat{O}_{2hv} = |v\rangle\langle v| \otimes |h\rangle\langle h| + |h\rangle\langle h| \otimes |v\rangle\langle v|. \quad (4.33)$$

All these operators are projectors. One can then obtain the probability of the corresponding outcomes described by each \hat{O} by calculating its mean value on the final state $|\Psi_f\rangle$. In particular, the probability of coincidences is

$$\text{Prob}(\mathcal{D}_h \text{ and } \mathcal{D}_v) = \langle \Psi_f | \hat{O}_{2hv} | \Psi_f \rangle. \quad (4.34)$$

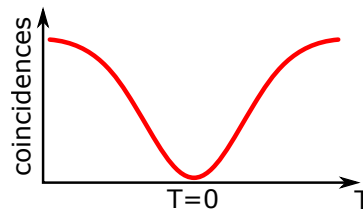
We insert the expression for $|\Psi_f\rangle$ given in (4.28), we use the orthogonality of the vertical and horizontal states and we use the relations of the coefficients r , t , and we obtain

$$\text{Prob}(\mathcal{D}_h \text{ and } \mathcal{D}_v) = 0. \quad (4.35)$$

Thus, the probability for simultaneous detection of one photon in each detector is zero.

This effect is a main tool in quantum optics experiments for three main reasons:

1. First of all, when the two photons used are emitted from the same source, it allows one to measure the rate of emission of the source. Indeed, controlling the optical path followed on each port of the beam splitter gives a way to derive the delay at which each emission process has occurred. In practice the following type of curve is measured (called the *HOM dip*), where the time delay $T = 0$ corresponds to the delay when the two pulses are synchronized on the beam splitter.



Of course, this is usable only with sources that emit photons at a constant rate.

2. Secondly, since the HOM effect occurs when the configurations that carry the photons are identical, it gives a way to measure whether the source is stable regarding the emission process (since a stable emission process should produce photons on identical configurations).
3. Last but not least, it is a fundamental tool to test whether the source emits quantum or classical light. Indeed, as we shall see now, the HOM effect (vanishing of coincidences) cannot be interpreted in any classical way.

4.3.3 Discussion on classical dynamics

To understand the importance of the Hong-Ou-Mandel effect, one can compare it to classical interpretations of light. We identify two possible classical descriptions:

1. Light as classical particles;
2. Light as classical waves.

The action of the beam splitter acquires a different interpretation depending on which description of light we use. For classical waves, it acts by dividing the amplitude of the wave and two waves emerge from the BS, one transmitted and one reflected (which is the description we used on the electromagnetic configurations which carry the photon states). For classical particles, the BS acquires a probabilistic power: each grain of light incoming onto the BS is either transmitted or reflected (the chance being given by the (r, t) coefficients).

Hence if we describe light as classical waves, both detectors should always, simultaneously, detect a part of the wave. There would thus always be coincidences occurring. If light were classical particles, on the other side, two impinging particles would have as much chance to be detected on different detectors than on the same. Both results are contradicted by the observation of the Hong-Ou-Mandel effect.

The Hong-Ou-Mandel effect can thus be considered as a simple proof of a true quantum behavior of photons.

4.4 Hong-Ou-Mandel with a fast detector

This Section contains the main new results regarding the dynamics of photons. It provides a description of some non-intuitive effects in the Hong-Ou-Mandel effect when using fast detectors. We will see that this description is rather straightforward using the tools introduced earlier.

To understand some recent quantum optics experiments, we need to have a description of detectors with short detection time bins. The HOM effect described in the preceding section only required the detectors to integrate over the whole classical configuration to see whether it carries a photon or not. But in practice, some detectors have a sensitivity which allows to “scan” the configuration and resolve it in time.

In this Section we use a very simple model of time-resolved detection. We consider that the action of a detector is repeated over and over during the passage of the classical configuration. It can thus be described as two steps:

- Detection in a time bin, with a probability given by the integral of the (normalized) classical configuration over the corresponding time bin,
- Cancellation of the part of the configuration inside the time bin, and renormalization of the whole configuration (or cancellation if all remaining photons have been detected in the time bin).

This model is very simple and does not represent the true, precise phenomena that come into play in a real detector. However, it is a sufficient model to describe the time-resolved effects in the HOM experiment.

4.4.1 Time-resolved HOM effect

From the preceding model of fast detectors, we can investigate how the HOM effect may be affected by such a time resolution. In order to make it as simple as possible, we start with a classical configuration which is scanned twice by the detector (i.e., it is made of two time bins only).

Consider that, in the initial condition as presented in the usual HOM effect (Section 4.3.2), the temporal center of one classical pulse (and the other, since they are synchronized) is called t_0 , the front is at t_1 and the tail is at t_{-1} . This pulse can be equivalently written as the sum of two pulses (see Figure 4.4), where the parts 1 and 2 correspond to the time bins $t_1 - t_0$ and $t_0 - t_{-1}$ respectively.

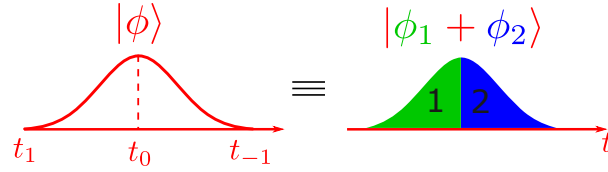


Figure 4.4 – Scheme of the initial classical configuration that carries the one-photon states, and how it is split into two time bins of detection.

The initial 2-photon state is the same as in Section 4.3.2, and it can now be written

$$|\Psi_i\rangle = |v\rangle \otimes_s |h\rangle = |v_1 + v_2\rangle \otimes_s |h_1 + h_2\rangle, \quad (4.36)$$

where the indices 1 and 2 refer to the first and the second time bin where the detection can occur.

| **Remark:** If the pulses are symmetric, then ϕ_1 and ϕ_2 are normalized to 1/2.

The BS acts in the same way on ϕ_1 and ϕ_2 (and preserves the time sequence). The final state is thus

$$|\Psi_f\rangle = |t(v_1 + v_2) + r(h_1 + h_2)\rangle \otimes_s |t(h_1 + h_2) + r(v_1 + v_2)\rangle \quad (4.37)$$

$$\begin{aligned} &= (t^2 + r^2)|v_1 + v_2\rangle \otimes_s |h_1 + h_2\rangle \\ &\quad + r t \left(|h_1\rangle \otimes |h_1\rangle + |h_2\rangle \otimes |h_2\rangle + |v_1\rangle \otimes |v_1\rangle + |v_2\rangle \otimes |v_2\rangle \right. \\ &\quad \left. + 2|h_1\rangle \otimes_s |h_2\rangle + 2|v_1\rangle \otimes_s |v_2\rangle \right). \end{aligned} \quad (4.38)$$

Under the condition of a balanced BS, we again have $t^2 + r^2 = 0$ and so (4.38) reduces to

$$\begin{aligned} |\Psi_f\rangle &= \frac{i}{2} \left(|h_1\rangle \otimes |h_1\rangle + |h_2\rangle \otimes |h_2\rangle + |v_1\rangle \otimes |v_1\rangle + |v_2\rangle \otimes |v_2\rangle \right. \\ &\quad \left. + 2|h_1\rangle \otimes_s |h_2\rangle + 2|v_1\rangle \otimes_s |v_2\rangle \right). \end{aligned} \quad (4.39)$$

This state has an interpretation which is consistent with the usual HOM effect. Indeed it tells us that:

- there is a probability to observe pairs of photons in the same time bin [first line of (4.39)];
- there is a probability to observe photons distributed in the two time bins of one pulse [second line of (4.39)];
- there is **no** possibility to observe photons on different pulses (whether in the same time bin or not).

This description where the photon state is decomposed as two connected parts is perfectly equivalent to considering a photon state occupying a classical mode made of two pulses (i.e., the mathematical trick of splitting into time bins is not contradictory with what one can create in the lab [20–22]). There might be technical differences in the experiment, but the predictions are the same whether the time bins refer to sub-parts of one pulse or different pulses in a train.

Remark: This result can easily be extended to a situation where the splitting time t_0 is not at the center of the pulse (or equivalently if the pulse is not symmetric); one simply has to remember that the sub-pulses composing the full pulse are normalized differently, depending on the area of the pulse they cover.

Furthermore, this result can also be extended to N splittings of the pulse if one wants to describe a more resolved instrument to measure the photons. This will be written in a general way in Section 4.4.3.

4.4.2 Time-resolved HOM with phase flip

The preceding case in study – though of particular interest to investigate experiments with time-resolved detectors or two-pulse photons – is in agreement with what one could already observe in the standard “time-integrated” HOM experiment of Section 4.3.2. The next step in our discussion proposes a variant of the HOM effect which can exhibit counter-intuitive results compared to the usual one. This will lead us to restate more precisely the conditions to observe the HOM effect.

Since the two first conditions to obtain a HOM effect are (1) using a balanced BS and (2) having identical pulses synchronized on the BS, it may look vain to hope altering this effect without destroying it completely. What can someone change **and** maintain a non-crossed probability without it being necessarily balanced by crossed ones? The answer to that is included in the word *identical*. Although the temporal/spatial shape should be maintained, it is not necessarily the case of the phase.

Let us consider the time-resolved experiment described in Section 4.4.1, and let us now apply a constant phase flip of φ on the second time bin of one photon (say, ν_2). We will note $|\nu_2^\varphi\rangle = e^{i\varphi}|\nu_2\rangle$. We also assume that this change of phase is not affected by the BS.

The initial 1-photon states are drawn in Figure 4.5 and the initial 2-photon state reads

$$|\Psi_i\rangle = |\nu_1 + \nu_2^\varphi\rangle \otimes_s |h_1 + h_2\rangle. \quad (4.40)$$

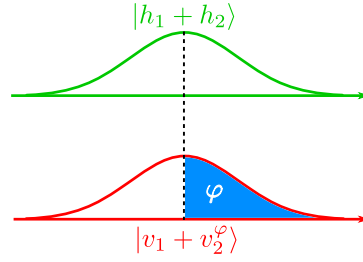


Figure 4.5 – Scheme of the initial classical configurations that carry the one-photon states, when a phase is applied on the second time bin of the configuration incoming on the vertical arm.

It evolves similarly as before, with a preservation of the phase:

$$|\Psi_f\rangle = |t(v_1 + v_2^\varphi) + r(h_1 + h_2^\varphi)\rangle \otimes_s |t(h_1 + h_2) + r(v_1 + v_2)\rangle \quad (4.41)$$

$$\begin{aligned} &= [t^2 + e^{i\varphi}r^2]|v_1\rangle \otimes_s |h_2\rangle + [e^{i\varphi}t^2 + r^2]|v_2\rangle \otimes_s |h_1\rangle \\ &\quad + r t \left\{ |h_1\rangle \otimes_s |h_1\rangle + |v_1\rangle \otimes_s |v_1\rangle + e^{i\varphi} (|h_2\rangle \otimes_s |h_2\rangle + |v_2\rangle \otimes_s |v_2\rangle) \right\} \\ &\quad + r t (1 + e^{i\varphi}) (|h_1\rangle \otimes_s |h_2\rangle + |v_1\rangle \otimes_s |v_2\rangle). \end{aligned} \quad (4.42)$$

A first remark should be made here: for any phase φ , there is no term of the form $|v_i\rangle \otimes_s |h_i\rangle$ (i.e., no cross detection in the same time bin). In the case of a balanced BS, we can make the following observations:

- $\forall \varphi$, if no photon has been detected in the first time bin (neither on \mathcal{D}_h nor \mathcal{D}_v), then the photons will be detected **both on one detector** in the second time bin. In other words, the HOM effect takes place as usual in the time bin left, even if the pulses in this time bin are of different phases (0 and φ);
- if $\varphi = 0$, if only one photon has been detected on one detector in the first time bin, the second photon will be detected **on the same detector** in the second time bin. This is again the result (4.39) of the time-resolved HOM effect;

These two points are consistent with a HOM resolved in time. A more interesting observation can however be added:

- if $\varphi = \pi$, if only one photon has been detected on one detector in the first time bin, the second photon will be detected **on the other detector** in the second time bin.

These three possibilities are summarized in Figure 4.6.

Remark: In the literature, authors sometimes write that this last behavior of photons (when $\varphi = \pi$ and detection occurs in different time bins) is “quasi-fermionic” (see, e.g., [21]). This is explained by the *only* fact that photons are detected on opposite detectors instead of the same one, which is what is seen in the usual HOM effect using fermions [49]. Such an argument evades all considerations of the *time* of detection. In particular, if the detection occurs in the same time bin, the usual bosonic HOM effect is recovered (i.e., both photons are detected on the same detector), which would not happen with fermions. The use of an expression like “fermionic” or “quasi-fermionic” would seem appropriate if fermions gave the same results in this experiment, which is not true: they still give opposite results compared to bosons.

One should simply remember that the usual HOM effect describes an experiment where photons have a constant phase difference throughout the detection process, and that a phase change in this process might bring out some new interference effects not considered originally – es-

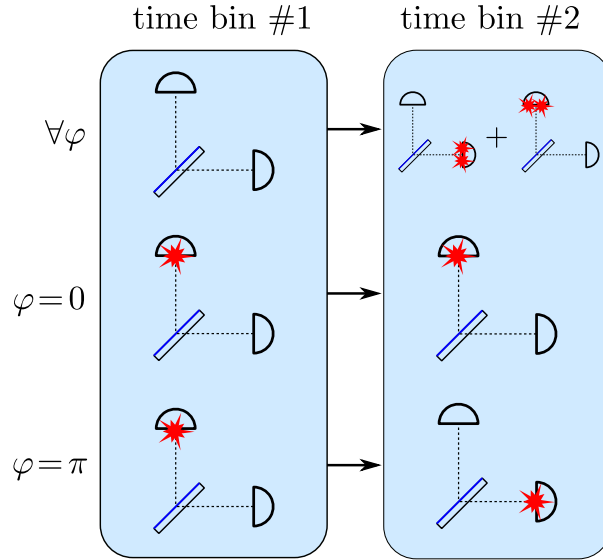


Figure 4.6 – Three possible outcomes of the HOM experiment with two time bins. The red star depicts a detection of one photon.

pecially since such an observation requires time-resolved detection, which can be difficult to achieve with common detectors, and therefore requires very long photons (experimental implementations have been performed with temporal length of the classical configurations typically of a few hundred nanoseconds, see [19, 20, 22]).

4.4.3 Multi-pulses HOM with phase flips

In this section we generalize the study of the HOM effect to pulses made of N time bins with arbitrary phase flips. To vary with the description and to get closer to the experiments investigating such effects [20–22], we change the way of generation of the time bins: the photons are now shaped as trains of N pulses with their own phase instead of one pulse enduring N phase flips. The theoretical description is the same in both cases, but using trains of pulses has the advantage that one can apply the phase flips in the generation of the photon (by shaping the phase of the laser which pumps the single-photon source), and not *a posteriori*. The input states are sketched in Figure 4.7.

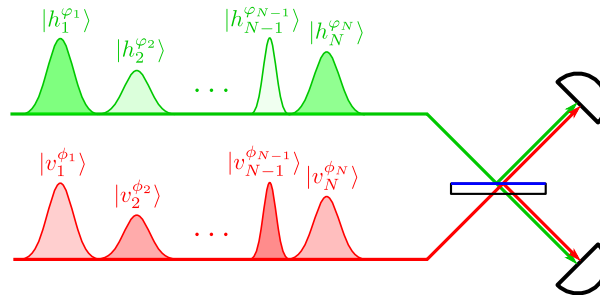


Figure 4.7 – Generalized HOM effect with photon states carried by a train of N classical pulses (equivalent to time bins) with arbitrary phases on each pulse.

The initial 2-photon state reads

$$|\Psi_i\rangle = \sum_{i,j=1}^N |v_i^{\phi_i}\rangle \otimes_s |h_j^{\phi_j}\rangle, \quad (4.43)$$

and we emphasize that the states $|v_i^{\phi_i}\rangle$ and $|h_j^{\varphi_j}\rangle$ are not normalized. The normalization condition reads

$$\sum_i \langle v_i^{\phi_i} | v_i^{\phi_i} \rangle = \sum_j \langle h_j^{\varphi_j} | h_j^{\varphi_j} \rangle = 1 \quad (4.44)$$

Like in the preceding section, we assume that the passage through the BS does not impact the phases:

$$\begin{aligned} v_i^{\phi_i} &\xrightarrow{BS} t v_i^{\phi_i} + r h_i^{\phi_i}, \\ h_j^{\varphi_j} &\xrightarrow{BS} t h_j^{\varphi_j} + r v_j^{\varphi_j}. \end{aligned}$$

Ultimately, the final state reads

$$|\Psi_f\rangle = \sum_{ij} |t v_i^{\phi_i} + r h_i^{\phi_i}\rangle \otimes_s |t h_j^{\varphi_j} + r v_j^{\varphi_j}\rangle \quad (4.45)$$

$$\begin{aligned} &= \sum_{ij} \left\{ [t^2 e^{i(\phi_i + \varphi_j)} + r^2 e^{i(\phi_j + \varphi_i)}] |v_i\rangle \otimes_s |h_j\rangle \right. \\ &\quad \left. + r t e^{i(\phi_i + \varphi_j)} (|v_i\rangle \otimes_s |v_j\rangle + |h_i\rangle \otimes_s |h_j\rangle) \right\}. \end{aligned} \quad (4.46)$$

For $i = j$, we can show that the first term in (4.46) vanishes (since $t^2 + r^2 = 0$), hence we can write

$$\begin{aligned} |\Psi_f\rangle &= \sum_{ij} [t^2 e^{i(\phi_i + \varphi_j)} + r^2 e^{i(\phi_j + \varphi_i)}] |v_i\rangle \otimes_s |h_j\rangle \\ &\quad + \sum_{ij} r t e^{i(\phi_i + \varphi_j)} (|v_i\rangle \otimes_s |v_j\rangle + |h_i\rangle \otimes_s |h_j\rangle), \quad \text{where } \sum_{\substack{ij \\ i \neq j}} \equiv \sum_{ij}. \end{aligned} \quad (4.47)$$

We see again that this general result is compatible with HOM effect, since in the same time bin ($i = j$) the first line with cross detection vanishes. For detections at different time bins ($i \neq j$), similar intermediary outcomes as described in Section 4.4.2 appear. This was demonstrated experimentally up to four pulses [21] and was shown to be usable for encoding information.

4.5 Summary on the dynamics of photons

The development of single photon sources has allowed the community to probe experimentally some fundamental aspects of quantum light. In this regard the Hong-Ou-Mandel experiment is a pioneer interference setup which is widely used nowadays. It is probably the simplest setup to verify that a source of light emits quantum photons that are *identical* (i.e., they are associated with identical classical configuration). Most of the time, it is sufficient to expect two main outcomes in this experiment: either the configurations are identical and the effect occurs, or they are not and the effect is reduced. More recently, some experiments have demonstrated the Hong-Ou-Mandel effect using only partly identical photons whose configuration can be shaped in a controlled manner and whose states can be detected with short temporal resolution. The results can be counter-intuitive and, to our knowledge, had not been described in a simple way before.

In this Chapter we emphasized that the classical dynamics of the configuration (together with the bosonic condition of symmetry) is sufficient to determine the quantum dynamics of the photon state through a beam splitter. Provided a simplified model for time-resolved detection, we have shown that this new type of Hong-Ou-Mandel effect can be rather easily analyzed with our approach.

The approximated role of the beam splitter (simply introducing coefficients of transmission and reflection) does neglect local effects which could be addressed with the quantum theory of light in passive media as constructed in the preceding chapters. Other types of Hong-Ou-Mandel experiments such as the plasmonic one should require a quantum theory of plasmons, which we construct in the next chapters.

Part II

Plasmons

Canonical plasmonics

The macroscopic Maxwell equations (1.6) describe how the electromagnetic field interacts with a linear medium. In the same way as we used them in a passive environment to have a classical description of light and to build a quantum theory of photons, it is reasonable to use them as well to describe classical light around plasmon resonances and to build a quantum theory of plasmons.

In a non-passive medium, the induced polarization density describes a retard electric response. In the Fourier domain, this translates into a dielectric permittivity which is frequency-dependent (i.e., the medium is dispersive) and complex with a positive imaginary part (i.e., the medium is dissipative). Because of this, the macroscopic Maxwell equations do not have a Hamiltonian structure. In order to go around this problem, we need to quantize a system that encompasses all sub-systems where the energy may flow, i.e., the electromagnetic field and the medium. The goal of the present Chapter is to construct such a system, and it should be Hamiltonian/canonical as for photonics.

In Section 5.1 we describe the Hamiltonian model containing the degrees of freedom of light and of the medium, and we show that this model is compatible with the macroscopic Maxwell equations. In Section 5.2, we construct a method of diagonalization of the Hamiltonian based on its transformation into a harmonic-like form, and then the diagonalization of its frequency operator.

Contents

5.1 Microscopic model	78
5.1.1 Light	79
5.1.2 Matter	79
5.1.3 Interaction	80
5.1.4 Equivalence with Maxwell's macroscopic equations	81
5.1.5 Hamiltonian structure	83
5.1.6 Coupling function in standard models	84
5.2 Canonical diagonalization of the model	86
5.2.1 Pre-diagonalization of the electromagnetic part	86
5.2.2 Integral operators, matrix form and canonical transformations	87
5.2.3 Finding the harmonic-like Hamiltonian	89

5.2.4	Møller wave operator	90
5.2.5	Lippmann-Schwinger equation	92
5.2.6	Degeneracy and block structure	94
5.2.7	Phase space of plasmonic configurations	96
5.2.8	Orthonormalization and completeness of the eigenconfigurations . .	97
5.2.9	Diagonal Hamiltonian	98
5.3	Summary on the classical Hamiltonian system	99

5.1 Microscopic model

Surface plasmon phenomena have been first observed in the late 50s by Ritchie [50] and are the subject of many recent studies, both experimental and theoretical, both classical and quantum. Classically, plasmons are some particular solutions of the macroscopic Maxwell equations which are confined at the interface between a metallic structure and a passive medium. This confinement is probably the most interesting feature of classical plasmons since they can be localized and propagate in volumes smaller than the diffraction limit. This has led the development of many devices to apply the general scheme of photonic circuits described in Chapter 1 Section 1.1 to plasmons. The emission of plasmons propagating at the surface of a metal is mostly performed by conversion of classical light into plasmons, using scatterers. However, more exotic sources of plasmons are under development such as spasers [52–56] which use analogies with lasers to emit plasmons. The subwavelength propagation is achieved using plasmonic waveguides [57–59] and some devices have been developed such as high-speed modulators [60] and plasmonic photodetectors [61]. Note that on a more fundamental perspective, some teams have recently constructed new platforms to excite a certain type of plasmon modes called *lattice plasmons* [62–64].

Similarly to photonic circuits, most studies assume that the plasmons that appear in their setup (and particularly their propagation) can be described classically with Maxwell’s equations. More and more studies, however, emphasize on the importance to study quantum plasmons [65–67] since it could open new doors in, e.g., integrated quantum computing. The main motivation of this Chapter and the two next is thus to quantize the macroscopic Maxwell equations and construct a theory of quantum plasmons as precise as what we could construct for photons in passive media.

We use a microscopic model made of three parts:

- The electromagnetic field in the free dielectric environment (i.e., with no metal);
- The free metallic medium;
- The interaction.

The first part was already treated in the previous chapters, and to simplify our study we consider the environment to be vacuum. We draw a general scheme of the configuration in Figure 5.1.

Our first goal is to show that the three parts of the system can be constructed in such a way that the whole system takes a Hamiltonian form compatible with the macroscopic Maxwell

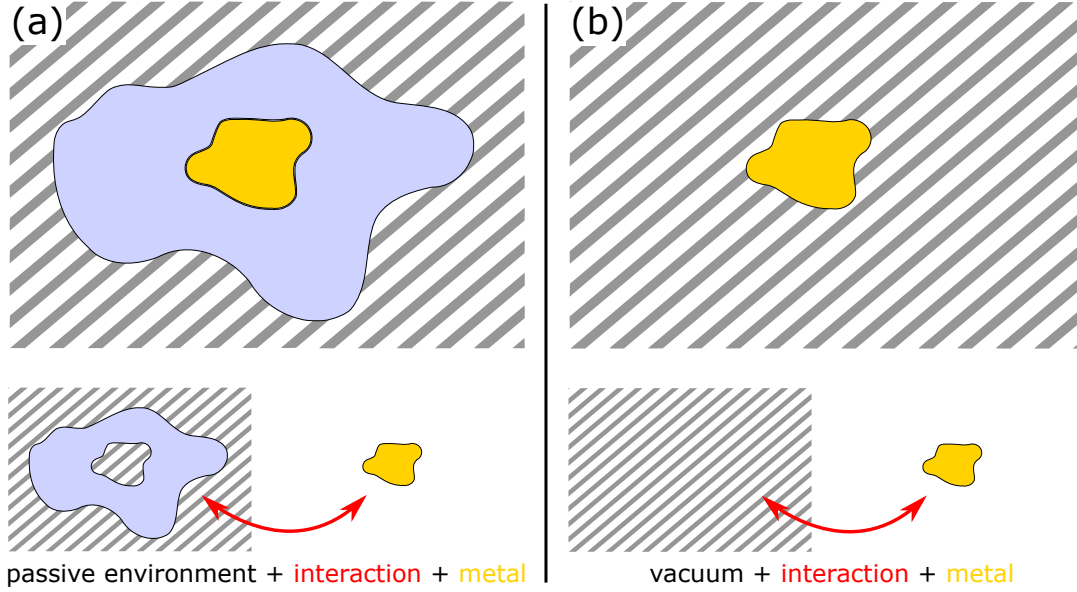


Figure 5.1 – Scheme of the general configurations in plasmonics: (a) the metal is embedded in a passive dielectric matrix surrounded by vacuum; (b) the metal is surrounded by vacuum only. On the bottom: decomposition into the three parts of the microscopic model. In this thesis, we study the configuration (b) only, but extensions to (a) can be naturally developed from the preceding chapters.

equations in a linear, non-magnetic, dispersive and dissipative medium.

The constructions of this Section are based on the results of Refs. [26, 51].

5.1.1 Light

The Hamiltonian description of classical light has been addressed in Chapter 2 in a passive dielectric environment. We can consider that this environment is vacuum at any point of the construction simply by choosing $\epsilon_R = 1$ (this is the only case for which the passive dielectric response verifies the Kramers-Kronig relations since they allow $\epsilon_R = 1$ when $\epsilon_I = 0$). The Hamiltonian reads

$$H_{\text{em}} = \frac{1}{2} \int d^3 r \left[\epsilon_0 \vec{E} \cdot \vec{E} + \frac{1}{\mu_0} \vec{B} \cdot \vec{B} \right], \quad (5.1)$$

or

$$H_{\text{em}} = \frac{1}{2} \int d^3 r \left[\epsilon_0 \vec{E} \cdot \vec{E} + \frac{1}{\mu_0} (\nabla \times \vec{A})^2 \right]. \quad (5.2)$$

We do not yet introduce canonically conjugate variables as in Chapter 2 since they will now depend on the matter variables and on the interaction. We shall however keep in mind that any choice of canonical variables should remain consistent with the limit when the interaction vanishes or when the degrees of freedom of matter are eliminated.

5.1.2 Matter

The material medium can be described by various models. The main criterion for the choice of the microscopic model is that if one integrates the equations for the medium and

one inserts the obtained currents into the microscopic Maxwell equations one should obtain the macroscopic Maxwell equations. The first model specifically addressed in the literature by Suttorp and Wubs [23, 24] consists of a set of charges coupled to the electromagnetic field and to a bath of oscillators. However it was shown ([26] and references therein) that a microscopic description consisting on a bath of oscillators only is sufficient to fulfill the criterion. This effective description of matter is the result of the pre-diagonalization of more detailed models. We will hence use this simplest model where the medium consists of an infinite set of harmonic oscillators attached to each point of space and interacting dipolarly with the electric field. Hence, it can be seen as a continuous ensemble of electric dipoles.

We call the frequency of these oscillators ν . We represent the medium by a vector field where $\vec{X}'(\nu, \vec{r})$ is the position field and $\vec{\Pi}'_X(\nu, \vec{r})$ is the momentum field, with \vec{r} restricted to the volume inside the medium). The Hamiltonian of this system reads

$$H_{\text{medium}} = \int_0^\infty d\nu \int_V d^3r \left[\frac{1}{2\rho(\nu, \vec{r})} \vec{\Pi}'_X{}^2(\nu, \vec{r}) + \rho(\nu, \vec{r}) \nu^2 \vec{X}'^2(\nu, \vec{r}) \right], \quad (5.3)$$

with V the region of space occupied by the medium and ρ a density of mass per frequency and volume units. It is worth noting that the position \vec{r} inside the medium plays the role of a (continuous) degeneracy index for the harmonic oscillators, while the three components of the vectors are a discrete degeneracy index.

In order to lighten the notation, we include the mass density in the canonical variables by performing the change of variable

$$\vec{\Pi}_X := \frac{1}{\sqrt{\rho}} \vec{\Pi}'_X, \quad \vec{X} := \sqrt{\rho} \vec{X}'. \quad (5.4)$$

Hence the Hamiltonian (5.3) reads

$$H_{\text{medium}} = \int_0^\infty d\nu \int_V d^3r \left[\frac{1}{2} \vec{\Pi}_X^2 + \nu^2 \vec{X}^2 \right]. \quad (5.5)$$

5.1.3 Interaction

In order to construct the interaction between the material medium and light, we need to define how the degrees of freedom of the medium are affected by the electromagnetic field. The charged oscillators interact with the electric field through the electric Lorentz force (we consider no magnetic response), such that the equation of motion of the matter field reads

$$\rho(\nu, \vec{r}) \partial_t^2 \vec{X}'(\nu, \vec{r}, t) = -\rho(\nu, \vec{r}) \nu^2 \vec{X}'(\nu, \vec{r}, t) + \alpha'(\nu, \vec{r}) \vec{E}(\vec{r}, t), \quad (5.6)$$

where α' is the charge density of the dipoles and the temporal dependence is implicit in the vector fields. The dipoles create a current density which sums up current densities of each frequency of oscillation:

$$\vec{j}(\vec{r}, t) = \int_0^\infty d\nu \alpha'(\nu, \vec{r}) \partial_t \vec{X}'(\nu, \vec{r}, t). \quad (5.7)$$

With the change of variable (5.4), Eq. (5.6) becomes

$$\partial_t^2 \vec{X}(\nu, \vec{r}, t) = -\nu^2 \vec{X}(\nu, \vec{r}, t) + \alpha(\nu, \vec{r}) \vec{E}(\vec{r}, t), \quad (5.8)$$

where we have introduced

$$\alpha = \frac{\alpha'}{\sqrt{\rho}}. \quad (5.9)$$

We can link the current density (5.7) to a macroscopic polarization density through $\vec{j} = \partial_t \vec{\mathfrak{P}}$, which leads to

$$\vec{\mathfrak{P}}(\vec{r}, t) = \int_0^\infty dv \alpha'(v, \vec{r}) \vec{X}'(v, \vec{r}, t) = \int_0^\infty dv \alpha(v, \vec{r}) \vec{X}(v, \vec{r}, t). \quad (5.10)$$

We thus have an expression of the polarization density in terms of the degrees of freedom of matter and a coupling function α yet to be determined. The justification of this interaction model will be found in the following section by its relation with the macroscopic Maxwell equations. A key point is to find the connection between the coupling function α and the causal response function χ (or equivalently, with the dielectric function).

5.1.4 Equivalence with Maxwell's macroscopic equations

The macroscopic Maxwell equations for a non-magnetic medium read

$$\partial_t \vec{E} = c^2 \nabla \times \nabla \times \vec{A} - \frac{1}{\epsilon_0} \partial_t \vec{\mathfrak{P}}, \quad (5.11a)$$

$$\partial_t \vec{A} = -\vec{E} - \nabla U, \quad (5.11b)$$

$$\nabla \cdot \vec{E} = -\frac{1}{\epsilon_0} \nabla \cdot \vec{\mathfrak{P}}, \quad (5.11c)$$

$$\vec{B} = \nabla \times \vec{A}, \quad (5.11d)$$

with a polarization density that can be split into a spontaneous term $\vec{\mathfrak{P}}_{sp}$ and an induced term $\vec{\mathfrak{P}}_{ind}$ (since the medium is supposed surrounded by vacuum, there is no external term). The spontaneous polarization density depends on initial conditions of the medium that are unknown in general. The induced polarization density is related to the electric field with a causal response function χ :

$$\vec{\mathfrak{P}}_{ind}(\vec{r}, t) = \epsilon_0 \int_{-\infty}^\infty dt' \chi(\vec{r}, t - t') \vec{E}(\vec{r}, t'), \quad (5.12)$$

with $\chi = 0$ for \vec{r} in the exterior of the medium. We show now that the microscopic model constructed in the preceding paragraphs can be equivalent to the macroscopic Maxwell equations.

We first write the general solution of the equation of motion of the matter field (5.8):

$$\vec{X}(v, \vec{r}, t) = \vec{a}(v, \vec{r}) \cos(vt) + \frac{\vec{b}(v, \vec{r})}{v} \sin(vt) + \frac{\alpha(v, \vec{r})}{v} \int_{-\infty}^t dt' \sin[v(t - t')] \vec{E}(\vec{r}, t'), \quad (5.13)$$

where \vec{a} and \vec{b} are arbitrary vectors constant in time. Inserting this solution into the polarization density (5.10) gives two contributions which we identify to a spontaneous and an induced term:

$$\vec{\mathfrak{P}}_{sp}(\vec{r}, t) = \int_0^\infty dv' \alpha(v', \vec{r}) \left[\vec{a}(v', \vec{r}) \cos(v't) + \frac{\vec{b}(v', \vec{r})}{v'} \sin(v't) \right], \quad (5.14a)$$

$$\vec{\mathfrak{P}}_{ind}(\vec{r}, t) = \int_0^\infty dv' \alpha(v', \vec{r}) \left[\int_{-\infty}^t dt' \frac{\alpha(v', \vec{r})}{v'} \sin[v'(t - t')] \vec{E}(\vec{r}, t') \right]. \quad (5.14b)$$

Since the variables v' and t' are independent, we can exchange the order of the integrals in Eq. (5.14b), which gives exactly the definition (5.12) but with a response function given by

$$\chi(\vec{r}, t - t') = \theta(t - t') \int_0^\infty dv' \frac{\alpha^2(v', \vec{r})}{\epsilon_0 v'} \sin[v'(t - t')]. \quad (5.15)$$

The Heaviside function $\theta(t - t')$ stands for the causality of the response of the medium. We have thus made the link between the polarization density as introduced in the Maxwell equations and the one constructed in the microscopic model. This link depends on the coupling function α which we shall calculate now.

We take the Fourier transform of Eq. (5.15):

$$\tilde{\chi}(v, \vec{r}) = \int_0^\infty dv' \frac{\alpha^2(v', \vec{r})}{\epsilon_0 v'} \int_0^\infty dt e^{ivt} \sin(v't), \quad \text{with } v \in \mathbb{R}, v' \in \mathbb{R}_+. \quad (5.16)$$

We evaluate the last integral using

$$\begin{aligned} \int_0^\infty dt e^{ivt} \sin(v't) &= \frac{1}{2i} \int_0^\infty dt \left[e^{i(v'+v)t} - e^{-i(v'-v)t} \right], \\ &= \frac{1}{2} \left[\frac{1}{v' + v + i0^+} + \frac{1}{v' - v - i0^+} \right], \end{aligned} \quad (5.17)$$

where 0^+ stands for the limit $\frac{1}{\lambda \pm 0^+} \equiv \lim_{\epsilon \rightarrow 0} \frac{1}{\lambda \pm \epsilon}$ with $\epsilon > 0$. These terms can be interpreted as distributions depending on the variable v and they satisfy the identity

$$\frac{1}{v' \pm v \pm i0^+} = \mathcal{P} \frac{1}{v' \pm v} \mp i\pi \delta(v' \pm v), \quad (5.18)$$

with \mathcal{P} the Cauchy principal value as defined in Eq. (1.18). The Fourier transform of the response function χ thus gives $\tilde{\chi} = \tilde{\chi}_R + i\tilde{\chi}_I$, with

$$\tilde{\chi}_R(v, \vec{r}) = \frac{1}{\epsilon_0} \mathcal{P} \int_0^\infty dv' \frac{\alpha^2(v', \vec{r})}{v'^2 - v^2}, \quad (5.19a)$$

$$\tilde{\chi}_I(v, \vec{r}) = -\frac{\pi}{2} \int_0^\infty dv' \delta(v' + v) \frac{\alpha^2(v')}{\epsilon_0 v'} + \frac{\pi}{2} \int_0^\infty dv' \delta(v' - v) \frac{\alpha^2(v')}{\epsilon_0 v'}. \quad (5.19b)$$

For these expressions to be well defined, the function $\alpha^2(v')$ must be integrable for $v' \rightarrow 0$. We have to distinguish the positive and the negative values of v , for which either the first or the second term of the right-hand side of (5.19b) vanishes (due to the delta functions):

$$\tilde{\chi}_I(v, \vec{r}) = \begin{cases} -\frac{\pi}{2} \frac{\alpha^2(|v|, \vec{r})}{\epsilon_0 |v|} & \text{for } v < 0 \\ \frac{\pi}{2} \frac{\alpha^2(|v|, \vec{r})}{\epsilon_0 v} & \text{for } v > 0 \end{cases} = \frac{\pi}{2} \frac{\alpha^2(|v|, \vec{r})}{\epsilon_0 v}. \quad (5.20)$$

We remark that

$$\tilde{\chi}_R(-v) = \tilde{\chi}_R(v), \quad (5.21a)$$

$$\tilde{\chi}_I(-v) = -\tilde{\chi}_I(v), \quad (5.21b)$$

$$\tilde{\chi}(-v) = \tilde{\chi}^*(v). \quad (5.21c)$$

Finally, since by definition the dielectric coefficient is $\epsilon = 1 + \tilde{\chi}$, the coupling function can be expressed in terms of the imaginary part of the dielectric coefficient as

$$\alpha^2(\nu, \vec{r}) = \frac{2\epsilon_0}{\pi} \nu \epsilon_I(\nu, \vec{r}), \quad \nu > 0. \quad (5.22)$$

The microscopic model is thus consistent with the macroscopic Maxwell equations with a polarization density expressed in terms of the coupling function α and the matter degrees of freedom. Note that since ϵ_I is necessarily positive in a lossy medium, then α is real.

Because of Eq. (5.22), the relations (5.19a) and (5.19b) are the same as the Kramers-Kronig relations (1.25). For the microscopic model to be well-defined, the dielectric function must therefore be chosen such that it satisfies the Kramers-Kronig relations.

5.1.5 Hamiltonian structure

In order to construct the Hamiltonian structure of the system, we start by choosing a gauge for the electromagnetic variables (the matter vector fields are not constrained). We adopt a Coulomb gauge such that $\nabla \cdot \vec{A} = 0$ and such that the equations for \vec{A} are decoupled from the scalar potential U . For this purpose, we separate the polarization into its transverse and longitudinal parts

$$\vec{\mathfrak{P}} = \vec{\mathfrak{P}}^\perp + \vec{\mathfrak{P}}^\parallel. \quad (5.23)$$

One can show that there is a gauge transformation such that

$$\nabla \cdot \vec{A} = 0, \quad \nabla U = \frac{1}{\epsilon_0} \vec{\mathfrak{P}}^\parallel. \quad (5.24)$$

We can write the wave equation from Maxwell's equations by introducing Eq. (5.11b) into Eq. (5.11a):

$$\partial_t^2 \vec{A} = c^2 \Delta \vec{A} + \frac{1}{\epsilon_0} \partial_t \vec{\mathfrak{P}}^\perp, \quad (5.25)$$

where $\Delta = (\nabla \nabla \cdot) - (\nabla \times \nabla \times)$ is the Laplacian operator. Replacing the polarization density by its expression (5.10), we get

$$\partial_t^2 \vec{A}(\vec{r}, t) = c^2 \Delta \vec{A}(\vec{r}, t) + \frac{1}{\epsilon_0} \left[\int_0^\infty d\nu \alpha(\nu, \vec{r}) \partial_t \vec{X}(\nu, \vec{r}, t) \right]^\perp. \quad (5.26)$$

We now introduce a new vector $\vec{\Pi}_A$ verifying

$$\vec{\Pi}_A := -\epsilon_0 \vec{E} - \vec{\mathfrak{P}} = -\epsilon_0 \vec{E}^\perp - \vec{\mathfrak{P}}^\perp = -\vec{\mathfrak{D}}, \quad (5.27)$$

with $\vec{\mathfrak{D}}$ the *electric displacement*. It satisfies the gauge condition $\nabla \cdot \vec{\Pi}_A = 0 = \nabla \cdot \vec{\mathfrak{D}}$. Eq. (5.26) can be split into two coupled equations:

$$\partial_t \vec{\Pi}_A(\vec{r}, t) = \epsilon_0 c^2 \Delta \vec{A}(\vec{r}, t), \quad (5.28a)$$

$$\partial_t \vec{A}(\vec{r}, t) = \frac{1}{\epsilon_0} \vec{\Pi}_A(\vec{r}, t) + \frac{1}{\epsilon_0} \left[\int_0^\infty d\nu \alpha(\nu, \vec{r}) \vec{X}(\nu, \vec{r}, t) \right]^\perp. \quad (5.28b)$$

We also split the equation of motion (5.8) into first-order equations with the momentum $\vec{\Pi}_X$:

$$\partial_t \vec{X}(\nu, \vec{r}, t) = \vec{\Pi}_X(\nu, \vec{r}, t), \quad (5.28c)$$

$$\begin{aligned} \partial_t \vec{\Pi}_X(\nu, \vec{r}, t) &= -\nu^2 \vec{X}(\nu, \vec{r}, t) + \alpha(\nu, \vec{r}) \vec{E}(\vec{r}, t) \\ &= -\nu^2 \vec{X}(\nu, \vec{r}, t) - \frac{\alpha(\nu, \vec{r})}{\epsilon_0} \left[\vec{\Pi}_A(\nu, \vec{r}, t) + \vec{\mathfrak{P}}(\vec{r}, t) \right]. \end{aligned} \quad (5.28d)$$

Remark: The transversality conditions are preserved by the time evolution. It follows from the infinitesimal time evolution determined by Eqs. (5.28a),(5.28b):

$$\vec{\Pi}_A(\vec{r}, t + \delta t) = \vec{\Pi}_A(\vec{r}, t) + \delta t \epsilon_0 c^2 \Delta \vec{A}(\vec{r}, t), \quad (5.29a)$$

$$\vec{A}(\vec{r}, t + \delta t) = \vec{A}(\vec{r}, t) + \delta t \frac{1}{\epsilon_0} \left[\vec{\Pi}_A(\vec{r}, t) + \vec{\mathfrak{P}}^\perp(\vec{r}, t) \right]. \quad (5.29b)$$

Thus if $\nabla \cdot \vec{\Pi}_A(\vec{r}, t) = 0 = \nabla \cdot \vec{A}(\vec{r}, t)$ at some time t , then it will also be the case for all later times.

The system of equations (5.28) forms a set of Hamilton equations with a Hamiltonian function H , such that

$$\partial_t \vec{\Pi}_A = -\frac{\delta H}{\delta \vec{A}}, \quad \partial_t \vec{A} = \frac{\delta H}{\delta \vec{\Pi}_A}, \quad (5.30a)$$

$$\partial_t \vec{\Pi}_X = -\frac{\delta H}{\delta \vec{X}}, \quad \partial_t \vec{X} = \frac{\delta H}{\delta \vec{\Pi}_X}, \quad (5.30b)$$

with the Hamiltonian given by

$$H = H_{\text{elm}} + H_{\text{med}} + H_s + H_i, \quad (5.31)$$

$$\text{with } H_{\text{elm}} = \int d^3 r \left[\frac{1}{2\epsilon_0} \vec{\Pi}_A^2 - \frac{1}{2\mu_0} \vec{A} \cdot \Delta \vec{A} \right], \quad (5.32)$$

$$H_{\text{med}} = \int_0^\infty dv \int_V d^3 r \left[\frac{1}{2} \vec{\Pi}_X^2 + \frac{1}{2} v^2 \vec{X}^2 \right], \quad (5.33)$$

$$H_s = \frac{1}{2\epsilon_0} \int_V d^3 r \left[\int_0^\infty dv \alpha \vec{X} \right]^2, \quad (5.34)$$

$$\begin{aligned} H_i &= \frac{1}{\epsilon_0} \int d^3 r \vec{\Pi}_A \cdot \mathcal{P}^\perp \int_0^\infty dv \alpha \vec{X}, \\ &= \frac{1}{\epsilon_0} \int d^3 r \mathcal{P}^\perp \vec{\Pi}_A \cdot \int_0^\infty dv \alpha \vec{X}, \end{aligned} \quad (5.35)$$

where \mathcal{P}^\perp is the projector onto transverse fields. The first contribution H_{elm} corresponds to the classical energy of radiation (2.13) but with a polarization density (5.10) which now includes an inhomogeneous and dispersive coupling with the medium. The term H_{med} is the Hamiltonian of the harmonic oscillators of the medium. H_i and H_s are respectively a contribution *induced* by the interaction between the oscillators and the field, and a contribution of *self-interaction* inside the medium. In the no-coupling limit where $\alpha = 0$, H_{elm} tends to the energy of electromagnetic radiation in vacuum, H_{med} tends to the energy of free oscillators, and both interaction parts go to zero.

Remark: A careful inspection of Hamilton's equations (5.30) shows that it does give the equations (5.28) except for the term with $\vec{\Pi}_A$ in (5.28d) which is replaced by $\mathcal{P}^\perp \vec{\Pi}_A$. They however coincide when the fields are chosen transverse at an initial condition since in that case $\mathcal{P}^\perp \vec{\Pi}_A(t) = \vec{\Pi}_A(t)$ for all t .

5.1.6 Coupling function in standard models

There exists a model described by the Hamiltonian (5.31) for each coupling function α satisfying the condition (5.22), i.e., for each model of the permittivity one can consider physically relevant in a given scenario. We give here explicit formulas for the coupling function in two standard models: the Drude and the Lorentz models. Since they have been constructed in Chapter 1 Section 1.3, we can start from the results therein.

Drude model

In the Drude model, the Fourier transform of the susceptibility is

$$\tilde{\chi}(\nu) = -\frac{\omega_p^2}{(\nu + i0^+)(\nu + i\gamma)}, \quad (5.36)$$

with ω_p the plasma frequency given in Eq. (1.55), and γ a damping coefficient which is small compared to ω_p . We can isolate the real and imaginary parts:

$$\begin{aligned} \tilde{\chi}(\nu) &= \frac{\omega_p^2}{\gamma} \left(\left[\pi\delta(\nu) - \frac{\gamma}{\nu^2 + \gamma^2} \right] + i \left[\mathcal{P} \frac{1}{\nu} - \frac{\nu}{\nu^2 + \gamma^2} \right] \right), \\ &= \frac{\omega_p^2}{\gamma} \left(\left[\pi\delta(\nu) - \frac{\gamma}{\nu^2 + \gamma^2} \right] + i \left[\mathcal{P} \frac{\gamma^2}{\nu(\nu^2 + \gamma^2)} \right] \right). \end{aligned} \quad (5.37)$$

Since the dielectric coefficient verifies $\epsilon = 1 + \tilde{\chi}$, we have

$$\epsilon_i(\nu) = \omega_p^2 \left[\mathcal{P} \frac{\gamma}{\nu(\nu^2 + \gamma^2)} \right], \quad (5.38)$$

and the coupling function is thus given by

$$\alpha^2(\nu) = \frac{2\epsilon_0}{\pi} \omega_p^2 \frac{\gamma}{\nu^2 + \gamma^2}. \quad (5.39)$$

It has the following asymptotic behavior:

$$\alpha(\nu) \rightarrow \omega_p \sqrt{\frac{2\epsilon_0}{\pi\gamma}}, \quad \text{for } \nu \rightarrow 0, \quad (5.40)$$

$$\sim \frac{\omega_p}{\nu} \sqrt{\frac{2\epsilon_0\gamma}{\pi}} \rightarrow 0, \quad \text{for } \nu \rightarrow +\infty. \quad (5.41)$$

Lorentz model

For the Lorentz model, the susceptibility is given by

$$\tilde{\chi}(\nu) = -\frac{\omega_p^2}{-\omega_0^2 + \nu(\nu + i\gamma)}, \quad (5.42)$$

with ω_0 the normal frequency of the medium. We separate the real and imaginary parts:

$$\tilde{\chi}(\nu) = -\omega_p^2 \frac{\nu^2 - \omega_0^2 - i\gamma\nu}{[\nu^2 - \omega_0^2]^2 + [\gamma\nu]^2}, \quad (5.43)$$

and thus

$$\epsilon_i(\nu) = \omega_p^2 \frac{\gamma\nu}{[\nu^2 - \omega_0^2]^2 + [\gamma\nu]^2}. \quad (5.44)$$

The coupling function is thus

$$\alpha^2(\nu) = \frac{2\epsilon_0}{\pi} \omega_p^2 \frac{\gamma\nu^2}{[\nu^2 - \omega_0^2]^2 + [\gamma\nu]^2}, \quad (5.45)$$

which has the following asymptotic behavior

$$\alpha(\nu) \rightarrow \omega_p \sqrt{\frac{2\epsilon_0\gamma}{\pi}} \frac{\nu}{\omega_0} \rightarrow 0, \quad \text{for } \nu \rightarrow 0, \quad (5.46)$$

$$\sim \sqrt{\frac{2\epsilon_0\gamma}{\pi}} \frac{\omega_p}{\nu} \rightarrow 0, \quad \text{for } \nu \rightarrow +\infty. \quad (5.47)$$

5.2 Canonical diagonalization of the model

The standard approach for diagonalizing the Hamiltonian (5.31) is used in the quantum domain: one assumes a particular structure of the quantized diagonal Hamiltonian and uses this assumption to derive expressions of the fields in terms of the diagonalizing creation-annihilation operators. This is called the Friedrichs-Fano (or simply Fano) method. The diagonalization is however non-unique and depends on free functions. Since one needs the transformation to be canonical, an important step is to find an expression of the free functions that ensures it (which is equivalent to imposing the commutation relation of the operators in the quantum model). This method brings some issues that will be described in Chapter 6. We therefore follow instead the approach described in the main introduction, i.e., we start by finding appropriate canonical transformations that put the Hamiltonian into a harmonic-like form, and then we diagonalize its frequency operator. This method does not require to quantize in order to find the adequate diagonalizing transformation, and most importantly, it does not need any *a priori* assumption on the structure of the result.

5.2.1 Pre-diagonalization of the electromagnetic part

Before diagonalizing the whole Hamiltonian, we will first pre-diagonalize the electromagnetic part, which will thus follow the ideas used in Chapter 2 for a passive environment. We expand the fields \vec{A} and $\vec{\Pi}_A$ on a complete and orthonormal basis of eigenfunctions of the operator $c^2 \nabla \times \nabla \times$ (i.e., a complete basis of $-c^2 \Delta$ restricted to the transverse subspace), and we remove the constant ϵ_0 :

$$\vec{A}(\vec{r}) = \int d\kappa \frac{1}{\sqrt{\epsilon_0}} \vec{\varphi}_\kappa(\vec{r}) q'_\kappa, \quad (5.48a)$$

$$\vec{\Pi}_A(\vec{r}) = \int d\kappa \sqrt{\epsilon_0} \vec{\varphi}_\kappa(\vec{r}) p'_\kappa, \quad (5.48b)$$

with

$$-c^2 \Delta \vec{\varphi}_\kappa(\vec{r}) = \omega_\kappa^2 \vec{\varphi}_\kappa(\vec{r}). \quad (5.49)$$

The index κ contains all the spectral structure of the operator $-c^2 \Delta$ restricted to the transverse subspace. We choose real eigenfunctions as described in vacuum in Section 2.2.4:

$$\vec{\varphi}_{\vec{k}, \sigma, \zeta}(\vec{r}) = \begin{cases} \frac{1}{2\pi^{3/2}} \vec{\epsilon}_\sigma(\vec{k}) \cos(\vec{k} \cdot \vec{r}), & \zeta = c, \\ \frac{1}{2\pi^{3/2}} \vec{\epsilon}_\sigma(\vec{k}) \sin(\vec{k} \cdot \vec{r}), & \zeta = s, \end{cases} \quad (5.50)$$

hence $\kappa = (\vec{k}, \sigma, \zeta)$, with \vec{k} the wave vector, $\sigma = \pm$ the index for the basis of linear polarization, and $\epsilon_\pm(\vec{k})$ two real unit vectors orthogonal to \vec{k} and to each other. We have $\omega_\kappa = c|\vec{k}|$. Sometimes we may drop the label κ on ω_κ to simplify the notation.

We emphasize that the vectors $\vec{\varphi}_\kappa$ satisfy the same transversality condition as \vec{A} and $\vec{\Pi}_A$: $\nabla \cdot \vec{\varphi}_\kappa(\vec{r}) = 0$. Contrary to the passive medium, they are no longer eigenconfigurations, since they are not eigenfunctions of the frequency operator of the coupled system.

The transformation (5.48) is conceptually similar to a Fourier transform, where the phase space of electromagnetic configurations $(\vec{A}, \vec{\Pi}_A)$ is transformed into its Fourier space $(\underline{q}', \underline{p}')$, with the notation $\underline{q}' = \{q'_1, q'_2, \dots\}$. As in the expansion performed in Section 2.2.3 for passive

media, Appendix B shows that this transformation is canonical and therefore preserves the Hamiltonian structure of the model.

The Hamiltonian contributions (5.31)–(5.34) become

$$H = H_{\text{elm}} + H_{\text{med}} + H_i + H_s, \quad (5.51)$$

$$\text{with } H_{\text{elm}} = \frac{1}{2} \int d\kappa [p_\kappa'^2 + \omega_\kappa^2 q_\kappa'^2], \quad (5.52)$$

$$H_{\text{med}} = \frac{1}{2} \int_V d^3r \int_0^\infty dv [\vec{\Pi}_X^2 + v^2 \vec{X}^2], \quad (5.53)$$

$$H_i = \int d\kappa p_\kappa' \int_V d^3r \mathcal{P}^\perp \vec{\varphi}_\kappa \cdot \int_0^\infty dv \tilde{\alpha} \cdot \vec{X}, \quad (5.54)$$

$$H_s = \frac{1}{2} \int_V d^3r \left[\int_0^\infty dv \tilde{\alpha} \vec{X} \right]^2, \quad (5.55)$$

with $\tilde{\alpha} = \alpha/\sqrt{\epsilon_0}$. We have used the fact that $\alpha(\vec{r}) = 0$ for $\vec{r} \notin V$, such that the integral in H_i is reduced to an integral in the volume V only. We have also used the orthonormalization of the functions $\vec{\varphi}$:

$$\int d^3r \vec{\varphi}_\kappa(\vec{r}) \cdot \vec{\varphi}_{\kappa'}(\vec{r}) = \delta(\kappa - \kappa'), \quad (5.56)$$

where $\delta(\kappa - \kappa') = \delta(\vec{k} - \vec{k}') \delta_{\sigma\sigma'} \delta_{\zeta\zeta'}$. The transformation (5.48) therefore achieves two goals: (i) it removes the transversality constraint from the canonical variables of the electromagnetic field since this constraint is projected onto the basis of functions $\vec{\varphi}$, and (ii) it brings the Hamiltonian H_{elm} into a diagonal form.

Remark: The restriction of the Hamiltonian (5.51) to the transverse subspace can also be written as:

$$H = \frac{1}{2} \int d\kappa \omega_\kappa^2 q_\kappa'^2 + \frac{1}{2} \int_V d^3r \int_0^\infty dv [\vec{\Pi}_X^2(v, \vec{r}) + v^2 \vec{X}^2(v, \vec{r})] + \frac{1}{2} \int_V d^3r \left[\int d\kappa \vec{\varphi}_\kappa(\vec{r}) p_\kappa' + \int_0^\infty dv \tilde{\alpha}(v, \vec{r}) \vec{X}(v, \vec{r}) \right]^2. \quad (5.57)$$

This form shows explicitly that the restriction of the Hamiltonian is positive, which is an important feature to construct a harmonic-like form as will be done in Section 5.2.3.

5.2.2 Integral operators, matrix form and canonical transformations

We have shown in Chapter 2 a strategy to diagonalize a Hamiltonian of the form

$$H = \frac{1}{2} \int d\eta [P^2 + Q \cdot \Omega^2 Q], \quad (5.58)$$

with canonical variables $P(\eta)$ and $Q(\eta)$, a frequency operator Ω , and η a variable which contains all the degrees of freedom of the system (continuous or discrete, infinite or finite). In the passive environment, we had $\eta \equiv \vec{x}$, $P \equiv \vec{\Pi}_A$, $Q \equiv \vec{A}$ and $\Omega^2 = \frac{c}{\sqrt{\epsilon_R}} \nabla \times \nabla \times \frac{c}{\sqrt{\epsilon_R}}$. The diagonalization of the Hamiltonian comes down to diagonalizing the frequency operator, which was performed simply by expanding the canonical variables on a basis of its eigenfunctions. This procedure remains valid for any Hamiltonian of the harmonic-like form (5.58) and for any spectral structure. Thus, a starting step to diagonalize the Hamiltonian (5.51) is to find

its harmonic-like form. It is generally not straightforward, and one must ensure that the transformations leading to such form are canonical. In this subsection, we give tools that can help one in finding the adequate transformations.

A very practical tool is to express the Hamiltonian as the sum of scalar products. We use the notation $(\cdot|\cdot)$ for an arbitrary scalar product, meaning that for any type of variable x , the product of two functions of x can be written

$$\begin{aligned} (f|g) &= \int dx f(x)g(x) && \text{if } x \text{ is continuous,} \\ (f|g) &= \sum_x f(x)g(x) && \text{if } x \text{ is discrete.} \end{aligned}$$

The Hamiltonian (5.51) can thus be written

$$H = H_{\text{elm}} + H_{\text{med}} + H_i + H_s, \quad (5.59)$$

$$\text{with } H_{\text{elm}} = \frac{1}{2} (p'|p') + \frac{1}{2} (q'|\omega_\kappa^2 q'), \quad (5.60)$$

$$H_{\text{med}} = \frac{1}{2} (\vec{\Pi}_X|\vec{\Pi}_X) + \frac{1}{2} (\vec{X}|v^2 \vec{X}), \quad (5.61)$$

$$H_i = \frac{1}{2} (p'|B'_1 \vec{X}) + \frac{1}{2} (\vec{X}|B'_2 p'), \quad (5.62)$$

$$H_s = \frac{1}{2} (\vec{X}|A\vec{X}), \quad (5.63)$$

where A , B'_1 and B'_2 are integral operators defined by

$$[A\vec{X}](v, \vec{r}, j) := \tilde{\alpha}(v, \vec{r}) \int_V d^3 r' \int_0^\infty dv' \tilde{\alpha}(v', \vec{r}') \delta(\vec{r} - \vec{r}') X^j(v', \vec{r}'), \quad (5.64)$$

$$[B'_1 \vec{X}](\kappa) := \int_V d^3 r \int_0^\infty dv \tilde{\alpha}(v, \vec{r}) (\vec{\varphi}_\kappa(\vec{r}) \cdot \vec{X}(v, \vec{r})), \quad (5.65)$$

$$[B'_2 p'](v, \vec{r}, j) := \tilde{\alpha}(v, \vec{r}) \int d\kappa \varphi_\kappa^j(\vec{r}) p'_\kappa, \quad (5.66)$$

with j the component of the vectors. We can give a formal matrix representation of the Hamiltonian:

$$H = \frac{1}{2} \left(\begin{array}{c|c} p' & p' \\ \vec{\Pi}_X & \vec{\Pi}_X \\ \hline q' & q' \\ \vec{X} & \vec{X} \end{array} \middle| \overleftrightarrow{h} \right), \quad (5.67)$$

with

$$\overleftrightarrow{h} = \begin{bmatrix} 1 & 0 & 0 & B'_1 \\ 0 & 1 & 0 & 0 \\ 0 & 0 & I_{\omega_\kappa^2} & 0 \\ B'_2 & 0 & 0 & I_{v^2} + A \end{bmatrix}. \quad (5.68)$$

The matrix \overleftrightarrow{h} contains integral operators. The unit operator is defined by

$$[\mathbb{1}f](\eta) = \int d\eta' \delta(\eta - \eta') f(\eta') = f(\eta), \quad (5.69)$$

and

$$[I_{\omega_\kappa}^2 f](\kappa) = \int d\kappa' \omega_\kappa^2 \delta(\kappa - \kappa') f(\kappa') = \omega_\kappa^2 f(\kappa), \quad (5.70)$$

$$[I_{v^2} \vec{g}](v, \vec{r}, j) = \int dv' \int_V d^3 r' \sum_{j'} v'^2 \delta(v - v') \delta(\vec{r} - \vec{r}') \delta_{jj'} g^{j'}(v', \vec{r}') = v^2 g^j(v, \vec{r}). \quad (5.71)$$

A *diagonal* integral operator can be defined as an operator whose kernel is proportional to a delta function for each integrated variable. Thus, $\mathbb{1}$, $I_{\omega_\kappa}^2$ and I_{v^2} are diagonal operators, but not A , B_1' and B_2' . Diagonalizing the Hamiltonian H is equivalent to transforming it such that its matrix form \overleftrightarrow{h} consists of a diagonal block structure, whose blocks are diagonal operators. This representation allows one to use the intuition of linear algebra to find the adequate transformations.

We have to ensure that all transformations performed are canonical, since it is the only way to preserve the Hamiltonian structure of the initial model. We have seen in Appendix B that the pre-diagonalization was performed with a canonical transformation. In the matrix form, the definition of a canonical (or symplectic) transformation S simply has to verify

$$SJS^T = J, \quad \text{where } J = \begin{bmatrix} 0 & -\mathbb{1} \\ \mathbb{1} & 0 \end{bmatrix}. \quad (5.72)$$

With the structure of the Hamiltonian matrix form (5.68), the transformation matrices are 4×4 and we have

$$J = \begin{bmatrix} 0 & 0 & -\mathbb{1} & 0 \\ 0 & 0 & 0 & -\mathbb{1} \\ \mathbb{1} & 0 & 0 & 0 \\ 0 & \mathbb{1} & 0 & 0 \end{bmatrix}. \quad (5.73)$$

Now that we have a more practical and intuitive representation of the Hamiltonian structure of the problem, we can find the adequate (canonical) transformations to construct the harmonic-like form.

5.2.3 Finding the harmonic-like Hamiltonian

We want to write the Hamiltonian in the harmonic-like form

$$H = \frac{1}{2} (P|P) + \frac{1}{2} (Q|\Omega^2 Q). \quad (5.74)$$

Examining the matrix form (5.68), one can guess the adequate canonical transformation, which consists of swapping p' and q' and balancing the factor ω_κ^2 :

$$\begin{bmatrix} p_\kappa \\ q_\kappa \end{bmatrix} = \begin{bmatrix} -\omega_\kappa q'_\kappa \\ \frac{1}{\omega_\kappa} p'_\kappa \end{bmatrix}, \quad \forall \omega_\kappa \neq 0. \quad (5.75)$$

The transformation on all ω_κ can thus be written

$$\begin{pmatrix} p' \\ \vec{\Pi}_X \\ q' \\ \vec{X} \end{pmatrix} = S \begin{pmatrix} p \\ \vec{\Pi}_X \\ q \\ \vec{X} \end{pmatrix}, \quad \text{with } S = \begin{bmatrix} 0 & 0 & I_{\omega_\kappa} & 0 \\ 0 & \mathbb{1} & 0 & 0 \\ -I_{\omega_\kappa}^{-1} & 0 & 0 & 0 \\ 0 & 0 & 0 & \mathbb{1} \end{bmatrix}. \quad (5.76)$$

One can verify that the transformation S is canonical [it satisfies the condition (5.72) with (5.73)]. We make the change of coordinate in the Hamiltonian (5.67):

$$H = \frac{1}{2} \left(\begin{array}{c|ccc|c} p & & & & p \\ \vec{\Pi}_X & & & & \vec{\Pi}_X \\ q & & & & q \\ \vec{X} & & & & \vec{X} \end{array} \right) S^T \overleftrightarrow{\hbar} S \left(\begin{array}{c|ccc|c} p & & & & p \\ \vec{\Pi}_X & & & & \vec{\Pi}_X \\ q & & & & q \\ \vec{X} & & & & \vec{X} \end{array} \right) = \frac{1}{2} \left(\begin{array}{c|ccc|c} p & \mathbb{1} & 0 & 0 & p \\ \vec{\Pi}_X & 0 & \mathbb{1} & 0 & \vec{\Pi}_X \\ q & 0 & 0 & I_{\omega_\kappa} & q \\ \vec{X} & 0 & 0 & B_2 I_{\omega_\kappa} & \vec{X} \end{array} \right), \quad (5.77)$$

where we have used that $I_{\omega_\kappa} I_{\omega_\kappa} = I_{\omega_\kappa}^2$. We can finally write

$$H = \frac{1}{2} \left(\begin{array}{c|ccc|c} p & \mathbb{1} & 0 & 0 & p \\ \vec{\Pi}_X & 0 & \mathbb{1} & 0 & \vec{\Pi}_X \\ q & 0 & 0 & I_{\omega_\kappa} & q \\ \vec{X} & 0 & 0 & B_2 & \vec{X} \end{array} \right), \quad (5.78)$$

with $B_1 = I_{\omega_\kappa} B_1'$ and $B_2 = B_2' I_{\omega_\kappa}$ acting as

$$[B_1 \vec{X}](\kappa) := \int_V d^3 r \int_0^\infty dv \omega_\kappa \tilde{\alpha}(v, \vec{r}) (\vec{\varphi}_\kappa(\vec{r}) \cdot \vec{X}(v, \vec{r})), \quad (5.79)$$

$$[B_2 q](v, \vec{r}, j) := \tilde{\alpha}(v, \vec{r}) \int d\kappa \omega_\kappa \varphi_\kappa^j(\vec{r}) q_\kappa. \quad (5.80)$$

We introduce the new variables

$$Q = \begin{bmatrix} q \\ \vec{X} \end{bmatrix}, \quad P = \begin{bmatrix} p \\ \vec{\Pi}_X \end{bmatrix}, \quad (5.81)$$

therefore

$$H = \frac{1}{2} \left(\begin{array}{c|c} P & \mathbb{1} \\ \hline Q & \Omega^2 \end{array} \right) P = \frac{1}{2} (P|P) + \frac{1}{2} (Q|\Omega^2 Q), \quad (5.82)$$

which is the harmonic-like form with the (square of the) frequency operator given by

$$\Omega^2 = \begin{bmatrix} I_{\omega_\kappa} & B_1 \\ B_2 & I_{\nu^2} + A \end{bmatrix}. \quad (5.83)$$

We show in Appendix C that Ω^2 is self-adjoint (since it is real we simply need to show that it is symmetric).

Now that the Hamiltonian is written in the harmonic-like form, we aim at diagonalizing its frequency operator. The eigenfunctions of Ω (referred to as eigenconfigurations, like in a passive medium) will then be used to construct the quantum operators.

5.2.4 Møller wave operator

The frequency operator acts on two spaces of functions: the ‘‘electromagnetic’’ functions of $\kappa = (\vec{k}, \sigma, \zeta)$, and the ‘‘matter’’ functions of (v, \vec{r}, j) . The system thus consists of two coupled continuous spectra of frequencies ω_κ and ν respectively, with their own degeneracy structure. We can identify two scenarios: one where the frequency operator Ω contains the interaction between the two continua, and one with the frequency operator Ω_0 where the interaction is off. We can write

$$\Omega^2 = \Omega_0^2 + V, \quad (5.84)$$

with

$$\Omega_0^2 = \begin{bmatrix} I_{\omega_k^2} & 0 \\ 0 & I_{\nu^2} \end{bmatrix}, \quad V = \begin{bmatrix} 0 & B_1 \\ B_2 & A \end{bmatrix}. \quad (5.85)$$

One can choose an orthonormal basis of eigenconfigurations of the uncoupled operator Ω_0^2 (see the next subsection for our choice). We are therefore in a situation where we have a precise view of the uncoupled system and we wish to know how the coupling V perturbs it. This problem is similar to scattering processes, where an unperturbed wave travels freely from far away (typically, infinity) and encounters a local modification of the environment which modifies its shape and its trajectory. Hence, we can use a mathematical tool which is standard in scattering theories: the Møller *wave* operator. This operator can be defined in two versions, noted \mathfrak{M}_+ and \mathfrak{M}_- , as

$$\mathfrak{M}_\pm(\Omega^2, \Omega_0^2) = \lim_{t \rightarrow \mp\infty} e^{i\Omega^2 t} e^{-i\Omega_0^2 t}. \quad (5.86)$$

These operators verify $\mathfrak{M}_\pm^\dagger \mathfrak{M}_\pm = \mathbb{1}$, as well as the following *intertwining relation*:

$$\Omega^2 \mathfrak{M}_\pm = \mathfrak{M}_\pm \Omega_0^2. \quad (5.87)$$

Proof: From the definition (5.86) we add a finite time constant τ which does not modify \mathfrak{M}_\pm because of the limit:

$$\begin{aligned} \mathfrak{M}_\pm &= \lim_{t \rightarrow \mp\infty} e^{i\Omega^2(t+\tau)} e^{-i\Omega_0^2(t+\tau)} \\ &= e^{i\Omega^2\tau} \mathfrak{M}_\pm e^{-i\Omega_0^2\tau}. \end{aligned} \quad (5.88)$$

Since adding this constant should not make the Møller operator vary, i.e., $\partial\mathfrak{M}_\pm/\partial\tau = 0$, taking the derivative of (5.88) with respect to τ gives

$$0 = e^{i\Omega^2\tau} i\Omega^2 \mathfrak{M}_\pm e^{-i\Omega_0^2\tau} - e^{i\Omega^2\tau} \mathfrak{M}_\pm i\Omega_0^2 e^{-i\Omega_0^2\tau}. \quad (5.89)$$

We choose $\tau = 0$ in Eq. (5.89), which leads to Eq. (5.87).

If the spectra of Ω_0^2 and Ω^2 are absolutely continuous (which is the case in our model), \mathfrak{M}_\pm are unitary, i.e., they also satisfy $\mathfrak{M}_\pm \mathfrak{M}_\pm^\dagger = \mathbb{1}$, and the intertwining relation (5.87) implies that Ω_0^2 and Ω^2 are unitarily equivalent:

$$\Omega^2 = \mathfrak{M}_\pm \Omega_0^2 \mathfrak{M}_\pm^\dagger. \quad (5.90)$$

Thus they have the same spectrum, with the same degeneracy. Denoting ψ the eigenconfigurations of Ω^2 and ϕ the ones of Ω_0 , the Møller wave operator provides a unitary relation between them:

$$\psi = \mathfrak{M}_\pm \phi. \quad (5.91)$$

It is important to notice that ψ is associated to the same continuum eigenvalue and degeneracy as ϕ . This implies that there is a one-to-one correspondence between the uncoupled and the coupled eigenconfigurations.

The two Møller operators \mathfrak{M}_+ and \mathfrak{M}_- only differ by a unitary transformation in the degeneracy subspace:

$$\mathfrak{M}_- \phi_{\lambda, d^\lambda} = \sum_{d'^\lambda} U_{d^\lambda, d'^\lambda} \mathfrak{M}_+ \phi_{\lambda, d'^\lambda}. \quad (5.92)$$

This plays a role only in a time-dependent description of the scattering process in which we can identify *incoming* waves ϕ_{in} and *outgoing* waves ϕ_{out} (corresponding to a degeneracy of degree 2). It is standard to consider that \mathfrak{M}_+ determines the perturbation of ϕ_{in} and \mathfrak{M}_- , the one of ϕ_{out} . However in our representation, the eigenconfigurations of Ω_0^2 are stationary and both operators can be used equivalently. In this work, we arbitrarily choose to work with \mathfrak{M}_+ only.

Remark: To prove that the Møller operator is well-defined and that the basis of perturbed eigenfunctions is complete is not a trivial task. For the plasmonic model, this proof will be published in a later article.

We have two possible ways of finding the eigenfunctions of the frequency operator Ω : one is to calculate the Møller operator \mathfrak{M}_+ and apply it on the uncoupled eigenconfigurations; the other is to construct and solve a Lippmann-Schwinger, which is what we shall describe now.

5.2.5 Lippmann-Schwinger equation

Considering the definition of the Møller wave operator and how it connects the coupled eigenconfigurations to the uncoupled ones, we can deduce the following equation:

$$\psi = \phi - (\Omega^2 - \lambda^2 - i0^+)^{-1} V \phi. \quad (5.93)$$

Proof: Starting from the definition of the Møller wave operator

$$\mathfrak{M}_+(\Omega^2, \Omega_0^2) = \lim_{t \rightarrow -\infty} e^{i\Omega^2 t} e^{-i\Omega_0^2 t}, \quad (5.94)$$

we calculate the time derivative without the limit and we apply it on an eigenconfiguration ϕ of Ω_0^2 :

$$\begin{aligned} \frac{\partial}{\partial t} \left\{ e^{i\Omega^2 t} e^{-i\Omega_0^2 t} \right\} \phi &= i e^{i\Omega^2 t} (\Omega^2 - \Omega_0^2) e^{-i\Omega_0^2 t} \phi, \\ &= i e^{i\Omega^2 t} V e^{-i\Omega_0^2 t} \phi, \end{aligned} \quad (5.95)$$

where we have used $\Omega^2 = \Omega_0^2 + V$. We integrate:

$$e^{i\Omega^2 t} e^{-i\Omega_0^2 t} \phi = i \int_0^t dt' e^{i\Omega^2 t'} V e^{-i\Omega_0^2 t'} \phi + \phi. \quad (5.96)$$

We now take the limit $t \rightarrow -\infty$, hence the left-hand side becomes $\mathfrak{M}_+(\Omega^2, \Omega_0^2) \phi = \psi$. The limit in the right-hand side can be transformed using the *Abelian limit* representation [68]: if f is a bounded measurable function and the limit $t \rightarrow \mp\infty$ exists, then

$$\lim_{t \rightarrow \mp\infty} \int_0^t dt' f(t') = \lim_{\varepsilon \rightarrow \pm 0^+} \int_0^{\mp\infty} dt' f(t') e^{\pm \varepsilon t'}. \quad (5.97)$$

Thus, we have

$$\psi = \lim_{\varepsilon \rightarrow 0^+} \left[i \int_0^{-\infty} dt' e^{\varepsilon t'} e^{i\Omega^2 t'} V e^{-i\Omega_0^2 t'} \phi \right] + \phi. \quad (5.98)$$

Since ϕ is an eigenfunction of Ω_0^2 with a certain frequency λ , we use $e^{-i\Omega_0^2 t'} \phi = e^{-i\lambda^2 t'} \phi$, and

$$i \int_0^{-\infty} dt' e^{i(\Omega^2 - \lambda^2 - i\varepsilon)t'} = -(\Omega^2 - \lambda^2 - i\varepsilon)^{-1}, \quad (5.99)$$

which is introduced into Eq. (5.98) to give Eq. (5.93).

In order to evaluate the eigenconfigurations ψ explicitly using Eq. (5.93), one would need to calculate the action of the integral operator $(\Omega^2 - \lambda^2 - i\varepsilon)^{-1}$ on all functions of the form $V\phi$, which in general cannot be done before one knows the eigenvectors of Ω^2 . In other terms, in order to get an explicit expression of the action of this operator, one needs first to diagonalize it, which is essentially equivalent to diagonalizing Ω^2 .

To avoid this difficulty, instead of using Eq. (5.93), the coupled eigenconfigurations can be obtained as solutions of the *Lippmann-Schwinger equation*:

$$\psi = \phi - (\Omega_0^2 - \lambda^2 - i0^+)^{-1} V\psi. \quad (5.100)$$

Proof: For self-adjoint operators Ω_0^2 and $\Omega^2 = \Omega_0^2 + V$, we define the corresponding *resolvent operators* as

$$R_0(z) := (\Omega_0^2 - z)^{-1}, \quad (5.101)$$

$$R(z) := (\Omega^2 - z)^{-1}, \quad (5.102)$$

with $z \in \mathbb{C} \setminus \mathbb{R}$. Starting with the general identity

$$X^{-1} = Y^{-1} + Y^{-1}(Y - X)X^{-1}, \quad (5.103)$$

one obtains the following *resolvent identities*:

$$R = R_0 - R_0 V R \quad (5.104)$$

$$R_0 = R + R V R_0. \quad (5.105)$$

This also implies the identity

$$R V = R_0 V (\mathbb{1} - R V). \quad (5.106)$$

The equation (5.93) can be written as

$$\psi = (\mathbb{1} - R V) \phi. \quad (5.107)$$

Thus, we have

$$R V \phi = R_0 V (\mathbb{1} - R V) \phi = R_0 V \psi. \quad (5.108)$$

Introducing it into Eq. (5.107) gives

$$\psi = \phi - R_0 V \psi, \quad (5.109)$$

which is another way of writing the Lippmann-Schwinger equation (5.100).

We have thus shown that if ψ and ϕ satisfy the equation (5.93), then they also satisfy the Lippmann-Schwinger equation (5.100). The converse is not always true. However, if one can prove the uniqueness of the solution of the Lippmann-Schwinger equation, then it will also satisfy Eq. (5.93), and it will provide a unitary map between Ω^2 and Ω_0^2 . As shown in the next subsection, the action of the free resolvent $(\Omega_0^2 - \lambda^2 - i0^+)^{-1}$ on an arbitrary function is known explicitly in our model, which is what makes the Lippmann-Schwinger equation (5.100) useful for practical calculations.

5.2.6 Degeneracy and block structure

We use this subsection to analyze more precisely the degeneracy of the system and to provide a more detailed description of the eigenconfigurations ϕ and ψ . As mentioned earlier, the system consists of two coupled continuous spectra, one “electromagnetic” and one “material”. Each continuum has its own degeneracy structure (corresponding to all the degrees of freedom involved) which we combine in one multi-variable: κ for the electromagnetic part, μ for the matter part.

- The indices for the electromagnetic part are

$$\kappa = (\vec{k}, \sigma, \zeta). \quad (5.110)$$

This degeneracy structure is inherent of the uncoupled electromagnetic eigenvectors $\vec{\varphi}$ given in Eq. (5.50). In order to have a precise view on the degeneracy structure, we may express κ as (ω, d^ω) , i.e., the frequency ω spanning the whole spectrum and the degeneracy index d^ω associated with each frequency. The notation is however formal, and we must have a clear understanding of what it means to “count” the eigenvectors. This is given by the sum:

$$\begin{aligned} \int d\kappa &= \int d^3 k \sum_{\sigma, \zeta} \\ &= \int_0^\infty d\omega \frac{\omega^2}{c^3} \int_0^{\pi/2} d\vartheta \int_0^{2\pi} d\eta \sin \vartheta \sum_{\sigma, \zeta}, \end{aligned} \quad (5.111)$$

where we have decomposed \vec{k} on spherical coordinates using $|\vec{k}| = \omega/c$. Hence, $d^\omega \equiv (\vartheta, \eta, \sigma, \zeta)$, with

$$\sum_{d^\omega} = \frac{\omega^2}{c^3} \int_0^{\pi/2} d\vartheta \int_0^{2\pi} d\eta \sin \vartheta \sum_{\sigma, \zeta}. \quad (5.112)$$

- For the matter variables, we have

$$\mu \equiv (\nu, \vec{r}, j), \quad (5.113)$$

where \vec{r} is the position *inside* the medium only, and since the canonical variables for matter, \vec{X} and $\vec{\Pi}_X$, are 3-component vectors, $j = 1, 2, 3$ labels their components. We thus have the general form $\mu \equiv (\nu, d^\nu)$, with $d^\nu \equiv (\vec{r}, j)$ and

$$\sum_{d^\nu} = \int_V d^3 r \sum_j. \quad (5.114)$$

Figure 5.2 is a schematic representation of the spectral structures.

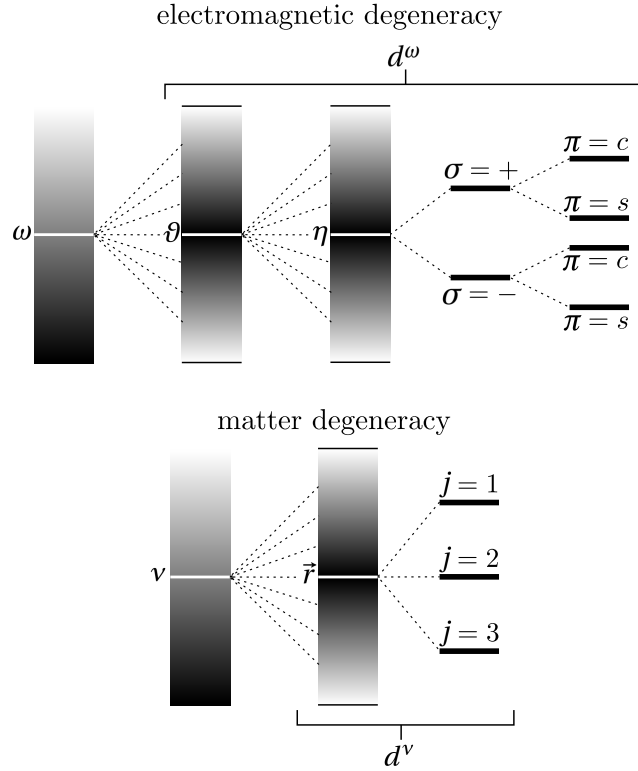


Figure 5.2 – Spectral structure of the two interacting continua that constitute the plasmonic model. Each frequency, ω or ν , is associated with a different set of continuous (but bounded) and finite discrete degeneracies.

In the space on which the frequency operator acts, the vectors have a two-block structure dictated by the matrix form of Ω^2 (or equivalently Ω_0^2) given in Eqs. (5.83) and (5.85). Thus in general, a vector ψ can be written in the same form as P and Q :

$$\psi = \begin{bmatrix} u(\kappa) \\ v(\mu) \end{bmatrix}. \quad (5.115)$$

The operator Ω_0^2 acts trivially on such a vector:

$$\Omega_0^2 \psi = \begin{bmatrix} \omega^2 u(\kappa) \\ \nu^2 v(\mu) \end{bmatrix}, \quad (5.116)$$

and similarly for any power of Ω_0 . We also have the resolvent

$$(\Omega_0^2 - \lambda^2 - i0^+)^{-1} \psi = \begin{bmatrix} \frac{1}{\omega^2 - \lambda^2 - i0^+} u(\kappa) \\ \frac{1}{\nu^2 - \lambda^2 - i0^+} v(\mu) \end{bmatrix}. \quad (5.117)$$

The eigenconfigurations of the uncoupled operator Ω_0^2 can be split into two groups: one associated with the electromagnetic spectral structure, and one with the material one. We denote the first by ϕ_κ^e and the latter by ϕ_μ^m . The choice of eigenconfigurations of Ω_0^2 is not unique; we choose the following generalized functions:

$$\phi_\kappa^e = \begin{bmatrix} \delta(\kappa - \kappa') \\ 0 \end{bmatrix} = \begin{bmatrix} \delta(\vec{k} - \vec{k}') \delta_{\zeta, \zeta'} \delta_{\sigma, \sigma'} \\ 0 \end{bmatrix}, \quad (5.118a)$$

$$\phi_\mu^m = \begin{bmatrix} 0 \\ \delta(\mu - \mu') \end{bmatrix} = \begin{bmatrix} 0 \\ \delta(\nu - \nu') \delta(\vec{r} - \vec{r}') \delta_{j, j'} \end{bmatrix}. \quad (5.118b)$$

One can easily verify, using the definition of Ω_0^2 in Eq. (5.85), that

$$\Omega_0^2 \phi_\kappa^e = \omega^2 \phi_\kappa^e, \quad (5.119)$$

$$\Omega_0^2 \phi_\mu^m = \nu^2 \phi_\mu^e, \quad (5.120)$$

assuming that

$$\int dy \delta(y - y') \delta(y - y'') = \delta(y' - y'') \quad (5.121)$$

for any continuous variable y . This is a standard assumption we will always consider valid in this thesis. The existence and unitarity of the Møller wave operator implies that the eigenvectors of Ω^2 can also be split into two groups, therefore preserving the spectral and degeneracy structures of the two continua:

$$\psi_\kappa^e = \begin{bmatrix} u_\kappa^e(\kappa') \\ v_\kappa^e(\mu') \end{bmatrix}, \quad \psi_\mu^m = \begin{bmatrix} u_\mu^m(\kappa') \\ v_\mu^m(\mu') \end{bmatrix}. \quad (5.122)$$

The one-to-one correspondence between the uncoupled and coupled eigenconfigurations is exhibited by the Lippmann-Schwinger equations:

$$\psi_\kappa^e = \phi_\kappa^e - (\Omega_0^2 - \omega^2 - i0^+) V \psi_\kappa^e, \quad (5.123a)$$

$$\psi_\mu^m = \phi_\mu^m - (\Omega_0^2 - \nu^2 - i0^+) V \psi_\mu^m. \quad (5.123b)$$

Separating the operators into their blocks given by Eq. (5.85) and using the fact that $I_\omega^{-1} = I_{\omega^{-1}}$, we have the two pairs of coupled equations for the blocks of ψ^e and ψ^m :

$$u_\kappa^e(\kappa') = \delta(\kappa - \kappa') - \frac{1}{\omega'^2 - \omega^2 - i0^+} [B_1 v_\kappa^e](\kappa'), \quad (5.124a)$$

$$v_\kappa^e(\mu') = -\frac{1}{\nu'^2 - \omega^2 - i0^+} \{ [B_2 u_\kappa^e](\mu') + [A v_\kappa^e](\mu') \}, \quad (5.124b)$$

$$u_\mu^m(\kappa') = -\frac{1}{\omega'^2 - \nu^2 - i0^+} [B_1 v_\mu^m](\kappa'), \quad (5.124c)$$

$$v_\mu^m(\mu') = \delta(\mu - \mu') - \frac{1}{\nu'^2 - \nu^2 - i0^+} \{ [B_2 u_\mu^m](\mu') + [A v_\mu^m](\mu') \}. \quad (5.124d)$$

One can therefore use these equations to find an eigenconfiguration of Ω for any frequency and degeneracy index. Finding all of the eigenconfigurations (i.e., solving the Lippmann-Schwinger equation for all κ and μ) is necessary to diagonalize entirely the frequency operator.

5.2.7 Phase space of plasmonic configurations

Because of the spectral structure of the problem, the complex phase space of the classical configurations is

$$\mathcal{P}_{\mathcal{C}, \Omega} = \mathcal{P}_{\mathcal{C}, \kappa} \oplus \mathcal{P}_{\mathcal{C}, \mu}, \quad (5.125)$$

where $\mathcal{P}_{\mathcal{C}, \kappa}$ is the phase space of (complex) electromagnetic configurations:

$$\mathcal{P}_{\mathcal{C}, \kappa}[u] = \{ u(\kappa) \mid \int d^3 k \sum_{\sigma, \zeta} |u(\vec{k}, \sigma, \zeta)|^2 < \infty \}, \quad (5.126)$$

and $\mathcal{P}_{\mathbb{C},\mu}$ is the equivalent space for the oscillators of the medium:

$$\mathcal{P}_{\mathbb{C},\mu}[\vec{v}] = \left\{ v(\mu) \mid \int dv \int_V d^3r \sum_j |v(v, \vec{r}, j)|^2 < \infty \right\}. \quad (5.127)$$

The plasmonic configurations in $\mathcal{P}_{\mathbb{C},\Omega}$ can be constructed similarly as in the passive medium:

$$\Psi = \frac{1}{\sqrt{2}} (\Omega^{1/2} Q + i\Omega^{-1/2} P), \quad (5.128)$$

and they are functions of the type

$$\Psi(\vec{k}, \sigma, \zeta, v, \vec{r}, j) = u(\vec{k}, \sigma, \zeta) \oplus v(v, \vec{r}, j), \quad (5.129)$$

or in a vector form:

$$\Psi = \begin{bmatrix} u(\vec{k}, \sigma, \zeta) \\ v(v, \vec{r}, j) \end{bmatrix}, \quad (5.130)$$

with the condition:

$$\int d\vec{k} \sum_{\sigma, \zeta} |u(\vec{k}, \sigma, \zeta)|^2 + \int dv \int d^3r \sum_j |v(v, \vec{r}, j)|^2 < \infty. \quad (5.131)$$

In the same way as in optics, we can construct plasmonic modes as classes of equivalence generated by the *normalized configurations* for which

$$\int d\vec{k} \sum_{\sigma, \zeta} |u(\vec{k}, \sigma, \zeta)|^2 + \int dv \int d^3r \sum_j |v(v, \vec{r}, j)|^2 = 1. \quad (5.132)$$

5.2.8 Orthonormalization and completeness of the eigenconfigurations

Another advantage of using the unitary Møller operator is that the orthonormality and completeness of the eigenconfigurations are preserved in the passage from Ω_0 to Ω . For any pair of eigenconfigurations $\psi_y = [u_y(\kappa) \ v_y(\mu)]^T$ and $\psi_{y'} = [u_{y'}(\kappa) \ v_{y'}(\mu)]^T$, with y and y' two labels of the spectral structure (either of type κ or μ), the orthonormality condition is given by

$$(\psi_y | \psi_{y'}) = \int d\kappa u_y^*(\kappa) u_{y'}(\kappa) + \int d\mu v_y^*(\mu) v_{y'}(\mu) = \delta(y - y'). \quad (5.133)$$

We notice that the passage to the dual space $|\psi\rangle \rightarrow (\psi|$ hides a complex conjugation which matters now that we work with complex functions (even if the uncoupled eigenconfigurations ϕ are real, the Lippmann-Schwinger equation brings complex terms to the ψ 's).

The completeness, on the other hand, is given by

$$\int dy (\psi_y) (\psi_y| = \mathbb{1}, \quad (5.134)$$

which can be more explicitly developed:

$$\begin{bmatrix} \int dy u_y(\kappa) u_y^*(\kappa') & \int dy u_y(\kappa) v_y^*(\mu) \\ \int dy v_y(\mu) u_y^*(\kappa) & \int dy v_y(\mu) v_y^*(\mu') \end{bmatrix} = \begin{bmatrix} \delta(\kappa - \kappa') & 0 \\ 0 & \delta(\mu - \mu') \end{bmatrix}. \quad (5.135)$$

Note that the integral must be performed over the whole spectral structure, i.e., $\int dy = \int d\kappa + \int d\mu$.

It is easy to verify that the eigenconfigurations of Ω_0^2 that we chose in Eq. (5.118) are orthonormal and form a complete basis, using Eq. (5.121).

5.2.9 Diagonal Hamiltonian

The diagonal form of the Hamiltonian is constructed in the complex representation, like in a passive medium (see Sec. 2.2.1). The configurations Ψ are given by (5.128) and the inverse of this equation gives

$$Q = \sqrt{\frac{1}{2}} \Omega^{-1/2} [\Psi + \Psi^*], \quad (5.136a)$$

$$P = -i \sqrt{\frac{1}{2}} \Omega^{1/2} [\Psi - \Psi^*], \quad (5.136b)$$

which can be inserted into the Hamiltonian (5.82) to give

$$H = \frac{1}{2} [(\Psi | \Omega \Psi) + c.c.]. \quad (5.137)$$

Remember that the “bra” notation implies a complex conjugation. The block structure reads

$$H = \frac{1}{2} \begin{pmatrix} \Psi & \Omega & 0 & \Psi \\ \Psi^* & 0 & \Omega & \Psi^* \end{pmatrix}. \quad (5.138)$$

We can now make use of the diagonalization that has been performed above. The eigenconfigurations of Ω^2 have been calculated using Lippmann-Schwinger equations and they can be gathered together to form the diagonalizing matrix:

$$U = \begin{bmatrix} u_\kappa^e & u_\mu^m \\ v_\kappa^e & v_\mu^m \end{bmatrix}. \quad (5.139)$$

Since the Lippmann-Schwinger equations derive from the Møller operator, it ensures that the transformation matrix U is unitary: $U^\dagger U = U U^\dagger = \mathbb{1}$. We have

$$U^\dagger \Omega^2 U = \Omega_D^2, \quad (5.140)$$

where Ω_D is the diagonalized frequency operator. Note that Eq. (5.140) is valid for any power of Ω . We introduce the operator U into the Hamiltonian (5.138):

$$\begin{aligned} H &= \frac{1}{2} \begin{pmatrix} \Psi & \left[\begin{array}{cc} U & 0 \\ 0 & U^* \end{array} \right] \left[\begin{array}{cc} U & 0 \\ 0 & U^* \end{array} \right]^\dagger \left[\begin{array}{cc} \Omega & 0 \\ 0 & \Omega \end{array} \right] \left[\begin{array}{cc} U & 0 \\ 0 & U^* \end{array} \right] \left[\begin{array}{cc} U & 0 \\ 0 & U^* \end{array} \right]^\dagger \\ \Psi^* & \end{pmatrix} \begin{pmatrix} \Psi \\ \Psi^* \end{pmatrix} \\ &= \frac{1}{2} \begin{pmatrix} \tilde{\Psi} & U^\dagger \Omega U & 0 \\ \tilde{\Psi}^* & 0 & (U^\dagger \Omega U)^* \end{pmatrix} \begin{pmatrix} \tilde{\Psi} \\ \tilde{\Psi}^* \end{pmatrix} \\ &= \frac{1}{2} \begin{pmatrix} \tilde{\Psi} & \Omega_D & 0 \\ \tilde{\Psi}^* & 0 & \Omega_D \end{pmatrix} \begin{pmatrix} \tilde{\Psi} \\ \tilde{\Psi}^* \end{pmatrix}, \end{aligned} \quad (5.141)$$

where we have used that Ω is a real operator and we introduced new complex vectors of the diagonal model:

$$\tilde{\Psi} = U^\dagger \Psi. \quad (5.142)$$

On the vectors $\tilde{\Psi}$, the diagonal operator Ω_D simply acts as a multiplication by the corresponding frequency, i.e., adopting the block structure $\tilde{\Psi} = [\tilde{z}_\kappa^e \ \tilde{z}_\mu^m]^T$,

$$\Omega_D \tilde{\Psi} = \Omega_D \begin{bmatrix} \tilde{z}_{k,\sigma,\zeta}^e \\ \tilde{z}_{v,\vec{r}}^m \end{bmatrix} = \begin{bmatrix} \omega \tilde{z}_{k,\sigma,\zeta}^e \\ \nu \tilde{z}_{v,\vec{r}}^m \end{bmatrix}. \quad (5.143)$$

Hence, the diagonal Hamiltonian (5.141) can be written as

$$H = \frac{1}{2} \int d\kappa \omega \left[\tilde{z}_\kappa^{e*} \tilde{z}_\kappa^e + \tilde{z}_\kappa^e \tilde{z}_\kappa^{e*} \right] + \frac{1}{2} \int d\mu \nu \left[\tilde{z}_\mu^{m*} \tilde{z}_\mu^m + \tilde{z}_\mu^m \tilde{z}_\mu^{m*} \right]. \quad (5.144)$$

5.3 Summary on the classical Hamiltonian system

In this Chapter we have seen that the macroscopic Maxwell equations with a dispersive and dissipative electric response can be reformulated as Hamilton equations of a Hamiltonian system, provided that we introduce a microscopic description of the medium. This description can be made with an infinite set of harmonic oscillators attached to each point of space occupied by the material medium.

We have then shown that with adequate canonical transformations, the Hamiltonian can be put in a harmonic-like form with a frequency operator Ω . The diagonalization of Ω is performed using the Møller wave operator and Lippmann-Schwinger equations, which ensure that the spectral/degeneracy structure of the initial (uncoupled) system is preserved when light interacts with the medium. We finally introduce a complex representation which paves the way to the quantization process, similarly to the passive-medium case.

Quantum plasmonics

Classical light can be thoroughly described with Maxwell's equations. Similarly, classical plasmonic fields can be analyzed using the macroscopic Maxwell equations with a choice of response function from the medium. It is the main goal of this Chapter to quantize the classical plasmonic model that we constructed in a harmonic-like form in the preceding chapter.

Section 6.1 is used to quantize the model in a way that is very similar to the procedure we used in Chapter 3 for photons. In fact, apart from technical differences stemming from the different spectral structures, the strategy and conceptual tools are the same. All difficulties that have been treated in Chapter 3 such as the isomorphism between phase spaces or the necessity to quantize first in a reduced finite-dimensional model before taking a limit to infinite dimensions in the Fock space – all these technical subtleties bring no more information than with photons; thus we leave them aside in the plasmonics model and we construct directly the quantum field model in the Bosonic Fock space.

The operators of the electromagnetic field (and in particular the electric field observable) are linked to the eigenconfigurations, i.e., the eigenfunctions of the frequency operator. In Section 6.2, we give some partial and perturbative results of the calculation of the eigenconfigurations. This requires solving a Lippmann-Schwinger equation.

The quantization of the initial plasmonic model of Chapter 5 was performed in the past, with results substantially different from our present results. In Section 6.3 we review the method used in the literature and we analyze some discrepancies it contains when applied to models with a finite medium.

Contents

6.1 Quantization	102
6.1.1 Bosonic operators and Hamiltonian	102
6.1.2 Fock space and quantum plasmons	103
6.1.3 Electric field operator	104
6.1.4 Other fields and commutation relations	105
6.1.5 No-coupling limit	106
6.2 Solving the Lippmann-Schwinger equation	107
6.2.1 Perturbative series	107
6.2.2 Small coupling regime	108

6.2.3	Small volume regime	111
6.3	Comments on the literature	115
6.3.1	Summary of the previous approaches in literature	116
6.3.2	The problem of the no-coupling limit	118
6.3.3	Justifications and proposed corrections in the literature	120
6.3.4	Addition of a modified free field	121
6.4	Summary on the quantum model	121

6.1 Quantization

6.1.1 Bosonic operators and Hamiltonian

The principle of correspondence we use to quantize the plasmonic model is the same as in a passive medium: the complex variables become quantum operators acting on the (finite) Hilbert space of configurations, then these quantum operators are associated with bosonic creation-annihilation operators of the Fock space, which are the only objects that are still well-defined when the limit to infinite dimensions is taken. Overall, this principle of correspondence can be formulated directly in the full (infinitely dimensional) model by disregarding the intermediary steps:

$$\tilde{z}_{\lambda,d\lambda} \mapsto \sqrt{\hbar} \hat{B}_{\psi_{\lambda,d\lambda}}, \quad \tilde{z}_{\lambda,d\lambda}^* \mapsto \sqrt{\hbar} \hat{B}_{\psi_{\lambda,d\lambda}}^\dagger. \quad (6.1)$$

We emphasize that, because of the diagonalizing transformation which helps construct the complex variables \tilde{z} [see Eq. (5.142)], each operator \hat{B} is associated with a plasmonic configuration Ψ , or with an eigenconfiguration $\psi_{\lambda,d\lambda}$ (i.e., an eigenfunction of Ω).

We adopt the general notation \hat{B} for the creation-annihilation operators in the Fock space. However, it is more convenient for later purposes to differentiate explicitly operators associated with the “electromagnetic” eigenconfiguration and the ones with the “matter” eigenconfiguration:

$$\tilde{z}_\kappa^e \mapsto \sqrt{\hbar} \hat{D}_{\psi_\kappa^e}, \quad \tilde{z}_\mu^m \mapsto \sqrt{\hbar} \hat{C}_{\psi_\mu^m}. \quad (6.2)$$

Since by definition each eigenconfiguration is associated with only one label κ or μ , we adopt the implicit notation

$$\hat{D}_{\psi_\kappa^e} \equiv \hat{D}_\kappa, \quad \hat{C}_{\psi_\mu^m} \equiv \hat{C}_\mu. \quad (6.3)$$

The configurations of the plasmonic field can be written as a linear combination of the eigenconfigurations,

$$\Psi = \int d\kappa a(\kappa) \psi_\kappa^e + \int d\mu b(\mu) \psi_\mu^m. \quad (6.4)$$

It can be more convenient to express it as a linear combination of the *uncoupled* eigenconfigurations,

$$\Psi = \int d\kappa c(\kappa) \phi_\kappa^e + \int d\mu d(\mu) \phi_\mu^m, \quad (6.5)$$

and because of Eq. (5.118) the coefficients are related by

$$c(\kappa) = \int d\kappa' a(\kappa') u_{\kappa'}^e(\kappa) + \int d\mu' b(\mu') u_{\mu'}^m(\kappa), \quad (6.6a)$$

$$d(\mu) = \int d\kappa' a(\kappa') v_{\kappa'}^e(\mu) + \int d\mu' b(\mu') v_{\mu'}^m(\mu). \quad (6.6b)$$

Hence, apart from very specific cases, general plasmonic configurations can be written as non-trivial combinations of purely electromagnetic and purely matter configurations.

The creation-annihilation operators associated with a configuration Ψ can be constructed as follow:

$$\hat{B}_\Psi = \hat{B} \int d\kappa a(\kappa) \psi_\kappa^e + \int d\mu b(\mu) \psi_\mu^m = \int d\kappa a^*(\kappa) \hat{D}_\kappa + \int d\mu b^*(\mu) \hat{C}_\mu. \quad (6.7)$$

Furthermore these operators satisfy the commutation relations,

$$[\hat{B}_\Psi, \hat{B}_{\Psi'}^\dagger] = (\Psi | \Psi') \mathbb{1}, \quad (6.8a)$$

$$[\hat{B}_\Psi, \hat{B}_{\Psi'}] = 0. \quad (6.8b)$$

This implies

$$[\hat{D}_\kappa, \hat{D}_{\kappa'}^\dagger] = \delta(\kappa - \kappa') \mathbb{1}, \quad [\hat{D}_\kappa, \hat{D}_{\kappa'}] = 0, \quad (6.9a)$$

$$[\hat{C}_\mu, \hat{C}_{\mu'}^\dagger] = \delta(\mu - \mu') \mathbb{1}, \quad [\hat{C}_\mu, \hat{C}_{\mu'}] = 0, \quad (6.9b)$$

and

$$[\hat{D}_\kappa, \hat{C}_\mu] = 0, \quad [\hat{D}_\kappa, \hat{C}_\mu^\dagger] = 0. \quad (6.9c)$$

Additionally, inserting the correspondence (6.2) in the diagonal Hamiltonian gives

$$\hat{H} = \frac{\hbar}{2} \int d\kappa \omega \left[\hat{D}_\kappa^\dagger \hat{D}_\kappa + \hat{D}_\kappa \hat{D}_\kappa^\dagger \right] + \frac{\hbar}{2} \int d\mu v \left[\hat{C}_\mu^\dagger \hat{C}_\mu + \hat{C}_\mu \hat{C}_\mu^\dagger \right]. \quad (6.10)$$

We however define it in the Wick ordering,

$$\hat{H} = \int d\kappa \hbar \omega \hat{D}_\kappa^\dagger \hat{D}_\kappa + \int d\mu \hbar v \hat{C}_\mu^\dagger \hat{C}_\mu. \quad (6.11)$$

6.1.2 Fock space and quantum plasmons

The Fock space is constructed in a similar way as the one for photons. It is based on the Hilbert space $\mathcal{P}_{\mathbb{C}, \Omega}$ of vectors $\Psi = [u(\kappa) v(\mu)]^T$ (described in Section 5.2.7). We remark that, like the plane waves in vacuum, the uncoupled eigenconfigurations are not square integrable and the coupled ones may not be in general. They can however be used to construct any vector Ψ from the expansions (6.4) or (6.5).

The construction of the bosonic Fock space is formally the same as in the passive medium, described in Section 3.2.1, but with the bosonic operators constructed in the preceding section. We note the plasmon states $|\Psi\rangle$ where Ψ is the classical configuration associated with the quantum state.

In passive media, we define photons as 1-quantum states in the Fock space constructed from the quantization of Maxwell's equations. We use the same approach in dispersive and dissipative media to provide a definition of quantum plasmons:

A *quantum plasmon* is a 1-quantum state in the bosonic Fock space constructed from the quantization of the macroscopic Maxwell equations with dispersion and dissipation.

Since the quantum states are built on configurations of the *coupled* system (electromagnetic field + matter field), they are generally hybrid quantum objects. This has led some authors to call them *plasmon-polaritons*.

6.1.3 Electric field operator

We can now express the electric field in terms of the complex variables \tilde{z} , then use the principle of correspondence (6.2) to transform the electric field into an operator acting on the Fock space.

We start with Eqs. (5.27) and (5.10):

$$\vec{E}(\vec{r}) = \frac{1}{\epsilon_0} [\vec{\mathfrak{D}}(\vec{r}) - \vec{\mathfrak{P}}(\vec{r})] = -\frac{1}{\epsilon_0} \vec{\Pi}_A(\vec{r}) - \frac{1}{\epsilon_0} \int_0^\infty dv \alpha(v, \vec{r}) \vec{X}(v, \vec{r}). \quad (6.12)$$

Then, we use the pre-diagonalizing transformation (5.48) combined with the transformation (5.75):

$$\vec{\Pi}_A(\vec{r}) = \int d\kappa \sqrt{\epsilon_0 \omega} \vec{\varphi}_\kappa(\vec{r}) q_\kappa, \quad (6.13a)$$

$$\vec{A}(\vec{r}) = -\int d\kappa \frac{1}{\sqrt{\epsilon_0 \omega}} \vec{\varphi}_\kappa(\vec{r}) p_\kappa, \quad (6.13b)$$

which leads to

$$\vec{E}(\vec{r}) = -\frac{1}{\sqrt{\epsilon_0}} \int d\kappa \omega \vec{\varphi}_\kappa(\vec{r}) q_\kappa - \frac{1}{\epsilon_0} \int_0^\infty dv \alpha(v, \vec{r}) \vec{X}(v, \vec{r}). \quad (6.14)$$

Inserting the unitary transformation U into Eq. (5.136a) gives

$$\begin{bmatrix} q \\ \vec{X} \end{bmatrix} = \sqrt{\frac{1}{2}} \left(U \Omega_D^{-1/2} \begin{bmatrix} \tilde{z}^e \\ \tilde{z}^m \end{bmatrix} + U^* \Omega_D^{-1/2} \begin{bmatrix} \tilde{z}^{e*} \\ \tilde{z}^{m*} \end{bmatrix} \right), \quad (6.15)$$

or more explicitly:

$$q_\kappa = \int d\kappa' \sqrt{\frac{1}{2\omega'}} u_{\kappa'}^e(\kappa) \tilde{z}_{\kappa'}^e + \int d\mu' \sqrt{\frac{1}{2\nu'}} u_{\mu'}^m(\kappa) \tilde{z}_{\mu'}^m + c.c., \quad (6.16a)$$

$$\vec{X}(v, \vec{r}) = \int d\kappa' \sqrt{\frac{1}{2\omega'}} \vec{v}_{\kappa'}^e(v, \vec{r}) \tilde{z}_{\kappa'}^e + \int d\mu' \sqrt{\frac{1}{2\nu'}} \vec{v}_{\mu'}^m(v, \vec{r}) \tilde{z}_{\mu'}^m + c.c. \quad (6.16b)$$

Now using the principle of correspondence (6.2), q and \vec{X} become operators,

$$\hat{q}_\kappa = \int d\kappa' \sqrt{\frac{\hbar}{2\omega'}} u_{\kappa'}^e(\kappa) \hat{D}_{\kappa'} + \int d\mu' \sqrt{\frac{\hbar}{2\nu'}} u_{\mu'}^m(\kappa) \hat{C}_{\mu'} + h.c., \quad (6.17a)$$

$$\vec{\hat{X}}(v, \vec{r}) = \int d\kappa' \sqrt{\frac{\hbar}{2\omega'}} \vec{v}_{\kappa'}^e(v, \vec{r}) \hat{D}_{\kappa'} + \int d\mu' \sqrt{\frac{\hbar}{2\nu'}} \vec{v}_{\mu'}^m(v, \vec{r}) \hat{C}_{\mu'} + h.c. \quad (6.17b)$$

We can finally insert them into the electric field (6.14), leading to two contributions:

$$\vec{E} = \vec{E}^e + \vec{E}^m, \quad (6.18)$$

with

$$\vec{E}^e(\vec{x}) = \int d\kappa [\vec{e}_\kappa(\vec{x}) \hat{D}_\kappa + \vec{e}_\kappa^*(\vec{x}) \hat{D}_\kappa^\dagger], \quad (6.19a)$$

$$\vec{E}^m(\vec{x}) = \int d\mu [\vec{m}_\mu(\vec{x}) \hat{C}_\mu + \vec{m}_\mu^*(\vec{x}) \hat{C}_\mu^\dagger], \quad (6.19b)$$

where

$$\vec{e}_\kappa(\vec{x}) = -\sqrt{\frac{\hbar}{2\epsilon_0\omega}} \left\{ \int d\kappa' \omega' \vec{\varphi}_{\kappa'}(\vec{x}) u_\kappa^e(\kappa') + \int_0^\infty dv' \tilde{\alpha}(v, \vec{x}) \vec{v}_\kappa^e(v', \vec{x}) \right\}, \quad (6.20a)$$

$$\vec{m}_\mu(\vec{x}) = -\sqrt{\frac{\hbar}{2\epsilon_0\nu}} \left\{ \int d\kappa' \omega' \vec{\varphi}_{\kappa'}(\vec{x}) u_\mu^m(\kappa') + \int_0^\infty dv' \tilde{\alpha}(v', \vec{x}) \vec{v}_\mu^m(v', \vec{x}) \right\}. \quad (6.20b)$$

We recall that

$$\vec{\varphi}_{\vec{k}, \sigma, \zeta}(\vec{x}) = \begin{cases} \frac{1}{2\pi^{3/2}} \vec{e}_\sigma(\vec{k}) \cos(\vec{k} \cdot \vec{x}), & \zeta = c, \\ \frac{1}{2\pi^{3/2}} \vec{e}_\sigma(\vec{k}) \sin(\vec{k} \cdot \vec{x}), & \zeta = s, \end{cases} \quad (6.21)$$

and

$$\tilde{\alpha}^2(v, \vec{x}) = \alpha^2(v, \vec{x})/\epsilon_0 = \begin{cases} \frac{2}{\pi} \nu \epsilon_I(v, \vec{x}) & \text{for } \vec{x} \in V, \\ 0 & \text{for } \vec{x} \notin V. \end{cases} \quad (6.22)$$

An important simplification takes place when one considers the observer's coordinate \vec{x} in the exterior of the medium, since there, $\alpha = 0$, and thus the second term vanishes in both expressions (6.20a) and (6.20b) (the vanishing terms correspond to the polarization density) and we end up with

$$\vec{e}_\kappa(\vec{x}_{\text{ext}}) = -\sqrt{\frac{\hbar}{2\epsilon_0\omega}} \int d\kappa' \omega' \vec{\varphi}_{\kappa'}(\vec{x}_{\text{ext}}) u_\kappa^e(\kappa'), \quad (6.23a)$$

$$\vec{m}_\mu(\vec{x}_{\text{ext}}) = -\sqrt{\frac{\hbar}{2\epsilon_0\nu}} \int d\kappa' \omega' \vec{\varphi}_{\kappa'}(\vec{x}_{\text{ext}}) u_\mu^m(\kappa'). \quad (6.23b)$$

Thus, in the exterior of the medium, the electric field operator is entirely determined by the knowledge of the *upper blocks* of the eigenconfigurations, u^e and u^m .

6.1.4 Other fields and commutation relations

For the sake of completeness, we derive here the other canonical variables and field observables. We recall the quantum version of Eq. (6.15) and the equivalent for the other two variables, coming from (5.136) and the principle of correspondence (5.142):

$$\left[\begin{array}{c} \hat{q} \\ \hat{X} \end{array} \right] = \sqrt{\frac{\hbar}{2}} \left(U \Omega_D^{-1/2} \left[\begin{array}{c} \hat{D} \\ \hat{C} \end{array} \right] + U^* \Omega_D^{-1/2} \left[\begin{array}{c} \hat{D}^\dagger \\ \hat{C}^\dagger \end{array} \right] \right), \quad (6.24)$$

$$\left[\begin{array}{c} \hat{p} \\ \hat{\Pi}_X \end{array} \right] = -i \sqrt{\frac{\hbar}{2}} \left(U \Omega_D^{1/2} \left[\begin{array}{c} \hat{D} \\ \hat{C} \end{array} \right] - U^* \Omega_D^{1/2} \left[\begin{array}{c} \hat{D}^\dagger \\ \hat{C}^\dagger \end{array} \right] \right), \quad (6.25)$$

or more explicitly,

$$\hat{q}_\kappa = \int d\kappa' \sqrt{\frac{\hbar}{2\omega'}} u_{\kappa'}^e(\kappa) \hat{D}_{\kappa'} + \int d\mu' \sqrt{\frac{\hbar}{2\nu'}} u_{\mu'}^m(\kappa) \hat{C}_{\mu'} + h.c., \quad (6.26a)$$

$$\hat{p}_\kappa = -i \left[\int d\kappa' \sqrt{\frac{\hbar\omega'}{2}} u_{\kappa'}^e(\kappa) \hat{D}_{\kappa'} + \int d\mu' \sqrt{\frac{\hbar\nu'}{2}} u_{\mu'}^m(\kappa) \hat{C}_{\mu'} - h.c. \right], \quad (6.26b)$$

$$\vec{\hat{X}}(\nu, \vec{r}) = \int d\kappa' \sqrt{\frac{\hbar}{2\omega'}} \vec{v}_{\kappa'}^e(\nu, \vec{r}) \hat{D}_{\kappa'} + \int d\mu' \sqrt{\frac{\hbar}{2\nu'}} \vec{v}_{\mu'}^m(\nu, \vec{r}) \hat{C}_{\mu'} + h.c., \quad (6.26c)$$

$$\vec{\hat{\Pi}}_X(\nu, \vec{r}) = -i \left[\int d\kappa' \sqrt{\frac{\hbar\omega'}{2}} \vec{v}_{\kappa'}^e(\nu, \vec{r}) \hat{D}_{\kappa'} + \int d\mu' \sqrt{\frac{\hbar}{2\nu'}} \vec{v}_{\mu'}^m(\nu, \vec{r}) \hat{C}_{\mu'} - h.c. \right]. \quad (6.26d)$$

We can derive the polarization density operator $\vec{\hat{\mathfrak{P}}}$ from Eq. (5.10) (note that it is non-zero inside the medium only), and the electric displacement operator $\vec{\hat{\mathfrak{D}}}$ from Eq. (6.12).

We can now calculate commutators using the bosonic commutation relations (6.9). We get

$$[\hat{q}_\kappa, \hat{p}_{\kappa'}] = i\hbar\delta(\kappa - \kappa'), \quad [\hat{X}^i(\nu, \vec{r}), \hat{\Pi}_X^j(\nu', \vec{r}')] = i\hbar\delta(\nu - \nu')\delta(\vec{r} - \vec{r}')\delta_{ij}, \quad (6.27)$$

where we have used the completeness of the eigenfunctions of Ω (5.135). Note that this condition is the only requirement to obtain the commutation relations (6.27). From this, we can use the transformations (6.13) and (6.14) to obtain two additional commutation relations:

$$[\hat{A}^i(\vec{r}), \hat{\Pi}_A^j(\vec{x})] = i\hbar\delta_T^{ij}(\vec{r} - \vec{x}), \quad [\hat{A}^i(\vec{r}), \hat{E}^j(\vec{x})] = -\frac{i\hbar}{\epsilon_0}\delta_T^{ij}(\vec{r} - \vec{x}), \quad (6.28)$$

with the transverse delta function defined as [69]

$$\delta_T^{ij}(\vec{r} - \vec{x}) = \frac{2}{3}\delta_{ij}\delta(\vec{r} - \vec{x}) - \frac{1}{4\pi|\vec{r} - \vec{x}|^3} \left(\delta_{ij} - \frac{3(r_i - x_i)(r_j - x_j)}{|\vec{r} - \vec{x}|^2} \right). \quad (6.29)$$

We have used the transversality condition of the basis of eigenfunctions of $-c^2\Delta$ given by Eq. (6.21), which reads

$$\int d\kappa \varphi_\kappa^i(\vec{r}) \varphi_\kappa^j(\vec{x}) = \delta_T^{ij}(\vec{r} - \vec{x}). \quad (6.30)$$

6.1.5 No-coupling limit

An important feature of our diagonalization and quantization procedure is that the limit $\epsilon_I \rightarrow 0$, corresponding to no coupling between the electromagnetic field and the medium, can be taken at any step of the derivation. In this scenario, the Hamiltonian is always diagonal and the quantization procedure gives the two sets of bosonic operators \hat{D}^0 and \hat{C}^0 corresponding to the bosonic operators of the two subsystems (hence, $\hat{D}^0 \equiv \hat{D}^{(\text{vac})}$). We have

$$\hat{H}^0 = \hat{H}_{\text{elm}}^0 + \hat{H}_{\text{med}}^0, \quad (6.31)$$

$$\hat{H}_{\text{elm}}^0 = \int d\kappa \hbar\omega \hat{D}_\kappa^{0\dagger} \hat{D}_\kappa^0, \quad (6.32)$$

$$\hat{H}_{\text{med}}^0 = \int d\mu \hbar\nu \hat{C}_\mu^{0\dagger} \hat{C}_\mu^0. \quad (6.33)$$

Furthermore, the Lippmann-Schwinger equation (5.123) simply gives

$$\psi_\kappa^e \rightarrow \phi_\kappa^e = \begin{bmatrix} \delta(\kappa - \kappa') \\ 0 \end{bmatrix}, \quad \psi_\mu^m \rightarrow \phi_\mu^m = \begin{bmatrix} 0 \\ \delta(\mu - \mu') \end{bmatrix}. \quad (6.34)$$

Inserting it into the expressions (6.20a) and (6.20b) gives

$$\vec{e}_\kappa(\vec{x}) \rightarrow -\sqrt{\frac{\hbar\omega}{2\epsilon_0}} \vec{\varphi}_\kappa(\vec{x}), \quad (6.35a)$$

$$\vec{m}_\mu(\vec{x}) \rightarrow 0, \quad (6.35b)$$

leading to

$$\vec{E}(\vec{x}) \rightarrow -\int d\kappa \sqrt{\frac{\hbar\omega}{2\epsilon_0}} \vec{\varphi}_\kappa(\vec{x}) [\hat{D}_\kappa^0 + \hat{D}_\kappa^{0+}]. \quad (6.36)$$

This is the expression of the electric field in vacuum (see Eq. (3.57a) with $\epsilon_R = 1$). The only difference comes from the bosonic operators which can be defined up to a phase (here of $-\pi/2$, giving the $-i$ extra factor; this difference is a result of the canonical transformation (5.75) which was not used in the passive medium).

The no-coupling limit is therefore consistent at any stage of the construction. This is a special issue that had not been addressed in any satisfying way in the previous attempts of diagonalization/quantization of the initial Hamiltonian (5.31). We discuss this in more details in Section 6.3.

6.2 Solving the Lippmann-Schwinger equation

Even though the quantum formalism for plasmonics has been constructed in the preceding sections, it is not precisely defined if one cannot calculate the normal configurations the diagonal operators are associated with. As mentioned in Section 5.2.4, one way would be to calculate directly the Møller operator. Another way is to solve the Lippmann-Schwinger equation (5.123), which is what we try to do here.

Solving the Lippmann-Schwinger equation is not trivial and cannot be done analytically because of the structure of the coupling. Solving it numerically requires a discretization of the equation and of the integral operator which will be analyzed later. First, we will give analytical techniques that can be used in perturbation theory. We will show that it depends on two perturbative parameters, which makes the perturbative regime more difficult to characterize.

6.2.1 Perturbative series

We recall the general form of the Lippmann-Schwinger equation:

$$\psi = \phi - R_0 V \psi, \quad (6.37)$$

with ψ and ϕ the eigenconfigurations of Ω and Ω_0 respectively, associated with frequency λ , R_0 the resolvent $R_0 = (\Omega_0^2 - \lambda^2 - i0^+)^{-1}$, and V the integral operator of interaction. We can rewrite this equation

$$[\mathbb{1} + R_0 V] \psi = \phi. \quad (6.38)$$

If the coupling V is small enough, we enter in the perturbative regime, and we can use $(1 + \varepsilon)^{-1} \simeq 1 - \varepsilon + \varepsilon^2 - \varepsilon^3 + \dots$, thus:

$$\psi \simeq [\mathbb{1} - R_0 V + (R_0 V)^2 - (R_0 V)^3 + \dots] \phi. \quad (6.39)$$

The coupling operator V consists of two parts, V_A for the self-interaction part, and V_B for the cross-interaction part:

$$V = V_A + V_B, \quad (6.40)$$

with

$$V_A = \begin{bmatrix} 0 & 0 \\ 0 & A \end{bmatrix}, \quad V_B = \begin{bmatrix} 0 & B_1 \\ B_2 & 0 \end{bmatrix}, \quad (6.41)$$

acting on vectors of the form $\psi = [u(\kappa) \vec{v}(\nu, \vec{r})]^T$, with the operators A , B_1 and B_2 acting as

$$[A\vec{v}](\nu, \vec{r}, j) := \tilde{\alpha}(\nu, \vec{r}) \int_0^\infty d\nu' \int_{V_m} d^3 r' \sum_{j'} \tilde{\alpha}(\nu', \vec{r}') \delta(\vec{r} - \vec{r}') \delta_{jj'} \nu'^{j'}(\nu', \vec{r}'), \quad (6.42a)$$

$$[B_1 \vec{v}](\kappa) := \int_0^\infty d\nu \int_{V_m} d^3 r \omega \tilde{\alpha}(\nu, \vec{r}) (\vec{\varphi}_\kappa(\vec{r}) \cdot \vec{v}(\nu, \vec{r})), \quad (6.42b)$$

$$[B_2 u](\nu, \vec{r}, j) := \tilde{\alpha}(\nu, \vec{r}) \int d\kappa \omega \varphi_\kappa^j(\vec{r}) u(\kappa). \quad (6.42c)$$

We can identify two main parameters which can be used to quantify the strength of the coupling: $\tilde{\alpha}$ (and thus the dissipation ε_i) and the volume of the medium V_m because of the integration over \vec{r} . The coupling has a non-trivial structure in terms of these parameters:

$$V \equiv \begin{bmatrix} 0 & \tilde{\alpha} V_m \\ \tilde{\alpha} & \tilde{\alpha}^2 \end{bmatrix}, \quad (6.43)$$

which gives rise to a perturbative series (6.39) which contains a non-trivial combination of powers of these two parameters. Thus the convergence has to be ensured both by a small dissipation factor and a small volume of the medium, almost independently. This regime will be denoted as a general *small coupling* regime and will be investigated up to the first order.

We will see further that a part of the coupling can be solved exactly, leading to a new series where the convergence can be obtained with a volume sufficiently small to compensate a strong $\tilde{\alpha}$, resulting in a *small volume* regime. This other regime will be calculated up to the second order.

6.2.2 Small coupling regime

A first regime one can investigate is the small coupling regime, where both the coefficient of losses α (i.e., the imaginary part of the dielectric function) and the volume of the medium V are small. This corresponds to calculating ψ with Eq. (6.39), stopping at any desired order of the perturbative series.

Zeroth order

The zeroth order (with no coupling) is simply given by ϕ . Thus,

$$\vec{E}(\vec{x})|_{0th} = \vec{E}^{(vac)}(\vec{x}). \quad (6.44)$$

First order

The perturbation of first order is $(R_0 V)\phi$, thus it follows straightforwardly from the definition of the coupling operator V [Eqs. (6.40)–(6.42)]:

$$(R_0 V)\phi_\kappa^e = \begin{bmatrix} 0 \\ \frac{\omega \tilde{\alpha}(\nu, \vec{r})}{\nu^2 - \omega^2 - i0^+} \vec{\varphi}_\kappa(\vec{r}) \end{bmatrix}, \quad (6.45)$$

$$(R_0 V)\phi_\mu^m = \begin{bmatrix} \frac{\omega \tilde{\alpha}(\nu, \vec{r})}{\omega^2 - \nu^2 - i0^+} \vec{\varphi}_\kappa(\vec{r}) \\ \frac{\tilde{\alpha}(\nu, \vec{r}) \tilde{\alpha}(\nu', \vec{r}')}{\nu'^2 - \nu^2 - i0^+} \delta(\vec{r} - \vec{r}') \end{bmatrix}. \quad (6.46)$$

This first order already gives an interesting result. Combining it with the zeroth order, the eigenconfigurations ψ read

$$\psi_\kappa|_{1st} = \begin{bmatrix} u_\kappa^e(\kappa') \\ v_\kappa^e(\mu) \end{bmatrix}_{1st} = \begin{bmatrix} \delta(\kappa - \kappa') \\ -\frac{\omega \tilde{\alpha}(\nu, \vec{r})}{\nu^2 - \omega^2 - i0^+} \vec{\varphi}_\kappa(\vec{r}) \end{bmatrix}, \quad (6.47a)$$

$$\psi_\mu|_{1st} = \begin{bmatrix} u_\mu^m(\kappa) \\ v_\mu^m(\mu') \end{bmatrix}_{1st} = \begin{bmatrix} -\frac{\omega \tilde{\alpha}(\mu)}{\omega^2 - \nu^2 - i0^+} \vec{\varphi}_\kappa(\vec{r}) \\ \delta(\mu - \mu') - \frac{\tilde{\alpha}(\mu') \tilde{\alpha}(\mu)}{\nu'^2 - \nu^2 - i0^+} \delta(\vec{r} - \vec{r}') \end{bmatrix}. \quad (6.47b)$$

Inserting the upper blocks into the electric field operator (6.19) gives

$$\vec{E}^e(\vec{x})|_{1st} = \vec{E}^{(\text{vac})}(\vec{x}), \quad (6.48a)$$

$$\vec{E}^m(\vec{x})|_{1st} = \sqrt{\frac{\hbar \mu_0}{\pi c^2}} \int_0^\infty d\nu \int_V d^3 r \nu^2 \epsilon_i^{1/2}(\nu, \vec{r}) [G_0(\nu; \vec{r}, \vec{x}) + F_{\text{nf}}(\nu; \vec{r}, \vec{x})] \hat{C}_{\nu, \vec{r}} + h.c., \quad (6.48b)$$

where G_0 is the Green function of the wave equation in vacuum:

$$G_0(\nu; \vec{r}, \vec{x}) = c^2 \int d\kappa \frac{\vec{\varphi}_\kappa(\vec{r}) \cdot \vec{\varphi}_\kappa(\vec{x})}{\omega^2 - \nu^2 - i0^+}, \quad (6.49)$$

and F_{nf} is a near-field term:

$$F_{\text{nf}}^{ij}(\nu; \vec{r}, \vec{x}) = -\frac{c^2}{4\pi\nu^2 |\vec{r} - \vec{x}|^3} \left(\delta_{ij} - \frac{3(r_i - x_i)(r_j - x_j)}{|\vec{r} - \vec{x}|^2} \right). \quad (6.50)$$

Proof: Introducing the upper block of (6.47b) into (6.19), replacing $\tilde{\alpha}$ by its expression (6.22) and expanding $\kappa = (\vec{k}, d)$ gives

$$E^m(\vec{x})|_{1st} = \int d^3 k \sum_d \omega \vec{\varphi}_{\vec{k}, d}(\vec{x}) \int_0^\infty d\nu \int_V d^3 r \sqrt{\frac{\hbar \epsilon_I(\nu, \vec{r})}{\pi \epsilon_0}} \frac{\omega \vec{\varphi}_{\vec{k}, d}(\vec{r})}{\omega^2 - \nu^2 - i0^+} \hat{C}_{\nu, \vec{r}} + h.c. \quad (6.51)$$

Rearranging the integrals leads to

$$E^m(\vec{x})|_{1st} = \sqrt{\frac{\hbar}{\pi \epsilon_0}} \frac{1}{c^2} \int_0^\infty d\nu \int d^3 r \epsilon_I^{1/2}(\nu, \vec{r}) L(\nu; \vec{r}, \vec{x}) \hat{C}_{\nu, \vec{r}} + h.c., \quad (6.52)$$

with

$$L(\nu; \vec{r}, \vec{x}) = c^2 \int d^3k \frac{\omega^2}{\omega^2 - \nu^2 - i0^+} \sum_d \vec{\varphi}_{\vec{k},d}(\vec{r}) \cdot \vec{\varphi}_{\vec{k},d}(\vec{x}). \quad (6.53)$$

We decompose the integrals on the spherical system of coordinates $\int dk \sum_d \equiv (1/c) \int d\omega \sum_{d_\omega}$ where

$$\sum_{d_\omega} \equiv \int_0^{\pi/2} d\vartheta \int_0^{2\pi} d\eta \frac{\omega^2}{c^2} \sin \vartheta \sum_{\sigma, \zeta}, \quad (6.54)$$

and we use the identity

$$\frac{1}{\omega^2 - \nu^2 - i0^+} = \frac{\mathcal{P}}{\omega^2 - \nu^2} + i \frac{\pi}{2\nu} \delta(\omega - \nu), \quad (\omega, \nu) > 0, \quad (6.55)$$

which gives

$$L(\nu; \vec{r}, \vec{x}) = c\mathcal{P} \int_0^\infty d\omega \frac{\omega^2}{\omega^2 - \nu^2} g(\omega; \vec{r}, \vec{x}) + i \frac{\pi c\nu}{2} g(\nu; \vec{r}, \vec{x}), \quad (6.56)$$

$$\text{with } g(\omega; \vec{r}, \vec{x}) = \sum_{d^\omega} \vec{\varphi}_{\omega, d^\omega}(\vec{r}) \cdot \vec{\varphi}_{\omega, d^\omega}(\vec{x}). \quad (6.57)$$

It is not clear whether the term in the integral converges. We can however rewrite it

$$\begin{aligned} & c\mathcal{P} \int d\omega \left(\frac{\omega^2}{\omega^2 - \nu^2} - 1 \right) g(\omega; \vec{r}, \vec{x}) + c \int d\omega g(\omega; \vec{r}, \vec{x}) \\ &= c\mathcal{P} \int d\omega \frac{\nu^2}{\omega^2 - \nu^2} g(\omega; \vec{r}, \vec{x}) + c \int d\omega g(\omega; \vec{r}, \vec{x}). \end{aligned}$$

Because of Eq. (6.57) and the completeness of the eigenfunctions $\vec{\varphi}$,

$$\int d\omega g(\omega; \vec{r}, \vec{x}) = c\delta_T(\vec{r} - \vec{x}),$$

with the transverse delta function given by Eq. (6.29). Since \vec{r} is integrated only inside the medium whereas \vec{x} is taken in the exterior, the first term in the right-hand side vanishes in our problem. Hence,

$$L(\nu; \vec{r}, \vec{x}) = \nu^2 \left[c\mathcal{P} \int d\omega \frac{g(\omega; \vec{r}, \vec{x})}{\omega^2 - \nu^2} + i \frac{\pi c}{2\nu} g(\nu; \vec{r}, \vec{x}) + F_{\text{nf}}(\nu; \vec{r}, \vec{x}) \right] \quad (6.58)$$

$$= \nu^2 \left[c \int d\omega \frac{g(\omega; \vec{r}, \vec{x})}{\omega^2 - \nu^2 - i0^+} + F_{\text{nf}}(\nu; \vec{r}, \vec{x}) \right], \quad (6.59)$$

$$= \nu^2 \left[c^2 \int d^3k \sum_d \frac{\vec{\varphi}_{\vec{k},d}(\vec{r}) \cdot \vec{\varphi}_{\vec{k},d}(\vec{x})}{\omega^2 - \nu^2 - i0^+} + F_{\text{nf}}(\nu; \vec{r}, \vec{x}) \right], \quad (6.60)$$

where

$$F_{\text{nf}}^{ij}(\nu; \vec{r}, \vec{x}) := -\frac{c^2}{4\pi\nu^2|\vec{r} - \vec{x}|^3} \left(\delta_{ij} - \frac{3(r_i - x_i)(r_j - x_j)}{|\vec{r} - \vec{x}|^2} \right). \quad (6.61)$$

In (6.60) we recognize the Green function in vacuum (see e.g. [70] Section 8.4, with an extra term to avoid the singularity):

$$G_0(v; \vec{r}, \vec{x}) = c^2 \int d^3k \sum_d \frac{\vec{\Phi}_{\vec{k},d}(\vec{r}) \cdot \vec{\Phi}_{\vec{k},d}(\vec{x})}{\omega^2 - v^2 - i0^+}, \quad (6.62)$$

hence

$$L = v^2 [G_0 + F_{\text{nf}}]. \quad (6.63)$$

Introducing it back into Eq. (6.52) and using $\epsilon_0 \mu_0 c^2 = 1$, we obtain the electric field (6.48b).

The result in first order perturbation theory is very interesting because it can easily be compared with the result of the literature. This comparison is provided in detail in Section 6.3.

6.2.3 Small volume regime

We have seen in the preceding subsection that one can solve the Lippmann-Schwinger equation analytically as a perturbation series, provided that both the coupling function $\tilde{\alpha}$ and the volume of the medium V_m are small. The result in first order also provides an interesting comparison with the earlier results in the literature. However, because of the structure of the coupling with two perturbative parameters, it is not easy to compare the strength of the different orders. Furthermore, having $\tilde{\alpha}$ as a perturbative parameter is problematic in some setups where the electromagnetic field highly couples with the dissipative medium.

In this subsection, we show how we can partially solve the Lippmann-Schwinger equation in an exact manner, removing the coupling function $\tilde{\alpha}$ from the parameters of the perturbation theory. We will thus enter into a small *volume* regime, since only the volume of the medium will have to be considered small. To be more precise, the coupling function will still appear alongside with the volume in the series, but never alone, meaning that the criterion for convergence will be to choose a volume small enough to compensate the strength of $\tilde{\alpha}$. This should be well-suited to analyze the coupling with nanostructures.

Partial exact diagonalization

The key idea here is in a first step to solve analytically the Lippmann-Schwinger equation (5.93) without the coupling V_B . It reads:

$$\Phi = \phi - (\Omega_A^2 - \lambda^2 - i0^+)^{-1} V_A \phi, \quad (6.64)$$

where $\Omega_A^2 = \Omega_0^2 + V_A$ and λ the eigenvalue associated with the eigenvectors ϕ of Ω_0 and Φ of Ω_A . Once we have calculated the vectors Φ we can construct a new Lippmann-Schwinger equation for the final vectors ψ in terms of the Φ 's:

$$\psi = \Phi - (\Omega_A^2 - \lambda^2 - i0^+)^{-1} V_B \psi. \quad (6.65)$$

This is shown following the same derivations as in Section 5.2.5, replacing ϕ by Φ , Ω_0 by Ω_A and V by V_B in every line. For the sake of simplicity, we will write the coupling operator V_A in a ket-bra form

$$V_A = \begin{matrix} |0\rangle \\ \tilde{\alpha} \end{matrix} \begin{matrix} \langle 0| \\ \tilde{\alpha} \delta \end{matrix}, \quad (6.66)$$

where δ implies a multiplication by $\delta(\vec{r} - \vec{r}')$.

Let us now solve Eq. (6.64) and find the Φ 's. To solve this equation, we need to calculate the operator

$$[\Omega_A^2 - \lambda^2 - i0^+]^{-1} V_A = [\Omega_A^2 - \lambda^2 - i0^+]^{-1} \begin{vmatrix} 0 \\ \tilde{\alpha} \end{vmatrix} \left\langle \begin{vmatrix} 0 \\ \tilde{\alpha} \delta \end{vmatrix} \right|. \quad (6.67)$$

We start by evaluating the “ket” part of this operator (we denote $z = \lambda^2 + i0^+$):

$$\begin{aligned} [\Omega_A^2 - z]^{-1} \begin{vmatrix} 0 \\ \tilde{\alpha} \end{vmatrix} &= [\Omega_0^2 - z]^{-1} \begin{vmatrix} 0 \\ \tilde{\alpha} \end{vmatrix} + ([\Omega_A^2 - z]^{-1} - [\Omega_0^2 - z]^{-1}) \begin{vmatrix} 0 \\ \tilde{\alpha} \end{vmatrix}, \\ &= [\Omega_0^2 - z]^{-1} \begin{vmatrix} 0 \\ \tilde{\alpha} \end{vmatrix} - [\Omega_0^2 - z]^{-1} V_A [\Omega_A^2 - z]^{-1} \begin{vmatrix} 0 \\ \tilde{\alpha} \end{vmatrix} \\ &= [\Omega_0^2 - z]^{-1} \begin{vmatrix} 0 \\ \tilde{\alpha} \end{vmatrix} - [\Omega_0^2 - z]^{-1} \begin{vmatrix} 0 \\ \tilde{\alpha} \end{vmatrix} \left\langle \begin{vmatrix} 0 \\ \tilde{\alpha} \delta \end{vmatrix} \right| [\Omega_A^2 - z]^{-1} \begin{vmatrix} 0 \\ \tilde{\alpha} \end{vmatrix}. \end{aligned} \quad (6.68)$$

We denote

$$f(z) := \left\langle \begin{vmatrix} 0 \\ \tilde{\alpha} \delta \end{vmatrix} \right| [\Omega_A^2 - z]^{-1} \begin{vmatrix} 0 \\ \tilde{\alpha} \end{vmatrix}, \quad (6.69)$$

hence

$$[\Omega_A^2 - z]^{-1} \begin{vmatrix} 0 \\ \tilde{\alpha} \end{vmatrix} = [\Omega_0^2 - z]^{-1} \begin{vmatrix} 0 \\ \tilde{\alpha} \end{vmatrix} - [\Omega_0^2 - z]^{-1} \begin{vmatrix} 0 \\ \tilde{\alpha} \end{vmatrix} f(z). \quad (6.70)$$

We recall that Ω_0 simply acts as a multiplication by the frequency, thus the only unknown is $F(z)$. Multiplying (6.70) from the left by $\left\langle \begin{vmatrix} 0 \\ \tilde{\alpha} \delta \end{vmatrix} \right|$, we obtain

$$f(z) = f_0(z) - f_0(z) f(z), \quad (6.71)$$

$$\text{with } f_0(z) = \left\langle \begin{vmatrix} 0 \\ \tilde{\alpha} \delta \end{vmatrix} \right| [\Omega_0^2 - z]^{-1} \begin{vmatrix} 0 \\ \tilde{\alpha} \end{vmatrix}. \quad (6.72)$$

We therefore have

$$f(z) = f_0(z)(1 + f_0(z))^{-1}. \quad (6.73)$$

It is easy to calculate explicitly f_0 . Indeed,

$$f_0(\lambda^2 + i0^+) = \int_0^\infty d\nu' \int_V d^3 r' \frac{|\tilde{\alpha}(\nu', \vec{r}')|^2}{\nu'^2 - \lambda^2 - i0^+} \delta(\vec{r}' - \vec{r}). \quad (6.74)$$

Using the fact that $\tilde{\alpha}^2(\vec{r}, \nu) = \frac{2}{\pi} \nu \epsilon_I(\vec{r}, \nu)$ with $\epsilon = \epsilon_R + i\epsilon_I$ the dielectric permittivity of the medium, we can make use of the Kramers-Kronig relation:

$$\int_0^\infty d\nu' \frac{\tilde{\alpha}^2(\nu', \vec{r}')}{\nu'^2 - \lambda^2 - i0^+} = \epsilon(\lambda, \vec{r}') - 1. \quad (6.75)$$

Therefore,

$$f_0(\lambda^2 + i0^+) \rightarrow f_0(\lambda^2) = \epsilon(\lambda, \vec{r}) - 1. \quad (6.76)$$

Introducing it into (6.73) gives

$$f(\lambda^2) = 1 - \frac{1}{\epsilon(\vec{r}, \lambda_\sigma)}. \quad (6.77)$$

We can now replace in (6.70):

$$[\Omega_A^2 - \lambda_\sigma^2 - i0^+]^{-1} \begin{bmatrix} 0 \\ \tilde{\alpha} \end{bmatrix} = \frac{1}{\epsilon(\vec{r}, \lambda_\sigma)} [\Omega_0^2 - \lambda_\sigma^2 - i0^+]^{-1} \begin{bmatrix} 0 \\ \tilde{\alpha} \end{bmatrix}. \quad (6.78)$$

We introduce this result into (6.67) then into (6.64); we use the expression of the uncoupled eigenvectors

$$\phi_\kappa = \begin{bmatrix} \delta(\kappa - \kappa') \\ 0 \end{bmatrix}, \quad \phi_\mu = \begin{bmatrix} 0 \\ \delta(\mu - \mu') \end{bmatrix}, \quad (6.79)$$

and we obtain

$$\Phi_\kappa := \begin{bmatrix} \tilde{u}_\kappa(\kappa') \\ \tilde{v}_\kappa(\mu') \end{bmatrix} = \begin{bmatrix} \delta(\kappa - \kappa') \\ 0 \end{bmatrix}, \quad (6.80a)$$

$$\Phi_\mu := \begin{bmatrix} \tilde{u}_\mu(\kappa') \\ \tilde{v}_\mu(\mu') \end{bmatrix} = \begin{bmatrix} 0 \\ \delta(\mu - \mu') - \frac{1}{\epsilon(\mu)} \frac{\tilde{\alpha}(\mu') \tilde{\alpha}(\mu)}{v'^2 - v^2 - i0^+} \delta(\vec{r} - \vec{r}') \end{bmatrix}. \quad (6.80b)$$

As one could expect, since the coupling V_A only acts on the lower block of the uncoupled eigenvectors, only the matter continuum (i.e., the $\phi^{m'}$'s) is affected. The vectors ϕ^e remain the same.

Now that the Φ 's have been calculated, we can insert them into Eq. (6.65). However, in order to solve this final equation, we need to know how the operator $(\Omega_A^2 - \lambda^2 - i0^+)^{-1} V_B$ acts.

First, we can write the operator V_B as the sum of two ket-bras:

$$V_B = \begin{bmatrix} 0 \\ \tilde{\alpha} \end{bmatrix} \langle \beta | + \begin{bmatrix} 1 \\ 0 \end{bmatrix} \langle 0 | \begin{bmatrix} 0 \\ \beta \tilde{\alpha} \end{bmatrix}, \quad (6.81)$$

where β is the multiplication by $\beta_\kappa(\vec{r}) = \omega \vec{\phi}_\kappa(\vec{r})$. We need to calculate how $(\Omega_A^2 - \lambda^2 - i0^+)^{-1}$ acts on the ket part of the two terms of V_B . The first one has already been calculated and gives Eq. (6.78). The second term can be calculated in a similar fashion. We find

$$(\Omega_A^2 - z)^{-1} \begin{bmatrix} 1 \\ 0 \end{bmatrix} = (\Omega_0^2 - z)^{-1} \begin{bmatrix} 1 \\ 0 \end{bmatrix} - (\Omega_0^2 - z)^{-1} \begin{bmatrix} 0 \\ \tilde{\alpha} \end{bmatrix} \langle \tilde{\alpha} \delta | (\Omega_A^2 - z)^{-1} \begin{bmatrix} 1 \\ 0 \end{bmatrix}, \quad (6.82)$$

we multiply it from the left by $\left\langle \begin{array}{c} 0 \\ \tilde{\alpha}\delta \end{array} \right|$ and we obtain

$$g(z) = g_0(z) - f_0(z)g(z), \quad (6.83)$$

$$\text{with } g(z) = \left\langle \begin{array}{c} 0 \\ \tilde{\alpha}\delta \end{array} \right| [\Omega_A^2 - z]^{-1} \left| \begin{array}{c} 1 \\ 0 \end{array} \right\rangle, \quad (6.84)$$

$$\text{and } g_0(z) = \left\langle \begin{array}{c} 0 \\ \tilde{\alpha}\delta \end{array} \right| [\Omega_0^2 - z]^{-1} \left| \begin{array}{c} 1 \\ 0 \end{array} \right\rangle, \quad (6.85)$$

and f_0 given by Eq. (6.76). Since $[\Omega_0^2 - z]^{-1}$ does not mix up the upper and lower blocks of the vectors it is applied onto (it is diagonal), thus $g_0 = 0$. Hence, using Eq. (6.76), the equation (6.83) gives

$$\epsilon(\lambda, \vec{r})g(\lambda^2) = 0. \quad (6.86)$$

We assume that $\epsilon \neq 0$ for all frequencies and points of space, implying that $g = 0$. Replacing into Eq. (6.82) gives

$$(\Omega_A^2 - z)^{-1} \left| \begin{array}{c} 1 \\ 0 \end{array} \right\rangle = (\Omega_0^2 - z)^{-1} \left| \begin{array}{c} 1 \\ 0 \end{array} \right\rangle. \quad (6.87)$$

Consequently, we have

$$(\Omega_A^2 - \lambda^2 - i0^+)^{-1} V_B = (\Omega_0^2 - \lambda^2 - i0^+)^{-1} \left\{ \frac{1}{\epsilon(\lambda, \vec{r})} \left| \begin{array}{c} 0 \\ \tilde{\alpha} \end{array} \right\rangle \left\langle \begin{array}{c} \beta \\ 0 \end{array} \right| + \left| \begin{array}{c} 1 \\ 0 \end{array} \right\rangle \left\langle \begin{array}{c} 0 \\ \beta\tilde{\alpha} \end{array} \right| \right\}. \quad (6.88)$$

In order to solve the new Lippmann-Schwinger equation (6.65), we expand it as a perturbative series in the same way as the initial equation was expanded in the small coupling regime:

$$\psi = [\mathbb{1} - R_A V_B + (R_A V_B)^2 - (R_A V_B)^3 + \dots] \Phi, \quad (6.89)$$

with $R_A = (\Omega_A^2 - \lambda^2 - i0^+)^{-1}$. We can insert in it the vector Φ from (6.80) and the operator $R_A V_B$ from (6.88), and thereby compute analytically the solutions. Since the part of the interaction involving $\tilde{\alpha}$ only is now thoroughly and exactly included as a factor $1/\epsilon$, the perturbative series as powers of $R_A V_B$ involves only powers of $\tilde{\alpha}V$, and thus the criterion for the convergence of the series is to have a volume V small enough to compensate $\tilde{\alpha}$.

Zeroth order

The zeroth order of the perturbation theory (i.e., with the coupling set to zero), we recover, as expected, the eigenvectors of Ω_0 , and thus the electric field is the one in vacuum:

$$\vec{E}(\vec{x})|_{0th} = \vec{E}^{(vac)}(\vec{x}). \quad (6.90)$$

First order

The first order of the perturbation series is given by

$$\psi|_{1st} = \Phi - (\Omega_A^2 - \lambda^2 - i0^+)^{-1} V_B \Phi, \quad (6.91)$$

with $(\Omega_A^2 - \lambda^2 - i0^+)^{-1} V_B$ given by Eq. (6.88) and Φ given by Eq. (6.80). We get straightforwardly:

$$\psi_\kappa|_{1st} = \begin{bmatrix} u_\kappa^e(\kappa') \\ v_\kappa^e(\mu) \end{bmatrix}_{1st} = \begin{bmatrix} \delta(\kappa - \kappa') \\ -\frac{1}{\epsilon(\omega, \vec{r})} \frac{\omega \tilde{\alpha}(\nu, \vec{r})}{\nu^2 - \omega^2 - i0^+} \vec{\varphi}_\kappa(\vec{r}) \end{bmatrix}, \quad (6.92a)$$

$$\psi_\mu|_{1st} = \begin{bmatrix} u_\mu^m(\kappa) \\ v_\mu^m(\mu') \end{bmatrix}_{1st} = \begin{bmatrix} -\frac{1}{\epsilon(\mu)} \frac{\omega \tilde{\alpha}(\mu)}{\omega^2 - \nu^2 - i0^+} \vec{\varphi}_\kappa(\vec{r}) \\ \delta(\mu - \mu') - \frac{1}{\epsilon(\mu)} \frac{\tilde{\alpha}(\mu') \tilde{\alpha}(\mu)}{\nu'^2 - \nu^2 - i0^+} \delta(\vec{r} - \vec{r}') \end{bmatrix}. \quad (6.92b)$$

We notice that these are the same expressions as Eq. (6.47) in the small *coupling* regime, however with the extra factor $1/\epsilon$ in v^e , u^m and v^m . Thus the electric field has the same form as Eq. (6.48) but with this extra factor:

$$\vec{E}^e(\vec{x})|_{1st} = \vec{E}^{(\text{vac})}(\vec{x}), \quad (6.93a)$$

$$\vec{E}^m(\vec{x})|_{1st} = \sqrt{\frac{\hbar \mu_0}{\pi c^2}} \int_0^\infty d\nu \int_V d^3r \nu^2 \frac{\epsilon_i^{1/2}(\nu, \vec{r})}{\epsilon(\nu, \vec{r})} [G_0(\nu; \vec{r}, \vec{x}) + F_{nl}(\nu; \vec{r}, \vec{x})] \hat{C}_{\nu, \vec{r}} + h.c. \quad (6.93b)$$

Second order

The second order term is obtained by applying twice the operator (6.88) onto the Φ 's. One can show that the different blocks up to the second order read

$$u_\kappa^e(\kappa')|_{2nd} = \delta(\kappa - \kappa') + \frac{\omega \omega'}{\omega'^2 - \omega^2 - i0^+} \int d^3r \left[1 - \frac{1}{\epsilon(\omega, \vec{r})} \right] (\vec{\varphi}_\kappa(\vec{r}) \cdot \vec{\varphi}_{\kappa'}(\vec{r})) \quad (6.94a)$$

$$v_\kappa^e(\mu)|_{2nd} = -\frac{1}{\epsilon(\omega, \vec{r})} \frac{\omega \tilde{\alpha}(\mu)}{\nu^2 - \omega^2 - i0^+} \vec{\varphi}_\kappa(\vec{r}), \quad (6.94b)$$

$$u_\mu^m(\kappa)|_{2nd} = -\frac{1}{\epsilon(\mu)} \frac{\omega \tilde{\alpha}(\mu)}{\omega^2 - \nu^2 - i0^+} \vec{\varphi}_\kappa(\vec{r}), \quad (6.94c)$$

$$v_\mu^m(\mu')|_{2nd} = \delta(\mu - \mu') - \frac{1}{\epsilon(\mu)} \frac{\tilde{\alpha}(\mu') \tilde{\alpha}(\mu)}{\nu'^2 - \nu^2 - i0^+} \delta(\vec{r} - \vec{r}') \\ + \frac{1}{\epsilon^2(\mu)} \frac{\tilde{\alpha}(\mu') \tilde{\alpha}(\mu)}{\nu'^2 - \nu^2 - i0^+} \int d\kappa \frac{\omega^2}{\omega^2 - \nu^2 - i0^+} (\vec{\varphi}_\kappa(\vec{r}') \cdot \vec{\varphi}_\kappa(\vec{r})). \quad (6.94d)$$

6.3 Comments on the literature

One can date the first article on the quantization of plasmons back to 1992, by Huttner and Barnett [71]. Their goal was to introduce dissipation in the quantization of light in a homogeneous (therefore infinite) medium. It was followed by many other works [1, 23–26, 51, 72–82, 87] which used two main approaches:

- a phenomenological approach formulated in terms of quantum Langevin equations first introduced by Gruner and Welsch in 1995 [72] and 1996 [73];

- microscopic oscillator models for the medium coupled to the electromagnetic field.

The latter are variations of models of the type first proposed by Hopfield [83], which was the approach originally used by Huttner and Barnett. Extensions of their work to inhomogeneous media were treated in [23–26]. They involve a Fano-type diagonalization in terms of bosonic creation and annihilation operators. The results of the microscopic approach were meant to provide a justification of the phenomenological quantum Langevin noise models. The main criterion for the choice of the microscopic model is that if one integrates the equations for the medium and one inserts the obtained currents into the microscopic Maxwell equations one should obtain the macroscopic Maxwell equations [26, 51].

The Hamiltonian model we have constructed in the preceding chapter thus follows the approach of Huttner and Barnett [71] and is equivalent to the construction made in [23] or in [26] without the magnetic response of the medium. However, starting from the same classical model, this approach leads to results substantially different from the formulas derived and used in the past literature. In particular, it gives a different spectral structure of the diagonalized system and a different expression of the electric field operator. Our interpretation of this discrepancy is that the former results [23–26, 51, 71–75] were obtained under the implicit hypothesis of an infinite bulk medium, although it has been extensively extrapolated to finite media in later works.

We will now summarize the quantization procedure of Refs. [23–26] and point out explicitly how the formulas obtained in this approach lead to inconsistent results in some regimes. Then we will briefly review some criticism of the bulk approach which have been formulated in the literature [81, 82].

6.3.1 Summary of the previous approaches in literature

The diagonalization and quantization of the model described by the Hamiltonian (5.31) was performed in the past using a *Fano-Friedrichs diagonalization* method (usually simply called *Fano* method), based on the seminal work of Friedrichs [84, 85] that was rederived by Fano [86]. We first review this method.

The initial point is the classical Hamiltonian of the system which we recall:

$$H = H_{\text{elm}} + H_{\text{med}} + H_{\text{int}}, \quad (6.95)$$

with

$$H_{\text{elm}} = \int d^3r \left[\frac{1}{2\epsilon_0} \vec{\Pi}_A^2 + \frac{\epsilon_0}{2} \vec{A} \cdot (c^2 \nabla \times \nabla \times \vec{A}) \right], \quad (6.96a)$$

$$H_{\text{med}} = \int_0^\infty d\nu \int_V d^3r \left[\frac{1}{2} \vec{\Pi}_X^2 + \frac{1}{2} \nu^2 \vec{X}^2 \right], \quad (6.96b)$$

$$H_{\text{int}} = \frac{1}{\epsilon_0} \int_V d^3r \vec{\Pi}_A \cdot \int_0^\infty d\nu \alpha \vec{X} + \frac{1}{2\epsilon_0} \int_V d^3r \left[\int_0^\infty d\nu \alpha \vec{X} \right]^2. \quad (6.96c)$$

In [23–26] the diagonalization of H is formulated along with the quantization. It consists in finding a family of bosonic operators $\vec{C}(\nu, \vec{r})$ satisfying the commutation relations

$$[\hat{C}_j(\nu, \vec{r}), \hat{C}_{j'}^\dagger(\nu', \vec{r}')] = \delta_{jj'} \delta(\vec{r} - \vec{r}') \delta(\nu - \nu'), \quad (6.97a)$$

$$[\hat{C}_j(\omega, \vec{r}), \hat{C}_{j'}(\omega', \vec{r}')] = 0, \quad (6.97b)$$

such that the Hamiltonian, once quantized, is equal to

$$\hat{H} = \int d^3 r \int_0^\infty d\nu \hbar \nu \vec{C}^\dagger(\nu, \vec{r}) \cdot \vec{C}(\nu, \vec{r}), \quad (6.98)$$

plus an (infinite) constant that can be dropped in the Wick ordering. We remark that the structure of this Hamiltonian is very different from the one we constructed (6.11) although it is the form used mostly in the literature [23–26, 71–79, 82, 87–107].

The construction proceeds by writing the bosonic operator as a linear combination of the canonical variables:

$$\begin{aligned} \vec{C}(\nu, \vec{r}) = & -\frac{i}{\hbar} \int d^3 r' \left\{ \vec{A}(\vec{r}') \cdot \vec{f}_{\Pi_A}^*(\vec{r}', \vec{r}, \nu) - \vec{\Pi}_A(\vec{r}') \cdot \vec{f}_A^*(\vec{r}', \vec{r}, \nu) \right. \\ & \left. + \int_0^\infty d\nu' \left[\vec{X}(\nu', \vec{r}') \cdot \vec{f}_{\Pi_X}^*(\vec{r}, \vec{r}, \nu', \nu) - \vec{\Pi}_X(\nu', \vec{r}') \cdot \vec{f}_X^*(\vec{r}', \vec{r}, \nu', \nu) \right] \right\}, \end{aligned} \quad (6.99)$$

with some unknown tensors f . The ansatz (6.98) implies that the bosonic operators must satisfy:

$$[\vec{C}(\nu, \vec{r}), \hat{H}] = \hbar \nu \vec{C}(\nu, \vec{r}). \quad (6.100)$$

We remark that this is only a necessary condition. In order to make it into a sufficient condition it must be complemented by imposing the commutation relations (6.97). This also ensures that the diagonalization is performed canonically, which also allows the quantization to be formally performed before the diagonalization.¹

Inserting the Hamiltonian (6.95) and (6.99) into Eq. (6.100), one obtains a system of linear integro-differential equations for the coefficients \vec{f} . After some suitable algebraic operations, the solution of this system can be expressed in terms of a Green tensor and some free undetermined functions. The latter are determined by imposing the commutation relations (6.97). The solution is still not unique, since there is always the freedom to perform a unitary transformation within each degeneracy subspace. For the remaining free functions one can make a choice that leads to the possibly simplest formulas (Eq. (88) of Ref. [26]).

The validity of this construction depends critically on the choice of the ansatz (6.98). In order to check whether this ansatz is justified we can consider two different ways to proceed:

a) One can check whether one recovers the initial Hamiltonian (6.95) when inserting the obtained coefficients \vec{f} into the expression (6.99) and then into Eq. (6.98). This check involves relatively complicated calculations and, to our knowledge, it has not been provided in the literature.

b) Another simpler check consists in verifying whether if one takes the limit of zero coupling $\alpha \rightarrow 0$ (i.e., $\epsilon \rightarrow 1$) one obtains the expressions corresponding to the uncoupled medium and the free electromagnetic field. We will show that if one starts with a finite medium, these limits lead to the expressions for the uncoupled medium, but one does not recover the electromagnetic field. The conclusion is that the ansatz (6.98) for the diagonalized Hamiltonian is not valid for a finite medium.

¹An advantage of the method we developed in Chapter 5 is that the diagonalization can be performed independently of the quantization.

6.3.2 The problem of the no-coupling limit

We analyze specifically the equations in Ref. [26], Sections 3 and 4 (without the magnetic part of the model), since it has become one of the main references on the quantization of plasmons. Our discussion can be formulated similarly for the models used in Refs. [23–25], since the quantization procedure followed and the final results are essentially the same as what was described in [26]. The first part of [26] is dedicated to prove that the initial classical Hamiltonian model is equivalent to the macroscopic Maxwell equations (what we have shown in Section 5.1.4 in a different manner), thus the discussion on the quantum model only refers to the second half of the article (from Section 3, and more specifically the results given in Section 4). What we present in this Section is based on the assumption of a finite medium. The case of an infinite bulk medium will be discussed later.

For the bosonic operators

We first analyze the limit of no coupling in the expression of the bosonic operators \vec{C} given by the linear combination (6.99). In order to check whether they split into the two families of operators of the uncoupled model (see Section 6.1.5), we need to calculate the coefficients \vec{f} . They are given by Eqs. (80)–(86) of [26]:

$$\vec{f}_{\Pi_A} = -\epsilon_0 \epsilon \vec{f}_E - \alpha \vec{h}_X, \quad (6.101a)$$

$$\vec{f}_A = -\frac{i}{v} [\vec{f}_E]_{\perp}, \quad (6.101b)$$

$$\vec{f}_{\Pi_X} = \alpha \vec{f}_E \frac{i}{v} \left(1 - v' \left[\frac{1}{v' - v - i\nu 0^+} + \frac{1}{v' + v - i\nu 0^+} \right] \right) - i v \vec{h}_X \delta(v - v'), \quad (6.101c)$$

$$\vec{f}_X = \frac{i}{v} \vec{f}_{\Pi_X}, \quad (6.101d)$$

and they are expressed in terms of two additional tensors,

$$\vec{f}_E(\vec{r}', \vec{r}, \nu) = \sqrt{\frac{\hbar}{2\nu}} \mu_0 \nu^2 \alpha(\nu, \vec{r}) \vec{G}(\vec{r}', \vec{r}'', \nu), \quad (6.102)$$

$$\vec{h}_X(\vec{r}', \vec{r}, \nu) = \left(\frac{\hbar}{2\nu} \right)^{1/2} \delta(\vec{r} - \vec{r}') \vec{\mathbb{1}}, \quad (6.103)$$

where \vec{G} is the Green tensor verifying

$$\left[\nabla \times \nabla \times - \epsilon(\vec{r}, \nu) \frac{\nu^2}{c^2} \right] \vec{G}(\vec{r}, \vec{r}', \nu) = \vec{\mathbb{1}} \delta(\vec{r} - \vec{r}'). \quad (6.104)$$

An inspection of these expressions allows one to show that the no-coupling limit $\alpha \rightarrow 0$ is well defined, and one can calculate it explicitly. We start with Eq. (6.102). The limit of the Green tensor is

$$\lim_{\alpha \rightarrow 0} \vec{G}(\vec{r}', \vec{r}'', \nu) = \vec{G}_0(\vec{r}', \vec{r}'', \nu), \quad (6.105)$$

and thus

$$\lim_{\alpha \rightarrow 0} \vec{f}_E(\vec{r}', \vec{r}, \nu) = 0. \quad (6.106)$$

Inserting this result in Eqs. (6.101), we obtain

$$\lim_{\alpha \rightarrow 0} \bar{f}_{\Pi_A} = 0, \quad (6.107a)$$

$$\lim_{\alpha \rightarrow 0} \bar{f}_A = 0, \quad (6.107b)$$

$$\lim_{\alpha \rightarrow 0} \bar{f}_{\Pi_X} = -i v \bar{h}_X \delta(v - v') = -i \left(\frac{\hbar v}{2} \right)^{1/2} \delta(\vec{r} - \vec{r}') \bar{\mathbb{1}} \delta(v - v'), \quad (6.107c)$$

$$\lim_{\alpha \rightarrow 0} \bar{f}_X = \bar{h}_X \delta(v - v') = \left(\frac{\hbar}{2v} \right)^{1/2} \delta(\vec{r} - \vec{r}') \bar{\mathbb{1}} \delta(v - v'). \quad (6.107d)$$

Inserting it into the expression for the bosonic operator (6.99), we obtain

$$\lim_{\alpha \rightarrow 0} \vec{C}(v, \vec{r}) = \frac{1}{\sqrt{2\hbar}} \left[v^{1/2} \vec{X}_v(\vec{r}) + i v^{-1/2} \vec{\Pi}_{X_v}(\vec{r}) \right] = \vec{C}_0, \quad (6.108)$$

with \vec{C}_0 the bosonic operator for the uncoupled medium introduced in Sec. 6.1.5. Thus, in the uncoupled limit, the bosonic operator \vec{C} becomes the bosonic operator for the free medium \vec{C}_0 and it contains no information on the bosonic operator $\hat{D}_{\vec{k}, \sigma, \zeta}^0$ of the electromagnetic field.

For the Hamiltonian

The limit (6.108) can be taken in the diagonal Hamiltonian (6.98) and compared with Eq. (6.31). One obtains

$$\begin{aligned} \lim_{\alpha \rightarrow 0} \hat{H} &= \lim_{\alpha \rightarrow 0} \int d^3 r \int_0^\infty dv \hbar v \vec{C}^\dagger(v, \vec{r}) \cdot \vec{C}(v, \vec{r}), \\ &= \int d^3 r \int_0^\infty dv \hbar v \vec{C}_0^\dagger(v, \vec{r}) \cdot \vec{C}_0(v, \vec{r}) = \hat{H}_{\text{med}}^0, \end{aligned} \quad (6.109)$$

i.e., one obtains the Hamiltonian of the uncoupled medium only; the Hamiltonian of the free electromagnetic field is missing. This could be expected from the structure of the ansatz (6.98) which integrates only over the degrees of freedom of matter (v, \vec{r}) .

For the electric field operator

In the construction of the diagonalization procedure from [23–26] (as well as in the phenomenological approach [72–75]), the electric field operator reads

$$\vec{E}(\vec{x}) = \sqrt{\frac{\hbar \mu_0}{\pi c^2}} \int_0^\infty dv \int_V d^3 r v^2 \epsilon_i^{1/2}(v, \vec{r}) \vec{G}(v; \vec{r}, \vec{x}) \vec{C}(v, \vec{r}) + h.c. \quad (6.110)$$

This formula has been widely used in the literature [23–25, 70, 77, 79, 88, 91–118, 131, 132, 136, 137]. In order to show that it cannot be applied to a finite medium, we follow the same procedure: the limits of the Green tensor (6.105) and of the bosonic operator (6.108) are regular and well defined. Since the limit $\alpha \rightarrow 0$ is equivalent to $\epsilon_i \rightarrow 0$, this limit yields

$$\lim_{\alpha \rightarrow 0} \vec{E} = 0, \quad (6.111)$$

i.e., the electric field observable would disappear in the uncoupled limit, which of course is not consistent. This conclusion was already presented by [81, 82].

Remarks on an infinite bulk medium

The situation for an infinite bulk medium might be different. The uncoupled limit $\alpha \rightarrow 0$ is highly singular, since the dissipation disappears, and it does not seem likely to us that it allows one to recover the expressions of the uncoupled medium *and* electromagnetic field. The singularity of the limit entails that if one does not recover the expressions for the uncoupled fields, it does not mean that formulas for the infinite bulk medium are not correct. At this point we do not make any definite affirmation about the infinite bulk case. In particular, the diagonalization procedure presented in Chapter 5 is not applicable to this scenario, since it relies on a Møller wave operator which may not exist in an infinite medium. In that case, the spectral structure of the coupled model can be different from the one of the uncoupled model, leading to a possible loss of degrees of freedom. The singular nature of an infinite medium was also evoked in [119] as a reason for the lack of electromagnetic degrees of freedom in the final results of [72, 73] and subsequent works.

We emphasize that for the applications, in particular those involving nanostructures, the relevant models involve a finite medium. A bulk model can be a good approximation for some specific experimental setups, e.g., if one considers an emitter embedded in the interior of the medium. It is however not appropriate when the emitters are outside the medium, which is a far more common situation, particular for metallic media.

6.3.3 Justifications and proposed corrections in the literature

It has been remarked in several instances in the literature [81, 82, 120] that the expression of the electric field observable (6.110) cannot yield the free electric field observable in the limit $\epsilon_i \rightarrow 0$. Since this formula is of fundamental importance to study plasmonics structures, some authors have tried to either justify its validity nonetheless, or to correct it.

Addition of a fictitious homogeneous dissipative medium

An approach to justify the validity of Eq. (7.50) in the case of a finite medium can be found, e.g., in [75, 118, 120]. It consists of adding artificially to the dielectric coefficient $\epsilon(\nu, \vec{r})$ a small homogeneous dissipative background term $\epsilon_\infty(\nu)$, which is set to zero at the very end of the calculations, when one has obtained an expression for a quantity of physical interest, like the spontaneous decay rate of an emitter or the expectation value of a Casimir force. This is a mathematical trick that would allow one to use for practical calculations for a finite medium the expressions obtained for an infinite medium. The difficulty is that the validity of this trick is not easy to justify for the following reasons:

- Certainly, the infinite background medium does not correspond to the considered physical situation. It can only be seen as a mathematical trick, and one has to determine in which sense it can be justified, which does not seem to be an easy task. The procedure clearly shows that taking the limit $\epsilon_\infty(\nu) \rightarrow 1$ at the beginning of the calculation does not give the same result as taking the limit at the end. Thus the exchange of the limit and the intermediate calculations do not commute. Cases like this are difficult to handle mathematically and one has to figure out why one order of the operations can be declared correct and not the other one.
- One can ask how to determine whether the results obtained with this trick are correct. In order to make this verification one needs to have an independent method of calculating the desired physical quantities that is known to yield the correct results. The exact diagonalization described in Chapter 5 provides such an independent method.

Until such a comparison is made we cannot make any definite claim on the status of this trick.

6.3.4 Addition of a modified free field

Some authors [81, 82] have stated that the formula (6.110) is not complete when a finite medium is considered. Although these authors did not derive a formula from the diagonalization of the initial model, they proposed to correct it by adding to the electric field observable (6.110) a contribution \vec{E}_0 ,

$$\vec{E}(\vec{x}) = \vec{E}_0(\vec{x}) + \vec{E}_G(\vec{x}), \quad (6.112)$$

with \vec{E}_G given by Eq. (6.110), and \vec{E}_0 is related to the vacuum field and converges to it in the no-coupling limit. The expression (6.112) has by construction the correct limit when $\epsilon_i \rightarrow 0$. However, there is no justification for claiming that this is the expression that one would obtain from the exact diagonalization of the Hamiltonian (6.95). In fact, the result of Chapters 5 and 6 show that the exact diagonalization in a finite medium leads to an expression for the electric field observable that is different from (6.112), although they coincide in first order perturbation theory aside from a diverging term close to the medium (see Section 6.2.2).

6.4 Summary on the quantum model

The quantization of the plasmonic model constructed in Chapter 5 follows the same logic as the quantization of the dielectric model as performed in Chapter 3. It relies on the identification of the space of classical configurations which are used to define bosonic creation-annihilation operators acting on a Fock space of quantum states. Specific configurations (called *eigenconfigurations*) are calculated and used to formally define bosonic operators which diagonalize the Hamiltonian. These eigenconfigurations are generally non square-integrable and the subsequent diagonal bosonic operators are not well-defined in the Fock space of quantum states, however they are a useful mathematical tool to characterize the states.

The diagonalizing transformation can be inverted to express the electric or magnetic field observable in terms of these particular operators and eigenconfigurations. For the free field, this task is rather straightforward since the diagonalizing transformation is more or less equivalent to a Fourier transform, and in many experiments in optics this is sufficient to analyze the interaction with passive media as shown in Chapter 4. In the plasmonic model, however, it requires to solve the Lippmann-Schwinger equation as constructed in Chapter 5. This is a non-trivial task that is not easy to perform analytically. We have shown a way to calculate it in two perturbative regimes: one assuming that both the dissipation of the medium and its volume are small, the other counting on a volume sufficiently small to compensate a potentially high dissipation coefficient.

The classical configurations (and therefore the quantum states) are associated with all initial degrees of freedom of the system – both electromagnetic and of matter. This is ensured by the existence of the Møller wave operator and the Lippmann-Schwinger equation, and this was one of the main results of Chapter 5. In Chapter 6 we have seen the consequences of this: two families of bosonic operators can be identified, and the diagonal Hamiltonian

and the electric field observable have two contributions: one for each set of degrees of freedom. A fundamental feature we could describe is the no-coupling limit consistent with the results in vacuum. This feature was mostly absent in the literature, and only in very few instances a correction was proposed but with no justification *a priori*. To our knowledge, it is the first time that a complete, consistent expression of the electric field observable in a plasmonic environment was derived from the diagonalization and quantization of an initial microscopic model (equivalent to the macroscopic Maxwell equations). We have reviewed the method commonly used in the literature and we have described how it fails to give the correct no-coupling limit.

Plasmon dynamics

In the preceding chapter we have shown that the question of quantizing the electromagnetic field when interacting with a dispersive and dissipative medium (such as a metal) can be addressed in a way very similar to the quantization of the free field. One can even go further by assuming that the fundamental difference between photons and plasmons is of the same nature as the difference between photons in a perfect cavity and photons in free space, i.e., a change in the degeneracy structure. Therefore the intuition we used in Chapter 4 to investigate photon dynamics can be extrapolated to plasmons. Hence one can use the formalism of Section 6.1.1 to describe the propagation of plasmon wave packets in plasmonic circuits. However in this Chapter we focus on the very first part of a plasmonic experiment: the emission of individual plasmons.

We present the model of an emitter interacting with the (photonic or plasmonic) electromagnetic field in Section 7.1. We show in Sections 7.2 and 7.3 two ways of calculating the spontaneous rate of emission: the Fermi golden rule, and the Wigner-Weisskopf theory. We also introduce a coefficient of losses which quantifies the amount of the energy of the plasmon state that gets lost inside the medium. From the quantization procedure for plasmons used in the past, many works have studied spontaneous emission of plasmons. Because of the criticisms we made in the preceding Chapter and some additional discrepancies in the formulas used for finite media, we add some comments of this specific question in Section 7.4.

Contents

7.1 The model	124
7.2 Fermi Golden rule	125
7.2.1 Emitter in a plasmonic environment	126
7.2.2 Emitter in vacuum	127
7.2.3 The Purcell factor	128
7.3 Wigner-Weisskopf theory	129
7.3.1 Emitted quantum state	129
7.3.2 Tracking the dissipation	130
7.4 Comments on the literature	132
7.4.1 Summary of the result in the literature	132
7.4.2 Fermi golden rule assuming Eq. (6.110)	133
7.4.3 Spontaneous emission in a 1D model assuming Eq. (6.110)	135
7.5 Summary on the dynamics of plasmons	138

7.1 The model

Consider a two-level system (typically an atom, a molecule or a quantum dot with appropriate level structure) consisting of a ground level and an excited one, separated by an energy of $\hbar\omega_0$. We make the standard assumption [121] that this system can be modeled as a point dipole at position \vec{x}_0 , emitting resonantly with its normal frequency ω_0 . This system is permanently coupled with the surrounding quantized electromagnetic field, whether it is excited (i.e., it contains several photons/plasmons) or not (i.e., it is in its ground “vacuum” state).

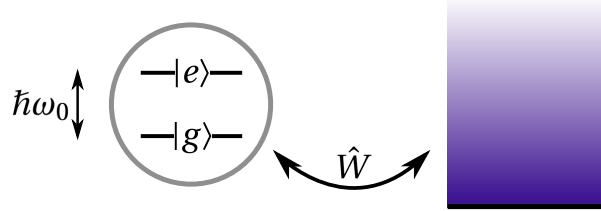


Figure 7.1 – Scheme of a two-level system coupled to the quantized electromagnetic field with a coupling operator \hat{W} .

In general, the global state of the coupled system is a linear combination of tensor products of the state of the atom (either $|g\rangle$ or $|e\rangle$ or a combination of both) with the state of the electromagnetic field (i.e., a state created by the application of 0, 1, or N bosonic operators as defined in Section 6.1.1). For the sake of simplicity we consider that the electromagnetic field is initially in its vacuum state $|\emptyset\rangle$.

The Hamiltonian of the global system reads

$$\hat{H} = \hat{H}_{field} + \hat{H}_{atom} + \hat{W}, \quad (7.1)$$

where \hat{H}_{field} corresponds to the energy of the background field (either photons or plasmons), which takes the diagonal form:

$$\hat{H}_{field} = \int d\lambda \sum_{d^\lambda} \hbar\lambda \hat{B}_{\lambda,d^\lambda}^\dagger \hat{B}_{\lambda,d^\lambda}, \quad (7.2)$$

where λ, d^λ refer to ω or ν and their associated degeneracy indices, and \hat{B} is either of type \hat{D} or \hat{C} . Note that we use the Hamiltonian and bosonic operators of the plasmonic model; the formulas can however be easily adapted to passive media by canceling out the degrees of freedom of matter and setting $\alpha = 0$.

The two-level system is initially in its excited state. Setting the ground state at energy zero, we have

$$\hat{H}_{atom} = \hbar\omega_0 |e\rangle\langle e|. \quad (7.3)$$

We assume a dipolar coupling operator:

$$\hat{W}(\vec{x}_0) = -\vec{d} \cdot \vec{E}(\vec{x}_0), \quad (7.4)$$

with \vec{x}_0 the position of the emitter. The operator \vec{d} is the dipole operator and it can be written

$$\vec{d} = \vec{d}[\hat{\sigma}_+ + \hat{\sigma}_-], \quad (7.5)$$

with \vec{d} the dipole moment; $\hat{\sigma}_+$ and $\hat{\sigma}_-$ are the rising and lowering ladder operators of the atom:

$$\hat{\sigma}_+ = |e\rangle\langle g|, \quad \hat{\sigma}_- = |g\rangle\langle e|, \quad \hat{\sigma}_+ = \hat{\sigma}_-^\dagger. \quad (7.6)$$

The coupling operator reads

$$\hat{W} = - \int d\lambda \sum_{d^\lambda} \left[g_{\lambda,d^\lambda}(\vec{x}_0) \hat{\sigma}_+ \hat{B}_{\lambda,d^\lambda} + g_{\lambda,d^\lambda}^*(\vec{x}_0) \hat{\sigma}_- \hat{B}_{\lambda,d^\lambda}^\dagger + \bar{g}_{\lambda,d^\lambda}(\vec{x}_0) \hat{\sigma}_+ \hat{B}_{\lambda,d^\lambda}^\dagger + \bar{g}_{\lambda,d^\lambda}^*(\vec{x}_0) \hat{\sigma}_- \hat{B}_{\lambda,d^\lambda} \right]. \quad (7.7)$$

The functions g and \bar{g} are the so-called *rotating* and *counter-rotating* coupling constants, respectively. We use the *Rotating Wave Approximation* (RWA), which assumes that $\bar{g} = 0$. Hence, the coupling operator reduces to

$$\hat{W} = - \int d\lambda \sum_{d^\lambda} \left[g_{\lambda,d^\lambda}(\vec{x}_0) \hat{\sigma}_+ \hat{B}_{\lambda,d^\lambda} + g_{\lambda,d^\lambda}^*(\vec{x}_0) \hat{\sigma}_- \hat{B}_{\lambda,d^\lambda}^\dagger \right]. \quad (7.8)$$

The two remaining terms are *elastic* interactions since they preserve the number of quanta: the first term excites the atom while absorbing a photon/plasmon, and the second term lowers the atom down to its ground state while releasing a quantum in the electromagnetic field.

If the background field described by \hat{H}_{field} is the plasmonic field constructed in Chapter 6, the coupling constant g can be split into two functions: one for the interaction with the operators \hat{D} and one for the interaction with \hat{C} , which we denote g^e and g^m respectively. The electric field being given by Eq. (6.19):

$$\vec{\tilde{E}} = \vec{\tilde{E}}^e + \vec{\tilde{E}}^m, \quad (7.9)$$

with

$$\vec{\tilde{E}}^e(\vec{x}) = \int d\kappa [\vec{e}_\kappa(\vec{x}) \hat{D}_\kappa + \vec{e}_\kappa^*(\vec{x}) \hat{D}_\kappa^\dagger], \quad (7.10a)$$

$$\vec{\tilde{E}}^m(\vec{x}) = \int d\mu [\vec{m}_\mu(\vec{x}) \hat{C}_\mu + \vec{m}_\mu^*(\vec{x}) \hat{C}_\mu^\dagger], \quad (7.10b)$$

we can identify in (7.8):

$$g_\kappa^e(\vec{x}_0) = \vec{d} \cdot \vec{e}_\kappa(\vec{x}_0), \quad g_\mu^m(\vec{x}_0) = \vec{d} \cdot \vec{m}_\mu(\vec{x}_0). \quad (7.11)$$

The model is completely defined and can be used either with \vec{e} and \vec{m} calculated with the Lippmann-Schwinger equation, or in the case of vacuum by replacing them by their special expressions (6.35).

7.2 Fermi Golden rule

The Fermi golden rule is a very standard derivation of the decay rate of an emitter, based on the calculation of the probability of transition in first order perturbation theory, and on the definition of a density of final states accessible when the atom emits. Its derivation can be found in many textbooks (see, e.g., [70]). The final expression of the decay rate reads

$$\Gamma(\vec{x}_0, \omega_0) = \frac{2\pi}{\hbar^2} \sum_f |\langle f | \hat{W} | i \rangle|^2 \delta(\omega_f - \omega_0), \quad (7.12)$$

with $|i\rangle = |\emptyset \otimes e\rangle$ the initial state, $|f\rangle$ the final state, and ω_f its associated energy. Note that it is formulated for initial and final states that are eigenstates of the system, to which we can associate a single energy. Thus, the sum over all final states can be replaced by a sum over all the degrees of freedom of the quantized electromagnetic field:

$$\Gamma = \Gamma^e + \Gamma^m, \quad (7.13)$$

with

$$\Gamma^e(\vec{x}_0, \omega_0) = \frac{2\pi}{\hbar^2} \int d^3k \sum_d \left| \langle 1_{\vec{k},d} \otimes g | \hat{W} | \emptyset \otimes e \rangle \right|^2 \delta(\omega - \omega_0), \quad (7.14a)$$

$$\Gamma^m(\vec{x}_0, \omega_0) = \frac{2\pi}{\hbar^2} \int d\nu \int_V d^3r \sum_j \left| \langle 1_{\nu, \vec{r}, j} \otimes g | \hat{W} | \emptyset \otimes e \rangle \right|^2 \delta(\nu - \omega_0). \quad (7.14b)$$

Replacing \hat{W} by its expression (7.4), one can use the expression of the electric field in a passive medium or in the plasmonic environment to evaluate the decay rate of the emitter, since its expression in terms of bosonic operators allows us to apply it on the initial/final states.

7.2.1 Emitter in a plasmonic environment

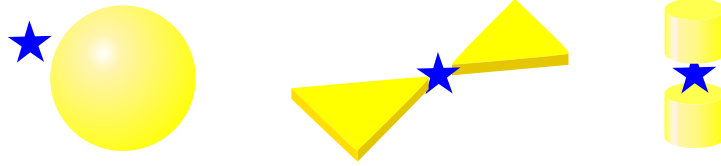


Figure 7.2 – Examples of plasmonic structures interacting with an emitter. *Left*: a spherical nanoparticle, mostly studied theoretically because of the spherical symmetry which simplifies computations; *Middle*: a bow-tie nanoantenna; *Right*: a plasmonic cavity.

We would in general consider that the emitter is placed in the surrounding of a metallic medium we may call a plasmonic environment, even though it can be extended to any medium which can be described by the dispersive and dissipative model of Chapter 5. Examples of plasmonic structures commonly used in experiments or studied in theoretical works are shown in Figure 7.2. In this scenario, the electric field operator is given by Eq. (6.19) in the exterior of the medium and, replacing \vec{d} by its expression (7.5), we obtain

$$\Gamma^e(\vec{x}_0, \omega_0) = \frac{2\pi}{\hbar^2} \int d^3k \sum_d \left| \langle 1_{\vec{k},d} \otimes g | [\hat{\sigma}_+ + \hat{\sigma}_-] \vec{d} \cdot [\vec{\tilde{E}}^e + \vec{\tilde{E}}^m] | \emptyset \otimes e \rangle \right|^2 \delta(\omega - \omega_0), \quad (7.15a)$$

$$\Gamma^m(\vec{x}_0, \omega_0) = \frac{2\pi}{\hbar^2} \int d\nu \int_V d^3r \left| \langle 1_{\nu, \vec{r}} \otimes g | [\hat{\sigma}_+ + \hat{\sigma}_-] \vec{d} \cdot [\vec{\tilde{E}}^e + \vec{\tilde{E}}^m] | \emptyset \otimes e \rangle \right|^2 \delta(\nu - \omega_0), \quad (7.15b)$$

where we hide the degeneracy j to lighten the equations. We first evaluate

$$\begin{aligned} [\hat{\sigma}_+ + \hat{\sigma}_-] [\vec{\tilde{E}}^e + \vec{\tilde{E}}^m] | \emptyset \otimes e \rangle &= \int d^3k' \sum_{d'} [\hat{\sigma}_+ + \hat{\sigma}_-] [\vec{e}_{\vec{k}', d'} \hat{D}_{\vec{k}', d'} + \vec{e}_{\vec{k}', d'}^* \hat{D}_{\vec{k}', d'}^\dagger] | \emptyset \otimes e \rangle \\ &+ \int d\nu \int_V d^3r [\hat{\sigma}_+ + \hat{\sigma}_-] [\vec{m}_{\nu, \vec{r}} \vec{C}_{\nu, \vec{r}} + \vec{m}_{\nu, \vec{r}}^* \vec{C}_{\nu, \vec{r}}^\dagger] | \emptyset \otimes e \rangle, \end{aligned} \quad (7.16)$$

with \vec{e} and \vec{m} given by Eq. (6.23) in the exterior of the medium. We use that $\hat{D}_{\vec{k},d}|\emptyset\rangle = 0$ and $\vec{C}_{\nu,\vec{r}}|\emptyset\rangle = 0$, as well as $\hat{\sigma}_+|e\rangle = 0$, and we obtain

$$[\hat{\sigma}_+ + \hat{\sigma}_-][\vec{E}^e + \vec{E}^m]|\emptyset \otimes e\rangle = \int d^3 k' \sum_{d'} \vec{e}_{\vec{k}',d'}^* |1_{\vec{k}',d'} \otimes g\rangle + \int d\nu \int_V d^3 r \vec{m}_{\nu,\vec{r}}^* |1_{\nu,\vec{r}} \otimes g\rangle. \quad (7.17)$$

We now multiply it on the left by $\langle 1_{\vec{k},d} \otimes g|$ and we use that

$$\langle 1_{\vec{k},d} \otimes g | 1_{\vec{k}',d'} \otimes g \rangle = \delta_{dd'} \delta(\vec{k} - \vec{k}'), \quad \langle 1_{\vec{k},d} \otimes g | 1_{\nu,\vec{r}} \otimes g \rangle = 0, \quad (7.18)$$

leading to

$$\langle 1_{\vec{k},d} \otimes g | [\hat{\sigma}_+ + \hat{\sigma}_-][\vec{E}^e + \vec{E}^m]|\emptyset \otimes e\rangle = \vec{e}_{\vec{k},d}^*. \quad (7.19)$$

Similarly we can show that

$$\langle 1_{\nu,\vec{r}} \otimes g | [\hat{\sigma}_+ + \hat{\sigma}_-][\vec{E}^e + \vec{E}^m]|\emptyset \otimes e\rangle = \vec{m}_{\nu,\vec{r}}^*. \quad (7.20)$$

We introduce it into Eqs. 7.15a and 7.15b:

$$\Gamma^e(\vec{x}_0, \omega_0) = \frac{2\pi}{\hbar^2} \int d^3 k \sum_d \left| \vec{d} \cdot \vec{e}_{\vec{k},d}(\vec{x}_0) \right|^2 \delta(\omega - \omega_0), \quad (7.21a)$$

$$\Gamma^m(\vec{x}_0, \omega_0) = \frac{2\pi}{\hbar^2} \int d\nu \int_V d^3 r \left| \vec{d} \cdot \vec{m}_{\nu,\vec{r}}(\vec{x}_0) \right|^2 \delta(\nu - \omega_0), \quad (7.21b)$$

with \vec{e} and \vec{m} calculated from the diagonalization of the frequency operator as described in Chapter 6.

7.2.2 Emitter in vacuum

Once the general formula of the decay rate is derived in a plasmonic environment, one can easily recover the one in vacuum by taking the no-coupling limit (see Section 6.1.5). In this limit, we have

$$\vec{e}_{\vec{k},d}(\vec{x}_0) \rightarrow -\sqrt{\frac{\hbar\omega}{2\epsilon_0}} \vec{\varphi}_{\vec{k},d}(\vec{x}_0), \quad (7.22a)$$

$$\vec{m}_{\nu,\vec{r}}(\vec{x}_0) \rightarrow 0, \quad (7.22b)$$

with $\vec{\varphi}_{\vec{k},d}(\vec{x})$ satisfying the wave equation in vacuum:

$$\nabla \times \nabla \times \vec{\varphi}_{\vec{k},d}(\vec{x}) - \frac{\omega^2}{c^2} \vec{\varphi}_{\vec{k},d}(\vec{x}) = 0. \quad (7.23)$$

Hence, the two contributions of the decay rate (7.21a) and (7.21b) become

$$\Gamma_{vac}^e(\vec{x}_0, \omega_0) = \frac{\pi}{\hbar\epsilon_0} \int d^3 k \sum_d \omega \left| \vec{d} \cdot \vec{\varphi}_{\vec{k},d}(\vec{x}_0) \right|^2 \delta(\omega - \omega_0), \quad (7.24a)$$

$$\Gamma_{vac}^m(\vec{x}_0, \omega_0) = 0. \quad (7.24b)$$

A calculation in spherical coordinates shows that

$$\Gamma_{vac}(\vec{x}_0, \omega_0) = \Gamma_{vac}^e(\vec{x}_0, \omega_0) = \frac{\omega_0^3 |\vec{d}|^2}{3\pi \hbar \epsilon_0 c^3}. \quad (7.25)$$

Proof: We evaluate the integral

$$\int d^3k \sum_d \omega \left| \vec{d} \cdot \vec{\varphi}_{\vec{k},d}(\vec{x}_0) \right|^2 \delta(\omega - \omega_0) \quad (7.26)$$

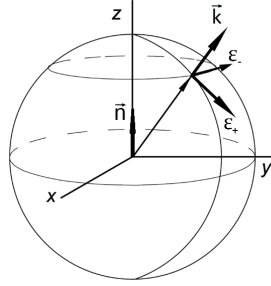
by projecting \vec{k} onto spherical coordinates:

$$\int d\vec{k} \rightarrow \frac{1}{c^3} \int_0^\infty d\omega \int_0^{\pi/2} d\vartheta \int_0^{2\pi} d\eta \omega^2 \sin \vartheta. \quad (7.27)$$

We recall that the wave functions $\vec{\varphi}$ read (in real representation)

$$\vec{\varphi}_{\vec{k},\sigma,\zeta}(\vec{x}) = \begin{cases} \frac{1}{2\pi^{3/2}} \vec{\epsilon}_\sigma(\vec{k}) \cos(\vec{k} \cdot \vec{x}), & \zeta = c, \\ \frac{1}{2\pi^{3/2}} \vec{\epsilon}_\sigma(\vec{k}) \sin(\vec{k} \cdot \vec{x}), & \zeta = s, \end{cases} \quad (7.28)$$

where the degeneracy d contains both the index of polarization $\sigma = \pm$ and the index $\zeta = c/s$ for the cosine and sine contributions. The vectors $\vec{\epsilon}_\pm$ are unit polarization vectors, orthogonal to \vec{k} and to each other, as represented on the figure below.



Furthermore, we choose $\vec{x}_0 = 0$ so that $\cos(\vec{k} \cdot \vec{x}_0) = 1$, and the degeneracy $\zeta = s$ does not contribute. Thus, the decay rate (7.24a) reads

$$\Gamma_{vac}^e(\vec{x}_0, \omega_0) = \frac{\omega_0^3}{4\pi^2 \hbar \epsilon_0 c^3} \int_0^{\pi/2} d\vartheta \int_0^{2\pi} d\eta \sin \vartheta \left\{ \left| \vec{d} \cdot \vec{\epsilon}_+(\vartheta, \eta) \right|^2 + \left| \vec{d} \cdot \vec{\epsilon}_-(\vartheta, \eta) \right|^2 \right\}. \quad (7.29)$$

We can choose the direction of \vec{d} arbitrarily in vacuum; we choose it along the z -axis such that $\vec{d} \cdot \vec{\epsilon}_- = 0$ and $\vec{d} \cdot \vec{\epsilon}_+ = -|\vec{d}| \sin \vartheta$. Hence, Eq. (7.29) becomes

$$\Gamma_{vac}^e(\vec{x}_0, \omega_0) = \frac{\omega_0^3 |\vec{d}|^2}{2\pi \hbar \epsilon_0 c^3} \underbrace{\int_0^{\pi/2} d\vartheta \sin^3 \vartheta}_{2/3} = \frac{\omega_0^3 |\vec{d}|^2}{3\pi \hbar \epsilon_0 c^3}. \quad (7.30)$$

We note that the decay rate in vacuum does not depend on the position nor on the direction of the emitter.

7.2.3 The Purcell factor

In practice, it is often more adequate to study the ratio between the calculated (or measured) decay rate in a given environment and the decay rate in vacuum. We define the Purcell factor,

$$P(\vec{x}_0, \omega_0) = \Gamma(\vec{x}_0, \omega_0) / \Gamma_{vac}(\omega_0), \quad (7.31)$$

which is a measure of the impact of the environment on the spontaneous emission of the two-level system. The use of plasmonic structures is often justified because they highly enhance the decay rate near the surface of the metal, i.e., the Purcell factor for an emitter is very large compared to one (factors from around a hundred [122–125] to several hundreds or thousands [126–129] have been obtained experimentally). This phenomenon is called the Purcell enhancement and highly depends on the plasmonic structure (see Ref. [130] for a detailed review on the subject).

7.3 Wigner-Weisskopf theory

The Fermi golden rule is a very common way to express the rate of spontaneous emission of the emitter in a regime where the emitter is weakly coupled to its environment. There is another way to obtain it, however, which relies on other approximations and has the advantage to provide a more detailed description of the quantum state which is emitted in the process. This is what is called the Wigner-Weisskopf theory.

We start by writing the Hamiltonian of the coupled system emitter+plasmonic field in the Rotating Wave Approximation:

$$\hat{H} = \hbar\omega_0|e\rangle\langle e| + \int_0^\infty d\lambda \sum_{d^\lambda} \hbar\lambda \hat{B}_{\lambda,d^\lambda}^\dagger \hat{B}_{\lambda,d^\lambda} - \int_0^\infty d\lambda \sum_{d^\lambda} [g_{\lambda,d^\lambda}(\vec{x}_0) \hat{B}_{\lambda,d^\lambda} |e\rangle\langle g| + h.c.]. \quad (7.32)$$

The notation (λ, d^λ) contains both electromagnetic $\kappa = (\vec{k}, \sigma, \zeta)$ and matter $\mu = (v, \vec{r}, j)$ degrees of freedom. As in Section 7.1, we have $g_\kappa \equiv g_\kappa^e = \vec{d} \cdot \vec{e}_\kappa$ and $g_\mu \equiv g_\mu^m = \vec{d} \cdot \vec{m}_\mu$.

This initial Hamiltonian will serve as the basis to extract the emitted quantum state and the rate of its emission.

7.3.1 Emitted quantum state

A general state of the coupled system restricted to one-quantum excitation can be written

$$|\Psi\rangle = C_0^e(t) e^{-i\omega_0 t} |\emptyset \otimes e\rangle + \int_0^\infty d\lambda \sum_{d^\lambda} C_{1,\lambda,d^\lambda}^g(t) e^{-i\lambda t} |1_{\lambda,d^\lambda} \otimes g\rangle, \quad (7.33)$$

with $|C_0^e|^2$ the population of the state $|\emptyset \otimes e\rangle$, and $|C_{1,\lambda,d^\lambda}^g|^2$ the population of the state $|1_{\lambda,d^\lambda} \otimes g\rangle$. Developing both left-hand side and right-hand side of the Schrödinger equation $i\hbar\partial_t|\Psi\rangle = \hat{H}|\Psi\rangle$ using the Hamiltonian (7.32) leads to the following coupled differential equations for the coefficients:

$$i\hbar\dot{C}_0^e = - \int_0^\infty d\lambda \sum_{d^\lambda} g_{\lambda,d^\lambda} C_{1,\lambda,d^\lambda}^g e^{i(\omega_0-\lambda)t}, \quad (7.34a)$$

$$i\hbar\dot{C}_{1,\lambda,d^\lambda}^g = -g_{\lambda,d^\lambda}^* C_0^e e^{-i(\omega_0-\lambda)t}. \quad (7.34b)$$

We solve (7.34b) and we introduce it into (7.34a):

$$\dot{C}_0^e(t) = -\frac{1}{\hbar^2} \int_0^\infty d\lambda \sum_{d^\lambda} |g_{\lambda,d^\lambda}|^2 \int_0^t dt' C_0^e(t') e^{i(\lambda-\omega_0)(t-t')}. \quad (7.35)$$

We now use the Wigner-Weisskopf approximations: we consider that the time-evolution of C_0^e depends only on the amplitude C_0^e at time t (hence we can move it out of the integrand), and we extent $t \rightarrow \infty$. Then we can use the identity

$$\int_0^\infty dt' e^{i(\lambda - \omega_0)(t-t')} = \pi \delta(\lambda - \omega_0) + i \frac{\mathcal{P}}{\lambda - \omega_0}, \quad (7.36)$$

which gives

$$\dot{C}_0^e = -\frac{1}{\hbar^2} \left[\pi \sum_{d^\lambda} |g_{\omega_0, d^\lambda}|^2 + i \mathcal{P} \int_0^\infty d\lambda \frac{e^{-i(\lambda - \omega_0)t}}{\lambda - \omega_0} \sum_{d^\lambda} |g_{\lambda, d^\lambda}|^2 \right] C_0^e(t). \quad (7.37)$$

This is a differential equation of the form $\dot{a} = -Fa$, whose solution reads in general $a = e^{-Ft}$ with the initial condition $a(t=0) = 1$. Thus we can write

$$C_0^e(t) = e^{-\left(\frac{\Gamma}{2} + i\Delta\right)t}, \quad (7.38)$$

where we identify Γ as the decay rate of the emitter:

$$\Gamma(\omega_0, \vec{x}_0) = \frac{2\pi}{\hbar^2} \sum_{d^\lambda} |g_{\lambda=\omega_0, d^\lambda}(\vec{x}_0)|^2, \quad (7.39)$$

and Δ as the Lamb shift:

$$\Delta(\omega_0, \vec{x}_0) = \frac{1}{\hbar^2} \int_0^\infty d\lambda \frac{e^{-i(\lambda - \omega_0)t}}{\lambda - \omega_0} \sum_{d^\lambda} |g_{\lambda, d^\lambda}(\vec{x}_0)|^2. \quad (7.40)$$

The decay rate has here a direct physical meaning: since the population in the excited state decreases exponentially with time as

$$|C_0^e|^2(t) = e^{-\Gamma t}, \quad (7.41)$$

Γ is the inverse of the *mean lifetime*, which is the time it takes for the probability of the atom to be in its excited state to be reduced by a factor $1/e \approx 0.37$. We notice that the expression of the decay rate (7.39) is the same as with the Fermi golden rule, even though we have not considered a weak-coupling regime for the emitter.

The Wigner-Weisskopf gives us a way to calculate the quantum state emitted by the emitter, through time, from the calculation of the decay rate. We may now use the quantum state to evaluate other physical quantities.

7.3.2 Tracking the dissipation

One of the drawbacks of plasmonics applications is the high losses of metals. Depending on the metal, its geometry, and the frequency of the plasmon excitation, a part of the energy of the quantum plasmon may get converted into pure matter oscillations, without ever being radiatively emitted out of the structure. Such conversion is considered the main undesired loss in a plasmonic system, since this energy does not contribute to a surface propagation nor to interactions with atoms, molecules, structures, or measuring devices in the exterior of the metal.

Although the description of quantum plasmons developed in this thesis is fundamentally based on a closed system (with the inclusion of the matter field), it offers a clear picture of

lossy states that we describe in the present subsection.

We recall that the (uncoupled) eigenconfigurations ϕ_μ^m of the frequency operator [Eq. (5.118)] are pure matter oscillations; hence, we can evaluate how much of the emission is lost into pure matter excitation by projecting the one-plasmon state $|\Psi\rangle$ onto all generalized configurations $|\phi_\mu^m\rangle$. More specifically, we introduce a coefficient of losses:

$$\gamma(t) = \int d\mu \left| \langle \phi_\mu^m | \Psi(t) \rangle \right|^2, \quad (7.42)$$

which quantifies the part of the quantum state generated by pure matter excitation, thus inside the medium and non-contributing to any near- or far-field radiation outside the metal. Identifying the two blocks of the quantum state, $\Psi = [u \ v]^T$, this coefficient can be written

$$\gamma(t) = \int d\mu |v(\mu)|^2. \quad (7.43)$$

We can distinguish three scenarios for a given state $|\Psi(t)\rangle$:

- $\gamma = 0$: the state is purely photonic;
- $\gamma = 1$: the state is purely material;
- $0 < \gamma < 1$: the state is in a superposition of photonic and material contributions. This can correspond to a localized surface state, or to a partially radiative state, or to a combination of both.

For general applications in integrated plasmonics, one would wish to prepare a state which is localized at the surface but with γ as small as possible to prevent losses.

Remark: It is important to note that the state $|\phi_\mu^m\rangle$, despite being associated with an eigenconfiguration of the uncoupled frequency operator, is a state of the coupled system. It is generated by a creation annihilation $\hat{B}_{\phi_\mu^m}^\dagger$ as defined in Section 6.1.1.

One can evaluate the coefficient of losses γ for a state produced by spontaneous decay of an emitter. To do so, one needs to calculate the state $|\Psi(t)\rangle$ given by Eq. (7.33). Since we have solved the equation (7.37) for the population of the ground state of the emitter, we can now solve the equation (7.34b) for its excited state. We get straightforwardly

$$C_{1,\lambda,d\lambda}^g(t) = \frac{-i g_{\lambda,d\lambda}^* / \hbar}{\frac{\Gamma}{2} - i(\lambda - \omega_0 - \Delta)} \left[e^{i(\lambda - \omega_0)t} e^{-(\frac{\Gamma}{2} + i\Delta)t} - 1 \right], \quad (7.44)$$

with the condition $C_{1,\lambda,d\lambda}^g(t=0) = 0$. We can introduce it into (7.33):

$$\begin{aligned} |\Psi(t)\rangle &= e^{-i\omega_0 t} e^{-(\frac{\Gamma}{2} + i\Delta)t} |\emptyset, e\rangle \\ &\quad - \frac{i}{\hbar} \left[e^{-i\omega_0 t} e^{-(\frac{\Gamma}{2} + \Delta)t} - 1 \right] \int_0^\infty d\lambda \sum_{d\lambda} \frac{g_{\lambda,d\lambda}^*}{\frac{\Gamma}{2} - i(\lambda - \omega_0 - \Delta)} |1_{\lambda,d\lambda}, g\rangle. \end{aligned} \quad (7.45)$$

Hence, the quantum state of the system is entirely known, provided that we know the functions g , i.e., that we have calculated the eigenvectors of Ω and that we know the orientation and strength of the dipole moment of the emitter. We can project it onto the plasmon state

associated with configuration ϕ_μ^m , using that all 1-plasmon states of the coupled model satisfy $\langle \phi_\mu^m | \emptyset \rangle = 0$. Since the state Ψ also contains the information of the state of the emitter, we need to add that the projection does not affect it. We obtain

$$\begin{aligned} \langle \phi_\mu^m | \Psi(t) \rangle = & -\frac{i}{\hbar} \left[e^{-i\omega_0 t} e^{-(\frac{\Gamma}{2} + \Delta)t} - 1 \right] \left\{ \int d^3 k \sum_d \frac{\vec{d} \cdot \vec{e}_{\vec{k},d}^*(\vec{x}_0)}{\frac{\Gamma}{2} - i(\omega - \omega_0 - \Delta)} \vec{v}_{\vec{k},d}^e(\mu') \right. \\ & \left. + \int dV \int_V d^3 r \frac{\vec{d} \cdot \vec{m}_{\nu,\vec{r}}^*(\vec{x}_0)}{\frac{\Gamma}{2} - i(\nu - \omega_0 - \Delta)} \vec{v}_{\nu,\vec{r}}^m(\mu') \right\}, \end{aligned} \quad (7.46)$$

which can then be used to calculate the coefficient γ from Eq. (7.42).

7.4 Comments on the literature

We previously commented on certain discrepancies in the quantization procedure for plasmons as described in the literature (see Section 6.3). A main conclusion of the discussion was that using our method of diagonalization leads to a different expression of the electric field observable. Since this operator is used to derive the decay rate of the emitter in a plasmonic environment, it is reasonable to assume that its expression should be different as well. However, it appears that the decay rate as constructed and used in the literature does not contain inconsistencies when the limit of no coupling is taken. It is worth investigating whether or not the construction of the literature can be related to ours. We will see, in particular, that some terms are often forgotten in the usual construction.

7.4.1 Summary of the result in the literature

It is widely stated in the literature [70, 77, 79, 88, 92–107, 114–118, 121, 127, 130–137] that the spontaneous emission of a point-dipole emitter (or equivalently the power spectrum [87], coupling functions or commutators of the fields) in a plasmonic environment relies on the calculation of the imaginary part of a Green function at the position of the emitter \vec{x}_0 (which can be put inside or outside of the medium):

$$\Gamma(\vec{x}_0, \omega_0) = \frac{2\omega_0^2}{\hbar\epsilon_0 c^2} \left\{ \vec{d} \cdot \text{Im} \left[\bar{\bar{G}}(\omega_0, \vec{x}_0, \vec{x}_0) \right] \cdot \vec{d} \right\}, \quad (7.47)$$

with ω_0 the transition frequency of the emitter, \vec{d} its dipole moment and $\bar{\bar{G}}$ the Green function satisfying

$$\left[\nabla \times \nabla \times - \frac{v^2}{c^2} \epsilon(v, \vec{r}) \right] \bar{\bar{G}}(v, \vec{r}, \vec{x}) = \mathbb{1} \delta(\vec{r} - \vec{x}). \quad (7.48)$$

The decay rate (7.47) does not contain inconsistencies when the limit of no coupling is taken. Indeed, in this limit $\bar{\bar{G}}$ tends to the Green function in vacuum $\bar{\bar{G}}_0$ satisfying Eq. (7.48) with $\epsilon = 1$, and one can show [70] that we have

$$\Gamma_0(\vec{x}_0, \omega_0) = \frac{\omega_0^3 |\vec{d}|^2}{3\pi \hbar \epsilon_0 c^3}. \quad (7.49)$$

The expression (7.47) for the decay rate is obtained by inserting the expression (6.110) in the Fermi golden rule [88]. This calculation relies on the validity of Eq. (6.110), which is not justified for a finite medium, as shown in Section 6.3. Furthermore, we show in the present Section that the usual derivation assuming Eq. (6.110) also contains discrepancies which have failed to be fully addressed in past works.

7.4.2 Fermi golden rule assuming Eq. (6.110)

We will now describe how the spontaneous decay rate (7.47) is constructed in the literature using the Fermi golden rule and assuming the formula (6.110) for the electric field observable, which we recall:

$$\vec{\tilde{E}}(\vec{x}) = \sqrt{\frac{\hbar\mu_0}{\pi c^2}} \int_0^\infty d\nu \int_V d^3r \nu^2 \epsilon_i^{1/2}(\nu, \vec{r}) \bar{G}(\nu; \vec{r}, \vec{x}) \vec{C}(\nu, \vec{r}) + h.c., \quad (7.50)$$

where the Green function \bar{G} satisfies Eq. (7.48). We can insert it into the coupling operator $\hat{W} = -\vec{d} \cdot \vec{\tilde{E}}$ and then into the Fermi golden rule (7.12)

$$\Gamma(\vec{x}_0, \omega_0) = \frac{2\pi}{\hbar^2} \sum_f |\langle f | \hat{W} | i \rangle|^2 \delta(\omega_f - \omega_0). \quad (7.51)$$

Here the only states left are associated with the spectral structure of the medium (this is a key argument against the expression (7.50) as discussed in Section 6.3). Hence, the decay rate reads

$$\Gamma(\vec{x}_0, \omega_0) = \frac{2\pi}{\hbar^2} \int d\nu \int_V d^3r \left| \langle 1_{\nu, \vec{r}} \otimes g | [\hat{\sigma}_+ + \hat{\sigma}_-] \vec{d} \cdot \vec{\tilde{E}} | \emptyset \otimes e \rangle \right|^2 \delta(\nu - \omega_0). \quad (7.52)$$

After inserting the electric field observable (7.50) and making a few manipulations (in rotating wave approximation), we find

$$\Gamma(\vec{x}_0, \omega_0) = \frac{2\mu_0\omega_0^4}{\hbar c^2} \left\{ \vec{d} \cdot \left[\int_V d^3r \epsilon_I(\omega_0, \vec{r}) \bar{G}^T(\omega_0, \vec{r}, \vec{x}_0) \bar{G}^*(\omega_0, \vec{r}, \vec{x}_0) \right] \cdot \vec{d} \right\}. \quad (7.53)$$

It is usually stated [73, 74, 76–79, 88, 94, 97–100, 115–117] that the integral term can be simplified using

$$\frac{\omega_0^2}{c^2} \int_V d^3r \epsilon_I(\omega_0, \vec{r}) \bar{G}^T(\omega_0, \vec{r}, \vec{r}_A) \bar{G}^*(\omega_0, \vec{r}, \vec{r}_B) = \text{Im } \bar{G}(\vec{r}_A, \vec{r}_B). \quad (7.54)$$

If this were true, the decay rate would simplify into the expression that is mostly used in practice:

$$\Gamma(\vec{x}_0, \omega_0) = \frac{2\mu_0\omega_0^2}{\hbar} \left\{ \vec{d} \cdot \text{Im} \left[\bar{G}(\omega_0, \vec{x}_0, \vec{x}_0) \right] \cdot \vec{d} \right\}. \quad (7.55)$$

If one assumes the validity of this expression, the question of how to compute the decay rate of the emitter (and also field correlations and commutators) in a given configuration is narrowed to the question of how to find the Green tensor corresponding to this configuration [70, 77, 79, 88, 92–107, 114–118, 121, 127, 130–137]. Many analytical and numerical methods have been developed for this specific technique.

However, this expression is not true in general. An easy way to see it is by taking the limit $\epsilon \rightarrow 1$ in the Green identity (7.54), which cancels the left-hand side while the right-hand side is not zero in general. It is already not the case in vacuum, where the Green tensor reads [138]

$$\bar{G}_0^{ij}(\vec{r}_A, \vec{r}_B) = \delta_{ij} g_0 + \frac{c^2}{\omega^2} \frac{\partial^2 g_0}{\partial r_A^i \partial r_B^j}, \quad g_0(\vec{r}_A, \vec{r}_B) = \frac{e^{i\frac{\omega}{c}|\vec{r}_A - \vec{r}_B|}}{4\pi|\vec{r}_A - \vec{r}_B|}. \quad (7.56)$$

The correct evaluation of the left-hand side of Eq. (7.54) brings an extra boundary term, and we have the (complete) following identity instead:

$$\frac{v^2}{c^2} \int_V d^3 r \epsilon_I(\vec{r}) \bar{\bar{G}}^T(\vec{r}, \vec{r}_A) \bar{\bar{G}}^*(\vec{r}, \vec{r}_B) = \frac{1}{2i} [\bar{\bar{G}}^T(\vec{r}_B, \vec{r}_A) - \bar{\bar{G}}^*(\vec{r}_A, \vec{r}_B)] + \bar{\bar{F}}(\vec{r}_A, \vec{r}_B, \mathfrak{B}), \quad (7.57)$$

with

$$\bar{\bar{F}}(\vec{r}_A, \vec{r}_B, \mathfrak{B}) = [\bar{\bar{b}}^T(\vec{r}_B, \vec{r}_A, \mathfrak{B}) - \bar{\bar{b}}^*(\vec{r}_A, \vec{r}_B, \mathfrak{B})] / (2i), \quad (7.58)$$

$$\bar{\bar{b}}(\vec{r}_A, \vec{r}_B, \mathfrak{B}) = - \int_{\mathfrak{B}} ds (\vec{n} \times \bar{\bar{G}}^*(\vec{x}, \vec{r}_B))^T (\nabla \times \bar{\bar{G}}(\vec{x}, \vec{r}_A)), \quad (7.59)$$

where all frequency dependencies are implicit; \mathfrak{B} denotes a boundary surface which encapsulates \vec{r}_A and \vec{r}_B , \vec{n} is the outer unit normal vector on the surface, and ds is the surface element. This relation is valid for any tensor $\bar{\bar{G}}$ satisfying Eq. (7.48). For the particular cases where

$$\bar{\bar{G}}(\vec{r}_B, \vec{r}_A) = \bar{\bar{G}}^T(\vec{r}_A, \vec{r}_B), \quad (7.60)$$

the identity (7.57) can be expressed as

$$\frac{v^2}{c^2} \int_V d^3 r \epsilon_I(\omega_0, \vec{r}) \bar{\bar{G}}^T(\omega_0, \vec{r}, \vec{r}_A) \bar{\bar{G}}^*(\omega_0, \vec{r}, \vec{r}_B) = \text{Im } \bar{\bar{G}}(\vec{r}_A, \vec{r}_B) + \bar{\bar{F}}(\vec{r}_A, \vec{r}_B, \mathfrak{B}). \quad (7.61)$$

A brief proof of this was published in the first appendix of [119] and we write it in detail in Appendix D. One can show that all Green functions satisfying the asymptotic Sommerfeld radiation condition are among the cases where (7.60) is verified.

It is worth noting that for practical purposes, when used to calculate correlations or the decay rate of an emitter, the Green function is evaluated at a given observation point $\vec{x} = \vec{r}_A = \vec{r}_B$, relaxing the condition (7.60) to a simple symmetry condition of $\bar{\bar{G}}(\vec{x}, \vec{x})$.

We recover the correct limit in vacuum, in which case the identity (7.61) becomes

$$\bar{\bar{F}}_0(\vec{r}_A, \vec{r}_B, \mathfrak{B}) = -\text{Im } \bar{\bar{G}}_0(\vec{r}_A, \vec{r}_B). \quad (7.62)$$

In conclusion, if the usual formula (7.50) were correct for a finite medium, and if we use the correct Green identity for this case (7.61), the decay rate would be

$$\Gamma(\vec{x}_0, \omega_0) = \frac{2\mu_0\omega_0^2}{\hbar} \left\{ \vec{d} \cdot \left[\text{Im } \bar{\bar{G}}(\omega_0, \vec{x}_0, \vec{x}_0) + \bar{\bar{F}}(\vec{x}_0, \vec{x}_0, \mathfrak{B}) \right] \cdot \vec{d} \right\} \quad (7.63)$$

and not (7.55) as stated in the literature [70, 77, 88, 92, 94–100, 102–106, 114–117, 121, 127, 130–137] (some of these references study the power spectrum, which can be directly linked to the decay rate [87]). For a medium interacting weakly with the field (i.e., ϵ_i close to zero), the correction term $\bar{\bar{F}}$ can be estimated in perturbation theory by

$$\bar{\bar{F}} = -\text{Im } \bar{\bar{G}}_0 + \mathcal{O}(\epsilon_i), \quad (7.64)$$

and thus one would have

$$\Gamma(\vec{x}_0, \omega_0) = \frac{2\mu_0\omega_0^2}{\hbar} \left\{ \vec{d} \cdot \left[\text{Im } \bar{\bar{G}}(\omega_0, \vec{x}_0, \vec{x}_0) - \text{Im } \bar{\bar{G}}_0(\omega_0, \vec{x}_0, \vec{x}_0) \right] \cdot \vec{d} \right\} + \mathcal{O}(\epsilon_i). \quad (7.65)$$

Since we also have $\vec{\bar{G}} = \vec{\bar{G}}_0 + \mathcal{O}(\epsilon_i)$, we would conclude that

$$\Gamma = \mathcal{O}(\epsilon_i), \quad (7.66)$$

which implies $\lim_{\epsilon_i \rightarrow 0} \Gamma = 0$ instead of the vacuum value (7.49).

One could ask whether the addition of the boundary term in the Green identity has a significant effect on the decay rate in a non-perturbative scenario. In the next subsection we calculate it in detail in a one-dimensional configuration where the medium is a slab of metal (which is equivalent to a configuration analyzed, e.g., in [81, 118, 131]).

7.4.3 Spontaneous emission in a 1D model assuming Eq. (6.110)

We consider a 1D model where the material (dissipative and dispersive) medium consists of an homogeneous segment extending from $-\ell$ to ℓ . Its macroscopic electric response is given by the (complex) dielectric coefficient ϵ or equivalently by the (also complex) refractive index $n^2 = \epsilon$. This situation corresponds to a special case of a 3D model where only wave vectors \vec{k} normal to an infinite slab are considered, and where the electric field is constrained in one polarization orthogonal to \vec{k} . Figure 7.3 is a sketch of the system, with the notation used for each part of the total Green function. We note $[-L, L]$ the boundaries (which must include the coordinates of the source, x_S , and of the observer, x , and can be sent to infinity).

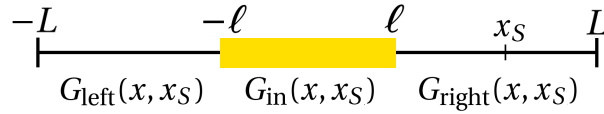


Figure 7.3 – Sketch of the 1D model. The Green function can be split into three contributions, with x_S the position of the source taken on the right side of the medium. The observation point x can be taken either on the left side of the medium, in the medium, or on the right side.

For an observing point x , we consider the Green function G satisfying

$$\left[-\partial_x^2 - \frac{\omega^2}{c^2} \epsilon(x, \nu) \right] G(x, x_S) = \delta(x - x_S), \quad (7.67)$$

which is the wave equation for \vec{E} in 1D but with the current density replaced by $\delta(x - x_S)$. We place arbitrarily the source on the right side of the slab ($x_S \in [\ell, L]$) as in Fig. 7.3. In Appendix E we have calculated the Green function for an observation point x on the left, inside the slab, or on the right. We have obtained the following expressions:

$$G_{\text{left}}(x, x_S) = \frac{i}{2k} A e^{-ik(2\ell+x-x_S)}, \quad (7.68)$$

$$G_{\text{in}}(x, x_S) = \frac{i}{2k} [B e^{-ik(nx-x_S)} + C e^{ik(nx+x_S)}], \quad (7.69)$$

$$G_{\text{right}}(x, x_S) = \frac{i}{2k} [D e^{-ik(2\ell-x-x_S)} + e^{ik|x-x_S|}], \quad (7.70)$$

where $k = \omega/c$, and

$$A = \frac{4n}{Y} e^{2ikn\ell}, \quad (7.71)$$

$$B = \frac{2(n+1)}{Y} e^{ik(n-1)\ell}, \quad (7.72)$$

$$C = \frac{2(n-1)}{Y} e^{ik(3n-1)\ell}, \quad (7.73)$$

$$D = \frac{(n^2-1)}{Y} [e^{4ikn\ell} - 1], \quad (7.74)$$

with

$$Y = (n+1)^2 - (n-1)^2 e^{4ikn\ell}. \quad (7.75)$$

We want to calculate the integral

$$\frac{\omega^2}{c^2} \int_{-L}^L dx \epsilon_i(x, \omega) G(x, x_A) G^*(x, x_B), \quad (7.76)$$

for two possible positions of the source x_A et x_B , using the Green identity (7.61), which in 1D reads:

$$\frac{\omega^2}{c^2} \int_{-L}^L dx \epsilon_i(x, \omega) G(x, x_A) G^*(x, x_B) = \text{Im } G(x_A, x_B) + F(x_A, x_B), \quad (7.77)$$

provided that the Green function satisfies the reciprocity condition $G(x, x') = G(x', x)$. The boundary term F is

$$F(x_A, x_B) = \frac{1}{2i} [b(x_B, x_A) - b^*(x_A, x_B)], \quad (7.78)$$

$$b(x_B, x_A) = -[G^*(x, x_B) \partial_x G(x, x_A)]_{-L}^L. \quad (7.79)$$

Since $L > \ell$, the term b reads

$$b(x_B, x_A) = G_{\text{left}}^*(x, x_B) \partial_x G_{\text{left}}(x, x_A) \Big|_{x=-L} - G_{\text{right}}^*(x, x_B) \partial_x G_{\text{right}}(x, x_A) \Big|_{x=L}. \quad (7.80)$$

We therefore need two Green function, one for each position of x close to a boundary. Using the expressions (7.68)–(7.70), a careful calculation leads to

$$G_{\text{left}}^*(x, x_B) \partial_x G_{\text{left}}(x, x_A) \Big|_{x=-L} = -\frac{i}{4k} |A|^2 e^{ik(x_A - x_B)}, \quad (7.81)$$

and

$$G_{\text{right}}^*(x, x_B) \partial_x G_{\text{right}}(x, x_A) \Big|_{x=L} = \frac{i}{4k} \left[|D|^2 e^{ik(x_A - x_B)} + e^{-ik(x_A - x_B)} + D e^{-ik(2\ell - x_A - x_B)} + D^* e^{ik(2\ell - x_A - x_B)} \right]. \quad (7.82)$$

For the result (7.82), we have used

$$e^{ik|x-x_A|} = e^{ik(x-x_A)} \Theta(x-x_A) + e^{-ik(x-x_A)} \Theta(x_A-x), \quad (7.83)$$

plus $\partial_x \Theta(x - x_A) = \delta(x - x_A)$, and finally the fact that for $x_A, x_B < L$, we have $\Theta(x - x_{A,B}) = 1$, $\Theta(x_{A,B} - x) = 0$ and $\delta(x - x_{A,B}) = 0$ when x is evaluated at the boundary $x = L$. We notice that the expressions (7.81) and (7.82) do not depend on the boundaries. We can finally insert them into (7.80) to obtain:

$$b(x_B, x_A) = -\frac{i}{4k} \left[(|A|^2 + |D|^2) e^{ik(x_A - x_B)} + e^{-ik(x_A - x_B)} + D e^{-ik(2\ell - x_A - x_B)} + D^* e^{ik(2\ell - x_A - x_B)} \right], \quad (7.84)$$

and

$$b^*(x_A, x_B) = -b(x_B, x_A). \quad (7.85)$$

Inserting it into Eq. (7.86):

$$F(x_A, x_B) = -\frac{1}{4k} \left[(|A|^2 + |D|^2) e^{ik(x_A - x_B)} + e^{-ik(x_A - x_B)} + 2\text{Re} \left\{ D e^{-ik(2\ell - x_A - x_B)} \right\} \right]. \quad (7.86)$$

Furthermore, we can express the identity (7.77) for $x_A = x_B = x_S$, with x_S on the right of the slab, which is what is usually considered to calculate e.g. the decay rate of an emitter. It reads:

$$\frac{\omega^2}{c^2} \int_{-L}^L dx \epsilon_i(x, \omega) |G(x, x_S)|^2 = \text{Im} G(x_S, x_S) + F(x_S, x_S). \quad (7.87)$$

From (7.70), the imaginary part of the Green function for a source outside the medium reads

$$\text{Im} G_{\text{right}}(x_S, x_S) = \text{Im} \left\{ \frac{i}{2k} \left[D e^{-2ik(\ell - x_S)} + 1 \right] \right\} = \frac{1}{2k} \left[1 + \text{Re} \left\{ D e^{-2ik(\ell - x_S)} \right\} \right], \quad (7.88)$$

and Eq. (7.86) gives

$$F(x_S, x_S) = -\frac{1}{4k} \left[1 + |A|^2 + |D|^2 + 2\text{Re} \left\{ D e^{-2ik(\ell - x_S)} \right\} \right]. \quad (7.89)$$

The sum of these two terms gives

$$\text{Im} G_{\text{right}}(x_S, x_S) + F(x_S, x_S) = \frac{1}{4k} [1 - |A|^2 - |D|^2], \quad (7.90)$$

which is a constant in x_S . Consequently, assuming that the integral (7.76) is adapted to calculate the Fermi golden rule, the decay rate of an emitter in the exterior of the slab would be constant and given by

$$\Gamma = \frac{\omega_0 |\vec{d}|^2}{2\hbar \epsilon_0 c S} [1 - |A|^2 - |D|^2], \quad (7.91)$$

whereas if the boundary terms were canceled, it would give

$$\Gamma_G = \frac{\omega_0 |\vec{d}|^2}{\hbar \epsilon_0 c S} \left[1 + \text{Re} \left\{ D e^{-2ik(\ell - x_S)} \right\} \right]. \quad (7.92)$$

This result in a one-dimensional model shows that the missing boundary terms in (7.54) can have a significant effect on the decay rate. Furthermore, the discrepancy with the no-coupling limit implies that one cannot use the expression (7.50) of the electric field to calculate the decay rate (or related quantities) as in Refs. [70, 77, 79, 88, 92–107, 114–118, 121, 127, 130–137].

Remark: It is easy to check that by taking the limit $n \rightarrow 1$, it gives

$$F(x_A, x_B) \rightarrow -\frac{1}{2k} \cos[k(x_A - x_B)] = -\text{Im } G_0(x_A, x_B), \quad (7.93)$$

where G_0 is the Green function satisfying the wave equation in free space (Eq. (7.67) with $\epsilon = 1$), which reads

$$G_0(\omega; x, x_S) = \frac{i}{2k} e^{ik|x-x_S|}. \quad (7.94)$$

Hence, Eq. (7.93) is consistent with the identity (7.77).

7.5 Summary on the dynamics of plasmons

Once the plasmonic model has been diagonalized (Chapter 5) and quantized (Chapter 6), the resulting quantum operators and quantum states can be used to describe many different problems. In this chapter we have focused on the process of spontaneous emission since the enhancement of the rate at which plasmons are emitted from an atom near a nanoparticle is one of the main reason why plasmonic structures are used in quantum experiments.

We have shown that the derivation of the spontaneous decay rate of the atom is straightforward when the electric field observable is explicitly known. Our result, once again, differs from the one used in the literature. We have verified that the two most common ways to derive the decay rate (the Fermi golden rule and the Wigner-Weisskopf theory) give the same result, which is expressed in terms of the functions found when solving the Lippmann-Schwinger equation. We have calculated the decay rate in a 1D model and compared it with the results from the literature.

A final construction we made in this thesis was a coefficient which quantifies how much of the plasmon state (either taken as an initial condition or as calculated from an emission process) is lost inside the medium. The calculation of this coefficient could be useful to characterize specific configurations for the design of plasmonic structures.

Additionally, we have analyzed how the spontaneous emission process is derived in the literature. It mostly relies on the expression for the electric field observable that is not valid for finite media (as discussed in the preceding chapter), but also on an identity for the Green tensor which also contains discrepancies in the case of finite media. The conclusion is that, even assuming that the usual expression for the quantum field is a good approximation of the exact result, one should take into account extra boundary terms in the calculation of the decay rate (or related quantities such as the commutators of the fields or the power spectrum). The impact of these missing terms on the local density of states or on Casimir forces [139, 140] is an open question.

Conclusion

This thesis describes a quantization procedure for light interacting with linear and inhomogeneous media, either passive or dispersive and dissipative. The former is used to characterize photons propagating in dielectric environments where neglecting dissipation and dispersion is justified. The effect of matter in this case mostly appears through coefficients of transmission and reflection during the propagation of the classical configuration the photon state is associated with. However, the construction of the quantum theory requires special care compared to the vacuum case because the Hamiltonian model depends critically on the response function corresponding to any given configuration of matter. The latter scenario, for metallic media, offers a theoretical basis to characterize quantum plasmons. Because of the introduction of dissipation and dispersion (i.e., with a dielectric function that is complex and frequency-dependent), the construction of a Hamiltonian structure necessary to quantize requires the inclusion of additional degrees of freedom associated with matter. The quantization of such a model provides sufficient tools to investigate spontaneous emission of single plasmons as in the present thesis, but it can also be used to characterize the propagation of single plasmons, their localization in space, as well as collective effects and stimulated emission.

A key message of this work is the range of applicability of the quantization procedure described in the main introduction (adapted from Refs. [13–15]). This procedure has been applied successfully to both scenarios. This contrasts with the literature, where quantization schemes have been developed specifically to the plasmonic models (either involving quantum noise and Langevin equations, or a Fano diagonalization method with a microscopic model for matter). One of our contributions was to show how such schemes fail to address configurations where the dispersive and dissipative material medium is of finite extent [2]. In the quantization procedure used in this work, the specificity of each scenario presents itself in the first step, when the Hamiltonian structure built from the equations of motion has to be transformed into a harmonic-like form,

$$H = \frac{1}{2} \underline{P} \cdot \underline{P} + \frac{1}{2} \underline{Q} \cdot \Omega^2 \underline{Q}, \quad (7.95)$$

with Ω a frequency operator. The diagonalization of the Hamiltonian thus reduces to the diagonalization of Ω^2 (or equivalently Ω), and the classical configurations of the field can be written as linear combinations of the eigenfunctions of Ω (called *eigenconfigurations*). Once this is achieved, a principle of correspondence can be applied and the field observables can be expressed in terms of the eigenconfigurations. The justification of the principle of correspondence is not trivial in a system with infinitely many degrees of freedom; we for-

mulated it in detail in the case of photons in passive media and similar arguments can be applied to the case of plasmons.

In passive media, the diagonalization of the frequency operator is not a trivial task because it depends on the dielectric function, which is different for every physical configuration. However, if one is interested only in the emission, propagation and detection of the photon in the exterior of the dielectric, its quantum state can be associated with the configurations of the free field and the presence of the dielectric can be handled in the propagation in the same way as in classical optics, through the introduction of coefficients of transmission and reflection.

The quantum theory of light in passive media provides a basis to describe quantum optics experiments. In particular, the detailed characterization of the quantum states and their association to classical configurations of the field provides the necessary tools to describe photons localized in pulses. In this thesis we gave the example of the Hong-Ou-Mandel experiment, a pioneer quantum interference effect. Recent experiments [20–22] require a description of the HOM effect with a detailed characterization of the classical configurations of the photons which we could provide from the quantization procedure.

A complete description of quantum optics experiments in passive media would include the emission process, the propagation, and the detection. While in this thesis we addressed mainly the propagation and emission, the detection part still raises some open questions. In particular, the construction of the quantum states shows that the localization of the photon depends on the definition of what particular type of detector measures actually. We described the detection in the Hong-Ou-Mandel experiments on the basis of the classical configuration, however it may have to be adapted to other local quantities such as the associated electric field observable.

In dispersive and dissipative media, the diagonalization of the frequency operator is more subtle and one cannot model the effect of the medium on external phenomena simply by introducing coefficients in the propagation. The difficulty of diagonalizing directly the plasmonic model has led many authors to use a special type of method, the Fano diagonalization method, where the result of the diagonalization is postulated and one then tries to extract the corresponding diagonalizing transformation. The novelty of our work is to have constructed a method to diagonalize the plasmonic model without postulating the result *a priori*. This was published in [1,3].

An advantage of our method is that it relies on canonical transformations. This ensures that the diagonalized and quantized model corresponds to the initial one. Furthermore, it also ensures that the commutation relations of the observables are the correct ones. In the literature, this latter point was usually dependent on a Green function which is different for every material environment. Here, it only requires the completeness of the eigenconfigurations, which is satisfied in the plasmonic model. Finally, our method gives a way to calculate the eigenconfigurations of the plasmonic field, which can then be used to characterize the field in detail. The structure of the quantum states also provides a rather simple method to track the dissipation inside the medium.

An interesting discussion comes from comparing the results of our diagonalization to the ones of the literature. An immediate observation is that our result is consistent with the limit when the coupling between light and the medium vanishes (corresponding to the dissipationless limit $\epsilon_i \rightarrow 0$). This limit has generated some debates in the literature, and

some attempts of justification that would allow one to use these results in practical calculations. Our interpretation is that the past results may be valid in a homogeneous (therefore infinite) medium, which was the case first studied [71, 72]. It is conceivable that using them in practical calculations (e.g., to compute the spontaneous decay rate of an emitter or Casimir forces) leads to good approximations. However, to check it, one needs an independent ansatz-free method to compare with. We provided such a method in [1, 3].

We compared our results with the ones of the literature in perturbation theory, in particular the expression of the electric field observable. In first order, they coincide with some proposed corrections from the literature [81, 82] taken at the same order of perturbation, aside from a diverging function very close to the surface (which is clearly outside the range of validity of the perturbation theory). In non-perturbative regimes, computational methods should be developed to solve the Lippmann-Schwinger equation. This is not an easy task because of the high degree of degeneracy of the model.

We described the spontaneous decay rate of a point-dipole emitter interacting with the plasmonic field, both from the Fermi golden rule and from the Wigner-Weisskopf theory (both approaches give the same results). The emitted quantum state was also expressed in terms of the eigenconfigurations, providing a potential starting point for future studies. This derivation was published in [3].

Aside of the direct comparison of formulas, we also investigated how the result of the literature for the spontaneous decay rate is derived. We showed that even assuming the commonly accepted expression for the electric field operator, the calculation of the decay rate from the Fermi golden rule or the Wigner-Weisskopf theory uses a identity for the Green tensor which is verified only in an infinite medium. In the context of finite media, extra terms appear in the identity, and we showed in a one-dimensional example that these terms have a significant impact on the result. Thus, even if the electric field observable could be approximated to the one of the literature, one should include the missing terms in practical applications.

Classical energy of radiation

The reason why the classical Hamiltonian of light in passive media, given by Eq. (2.15), can be identified as the energy of the system is not a trivial question which we try to answer in the present appendix.

A.1 From the power transfer to a set of external charges

One way to determine how the energy of an electromagnetic configuration should be defined is to make a link with a mechanical system for which the notion of kinetic energy is considered known [141]. We consider a system that can include a medium, and a possible coupling with a system of external charged particles. The coupling is given by the Lorentz force, i.e., the dynamics of each of the particles of charge Q_i , mass m , at position \vec{x}_i is determined by an equation of motion of the form

$$m \frac{d^2 \vec{x}_i}{dt^2} = Q_i \vec{E}(\vec{x}_i, t) + Q_i \frac{d\vec{x}_i}{dt} \times \vec{B}(\vec{x}_i, t). \quad (\text{A.1})$$

The kinetic energy of the i -th particle is given by

$$\mathcal{E}_{kin,i} = \frac{m}{2} \left(\frac{d\vec{x}_i}{dt} \right)^2, \quad (\text{A.2})$$

and the variation of the kinetic energy per time unit is

$$\frac{\partial \mathcal{E}_{kin,i}}{\partial t} = m \frac{d^2 \vec{x}_i}{dt^2} \cdot \frac{d\vec{x}_i}{dt}. \quad (\text{A.3})$$

Introducing (A.1) gives:

$$\frac{\partial \mathcal{E}_{kin,i}}{\partial t} = Q_i \vec{E}(\vec{x}_i, t) \cdot \frac{d\vec{x}_i}{dt} + \left(Q_i \frac{d\vec{x}_i}{dt} \times \vec{B}(\vec{x}_i, t) \right) \cdot \frac{d\vec{x}_i}{dt}. \quad (\text{A.4})$$

The last term is zero because it takes the scalar product of two orthogonal vectors. Thus,

$$\frac{\partial \mathcal{E}_{kin,i}}{\partial t} = \vec{E}(\vec{x}_i, t) \cdot \vec{j}_i, \quad (\text{A.5})$$

with $\vec{j}_i := Q_i d\vec{x}_i/dt$. We introduce $\vec{j}(\vec{x}) := \vec{j}_i \delta(\vec{x}_i - \vec{x})$:

$$\frac{\partial \mathcal{E}_{kin,i}}{\partial t} = \int d^3x \vec{E}(\vec{x}, t) \cdot \vec{j}(\vec{x}). \quad (\text{A.6})$$

If instead of a single point charge we consider N point charges or more generally a density of charge $\rho(\vec{x}) := \sum_i Q_i \delta(\vec{x}_i - \vec{x})$, the time derivative of the total kinetic energy can be written as

$$\frac{\partial}{\partial t} \sum_i \mathcal{E}_{kin,i} = \int d^3x \vec{E}(\vec{x}, t) \cdot \vec{j}(\vec{x}), \quad \vec{j}(\vec{x}) := \sum_i \vec{j}_i \delta(\vec{x}_i - \vec{x}). \quad (\text{A.7})$$

Writing

$$\sum_i \mathcal{E}_{kin,i} = \int d^3x \sum_i \mathcal{E}_{kin,i} \delta(\vec{x}_i - \vec{x}) \quad (\text{A.8})$$

and defining the density of kinetic energy

$$e_{kin}(\vec{x}) := \sum_i \mathcal{E}_{kin,i} \delta(\vec{x}_i - \vec{x}), \quad (\text{A.9})$$

the equation (A.7) becomes

$$\frac{\partial}{\partial t} \int d^3x e_{kin}(\vec{x}, t) = \int d^3x \vec{E}(\vec{x}, t) \cdot \vec{j}(\vec{x}), \quad (\text{A.10})$$

and we can write the relation between the local densities as

$$\frac{\partial}{\partial t} e_{kin}(\vec{x}, t) = \vec{E}(\vec{x}, t) \cdot \vec{j}(\vec{x}), \quad (\text{A.11})$$

which is valid for a discrete or a continuous density of charge. Thus, the quantity $\vec{E}(\vec{x}, t) \cdot \vec{j}(\vec{x})$ can be interpreted as the density of power, i.e., energy per time unit, transferred from the electromagnetic field to the external charge density.

If we denote by $u(\vec{x}, t)$ the energy density of the electromagnetic system, the global energy conservation is expressed by

$$\frac{\partial}{\partial t} \int d^3x [e_{kin}(\vec{x}, t) + u(\vec{x}, t)] = 0, \quad (\text{A.12})$$

implying

$$\frac{\partial}{\partial t} \int d^3x u(\vec{x}, t) = - \int d^3x \vec{E}(\vec{x}, t) \cdot \vec{j}(\vec{x}). \quad (\text{A.13})$$

Locally the electromagnetic energy density can change by two independent mechanisms: the first one is the transfer to the external charges that we have described above, and the second one is the transport by local energy flow. Thus locally, the conservation of energy is expressed by the following relation between densities:

$$\frac{\partial}{\partial t} u(\vec{x}, t) = -\nabla \cdot \vec{S} - \vec{E}(\vec{x}, t) \cdot \vec{j}(\vec{x}), \quad (\text{A.14})$$

where \vec{S} is the energy flow density, or *Poynting vector*. We remark that both the energy density and the Poynting vector take different expressions depending on the considered system (free field, electromagnetic field in a passive linear medium, in a non-passive medium, linear or non-linear...). For each system, the strategy is to start with the term $-\vec{E} \cdot \vec{j}$ and use Maxwell's equations to obtain an expression that has the structure of (A.14). Then the appearing expression for u can be identified as the energy density and the expression for \vec{S} as the Poynting energy flow density.

A.2 From the Hamiltonian structure

A second approach consists in starting with the considered Maxwell equations including the medium, but without the external test charges, and constructing a Hamiltonian representation. This construction involves the choice of canonical variables and a Hamiltonian functional H such that the corresponding Hamiltonian equations coincide with the Maxwell equations. In this approach, the energy density is defined by the Hamiltonian density $h(\vec{x})$,

$$H = \int d^3x h(\vec{x}). \quad (\text{A.15})$$

The energy flow density is obtained by calculating $\partial h / \partial t$.

This approach is certainly consistent from a mathematical point of view, but it seems important to have also the link between the electromagnetic energy and the mechanical energy provided in the preceding approach. As discussed in the next subsection, both approaches should lead to the same results.

A.3 Equivalence of the two approaches

For each concrete situation one can check whether the two functions u and h , expressed in suitable variables, coincide. This can be done explicitly for the linear systems treated in this thesis. In order to establish that the two definitions coincide in general we have to extend the Hamiltonian formulation to include the external test charges,

$$H = \int d^3x h(\vec{x}) + H_{ext}, \quad (\text{A.16})$$

and show that the corresponding Hamiltonian time evolution equations imply a relation of the form

$$\frac{\partial}{\partial t} h(\vec{x}, t) = -\nabla \cdot \vec{S} - \vec{E}(\vec{x}, t) \cdot \vec{j}(\vec{x}), \quad (\text{A.17})$$

and that the two energy densities coincide:

$$h(\vec{x}) = u(\vec{x}). \quad (\text{A.18})$$

In a passive medium with external charges and currents, Maxwell's equations can be written

$$\partial_t \vec{\mathcal{D}} = \nabla \times \vec{\mathcal{H}} - \vec{j}_{ext}, \quad (\text{A.19a})$$

$$\partial_t \vec{B} = -\nabla \times \vec{E}, \quad (\text{A.19b})$$

$$\nabla \cdot \vec{\mathcal{D}} = \rho_{ext}, \quad (\text{A.19c})$$

$$\nabla \cdot \vec{B} = 0, \quad (\text{A.19d})$$

where $\vec{\mathcal{D}}$ and $\vec{\mathcal{H}}$ are defined by

$$\vec{\mathcal{D}} := \epsilon_0 \epsilon_R \vec{E}, \quad (\text{A.20})$$

$$\vec{\mathcal{H}} := (\mu_0 \mu_R)^{-1} \vec{B}, \quad (\text{A.21})$$

with μ_R the relative magnetic permeability (which we have taken as 1 in this thesis, i.e., neglecting magnetic effects). The expressions for the energy density u and the flux \vec{S} can be determined starting from Eqs. (A.19a) and (A.19b):

$$-\vec{j}_{ext} \cdot \vec{E} = \vec{E} \cdot \partial_t \vec{\mathcal{D}} - \vec{E} \cdot (\nabla \times \vec{\mathcal{H}}). \quad (\text{A.22})$$

We can use the identity

$$\nabla \cdot (\vec{E} \times \vec{\mathcal{H}}) = \vec{\mathcal{H}} \cdot (\nabla \times \vec{E}) - \vec{E} \cdot (\nabla \times \vec{\mathcal{H}}), \quad (\text{A.23})$$

giving

$$\begin{aligned} -\vec{j}_{ext} \cdot \vec{E} &= \vec{E} \cdot \partial_t \vec{\mathcal{H}} + \nabla \cdot (\vec{E} \times \vec{\mathcal{H}}) - \vec{\mathcal{H}} \cdot (\nabla \times \vec{E}), \\ &= \vec{E} \cdot \partial_t \vec{\mathcal{D}} + \nabla \cdot (\vec{E} \times \vec{\mathcal{H}}) + \vec{\mathcal{H}} \cdot \partial_t \vec{B}, \end{aligned} \quad (\text{A.24})$$

where we have used (A.19b). For a passive linear medium where $\vec{\mathcal{D}}$ and $\vec{\mathcal{H}}$ are defined by Eqs. (A.20) and (A.21), we have the relations

$$\vec{E} \cdot \partial_t \vec{\mathcal{D}} = \frac{1}{2} \partial_t (\vec{E} \cdot \vec{\mathcal{D}}), \quad (\text{A.25})$$

$$\vec{\mathcal{H}} \cdot \partial_t \vec{B} = \frac{1}{2} \partial_t (\vec{B} \cdot \vec{\mathcal{H}}). \quad (\text{A.26})$$

We thus gather the different terms in (A.24):

$$-\vec{j}_{ext} \cdot \vec{E} = \frac{1}{2} \partial_t [\vec{E} \cdot \vec{\mathcal{D}} + \vec{B} \cdot \vec{\mathcal{H}}] + \nabla \cdot \vec{E} \times \vec{\mathcal{H}}. \quad (\text{A.27})$$

We can thus identify, and take as a definition, the energy density of the electromagnetic field as

$$u := \frac{1}{2} [\vec{E} \cdot \vec{\mathcal{D}} + \vec{B} \cdot \vec{\mathcal{H}}], \quad (\text{A.28})$$

and the Poynting energy flow as

$$\vec{S} := \vec{E} \times \vec{\mathcal{H}}. \quad (\text{A.29})$$

We remark that in absence of external charges, the relation

$$\partial_t u = -\nabla \cdot \vec{S} \quad (\text{A.30})$$

states the conservation of electromagnetic energy in the passive medium. The total energy of the system is then obtained by integrating the density over space, which gives exactly the Hamiltonian function constructed in Section 2.1.2, Eq. (2.15), with $\mu_R = 1$.

Symplectic structure for the electromagnetic field

In this Appendix we show that the transformation from the electromagnetic vector fields to the real diagonalizing variables, used in passive media, and in the plasmonic model for the pre-diagonalization, is canonical. To do so, we use the symplectic structure of the phase spaces.

The Hamiltonian structure with the constraints is first constructed in the phase space

$$\mathcal{P} := \mathcal{E}^\perp \oplus \mathcal{E}^\perp, \quad (\text{B.1})$$

$$\text{with } \mathcal{E}^\perp := \left\{ \vec{v}(\vec{x}) : \mathbb{R}^3 \mapsto \mathbb{R}^3 \mid \int_{\mathbb{R}^3} d^3x \vec{v}^2(\vec{x}) < \infty \text{ and } \nabla \cdot \vec{v} = 0 \right\}. \quad (\text{B.2})$$

Note that in passive media, the transversality condition is $\nabla \cdot [\sqrt{\epsilon_R} \vec{v}] = 0$ instead. The space \mathcal{P} has a symplectic structure defined by the following bilinear form

$$\mathfrak{S}_{\mathcal{P}} \left(\begin{bmatrix} \vec{\Pi} \\ \vec{A} \end{bmatrix}, \begin{bmatrix} \vec{\Pi}' \\ \vec{A}' \end{bmatrix} \right) = \langle \vec{A}, \vec{\Pi}' \rangle - \langle \vec{\Pi}, \vec{A}' \rangle. \quad (\text{B.3})$$

We can construct a Hamiltonian representation that is free of constraints, by defining another set of canonical variables (p, q) in another phase space defined as

$$\check{\mathcal{P}} := \check{\mathcal{E}} \oplus \check{\mathcal{E}}, \quad (\text{B.4})$$

$$\text{with } \check{\mathcal{E}} := \{ u(\vec{k}, \sigma, \zeta) \mid \sum_{\sigma=\pm} \sum_{\zeta=c,s} \int_{\mathbb{R}^3} d^3k u^2(\vec{k}, \sigma, \zeta) < \infty \} \quad (\text{B.5})$$

On $\check{\mathcal{P}}$ there is a symplectic structure defined by the bilinear form

$$\mathfrak{S}_{\check{\mathcal{P}}} \left(\begin{bmatrix} p \\ q \end{bmatrix}, \begin{bmatrix} p' \\ q' \end{bmatrix} \right) = \langle q, p' \rangle - \langle p, q' \rangle. \quad (\text{B.6})$$

Definition: A linear map

$$S : (\vec{\Pi}(\vec{x}), \vec{A}(\vec{x})) \mapsto (p, q) \quad (\text{B.7})$$

is symplectic if

$$\mathfrak{S}_{\check{\mathcal{P}}} \left(S \begin{bmatrix} \vec{\Pi} \\ \vec{A} \end{bmatrix}, S \begin{bmatrix} \vec{\Pi}' \\ \vec{A}' \end{bmatrix} \right) = \mathfrak{S}_{\mathcal{P}} \left(\begin{bmatrix} \vec{\Pi} \\ \vec{A} \end{bmatrix}, \begin{bmatrix} \vec{\Pi}' \\ \vec{A}' \end{bmatrix} \right). \quad (\text{B.8})$$

We consider a real orthonormal basis $\{\vec{\mu}_\kappa(\vec{x})\}$ of the space \mathcal{E}^\perp and the transformation $S : (\vec{\Pi}(\vec{x}), \vec{A}(\vec{x})) \mapsto (p, q)$ defined by

$$q_\kappa = \int d^3x \vec{\mu}_\kappa(\vec{x}) \cdot \vec{A}(\vec{x}) \equiv \langle \vec{\mu}_\kappa, \vec{A} \rangle, \quad (\text{B.9})$$

$$p_\kappa = \int d^3x \vec{\mu}_\kappa(\vec{x}) \cdot \vec{\Pi}(\vec{x}) \equiv \langle \vec{\mu}_\kappa, \vec{\Pi} \rangle. \quad (\text{B.10})$$

These vectors $\vec{\mu}_\kappa$ correspond to the eigenconfigurations in passive media, and to plane waves in the plasmonic model. They obey the same constraint as the vector fields \vec{A} and $\vec{\Pi}$.

Proposition: If $\{\vec{\mu}_\kappa(\vec{x})\}$ satisfies the completeness relation $\sum_\kappa |\vec{\mu}_\kappa\rangle\langle\vec{\mu}_\kappa| = \mathbb{1}_{\mathcal{E}^\perp}$ in the space \mathcal{E}^\perp then the transformation S is symplectic.

Proof:

$$\mathfrak{S}_{\mathcal{F}} \left(\begin{bmatrix} p \\ q \end{bmatrix}, \begin{bmatrix} p' \\ q' \end{bmatrix} \right) = \sum_\kappa q_\kappa p'_\kappa - p_\kappa q'_\kappa \quad (\text{B.11})$$

$$= \sum_\kappa \langle \vec{\mu}_\kappa, \vec{A} \rangle \langle \vec{\mu}_\kappa, \vec{\Pi}' \rangle - \langle \vec{\mu}_\kappa, \vec{\Pi} \rangle \langle \vec{\mu}_\kappa, \vec{A}' \rangle \quad (\text{B.12})$$

$$= \sum_\kappa \langle \vec{A}, \vec{\mu}_\kappa \rangle \langle \vec{\mu}_\kappa, \vec{\Pi}' \rangle - \langle \vec{\Pi}, \vec{\mu}_\kappa \rangle \langle \vec{\mu}_\kappa, \vec{A}' \rangle \quad (\text{B.13})$$

$$= \langle \vec{A} | \left(\sum_\kappa |\vec{\mu}_\kappa\rangle\langle\vec{\mu}_\kappa| \right) | \vec{\Pi}' \rangle - \langle \vec{\Pi} | \left(\sum_\kappa |\vec{\mu}_\kappa\rangle\langle\vec{\mu}_\kappa| \right) | \vec{A}' \rangle \quad (\text{B.14})$$

$$= \langle \vec{A}, \vec{\Pi}' \rangle - \langle \vec{\Pi}, \vec{A}' \rangle = \mathfrak{S}_{\mathcal{F}} \left(\begin{bmatrix} \vec{\Pi} \\ \vec{A} \end{bmatrix}, \begin{bmatrix} \vec{\Pi}' \\ \vec{A}' \end{bmatrix} \right), \quad (\text{B.15})$$

where we have used the completeness of the basis in \mathcal{E}^\perp : $\sum_\kappa |\vec{\mu}_\kappa\rangle\langle\vec{\mu}_\kappa| = \mathbb{1}_{\mathcal{E}^\perp}$. \square

One can further prove that a transformation is canonical if and only if it is symplectic.



Symmetry of the plasmonic frequency operator

In this appendix, we show that the frequency operator Ω^2 of the plasmonic model constructed in Chapter 5, is symmetric (since it is real, it implies that it is hermitian). We recall its form:

$$\Omega^2 = \begin{bmatrix} I_{\omega_{\kappa}^2} & B_1 \\ B_2 & I_{v^2} + A \end{bmatrix}, \quad (\text{C.1})$$

which acts on a configuration $[q \ \vec{X}]^T$ as

$$[I_{\omega_{\kappa}^2} q](\kappa) := \int d\kappa' \omega_{\kappa'}^2 \delta(\kappa - \kappa') q_{\kappa'} = \omega_{\kappa}^2 q_{\kappa}, \quad (\text{C.2a})$$

$$[I_{v^2} \vec{X}](v, \vec{r}, j) := \int d v' \int_V d^3 r' \sum_{j'} v'^2 \delta(v - v') \delta(\vec{r} - \vec{r}') \delta_{jj'} X^{j'}(v', \vec{r}') = v^2 X^j(v, \vec{r}), \quad (\text{C.2b})$$

$$[A \vec{X}](v, \vec{r}, j) := \tilde{\alpha}(v, \vec{r}) \int_0^{\infty} d v' \tilde{\alpha}(v', \vec{r}) X^j(v', \vec{r}), \quad (\text{C.2c})$$

$$[B_1 \vec{X}](\kappa) := \int_V d^3 r \int_0^{\infty} d v \omega_{\kappa} \tilde{\alpha}(v, \vec{r}) (\vec{\varphi}_{\kappa}(\vec{r}) \cdot \vec{X}_{v, \vec{r}}), \quad (\text{C.2d})$$

$$[B_2 q](v, \vec{r}, j) := \tilde{\alpha}(v, \vec{r}) \int d\kappa \omega_{\kappa} \varphi_{\kappa}^j(\vec{r}) q_{\kappa}. \quad (\text{C.2e})$$

In order to show that Ω^2 is symmetric, we need to show that (i) $I_{\omega_{\kappa}^2}$, I_{v^2} and A are symmetric, and that (ii) $B_1 = B_2^T$.

C.1 Definition of symmetric integral operators

Consider a real integral operator S acting on a space of real functions $f(x) \in \mathfrak{F}$. We denote by $g(x) \in \mathfrak{F}$ the resulting (real) function:

$$g(x) = (Sf)(x). \quad (\text{C.3})$$

The operator S is symmetric if

$$(g, Sf)_x = (Sg, f)_x, \quad (\text{C.4})$$

where $(\cdot, \cdot)_x$ refers to the scalar product in \mathfrak{F} .

The question is more subtle if the image of f through the application of S is in a different space. Let us denote $g(y) \in \mathfrak{G}$, with

$$g(y) = (Sf)(y). \quad (\text{C.5})$$

In this case, S^T (which is the transpose of S) acts on the space \mathfrak{G} and verifies

$$(S^T g, f)_y = (g, Sf)_x, \quad (\text{C.6})$$

where $(\cdot, \cdot)_y$ is the scalar product in \mathfrak{G} .

C.2 Symmetry of the diagonal blocks

The diagonal blocks of the frequency operator ($I_{\omega_\kappa^2}$, I_{v^2} and A) map elements from one space to the same space. With their definitions (C.2a)–(C.2c), it is easy to show that they are symmetric:

$$(q, I_{\omega_\kappa^2} q')_\kappa = \int d\kappa q_\kappa \omega_\kappa^2 q'_\kappa = (I_{\omega_\kappa^2} q, q')_\kappa, \quad (\text{C.7})$$

$$(\vec{X}, I_{v^2} \vec{X}')_{v, \vec{r}} = \int dv \int_V d^3 r \vec{X}(v, \vec{r}) \cdot v^2 \vec{X}'(v, \vec{r}) = (I_{v^2} \vec{X}, \vec{X}')_{v, \vec{r}}, \quad (\text{C.8})$$

$$\begin{aligned} (\vec{X}, A \vec{X}')_{v, \vec{r}} &= \int dv \int_V d^3 r \vec{X}(v, \vec{r}) \left[\tilde{\alpha}(v, \vec{r}) \int dv' \tilde{\alpha}(v', \vec{r}) \vec{X}'(v', \vec{r}) \right] \\ &= \iiint dv dv' \int_V d^3 r \vec{X}(v, \vec{r}) \tilde{\alpha}(v, \vec{r}) \cdot \alpha(v', \vec{r}) \vec{X}'(v', \vec{r}) = (A \vec{X}, \vec{X}')_{v, \vec{r}}, \end{aligned} \quad (\text{C.9})$$

where we have hidden the sum over the components j in the scalar product \cdot between vectors.

C.3 Symmetry of the off diagonal blocks

Since the operators B_1 and B_2 act on opposite spaces, we need to show that $B_1 = B_2^T$, thus:

$$(q, B_1 \vec{X})_\kappa = (B_2 q, \vec{X})_{v, \vec{r}}. \quad (\text{C.10})$$

From the definitions (C.2d) and (C.2e) we have

$$\begin{aligned} (q, B_1 \vec{X})_\kappa &= \int d\kappa q_\kappa \left[\int_V d^3 r \int dv \omega_\kappa \tilde{\alpha}(v, \vec{r}) (\vec{\varphi}_\kappa(\vec{r}) \cdot \vec{X}_{v, \vec{r}}) \right] \\ &= \int d\kappa \int dv \int_V d^3 r q_\kappa \omega_\kappa \tilde{\alpha}(v, \vec{r}) (\vec{\varphi}_\kappa(\vec{r}) \cdot \vec{X}(v, \vec{r})), \end{aligned} \quad (\text{C.11})$$

and

$$\begin{aligned} (B_2 q, \vec{X})_{v, \vec{r}} &= \int dv \int_V d^3 r \vec{X}(v, \vec{r}) \cdot \left[\tilde{\alpha}(v, \vec{r}) \int d\kappa \omega_\kappa \vec{\varphi}_\kappa(\vec{r}) q_\kappa \right] \\ &= \int d\kappa \int dv \int_V d^3 r q_\kappa \omega_\kappa \tilde{\alpha}(v, \vec{r}) (\vec{\varphi}_\kappa(\vec{r}) \cdot \vec{X}(v, \vec{r})) = (q, B_1 \vec{X})_\kappa. \end{aligned} \quad (\text{C.12})$$

Hence we have $B_2 = B_1^T$. Since the frequency operator is given by Eq. (C.1), we have

$$(\Omega^2)^T = \begin{bmatrix} I_{\omega_\kappa^2}^T & B_1^T \\ B_1^T & I_{v^2}^T + A^T \end{bmatrix} = \begin{bmatrix} I_{\omega_\kappa^2} & B_1 \\ B_2 & I_{v^2} + A \end{bmatrix} = \Omega^2, \quad (\text{C.13})$$

which concludes with the symmetry of the frequency operator of the plasmonic model.



Derivation of the Green identity

In this Appendix we derive the *Green identity*:

$$\frac{\omega^2}{c^2} \int_V d^3x \epsilon_i(\vec{x}) \bar{\bar{G}}^T(\vec{x}, \vec{x}_A) \bar{\bar{G}}^*(\vec{x}, \vec{x}_B) = \frac{1}{2i} \left[\bar{\bar{G}}^T(\vec{x}_B, \vec{x}_A) - \bar{\bar{G}}^*(\vec{x}_A, \vec{x}_B) \right] + \bar{\bar{F}}(\vec{x}_A, \vec{x}_B, \mathfrak{B}), \quad (\text{D.1})$$

where V is an arbitrary volume that contains \vec{x}_A and \vec{x}_B , and \mathfrak{B} is the surface of V . The Green tensor $\bar{\bar{G}}$ verifies the equation

$$\left(\nabla \times \nabla \times - \frac{\omega^2}{c^2} \epsilon(\vec{x}, \omega) \mathbb{1} \right) \bar{\bar{G}}(\vec{x}, \vec{x}_A) = \mathbb{1} \delta(\vec{x} - \vec{x}_A). \quad (\text{D.2})$$

In particular, we will show that the boundary term $\bar{\bar{F}}$ is given by

$$\bar{\bar{F}}(\vec{x}_A, \vec{x}_B, \mathfrak{B}) = [\bar{\bar{b}}^T(\vec{x}_B, \vec{x}_A, \mathfrak{B}) - \bar{\bar{b}}^*(\vec{x}_A, \vec{x}_B, \mathfrak{B})] / (2i), \quad (\text{D.3})$$

$$\bar{\bar{b}}(\vec{x}_A, \vec{x}_B, \mathfrak{B}) = - \int_{\mathfrak{B}} ds (\vec{n} \times \bar{\bar{G}}^*(\vec{x}, \vec{x}_B))^T (\nabla \times \bar{\bar{G}}(\vec{x}, \vec{x}_A)), \quad (\text{D.4})$$

with ds the surface element of \mathfrak{B} and \vec{n} the outer unit normal vector on the surface.

We start by multiplying Eq. (D.2) by $\bar{\bar{G}}^{*T}(\vec{x}, \vec{x}_B)$ from the left, and we integrate \vec{x} over a the volume V . Thus we obtain

$$\int_V d^3x \bar{\bar{G}}^{*T}(\vec{x}, \vec{x}_B) \nabla \times \nabla \times \bar{\bar{G}}(\vec{x}, \vec{x}_A) = \frac{\omega^2}{c^2} \int_V d^3x \epsilon(\vec{x}) \bar{\bar{G}}^{*T}(\vec{x}, \vec{x}_B) \bar{\bar{G}}(\vec{x}, \vec{x}_A) + \bar{\bar{G}}^{*T}(\vec{x}_A, \vec{x}_B). \quad (\text{D.5})$$

We then use the following identity for an integration by parts [138] (1.52):

$$\int_V d^3x (\nabla \times \nabla \times \bar{\bar{Q}})^T \bar{\bar{P}} = \int_V d^3x (\nabla \times \bar{\bar{Q}})^T (\nabla \times \bar{\bar{P}}) - \int_{\mathfrak{B}} ds (\nabla \times \bar{\bar{Q}})^T (\vec{n} \times \bar{\bar{P}}), \quad (\text{D.6})$$

which, by transposing both sides, can be written

$$\int_V d^3x \bar{\bar{P}}^T (\nabla \times \nabla \times \bar{\bar{Q}}) = \int_V d^3x (\nabla \times \bar{\bar{P}})^T (\nabla \times \bar{\bar{Q}}) - \int_{\mathfrak{B}} ds (\vec{n} \times \bar{\bar{P}})^T (\nabla \times \bar{\bar{Q}}). \quad (\text{D.7})$$

Applying this identity to the left hand side of (D.5), we obtain

$$\int_V d^3x \bar{\bar{G}}^{*T}(\vec{x}, \vec{x}_B) \nabla \times \nabla \times \bar{\bar{G}}(\vec{x}, \vec{x}_A) = \bar{\bar{I}}(\vec{x}_B, \vec{x}_A) + \bar{\bar{F}}(\vec{x}_B, \vec{x}_A, \mathfrak{B}), \quad (\text{D.8})$$

with

$$\bar{I}(\vec{x}_B, \vec{x}_A) := \int_V d^3x (\nabla \times G^*(\vec{x}, \vec{x}_B))^T (\nabla \times \bar{G}(\vec{x}, \vec{x}_A)), \quad (\text{D.9})$$

$$\bar{F}(\vec{x}_B, \vec{x}_A, \mathfrak{B}) := - \int_{\mathfrak{B}} ds (\vec{n} \times \bar{G}^*(\vec{x}, \vec{x}_B))^T (\nabla \times \bar{G}(\vec{x}, \vec{x}_A)). \quad (\text{D.10})$$

Equation (D.5) can thus be written as

$$\frac{\omega^2}{c^2} \int_V d^3x \epsilon(\vec{x}) \bar{G}^{*T}(\vec{x}, \vec{x}_B) \bar{G}(\vec{x}, \vec{x}_A) + \bar{G}^{*T}(\vec{x}_A, \vec{x}_B) = \bar{I}(\vec{x}_B, \vec{x}_A) + \bar{F}(\vec{x}_B, \vec{x}_A, \mathfrak{B}). \quad (\text{D.11})$$

We take the transpose and complex conjugate of this equation and we exchange the labels A and B :

$$\frac{\omega^2}{c^2} \int_V d^3x \epsilon^*(\vec{x}) \bar{G}^{*T}(\vec{x}, \vec{x}_B) \bar{G}(\vec{x}, \vec{x}_A) + \bar{G}(\vec{x}_B, \vec{x}_A) = \bar{I}^{*T}(\vec{x}_A, \vec{x}_B) + \bar{F}^{*T}(\vec{x}_A, \vec{x}_B, \mathfrak{B}). \quad (\text{D.12})$$

We can see from Eq. (D.9) that the tensor \bar{I} satisfies

$$\bar{I}(\vec{x}_B, \vec{x}_A) = \bar{I}^{*T}(\vec{x}_A, \vec{x}_B), \quad (\text{D.13})$$

thus (D.12) gives

$$\frac{\omega^2}{c^2} \int_V d^3x \epsilon^*(\vec{x}) \bar{G}^{*T}(\vec{x}, \vec{x}_B) \bar{G}(\vec{x}, \vec{x}_A) + \bar{G}(\vec{x}_B, \vec{x}_A) = \bar{I}(\vec{x}_B, \vec{x}_A) + \bar{F}^{*T}(\vec{x}_A, \vec{x}_B, \mathfrak{B}). \quad (\text{D.14})$$

We then subtract Eq. (D.14) from Eq. (D.11) and we divide by $2i$ such that the terms \bar{I} cancel. Finally we take the transpose, and we obtain the general Green identity (D.1), which completes the proof.

Green function for a 1D slab

In this appendix we perform the calculation of the Green function of the electromagnetic wave equation (with dispersion and dissipation) in a 1D model (see Figure E.1). The result of this calculation was partially given in [131].

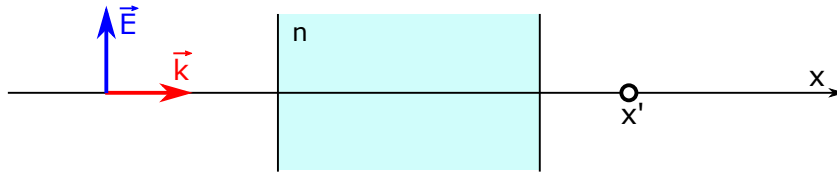


Figure E.1 – Scheme of the 1D model with a slab of refractive index n (which can include dissipation).

E.1 Continuity conditions

We start with the Green equation associated with the 1D wave equation:

$$\left[-\partial_x^2 - \frac{\omega^2}{c^2} \epsilon(x) \right] G(x, x') = \delta(x - x'), \quad (\text{E.1})$$

where x' is the position of the source and x is the observation point, ϵ is 1 outside of the medium, and constant (but complex) in the medium. All frequency dependencies are implicit in G and in ϵ . In order to calculate the Green function in the configuration of Figure E.1, we need to extract continuity conditions at the interfaces and at the point of the source.

1. Since the Green function should be continuous at the interfaces, we have the continuity condition:

$$G^{\triangleleft}(x = x_i, x') = G^{\triangleright}(x = x_i, x'), \quad (\text{E.2})$$

where the superscript \triangleleft stands for $x \leq x_i$ and \triangleright for $x \geq x_i$, with x_i the coordinate of an interface.

2. Since the Green function should be continuous for $x = x'$, we have the continuity condition:

$$G_1(x = x', x') = G_2(x = x', x'), \quad (\text{E.3})$$

where the subscript 1 stand for $x \leq x'$ and 2 for $x \geq x'$.

We also have continuity conditions for the derivatives of G :

- Integrating the homogeneous Green equation (Eq. (E.1) with no right-hand side), we see that the first derivative of G should also be continuous in the interface, that is,

$$\begin{aligned} \lim_{\varepsilon \rightarrow 0} \left\{ \left| \partial_x G(x, x') \right|_{x_i - \varepsilon}^{x_i + \varepsilon} \right\} &= 0, \\ \Leftrightarrow \quad \partial_x G^{\triangleleft}(x, x') \Big|_{x=x_i} &= \partial_x G^{\triangleright}(x, x') \Big|_{x=x_i}. \end{aligned} \quad (\text{E.4})$$

- Finally, we can extract a continuity condition for the derivative of G at the source x' . We integrate (E.1) over a small interval around x' :

$$\int_{x' - \varepsilon}^{x' + \varepsilon} \partial_x^2 G(x, x') dx + \frac{\omega^2}{c^2} \varepsilon(x') \int_{x' - \varepsilon}^{x' + \varepsilon} G(x, x') dx = -1, \quad (\text{E.5})$$

where we have used that ε is constant in this small interval. Since

$$\lim_{\varepsilon \rightarrow 0} \int_{x' - \varepsilon}^{x' + \varepsilon} G(x, x') dx = 0, \quad (\text{E.6})$$

and using (E.5) together with the condition (E.3), we deduce that

$$\begin{aligned} \lim_{\varepsilon \rightarrow 0} \left\{ \left| \partial_x G(x, x') \right|_{x' - \varepsilon}^{x' + \varepsilon} \right\} &= -1, \\ \Leftrightarrow \quad \partial_x G_1(x, x') \Big|_{x=x'} &= 1 + \partial_x G_2(x, x') \Big|_{x=x'}. \end{aligned} \quad (\text{E.7})$$

E.2 Source on the right of the slab

The calculation of the Green function for a source located on the right side of the slab is performed by using the Ohm-Rayleigh expansion. We consider four parts of the Green function, corresponding to each region of space:

$$G^{\triangleleft}(x, x') = A_+(x') e^{ikx} + A_-(x') e^{-ikx}, \quad (\text{E.8a})$$

$$G^{\circ}(x, x') = B_+(x') e^{iknx} + B_-(x') e^{-iknx}, \quad (\text{E.8b})$$

$$G_1^{\triangleright}(x, x') = C_+(x') e^{ikx} + C_-(x') e^{-ikx}, \quad (\text{E.8c})$$

$$G_2^{\triangleright}(x, x') = D_+(x') e^{ikx} + D_-(x') e^{-ikx}, \quad (\text{E.8d})$$

with $k = \omega/c$. We adopt a concise notation of superscripts $\triangleleft, \circ, \triangleright$ referring to the observation point x being on the left of the slab, inside the slab, and on the right, respectively. The index 1, 2 in (E.8c), (E.8d) refers to the observation point being on the left or on the right of the source (see Fig. E.2).

The general strategy to find the coefficients A, B, C, D is to insert the expansions (E.8) into each continuity condition for each critical point of the system (the interfaces and the source). This gives a set of equations that can be solved. There is however a faster way to calculate by introducing a matrix representation of the coefficients.

We introduce the following notations for x taken at specific points of the system (the interfaces x_L, x_R , or the source x'):

$$\begin{aligned} a_{\pm} &= A_{\pm} e^{\pm ikx_L}, & b_{\pm}^L &= B_{\pm} e^{\pm iknx_L}, & b_{\pm}^R &= B_{\pm} e^{\pm iknx_R}, \\ c_{\pm} &= C_{\pm} e^{\pm ikx_R}, & c'_{\pm} &= C_{\pm} e^{\pm ikx'}, & d'_{\pm} &= D_{\pm} e^{\pm ikx'}. \end{aligned}$$

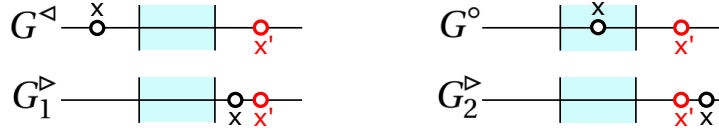


Figure E.2 – Notation used for the Green function depending on the position of the observation point x , when the source is on the right of the slab.

We use these coefficients to build two component vectors: $\underline{a} = [a_+ \ a_-]^T$, $\underline{b}^L = [b_+^L \ b_-^L]^T$ and so on. The propagation of waves through the system is described by the application of matrices of two kinds:

- Interfaces matrices $\bar{\bar{I}}$ connect the coefficients at the coordinates x_L and x_R . An interface matrix connecting a region A of index n_A to a region B of index n_B reads

$$\bar{\bar{I}}_{AB} = \begin{bmatrix} K_+^{AB} & K_-^{AB} \\ K_-^{AB} & K_+^{AB} \end{bmatrix}, \quad K_{\pm}^{AB} = \frac{1}{2} \left(1 \pm \frac{n_A}{n_B} \right). \quad (\text{E.9})$$

- Translation matrices $\bar{\bar{T}}$ add appropriate phases due to the propagation from one point x_1 to another point x_2 in a region A of index n_A :

$$\bar{\bar{T}}_{x_1 \rightarrow x_2}^A = \begin{bmatrix} e^{ikn_A(x_2-x_1)} & 0 \\ 0 & e^{-ikn_A(x_2-x_1)} \end{bmatrix}. \quad (\text{E.10})$$

The connections between the different regions can thus be made in the following way:

$$\underline{b}^L = \bar{\bar{I}}_{\leftarrow \circ} \underline{a}, \quad (\text{E.11})$$

$$\underline{b}^R = \bar{\bar{T}}_{x_L \rightarrow x_R}^{\circ} \underline{b}^L, \quad (\text{E.12})$$

$$\underline{c} = \bar{\bar{I}}_{\circ \triangleright} \underline{b}^R, \quad (\text{E.13})$$

$$\underline{c}' = \bar{\bar{T}}_{x_R \rightarrow x'}^{\triangleright}, \quad (\text{E.14})$$

$$\underline{d}' = \underline{c}' + \frac{i}{2k} \begin{bmatrix} 1 \\ -1 \end{bmatrix}. \quad (\text{E.15})$$

The last connection around the source was made using the continuity condition of the derivative of G at the source (E.7) together with the continuity of G (E.3).

The coefficients \underline{d}' for waves traveling to and from $+\infty$ can thus be linked to the coefficients \underline{a} for waves traveling to and from $-\infty$:

$$\underline{d}' = \frac{i}{2k} \begin{bmatrix} 1 \\ -1 \end{bmatrix} + \underbrace{\bar{\bar{T}}_{x_R \rightarrow x'}^{\triangleright} \bar{\bar{I}}_{\circ \triangleright} \bar{\bar{T}}_{x_L \rightarrow x_R}^{\circ} \bar{\bar{I}}_{\leftarrow \circ}}_{\bar{\bar{M}}} \underline{a}. \quad (\text{E.16})$$

Using $x_L = -\ell$ and $x_R = \ell$, a simple calculation gives the components of $\bar{\bar{M}}$:

$$M_{11} = \frac{1}{4n} \left[(n+1)^2 e^{2ikn\ell} - (n-1)^2 e^{-2ikn\ell} \right] e^{ik(x'-\ell)}, \quad (\text{E.17a})$$

$$M_{12} = \frac{1}{4n} \left[e^{4ikn\ell} - 1 \right] (n^2 - 1) e^{-2ikn\ell} e^{ik(x'-\ell)}, \quad (\text{E.17b})$$

$$M_{21} = \frac{-1}{4n} \left[e^{4ikn\ell} - 1 \right] (n^2 - 1) e^{-2ikn\ell} e^{-ik(x'-\ell)}, \quad (\text{E.17c})$$

$$M_{22} = \frac{1}{4n} Y e^{-2kn\ell} e^{-ik(x'-\ell)}, \quad (\text{E.17d})$$

with

$$Y = (n+1)^2 - (n-1)^2 e^{4ikn\ell}. \quad (\text{E.18})$$

We now impose a boundary condition at infinity. We consider that there is no source at infinity that could emit or reflect waves, such that all propagating waves from infinity are canceled. This is called the *Sommerfeld radiation condition*. In our calculation, it means imposing $a_+ = 0$ and $d'_- = 0$. The second component of Eq. (E.16) straightforwardly gives

$$a_- = \frac{i}{2kM_{22}} = \frac{i}{2k} \frac{4n}{Y} e^{2ikn\ell} e^{ik(x'-\ell)}. \quad (\text{E.19})$$

From this, we obtain the first component of (E.16):

$$d'_+ = \frac{i}{2k} + M_{12}a_- = \frac{i}{2k} \left\{ 1 + \frac{n^2-1}{Y} \left[e^{4ikn\ell} - 1 \right] e^{2ik(x'-\ell)} \right\}. \quad (\text{E.20})$$

Similarly, we introduce a_- and d'_+ in Eqs. (E.11)–(E.15) to obtain the remaining coefficients. We then insert everything into the Green functions (E.8) and we obtain

$$G^\triangleleft(x, x') = \frac{i}{2k} \frac{4n}{Y} e^{2ikn\ell} e^{-ik(2\ell+x-x')} \quad (\text{E.21})$$

for x on the left side of the slab, and

$$G^\circ(x, x') = \frac{i}{2k} \left[V e^{-ik(nx-x')} + W e^{ik(nx+x')} \right] \quad (\text{E.22})$$

for x in the slab, with

$$V = \frac{2(n+1)}{Y} e^{ik(n-1)\ell}, \quad W = \frac{2(n-1)}{Y} e^{ik(3n-1)\ell}. \quad (\text{E.23})$$

Finally, the Green function on the right side of the slab (where the source is) reads

$$\begin{aligned} G^\triangleright(x, x') &= G_1^\triangleright(x, x')\Theta(x'-x) + G_2^\triangleright(x, x')\Theta(x-x') \\ &= \frac{i}{2k} \left\{ \frac{n^2-1}{Y} \left[e^{4ikn\ell} - 1 \right] e^{-ik(2\ell-x-x')} + e^{ik|x-x'|} \right\}. \end{aligned} \quad (\text{E.24})$$

The Green functions are then associated to the ones used for the calculation of the Green identity in Section 7.4.3, with $G^\triangleleft \rightarrow G_{\text{left}}$, $G^\circ \rightarrow G_{\text{in}}$, and $G^\triangleright \rightarrow G_{\text{right}}$.

E.3 Other positions of the source

For the sake of completeness, we also give the Green function when the source is placed on the two other regions of space: on the left of the slab, and inside the slab.

E.3.1 On the left of the slab

The case where the position of the source x' is on the left of the medium is symmetric with the case on the right. We have trivially:

$$G^\triangleleft(x, x') \Big|_{x'>\ell} = G^\triangleright(-x, -x') \Big|_{x'<-\ell}, \quad (\text{E.25})$$

$$G^\circ(x, x') \Big|_{x'>\ell} = G^\circ(-x, -x') \Big|_{x'<-\ell}, \quad (\text{E.26})$$

$$G^\triangleright(x, x') \Big|_{x'>\ell} = G^\triangleleft(-x, -x') \Big|_{x'<-\ell}. \quad (\text{E.27})$$

E.3.2 Inside the slab

A similar calculation as performed in the other cases gives the Green function when the source is inside the medium. The notation is preserved but now refers to the cases as pictured in Fig. E.3.

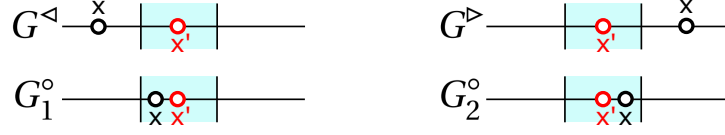


Figure E.3 – Notation used for the Green function depending on the position of the observation point x , when the source is on the right of the slab.

We obtain

$$G^<(x, x') = \frac{i}{2k} \left[V e^{ik(nx'-x)} + W e^{-ik(nx'+x)} \right], \quad (\text{E.28})$$

$$G^>(x, x') = \frac{i}{2k} \left[V e^{-ik(nx'-x)} + W e^{ik(nx'+x)} \right], \quad (\text{E.29})$$

and

$$G^o(x, x') = \frac{i}{2kn} \left\{ \frac{n^2 - 1}{Y} \left[e^{ikn(2\ell+x+x')} + e^{ikn(2\ell-x-x')} \right] + \right. \quad (\text{E.30})$$

$$\left. + \frac{n^2 - 1}{Y} \left[e^{ikn(4\ell+x-x')} + e^{ikn(4\ell-x+x')} \right] + e^{ikn|x-x'|} \right\}. \quad (\text{E.31})$$

Bibliography

- [1] V. Dorier, J. Lampart, S. Guérin, H. R. Jauslin (2019). Canonical quantization for quantum plasmonics with finite nanostructures. *Physical Review A*, 100 042111.
- [2] V. Dorier, S. Guérin, H.R. Jauslin, Critical review of quantum plasmonic models for finite-size media, arXiv:1911.03134 (2019).
- [3] V. Dorier, J. Lampart, S. Guérin, H. R. Jauslin (2020). Canonical quantization, spontaneous emission and dissipation of plasmon polaritons. In preparation.
- [4] J.F. Clauser, Experimental limitations to the validity of semiclassical radiation theories, *Phys. Rev. A* 6, 49 (1972).
- [5] J.F. Clauser, Experimental distinction between the quantum and classical field-theoretic predictions for the photoelectric effect, *Phys. Rev. D* 9, 853 (1974).
- [6] P. Grangier, G. Roger and A. Aspect, Experimental evidence for a photon anticorrelation effect on a beam splitter: a new light on single-photon interferences, *EPL* 1, 173 (1986).
- [7] R. Ghosh and L. Mandel, Observation of nonclassical effects in the interference of two photons, *Phys. Rev. Lett.* 59, 1903 (1987).
- [8] D.N. Klyshko, A.N. Penin and B.F. Polkovnikov, Parametric luminescence and light scattering by polaritons, *Soviet J. Exp. Th. Phys. Lett.* 11, 5 (1970).
- [9] D.C. Burnham and D.L. Weinberg, Observation of simultaneity in parametric production of optical photon pairs, *Phys. Rev. Lett.* 25, 84 (1970).
- [10] M.D. Eisaman, J. Fan, A. Migdall and S.V. Polyakov, Invited review article: Single-photon sources and detectors, *Review of Scientific Instruments* 82, 071101 (2011).
- [11] F. Flamini, S. Spagnolo and F. Sciarrino, Photonic quantum information processing: a review, *Rep. Prog. Phys.* 82, 016001 (2018).
- [12] J. Garrison and R. Chiao, *Quantum optics* (Oxford University Press, 2008).
- [13] S. de Bièvre; Local states of free bose fields; proceedings of “Summer School on large Coulomb systems,” Nordfjordeid, July 2003, *Lecture Notes in Physics* 695, p. 15-61 (2006), Springer Verlag.

-
- [14] S. de Bièvre; Where's that quantum?; in "Contributions in Mathematical Physics: A Tribute to Gerard G. Emch", Edited by: S. Twareque Ali, Kalyan B. Sinha; (2007) p. 123–146, Hindustan Book Agency.
- [15] S. de Bièvre; Classical and quantum oscillator fields: an introduction, unpublished preliminary version.
- [16] Glauber, R. J., Lewenstein, M. (1991). Quantum optics of dielectric media. *Physical Review A*, 43(1), 467.
- [17] M. Wubs, L. G. Suttorp, A. Legendijk; Multipole interaction between atoms and their photonic environment; *Physical Review A*, 68(2003)013822.
- [18] C. K. Hong, Z. Y. Ou, L. Mandel; Measurement of subpicosecond time intervals between two photons by interference; *Phys. Rev. Lett.* 59(1987)2044–2046.
- [19] Legero, T., Wilk, T., Kuhn, A., Rempe, G. (2006). Characterization of single photons using two-photon interference. *Advances In Atomic, Molecular, and Optical Physics*, 53, 253-289.
- [20] Nisbet-Jones, P. B., Dilley, J., Ljunggren, D., Kuhn, A. (2011). Highly efficient source for indistinguishable single photons of controlled shape. *New Journal of Physics*, 13(10), 103036.
- [21] Nisbet-Jones, P. B., Dilley, J., Holleccek, A., Barter, O., Kuhn, A. (2013). Photonic qubits, qutrits and ququads accurately prepared and delivered on demand. *New Journal of Physics*, 15(5), 053007.
- [22] Specht, H. P., Bochmann, J., Mücke, M., Weber, B., Figueroa, E., Moehring, D. L., Rempe, G. (2009). Phase shaping of single-photon wave packets. *Nature Photonics*, 3(8), 469.
- [23] L.G. Suttorp and M. Wubs, Field quantization in inhomogeneous absorptive dielectrics, *Phys. Rev. A* 70, 013816 (2004).
- [24] L.G. Suttorp and A.J. van Wonderen, Fano diagonalization of a polariton model for an inhomogeneous absorptive dielectric, *Europhys. Lett.* 70, 766 (2004).
- [25] L.G. Suttorp, Field quantization in inhomogeneous anisotropic dielectrics with spatio-temporal dispersion, *J. Phys. A: Math. Theor.* 40, 3697 (2007).
- [26] T.G. Philbin; Canonical quantization of macroscopic electromagnetism; *New J. Phys.* 12(2010)123008.
- [27] Jackson, J. D. (1999). *Classical electrodynamics*.
- [28] Zangwill, A. (2013). *Modern electrodynamics*. Cambridge University Press.
- [29] Lue, J. T., Hor, Y. S. (1989). Optical filters constructed from multilayers of dielectric and thin metallic films operating in the anomalous skin effect region. *JOSA B*, 6(6), 1103-1105.
- [30] Huang, W. C., Lue, J. T. (1994). Quantum size effect on the optical properties of small metallic particles. *Physical Review B*, 49(24), 17279.
- [31] S. M. Dutra; *Cavity quantum electrodynamics: the strange theory of light in a box*; John Wiley & Sons (2005).

-
- [32] M. Reed, B. Simon; *Methods of Modern Mathematical Physics*, volumes I-IV; Academic Press, San Diego, 1975.
- [33] Weinberg, S.; *The quantum theory of fields*; Cambridge University press, 1995.
- [34] Honegger, R., Rieckers, A. (2015). *Photons in Fock space and beyond*. World Scientific.
- [35] E. Zeidler; *Quantum Field Theory, Vol. 2, Quantum Electrodynamics*; Springer Vlg. Berlin, 2009.
- [36] B. R. Hunt, T. Sauer, J. A. Yorke; Prevalence: a translation-invariant “almost every” on infinite-dimensional spaces; *Bulletin of the American mathematical society*, 27(1992)217-238.
- [37] L., Mandel (1966). Configuration-space photon number operators in quantum optics. *Physical Review*, 144(4), 1071.
- [38] R. W. Heeres, L. P. Kouwenhoven, V. Zwiller; Quantum interference in plasmonic circuits; *Nature nanotechnology*, 8(2013)719.
- [39] G. Di Martino, Y. Sonnefraud, M.S. Tame, S. Kéna-Cohen, F. Dieleman, K. Özdemir, M.S. Kim, S.A. Maier; Observation of Quantum Interference in the Plasmonic Hong-Ou-Mandel Effect; *Phys. Rev. Appl.* 1(2014)034004.
- [40] J. S. Fakonas, H. Lee, Y. A. Kelaita, H. A. Atwater; Two-plasmon quantum interference; *Nature Photonics*, 8(2014)317.
- [41] Y. J. Cai, M. Li, X. F. Ren, C. L. Zou, X. Xiong, H. L. Lei, G. C. Guo; High-visibility on-chip quantum interference of single surface plasmons; *Physical Review Applied*, 2(2014)014004.
- [42] S. D. Gupta, G. S. Agarwal; Two-photon quantum interference in plasmonics: theory and applications; *Optics letters*, 39(2014)390-393.
- [43] B. Vest, M.-C. Dheur, E. Devaux, A. Baron, E. Rousseau, J.-P. Hugonin, J.-J. Greffet, G. Messin, and F. Marquier; Anti-coalescence of bosons on a lossy beam splitter; *Science* 356(2017)1373.
- [44] S. M. Barnett, J. Jeffers, A. Gatti, R. Loudon; Quantum optics of lossy beam splitters; *Phys. Rev. A* 57(1998)2134.
- [45] J. Jeffers; Interference and the lossless lossy beam splitter; *Journal of Modern Optics* 47(2000)1819-1824.
- [46] R. Uppu, T. A. Wolterink, T. B. Trentup, P. W. Pinkse; Quantum optics of lossy asymmetric beam splitters; *Optics express*, 24(2016)16440-16449.
- [47] T. Jonckheere, J. Rech, C. Wahl, T. Martin; Electron and hole hong-ou-mandel interferometry; *Physical Review B*, 86(2012)125425.
- [48] R. Lopes, A. Imanaliev, A. Aspect, M. Cheneau, D. Boiron, C. I. Westbrook; Atomic Hong–Ou–Mandel experiment; *Nature*, 520(2015)66.
- [49] Bose, S., & Home, D. (2002). Generic entanglement generation, quantum statistics, and complementarity. *Physical review letters*, 88(5), 050401.
- [50] R.H. Ritchie, Plasma losses by fast electrons in thin films, *Phys. Rev.* 106, 874 (1957).
-

-
- [51] N. A. Bhat, J. E. Sipe; Hamiltonian treatment of the electromagnetic field in dispersive and absorptive structured media; *Physical Review A*, 73(2006)063808.
- [52] D.J. Bergman and M.I. Stockman, Surface plasmon amplification by stimulated emission of radiation: quantum generation of coherent surface plasmons in nanosystems, *Phys. Rev. Lett.* 90, 027402 (2003).
- [53] M.A. Noginov, G. Zhu, A.M. Belgrave, R. Bakker, V.M. Shalaev, E.E. Narimanov, S. Stout, E. Herz, T. Suteewong and U. Wiesner, Demonstration of a spaser-based nanolaser, *Nature* 460, 1110 (2009).
- [54] A. Yang, Z. Li, M.P. Knudson, A.J. Hryn, W. Wang, K. Aydin and T.W. Odom, Unidirectional lasing from template-stripped two-dimensional plasmonic crystals, *ACS Nano* 9, 11582 (2015).
- [55] D. Wang, W. Wang, M.P. Knudson, G.C. Schatz and T.W. Odom, Structural engineering in plasmon nanolasers, *Chem. Rev.* 118, 2865 (2017).
- [56] Varguet, H., Guérin, S., Jauslin, H., & des Francs, G. C. (2019). Cooperative emission in quantum plasmonic superradiance. *Physical Review B*, 100(4), 041115.
- [57] S.I. Bozhevolnyi, V.S. Volkov, E. Devaux, J.Y. Laluet and T.W. Ebbesen, Channel plasmon subwavelength waveguide components including interferometers and ring resonators, *Nature* 440, 508 (2006).
- [58] T. Holmgaard, Z. Chen, S.I. Bozhevolnyi, L. Markey, A. Dereux, A.V. Krasavin and A.V. Zayats, Bend-and-splitting loss of dielectric-loaded surface plasmon-polariton waveguides, *Opt. Exp.* 16, 13585 (2008).
- [59] Ebbesen, T. W., Genet, C., & Bozhevolnyi, S. I. (2008). Surface-plasmon circuitry. *Physics Today*, 61(5), 44.
- [60] C. Haffner, W. Heni, Y. Fedoryshyn, J. Niegemann, A. Melikyan, D. L. Elder, B. Baeuerle, Y. Salamin, A. Josten, U. Koch, C. Hoessbacher, F. Ducry, L. Juchli, A. Emboras, D. Hillerkuss, M. Kohl, L. R. Dalton, C. Hafner and J. Leuthold, All-plasmonic Mach-Zehnder modulator enabling optical high-speed communication at the microscale, *Nat. Phot.* 9, 525 (2015).
- [61] Y. Salamin, P. Ma, B. Baeuerle, A. Emboras, Y. Fedoryshyn, W. Heni, B. Cheng, A. Josten, J. Leuthold, 100 GHz plasmonic photodetector, *ACS Phot.* 5, 3291 (2018).
- [62] H. Gao, J. Henzie and T.W. Odom, Direct evidence for surface plasmon-mediated enhanced light transmission through metallic nanohole arrays, *Nano Lett.* 6, 2104 (2006).
- [63] W. Zhou and T.W. Odom, Tunable subradiant lattice plasmons by out-of-plane dipolar interactions, *Nat. Nanotech.* 6, 423 (2011).
- [64] R. Li, M.R. Bourgeois, C. Cherqui, J. Guan, D. Wang, J. Hu, R.D. Schaller, G.C. Schatz and T.W. Odom, Hierarchical Hybridization in Plasmonic Honeycomb Lattices, *Nano Lett.* 19, 6435 (2019).
- [65] Barnes, W. L., Dereux, A., & Ebbesen, T. W. (2003). Surface plasmon subwavelength optics. *nature*, 424(6950), 824.
- [66] Tame, M. S., McEnery, K. R., Özdemir, Ş. K., Lee, J., Maier, S. A., & Kim, M. S. (2013). Quantum plasmonics. *Nature Physics*, 9(6), 329-340.

-
- [67] Bozhevolnyi, S. I., & Khurgin, J. B. (2017). The case for quantum plasmonics. *Nature Photonics*, 11(7), 398.
- [68] B. Simon; *Quantum Mechanics for Hamiltonians Defined as Quadratic Forms*; Princeton U. Press, 1971 (see p.136).
- [69] C. Cohen-Tannoudji, J. Dupont-Roc, G. Grynberg; *Photons and Atoms-Introduction to Quantum Electrodynamics*; ISBN 0-471-18433-0. Wiley-VCH, 1997, 486.
- [70] L. Novotny, B. Hecht; *Principles of nano-optics*; Cambridge university press, 2012.
- [71] B. Huttner, S.M. Barnett; Quantization of the electromagnetic field in dielectrics; *Phys. Rev. A* 46 (1992) 4306
- [72] T. Gruner and D.G. Welsch, Correlation of radiation-field ground-state fluctuations in a dispersive and lossy dielectric, *Phys. Rev. A* 51, 3246 (1995).
- [73] T. Gruner and D.G. Welsch, Green-function approach to the radiation-field quantization for homogeneous and inhomogeneous Kramers-Kronig dielectrics, *Phys. Rev. A* 53, 1818 (1996).
- [74] H.T. Dung, L. Knöll and D.G. Welsch, Three-dimensional quantization of the electromagnetic field in dispersive and absorbing inhomogeneous dielectrics, *Phys. Rev. A* 57, 3931 (1998).
- [75] S. Scheel, L. Knöll and D.G. Welsch, QED commutation relations for inhomogeneous Kramers-Kronig dielectrics, *Phys. Rev. A* 58, 700 (1998).
- [76] H.T. Dung, L. Knöll and D.G. Welsch, Spontaneous decay in the presence of dispersing and absorbing bodies: General theory and application to a spherical cavity, *Phys. Rev. A* 62, 053804 (2000).
- [77] L. Knöll, S. Scheel, D.-G. Welsch; QED in dispersing and absorbing media; contribution to *Coherence and Statistics of Photons and Atoms*, edited by J. Peřina, J. Wiley, New York 2001, arXiv e-print quant-ph/0006121.
- [78] C. Raabe, S. Scheel and D.G. Welsch, Unified approach to QED in arbitrary linear media, *Phys. Rev. A* 75, 053813 (2007).
- [79] S.A.R. Horsley and T.G. Philbin, Canonical quantization of electromagnetism in spatially dispersive media, *New J. Phys.* 16, 013030 (2014).
- [80] O. Di Stefano, S. Savasta, R. Girlanda; Electromagnetic-field quantization in absorbing confined systems; *Physical Review A*, 60(1999)1614.
- [81] O. Di Stefano, S. Savasta, R. Girlanda; Mode expansion and photon operators in dispersive and absorbing dielectrics; *Journal of Modern Optics* 48(2001)67-84.
- [82] A. Drezet; Quantizing polaritons in inhomogeneous dissipative systems; *Phys. Rev. A* 95(2017)023831.
- [83] J.J. Hopfield; Theory of the Contribution of Excitons to the Complex Dielectric Constant of Crystals; *Phys. Rev.* 112(1958)1555.
- [84] K.O. Friedrichs; Über die Spektralzerlegung eines Integraloperators.; *Math. Ann.* 115:249, 1937.
-

- [85] On the perturbation of continuous spectra, *Comm. Pure Appl. Math.* 1, 361 (1948).
- [86] U. Fano; Effects of Configuration Interaction on Intensities and Phase Shifts; *Phys. Rev.* 124(1961)1866.
- [87] Barnett, S. M., Huttner, B., & Loudon, R. (1992). Spontaneous emission in absorbing dielectric media. *Physical review letters*, 68(25), 3698.
- [88] Dung, H. T., Buhmann, S. Y., Knöll, L., Welsch, D. G., Scheel, S., & Kästel, J. (2003). Electromagnetic-field quantization and spontaneous decay in left-handed media. *Physical Review A*, 68(4), 043816.
- [89] Matloob, R. (2004). Electromagnetic field quantization in a linear isotropic dielectric. *Physical Review A*, 69(5), 052110.
- [90] Chen, X. W., Sandoghdar, V., & Agio, M. (2013). Coherent interaction of light with a metallic structure coupled to a single quantum emitter: from superabsorption to cloaking. *Physical review letters*, 110(15), 153605.
- [91] R. Fermani, S. Scheel and P.L. Knight, Spatial decoherence near metallic surfaces, *Phys. Rev A* 73, 032902 (2006).
- [92] D. Martin-Cano, A. González-Tudela, L. Martín-Moreno, F.J. Garcia-Vidal, C. Tejedor and E. Moreno, Dissipation-driven generation of two-qubit entanglement mediated by plasmonic waveguides, *Phys. Rev. B* 84, 235306 (2011).
- [93] T.G. Philbin, Casimir effect from macroscopic quantum electrodynamics, *New J. Phys.* 13, 063026 (2011).
- [94] A.L. Grimsmo, A.H. Vaskinn, P.K. Rekdal and B.S.K. Skagerstam, Memory effects in spontaneous emission processes, *Phys. Rev. A* 87, 022101 (2013).
- [95] Delga, A., Feist, J., Bravo-Abad, J., & Garcia-Vidal, F. J. (2014). Quantum emitters near a metal nanoparticle: strong coupling and quenching. *Physical review letters*, 112(25), 253601.
- [96] Delga, A., Feist, J., Bravo-Abad, J., & Garcia-Vidal, F. J. (2014). Theory of strong coupling between quantum emitters and localized surface plasmons. *Journal of Optics*, 16(11), 114018.
- [97] Hakami, J., Wang, L., & Zubairy, M. S. (2014). Spectral properties of a strongly coupled quantum-dot-metal-nanoparticle system. *Physical Review A*, 89(5), 053835.
- [98] Dzsotjan, D., Rousseaux, B., Jauslin, H. R., des Francs, G. C., Couteau, C., & Guérin, S. (2016). Mode-selective quantization and multimodal effective models for spherically layered systems. *Physical Review A*, 94(2), 023818.
- [99] Castellini, A., Jauslin, H. R., Rousseaux, B., Dzsotjan, D., des Francs, G. C., Messina, A., & Guérin, S. (2018). Quantum plasmonics with multi-emitters: application to stimulated Raman adiabatic passage. *European Physical Journal D*, 72(12), 223.
- [100] D.E. Chang, K. Sinha, J.M. Taylor and H.J. Kimble, Trapping atoms using nanoscale quantum vacuum forces, *Nat. Commun.* 5, 4343 (2014).
- [101] S. Ribeiro, S.Y. Buhmann, T. Stielow and S. Scheel, Casimir-Polder interaction from exact diagonalization and surface-induced state mixing, *Europhys. Lett.* 110, 51003 (2015).

-
- [102] Ge, R. C., & Hughes, S. (2015). Quantum dynamics of two quantum dots coupled through localized plasmons: An intuitive and accurate quantum optics approach using quasinormal modes. *Physical Review B*, 92(20), 205420.
- [103] Karanikolas, V. D., Marocico, C. A., Eastham, P. R., & Bradley, A. L. (2016). Near-field relaxation of a quantum emitter to two-dimensional semiconductors: Surface dissipation and exciton polaritons. *Physical Review B*, 94(19), 195418.
- [104] Varguet, H., Rousseaux, B., Dzsotjan, D., Jauslin, H. R., Guérin, S., & des Francs, G. C. (2016). Dressed states of a quantum emitter strongly coupled to a metal nanoparticle. *Optics letters*, 41(19), 4480-4483.
- [105] Thanopulos, I., Yannopapas, V., & Paspalakis, E. (2017). Non-Markovian dynamics in plasmon-induced spontaneous emission interference. *Physical Review B*, 95(7), 075412.
- [106] Yang, C. J., & An, J. H. (2017). Suppressed dissipation of a quantum emitter coupled to surface plasmon polaritons. *Physical Review B*, 95(16), 161408.
- [107] C.J. Yang, J.H. An and H.Q. Lin, Signatures of quantized coupling between quantum emitters and localized surface plasmons, *Phys. Rev. Res.* 1, 023027 (2019).
- [108] R. Carminati and J.J. Greffet, Near-field effects in spatial coherence of thermal sources, *Phys. Rev. Lett.* 82, 1660 (1999).
- [109] A.V. Shchegrov, K. Joulain, R. Carminati and J.J. Greffet, Near-field spectral effects due to electromagnetic surface excitations, *Phys. Rev. Lett.* 85, 1548 (2000).
- [110] C. Henkel, K. Joulain, R. Carminati and J.J. Greffet, Spatial coherence of thermal near fields, *Opt. Commun.* 186, 57-67 (2000).
- [111] K. Joulain, R. Carminati, J.P. Mulet and J.J. Greffet, Definition and measurement of the local density of electromagnetic states close to an interface, *Phys. Rev. B* 68, 245405 (2003).
- [112] K. Joulain, J.P. Mulet, F. Marquier, R. Carminati and J.J. Greffet, Surface electromagnetic waves thermally excited: Radiative heat transfer, coherence properties and Casimir forces revisited in the near field, *Surf. Sci. Rep.* 57, 59-112 (2005).
- [113] A. Archambault, T.V. Teperik, F. Marquier and J.J. Greffet, Surface plasmon Fourier optics, *Phys. Rev. B* 79, 195414 (2009).
- [114] R. Carminati, A. Cazé, D. Cao, F. Peragut, V. Krachmalnicoff, R. Pierrat and Y. De Wilde, Electromagnetic density of states in complex plasmonic systems, *Surf. Sc. Rep.* 70, 1-41 (2015).
- [115] Matloob, R., & Loudon, R. (1996). Electromagnetic field quantization in absorbing dielectrics. II. *Physical Review A*, 53(6), 4567.
- [116] Dzsotjan, D., Sørensen, A. S., & Fleischhauer, M. (2010). Quantum emitters coupled to surface plasmons of a nanowire: A Green's function approach. *Physical Review B*, 82(7), 075427.
- [117] Hümmer, T., García-Vidal, F. J., Martín-Moreno, L., & Zueco, D. (2013). Weak and strong coupling regimes in plasmonic QED. *Physical Review B*, 87(11), 115419.
- [118] T.G. Philbin, Damped vacuum states of light; *J. Opt.* 18, 095201 (2016).
-

-
- [119] A. Drezet; Equivalence between the Hamiltonian and Langevin noise descriptions of plasmon polaritons in a dispersive and lossy inhomogeneous medium; *Physical Review A*, 96(2017)033849.
- [120] S. Y. Buhmann; *Dispersion forces I*; Springer Verlag, Berlin, 2012.
- [121] P. Anger, P. Bharadwaj, L. Novotny; Enhancement and quenching of single-molecule fluorescence. *Physical review letters*, 96(2006)113002.
- [122] Jun, Y. C., Kekatpure, R. D., White, J. S., & Brongersma, M. L. (2008). Nonresonant enhancement of spontaneous emission in metal-dielectric-metal plasmon waveguide structures. *Physical Review B*, 78(15), 153111.
- [123] Sorger, V. J., Pholchai, N., Cubukcu, E., Oulton, R. F., Kolchin, P., Borschel, C., ... & Zhang, X. (2011). Strongly enhanced molecular fluorescence inside a nanoscale waveguide gap. *Nano letters*, 11(11), 4907-4911.
- [124] Ratchford, D., Shafiei, F., Kim, S., Gray, S. K., & Li, X. (2011). Manipulating coupling between a single semiconductor quantum dot and single gold nanoparticle. *Nano letters*, 11(3), 1049-1054.
- [125] Yuan, C. T., Wang, Y. C., Cheng, H. W., Wang, H. S., Kuo, M. Y., Shih, M. H., & Tang, J. (2013). Modification of fluorescence properties in single colloidal quantum dots by coupling to plasmonic gap modes. *The Journal of Physical Chemistry C*, 117(24), 12762-12768.
- [126] Kuttge, M., García de Abajo, F. J., & Polman, A. (2009). Ultrasmall mode volume plasmonic nanodisk resonators. *Nano letters*, 10(5), 1537-1541.
- [127] Akselrod, G. M. et al (2014). Probing the mechanisms of large Purcell enhancement in plasmonic nanoantennas. *Nature Photonics*, 8(11), 835.
- [128] Hoang, T. B., Akselrod, G. M., & Mikkelsen, M. H. (2015). Ultrafast room-temperature single photon emission from quantum dots coupled to plasmonic nanocavities. *Nano letters*, 16(1), 270-275.
- [129] Hoang, T. B., Akselrod, G. M., Argyropoulos, C., Huang, J., Smith, D. R., & Mikkelsen, M. H. (2015). Ultrafast spontaneous emission source using plasmonic nanoantennas. *Nature communications*, 6, 7788.
- [130] Koenderink, A. F. (2017). Single-photon nanoantennas. *ACS photonics*, 4(4), 710-722.
- [131] R. Matloob, R. Loudon, S. M. Barnett, J. Jeffers; Electromagnetic field quantization in absorbing dielectrics; *Physical Review A*, 52(1995)4823.
- [132] R. Matloob, H. Falinejad, Casimir force between two dielectric slabs, *Phys. Rev. A* 64, 042102 (2001).
- [133] Archambault, A., Marquier, F., Greffet, J. J., & Arnold, C. (2010). Quantum theory of spontaneous and stimulated emission of surface plasmons. *Physical Review B*, 82(3), 035411.
- [134] K. Sinha, B.P. Venkatesh and P. Meystre, Collective effects in Casimir-Polder forces, *Phys. Rev. Lett.* 121, 183605 (2018).

- [135] T.V. Shahbazyan, Spontaneous decay of a quantum emitter near a plasmonic nanostructure, *Phys. Rev. B* 98, 115401 (2018).
- [136] H. Falinejad, Quantization of the electromagnetic field at the presence of two dielectric slabs and application to the Casimir effect, *Euro. Phys. J. D* 71, 165 (2017).
- [137] H. Falinejad and S.N. Ardekani, Electromagnetic field quantization near a dielectric slab and spontaneous emission rate determination, *Appl. Phys. B* 125, 208 (2019).
- [138] C. T. Tai; *Dyadic Green functions in electromagnetic theory*; Institute of Electrical & Electronics Engineers (IEEE), 1994.
- [139] G. Barton, On van der Waals friction. II: Between atom and half-space, *New J. Phys.* 12, 113045 (2010).
- [140] F.S.S. Rosa, D.A.R. Dalvit and P.W. Milonni, Electromagnetic energy, absorption, and Casimir forces: Uniform dielectric media in thermal equilibrium, *Phys. Rev. A* 81, 033812 (2010).
- [141] L.D. Landau, E.M. Lifshitz; *The Classical Theory of Fields*; Elsevier, 1975.